UNIVERZITA OBRANY V BRNĚ
FAKULTA VOJENSKÉHO ZDRAVOTNICTVÍ
HRADEC KRÁLOVÉ

MOLEKULÁRNÍ MECHANIZMY PATOGENEZE MIKROBA *FRANCISELLA TULARENSIS*

Disertační práce

Mgr. Daniela Fabriková

Školitel: prof. MUDr. Jiří Stulík, CSc.

Doktorský studijní program: *Infekční biologie*

Hradec Králové
2018

Prohlášení:

Prohlašuji, že jsem tuto disertační práci vypracovala samostatně. Veškeré literární prameny a informace, které jsem v práci využila, jsou uvedeny v seznamu použité literatury.

V Hradci Králové dne 29. 6. 2018 ……

Mgr. Daniela Fabriková

Obsah

Poďakovanie

Na tomto mieste by som sa rada poďakovala môjmu školiteľovi prof. MUDr. Jiřímu Stulíkovi, CSc. za odborné vedenie a cenné rady počas môjho postgraduálneho štúdia. Moje veľké poďakovanie patrí taktiež PharmDr. Anette Švitorka Härtlovej, PhD. za nenahraditeľné skúsenosti získané vďaka nej počas spolupráce na tomto projekte.

Ďalej by som sa rada poďakovala Dr. Nelsonovi O. Gekarovi a celému jeho tímu, pôsobiacemu na Univerzite Umeå, bez ktorých by táto práca nemohla vzniknúť.

Ďakujem taktiež mojim kolegom a kolegyniam z Katedry molekulárnej patológie a biológie a taktiež bývalého Centra pokročilých štúdií za vytvorenie výbornej vedeckej atmosféry.

Avšak moje najväčšie ďakujem za trpezlivosť a neúnavnú podporu počas môjho štúdia patrí predovšetkým môjmu manželovi a zároveň kolegovi Mgr. Ivovi Fabrikovi, rodine a najbližším.

Použité skratky

AIM2 Absent in melanoma 2

AP-1 Activator protein 1

ASC Apoptosis-associated speck-like protein containing CARD

BMDMs Bone marrow-derived macrophages

CARD Caspase activation and recruitment domain

CDS Cytosolic DNA sensor

CFU Colony-forming unit

cGAS Cyclic GMP-AMP synthase

CTD Carboxy-terminal domain

FPI *Francisella* pathogenicity island

GBP Guanylate-binding protein

IFI16 IFN-γ inducible protein 16

IFN Interferon

IKK Inhibitor of NF-κB kinase

IL Interleukin

IPS1 IFN-β promoter stimulator 1

IRAK IL-1 receptor-associated kinase

IRF Interferon regulatory factor

LPS Lipopolysacharid

LRR	Leucine-rich repeat
LVS	Live vaccine strain
MAPKs	Mitogen-activated protein kinases
M-CSF	Macrophage colony-stimulating factor
MD2	Myeloid differentiation factor 2
MyD88	Myeloid differentiation factor 88
NF-κB	Nuclear factor-kappa B
NLR	NOD-like receptor
NOD	Nucleotide-binding oligomerization domain
PAMPs	Pathogen-associated molecular patterns
PRR	Pattern recognition receptors
PYD	Pyrin domain
RIG-I	Retinoic acid-inducible gene-I
RIP	Receptor-interacting protein
RLR	RIG-I-like receptor
RLU	Relative light unit
STING	Stimulator of IFN genes
T6SS	Type 6 **s**ecretion system
TAB	TAK1 binding protein
TAK1	TGF-ß-activated kinase 1
TBK1	TANK-binding kinase 1
TIR	Toll/interleukin 1 receptor
TLR	Toll-like receptor
TNF	Tumor necrosis factor
TRAF	TNF receptor-associated factor

TRAM TRIF-related adaptor molecule

TRIF TIR domain-containing adaptor-inducing IFN-β

VSV Vesicular stomatitis virus

1 Teoretická časť

1.1 *Francisella tularensis*

Francisella tularensis (*F. tularensis*) predstavuje pôvodcu zoonotického ochorenia nazývaného tularémia alebo zajačí mor. Tento aeróbny, nepohyblivý, gramnegatívny kokobacil bol prvýkrát identifikovaný u malých hlodavcoch trpiacich na ochorenie podobné moru v oblasti Tulare v Kalifornii, podľa ktorej bol pomenovaný *Bacterium tularense* (Mccoy and Chapin 1912). Prvý prípad ľudskej infekcie bol zaznamenaný v roku 1914 v Ohiu (Wherry and Lamb 1914). Etiologický agens bol avšak vyizolovaný z krvi pacientov postihnutých tzv. deer-fly fever až o pár rokov neskôr Dr. Edwardom Francisom, na ktorého počesť bol tento patogén premenovaný (Francis 1921).

1.1.1 Taxonómia a geografická distribúcia

Na základe sekvenačnej analýzy 16S rRNA bola *F. tularensis* zaradená do rodu *Francisella* v čeľadi *Francisellaceae*, ktorá prislúcha do triedy *Gammaproteobacteria* (Forsman et al. 1994; McLendon et al. 2006). V súčasnosti do druhu *F. tularensis* patria tri poddruhy, subsp. *tularensis*, *holarctica* a *mediasiatica*, líšiace sa svojim geografickým výskytom a patogenitou **(Tab. 1-1)** (Oyston 2008). Medzi najvirulentnejší poddruh sa radí *F. tularensis* subsp. *tularensis* (typ A), vyskytujúca sa najmä v Severnej Amerike. Rozlišujú sa tu dve geneticky rozdielne subpopulácie AI a AII (Johansson et al. 2004), pričom AI sa dodatočne delí na skupinu AIa a AIb. Tularémia u ľudí vyvolaná skupinou AIb má v porovnaní so subpopuláciami AIa a AII závažnejší priebeh a vyššiu mieru úmrtnosti (Carvalho et al. 2014). *F. tularensis* subsp. *holarctica* (typ B) vyvoláva miernejšiu formu ochorenia a objavuje sa hlavne v Severnej Amerike, Európe, ale taktiež Ázii. Tretí poddruh *F. tularensis* subsp. *mediasiatica* sa svojou virulenciou podobá *F. tularensis* typu B, avšak je ho možné nájsť len v Centrálnej Ázii. Za menej častého

pôvodcu tularémie u ľudí je považovaný druh *F. novicida*, ktorý sa vyskytuje hlavne v Severnej Amerike a Austrálii (Johansson et al.

2004; Larsson et al. 2009; Kingry and Petersen 2014).

Tab. 1-1: Geografické rozšírenie a virulencia *F. tularensis*

***F. tularensis* subsp.**	**Subpopulácie**	**Výskyt**	**LD_{50} (CFU) [a]**	
			Ľudia	Myši
tularensis	AI	Severná Amerika, Slovensko	<10	<10
	AII	Severná Amerika		
holarctica	BI	Eurázia	<1	$<10^3$
	BII	Severná Amerika, Švédsko		
	BIII	Severná Amerika, Eurázia		
	BIV	Severná Amerika, Švédsko, Španielsko, Francúzko		
	BV	Japonsko		
mediasiatica	-	Centrálna Ázia	n	n

[a] Všetky dávky boli podávané subkutánne. n, neznáma. Prevzaté a upravené z: (Ellis et al. 2002; Johansson et al. 2004).

1.1.2 Epidemiológia

V súčasnosti tularémia predstavuje ochorenie vyskytujúce sa s prírodnou ohniskovosťou v mnohých častiach severnej pologule. Prípady infekcie ľudí sú hlásené najmä z oblastí Severnej Ameriky, konkrétne z USA, ale taktiež z Japonska, Ruska, Škandinávie a centrálnej Európy (Tärnvik and Berglund 2003). V roku 2010 bolo európskym Centrom pre kontrolu a prevenciu chorôb zaznamenaných 891 prípadov tularémie v Európe, pričom najvyššia incidencia bola hlásená vo Švédsku, Fínsku a Maďarsku (Eliasson et al. 2002; Carvalho et al. 2014). Na druhú stranu, v niektorých krajinách, ako je Rakúsko alebo Veľká Británia, bol výskyt ochorenia pozorovaný len sporadicky (Carvalho et al. 2014).

Napriek tomu, že tularémia postihuje širokú škálu divoko žijúcich zvierat, vrátane hlodavcov, zajacovitých, hmyzožravcov, mäsožravcov, kopytníkov, vačkovcov, vtákov, obojživelníkov, rýb a taktiež bezstavovcov, zostáva jej primárny rezervoár stále neznámy (Mörner 1992; Pechous et al. 2009; Santic et al. 2010). Výskyt tularémie v prírode je

primárne spájaný s rôznymi druhmi hlodavcov, králikov alebo zajacov, u ktorých má ale ochorenie v mnohých prípadoch akútny priebeh (Pechous et al. 2009). Nedávne štúdie odhalili schopnosť *F. tularensis* subsp. *holarctica* prežívať a rásť v *Acanthamoeba castellanii*, ktorá môže predstavovať dlho hľadaný rezervoár tohto patogéna (Santic et al. 2010).

Za primárnu cestu nákazy je u tularémie považovaný transmisívny prenos *F. tularensis* článkonožcami, konkrétne kliešťami, komármi alebo ovadmi (Santic et al. 2010). Okrem toho môže dochádzať k infekcii aj požitím kontaminovanej vody či jedla, inhaláciou aerosólu obsahujúceho *F. tularensis* alebo priamym kontaktom s infikovanými zvieratami (Mörner 1992; Tärnvik and Berglund 2003).

1.1.3 *F. tularensis* ako potenciálna biologická hrozba

Z dôvodu nízkej infekčnej dávky, možnému prenosu aerogénnou cestou a schopnosti vyvolať smrteľné ochorenie bola *F. tularensis* klasifikovaná americkým Centrom pre kontrolu a prevenciu chorôb ako biologický agens kategórie A (Centers for Disease Control and Prevention. 2000). Prvé zmienky o jej možnom zneužití ako biologickej zbrane pochádzajú už zo staroveku z oblasti Malej Ázie. Predpokladá sa, že Chetiti zámerne zasielali kontaminované zvieratá *F. tularensis* svojim nepriateľom s cieľom infikovať protivníka (Trevisanato 2007). Záujem o *F. tularensis* v novodobých dejinách významne narástol v období 2. svetovej vojny. Nielen v Japonsku, ale i v USA a Sovietskom zväze začalo rozsiahle štúdium biologických agens za účelom vojenského využitia (Dennis et al. 2001). Svetová zdravotnícka organizácia označila *F. tularensis* za biologickú hrozbu a odhadla, že rozptýlenie 50 kg tejto baktérie vo forme aerosólu nad oblasťou s 5 miliónmi obyvateľov by mohlo vyvolať 19 000 úmrtí a závažné ochorenie postihujúce 250 000 ľudí (World Health Organization 1970). Krátko na to bol vydaný Dohovor o zákaze vývoja, výroby a hromadenia zásob bakteriologických a toxínových zbraní, na základe ktorého bol v mnohých krajinách ukončený vyzbrojovací program (UNODA 2017; IC 2017). Do popredia sa opätovne dostalo štúdium biologických agens, vrátane *F. tularensis,* po roku 2001 v dôsledku narastajúcej hrozby ich možného zneužitia počas teroristického útoku.

1.1.4 Tularémia

Tularémia je akútne febrilné ochorenie, ktoré postihuje ako zvieratá tak i ľudí. Priebeh tohto ochorenia závisí na mieste vstupu *F. tularensis*, infekčnej dávke, virulencii baktérie a stave imunitného systému hostiteľa (Ellis et al. 2002). Náhlemu prepuknutiu ochorenia predchádza inkubačná doba trvajúca 3 až 5 dní, výnimočne až 21 dní. Vysoké teploty sprevádzané symptómami pripomínajúcimi chrípku môžu viesť v skorej fáze tularémie k nesprávnej diagnóze a oddialeniu účinnej liečby, čo môže mať v niektorých prípadoch fatálne následky (Tärnvik and Berglund 2003).

1.1.4.1 Klinické formy tularémie

V závislosti na mieste vstupu infekcie je rozlišovaných niekoľko klinických foriem ochorenia. Najbežnejšou podobou je ulceroglandulárna tularémia, ktorá vzniká transmisívnym prenosom článkonožcami alebo priamym kontaktom s nakazenými zvieratami (Tärnvik and Berglund 2003). V mieste vstupu infekcie sa vytvára bolestivý vred, ktorý je nasledovaný zväčšením regionálnych lymfatických uzlín (Ohara et al. 1991).

Okuloglandulárna tularémia je menej častá forma ochorenia a je spôsobená priamym kontaktom baktérie s okom. V prípade požitia kontaminovanej vody alebo jedla dochádza ku vzniku orofaryngeálnej tularémie, ktorá je doprevádzaná ulceratívnou stomatitídou a faryngitídou. Touto cestou prenosu môže byť vyvolaná aj gastrointestinálna forma ochorenia, ktorej priebeh avšak závisí od množstva infekčnej dávky (Tärnvik and Berglund 2003).

Za najzávažnejší stav je považovaná respiračná tularémia, ktorá vzniká v dôsledku inhalácie aerosólu obsahujúceho *F. tularensis* alebo bakteriálneho šírenia sa hematogénnou cestou. Pokiaľ je ochorenie vyvolané najvirulentnejším poddruhom *F. tularensis* a nie je včas stanovená efektívna liečba, môže byť miera úmrtnosti až 60 % (Tärnvik and Berglund 2003).

1.1.4.2 Terapia tularémie

Liečba tularémie spočíva v podávaní aminoglykozidových, tetracyklínových a fluorochinolónových antibiotík. Historicky sa používali ako liek prvej voľby

aminoglykozidy, ktoré majú baktericídnu aktivitu a je tu pomerne malé riziko relapsu ochorenia. Avšak z dôvodu ich cytotoxického pôsobenia a nutnosti parenterálnej a intravenóznej aplikácie sa podávajú nakoniec len v najzávažnejších prípadoch. Ako alternatívna terapia sú využívané tetracyklíny aj napriek ich bakteriostatickému pôsobeniu a vysokému riziku relapsu choroby (Dennis et al. 2001; Oyston 2008). Dôležitého zástupcu predstavuje doxycyklín, ktorý bol účinný pri liečbe tularémie vyvolanej *F. tularensis* subsp. *holarctica* (Tärnvik and Berglund 2003). Ďalšou možnosťou voľby sú taktiež fluorochinolónové antibiotiká, kde sa v *in vitro* a *in vivo* testoch osvedčil napr. ciprofloxacín (Dennis et al. 2001; Johansson et al. 2001; Oyston 2008).

1.1.4.3 Vakcíny proti tularémii

Vakcíny predstavujú jeden z dôležitých nástrojov prevencie a profylaxie infekčných chorôb. Bohužiaľ, v prípade tularémie sú navzdory dlhoročnému úsiliu o ich vývoj stále nedostupné. V minulosti si zaslúžila najväčšiu pozornosť živá atenuovaná vakcína, tzv. live vaccine strain (LVS), ktorá bola pripravená mnohopočetným pasážovaním atenuovanej *F. tularensis* subsp. *holarctica* (Eigelsbach and Downs 1961). Z dát získaných na dobrovoľníkoch je známe, že podanie LVS vo forme aerosólu poskytovalo protektívnu ochranu proti infekcii spôsobenej najvirulentnejším poddruhom *F. tularensis* (McCrumb 1961). Avšak vakcína nebola schválená Úradom pre kontrolu potravín a liečiv z dôvodu neznámeho mechanizmu atenuácie, možnej reverzie virulencie a variabilnej imunogenicite (Hornick and Eigelsbach 1966; Hartley et al. 2006; Petrosino et al. 2006). Preto sa v súčasnosti sústreďujú všetky snahy na vývoj bezpečnej a efektívnej vakcíny, u ktorej bude známy presný mechanizmus pôsobenia a ktorá bude schopná navodiť protektívnu imunitnú odpoveď voči respiračnej tularémii vyvolanej *F. tularensis* subsp. *tularensis*.

1.1.5 Hostiteľská imunitná odpoveď voči *F. tularensis*

Vzhľadom na intracelulárny parazitizmus *F. tularensis* sa dlhú dobu predpokladalo, že najdôležitejšiu úlohu v hostiteľskej obrane bude zohrávať bunkami sprostredkovaná imunitná odpoveď. Odhaľovaním nových poznatkov sa však ukazuje, že pre potlačenie infekcie vyvolanej touto baktériou je dôležitá súčinnosť bunkovej aj

humorálnej imunity, a to hlavne profesionálnych fagocytov, cytokínov produkovaných T-lymfocytmi ako aj protilátkovej odpovede (Kirimanjeswara et al. 2008; Cole et al. 2011).

Hostiteľská imunitná obrana je v skorej fáze infekcie *F. tularensis* kontrolovaná profesionálnymi fagocytmi, ako sú makrofágy, dendritické bunky alebo neutrofily (Kirimanjeswara et al. 2008). Po prvotnom kontakte s baktériou dochádza prostredníctvom signalizačnej dráhy tzv. Toll-like receptor (TLR) 2 ku produkcii prozápalových cytokínov a chemokínov, ktoré ovplyvňujú diferenciáciu T-lymfocytov ako aj indukciu antimikrobiálnych molekúl (Katz et al. 2006; Cole et al. 2007; Cowley and Elkins 2011). Hlavnou úlohou kľúčového proteínu Th1-cytokínovej odpovede interferónu (IFN)-γ je navodenie mikrobicídneho stavu v infikovaných bunkách prostredníctvom aktivácie inducibilnej NO syntázy (Anthony et al. 1992; Lindgren et al. 2004b). Jeho hlavným zdrojom sú T-lymfocyty a NK-bunky, pričom jeho produkcia je regulovaná pomocou interleukínu (IL)-12p40, ale aj IL-17A (Karttunen et al. 1991; Elkins et al. 2002; De Pascalis et al. 2008; Lin et al. 2009). Okrem IFN-γ prispieva k potlačeniu infekcie vyvolanej *F. tularensis* aj tzv. tumor necrosis factor α (TNF-α), cytokín žírnych buniek IL-4 (Ketavarapu et al. 2008) a anti-lipopolysacharidové protilátky tvorené B1a B-lymfocytmi (Cowley and Elkins 2011).

Niekoľko dní po infekcii sa objavujú špecifické $CD4^+$ a $CD8^+$ T-lymfocyty, ktoré zabezpečujú dlhotrvajúcu protektívnu imunitnú odpoveď (Koskela and Herva 1982; Surcel et al. 1991; Ericsson et al. 2001). Z pohľadu potlačenia primárnej infekcie predstavujú αβ T-lymfocyty dôležitú zložku protektívnej imunity a to aj vďaka produkcii efektorových cytokínov IL-17A, IFN-γ ako aj TNF-α a následnej amplifikácii tvorby reaktívnych dusíkatých metabolitov (Surcel et al. 1991; Sjöstedt et al. 1992; Lin et al. 2009). Počas skorej fáze infekcie bola však detegovaná aj prítomnosť γδ Tlymfocytov rozlišujúcich špecifické fosfoantigény *F. tularensis.* Predpokladá sa, že vzhľadom na ich schopnosť perzistovať u pacientov až vyše roka bude ich úloha významná (Poquet et al. 1998; Kroca et al. 2000).

Okrem T-lymfocytov majú svoj podiel na protektívnej imunite aj špecifické Blymfocyty a protilátková odpoveď (Lavine et al. 2007; Kirimanjeswara et al. 2008; Cole et al. 2011; Kubelkova et al. 2012). V priebehu 1. týždňa infekcie sa objavujú v krvi pacientov sérové protilátky IgM, IgG a IgA, ktoré sú namierené primárne proti

lipopolysacharidu (LPS) *F. tularensis* (Koskela and Salminen 1985). Ďalšie ciele vznikajúcich protilátok predstavujú proteíny vonkajšej membrány *F. tularensis* FopA a OmpA ako aj intracelulárne proteíny GroEL a KatG (Sundaresh et al. 2007).

1.1.6 Intracelulárny osud *F. tularensis*

F. tularensis predstavuje baktériu známu svojou schopnosťou invadovať a množiť sa v rade hostiteľských buniek. U cicavcov tvoria primárny cieľ makrofágy, ktoré jej poskytujú úkryt pred pôsobením extracelulárnych zložiek vrodenej imunity, ale taktiež miesto pre replikáciu a následnú diseminaciu do distálnych orgánov. Okrem toho je *F. tularensis* však schopná infikovať aj iné typy buniek, vrátane ďalších fagocytujúcich (dendritické bunky, neutrofily), ako aj nefagocytujúcich (hepatocyty, endoteliálne bunky alebo fibroblasty) (Hall et al. 2008; Jones et al. 2012a; PizarroCerdá et al. 2016).

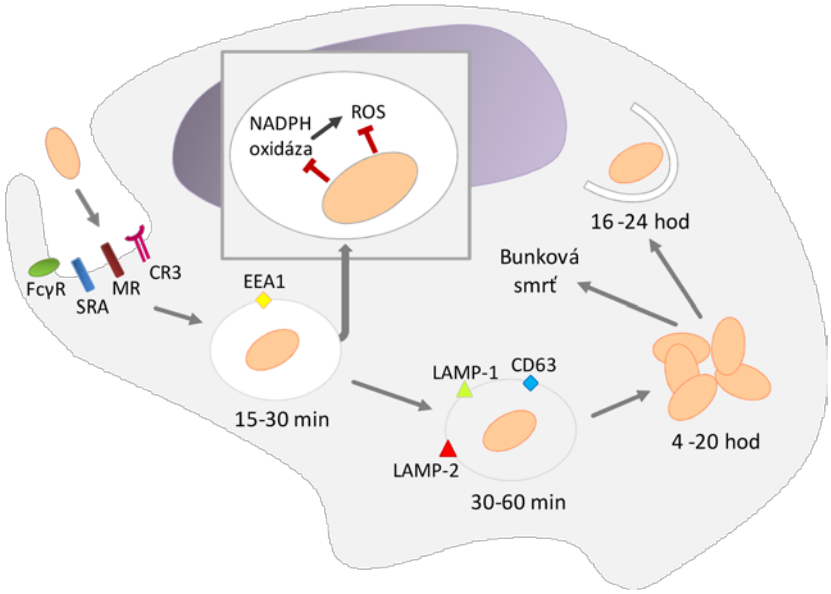

Obr. 1-1: Štádia intracelulárneho života *F. tularensis* v makrofágoch. *F. tularensis* je rozlišovaná celou radou makrofágových receptorov (FcγR, SRA, MR alebo CR3). Po jej pohltení sa nachádza vo fagozóme, ktorý postupne získava znaky skorého (EEA1) ako aj neskorého (Lamp1/2, CD63) endozómu. *F. tularensis* následne využíva množstvo mechanizmov, ktoré jej umožňujú zmierniť pôsobenie antimikrobiálnej obrany. Jeden z nich je schopnosť blokovať NADPH oxidázu alebo detoxikovať reaktívne formy kyslíka. Po úteku *F. tularensis* do cytosólu dochádza k výraznému pomnoženiu baktérie, autofágii a indukcii bunkovej smrti. Prevzaté a upravené z: (Pechous et al. 2009; Jones et al. 2012a).

1.1.6.1 Invázia do hostiteľskej bunky

Po prvom kontakte *F. tularensis* s hostiteľskou bunkou, dochádza k jej naviazaniu sa na povrchové receptory a k následnému pohlteniu unikátnym fagocytóze podobným mechanizmom prostredníctvom tzv. pseuodpod loops **(Obr. 1-1)**. Tieto asymetrické výbežky plazmatickej membrány vytvárajú priestornú štruktúru, ktorá obkľučuje patogén a vedie k jeho následnej internalizácii za účasti aktínových mikrofilament (Clemens et al. 2005). *F. tularensis* využíva pre inváziu do hostiteľskej bunky celú radu membránových receptorov, pričom miera jej inkorporácie a intracelulárny osud závisí taktiež na prítomnosti a povahe opsonizácie. Na vstupe *F. tularensis* opsonizovanej sérom sa podieľajú komplementové receptory (hlavne CR3, CR1, a CR4), scavengerový receptor A (SRA) a taktiež membránový nukleolín (Pierini 2006; Barel et al. 2008; Moreau and Mann 2013). V prípade opsonizácie baktérie protilátkou, najmä IgG, zohráva svoju rolu i Fc receptor (FcγR). Fagocytóza sprostredkovaná CR3 a FcγR receptormi má za následok oddialenie fagozomálneho úniku baktérie a obmedzenie jej replikácie v cytosóle (Geier and Celli 2011). Príjem neopsonizovanej *F. tularensis* cez manózový receptor (MR) vedie naopak k urýchleniu bakteriálneho úteku do cytosólu a početnému pomnoženiu sa (Balagopal et al. 2006; Schulert and Allen 2006). Dôležitú úlohu v internalizácii *F. tularensis* zohrávajú i lipidové rafty s vysokým podielom cholesterolu. Tieto membránové mikrodomény predstavujú výrazne koncentrovanú oblasť receptorov a signalizačných molekúl, ktoré interagujú s baktériou pri jej vstupe (Moreau and Mann 2013).

1.1.6.2 Fagozómálne štádium

Po pohltení baktérie vzniká tzv. *Francisella*-containing phagosome (FCP), ktorý získava počas endocytického vývoja znaky skorého (EEA1), ale aj neskorého endozómu (Lamp1/2, Rab7GTPáza, CD63) **(Obr. 1-1)**. Celý tento proces od začiatku biogenézy FCP je pomerne krátky a trvá zhruba 15 až 30 minút. Za normálnych okolností fagozóm, ktorý bol acidifikovaný pomocou protónových ATPázových púmp, fúzuje s lyzozómom, kde sa degraduje väčšina pohltených baktérii. Avšak v prípade *F. tularensis* k tomuto hostiteľskému obrannému mechanizmu nedochádza. V priebehu 30 až 60 minút neopsonizovaná baktéria uniká do bunkového cytosólu, kde sa mohutne replikuje. Tento proces je za prítomnosti opsonizácie oddialený a dochádza k nemu až v priebehu 2 až 4 hodín. Molekulárne mechanizmy, ktoré využíva *F. tularensis* ku svojmu úniku zostávajú

aj naďalej otázne (Santic et al. 2010; Pizarro-Cerdá et al. 2016). Predpokladá sa, že by v tomto deji mohol zohrávať dôležitú úlohu sekrečný systém typu 6 (T6SS) (Nano and Schmerk 2007; Spidlova and Stulik 2017; Brodmann et al. 2017).

T6SS bol objavený pomerne nedávno a predstavuje dôležitý virulenčný faktor mnohých gram-negatívnych patogénov, vrátane *Vibrio cholerae*, *Salmonella enterica* alebo *Escherichia coli*. Tento špecializovaný aparát umožňuje baktériam transportovať ich efektorové proteíny do cieľových hostiteľských buniek (Pizarro-Cerdá et al. 2016). V prípade *F. tularensis* zohráva T6SS dôležitú úlohu vo fagozomálnom úniku baktérie. Tento sekrečný systém je kódovaný tzv. *Francisella* pathogenicity island (FPI) predstavujúcim zhruba 30 kb veľkú oblasť genómu, ktorá je zdvojená u všetkých poddruhov *F. tularensis* (Nano and Schmerk 2007; Larsson et al. 2009). U mnohých génov exprimovaných z tejto oblasti (*iglC, pdpA, vrgG*) alebo regulujúcich ich expresiu (*mglA, fevR*) bola preukázaná účasť na fagozomálnom úniku a cytosólickej replikácii *F. tularensis* (Baron and Nano 1998; Lindgren et al. 2004a; Santic et al. 2005; Brotcke and Monack 2008; Barker et al. 2009). Okrem toho, kryo-elektrónová mikroskopia odhalila, že puzdro tohto sekrečného systému je tvorené produktmi génov FPI, a to *iglA* a *iglB* (Clemens et al. 2015). Presný mechanizmus pôsobenia T6SS avšak aj naďalej zostáva predmetom štúdií.

Pred tým, než *F. tularensis* unikne do cytosólu musí čeliť fagozómalnej antimikrobiálnej obrane, vrátane pôsobenia reaktívnych foriem kyslíka (ROS). Ich tvorba je zabezpečená prostredníctvom NADPH oxidázy, ktorá stojí za produkciou superoxidových radikálov z molekulárneho kyslíka **(Obr. 1-1)**. Tento mnohopočetný enzýmový komplex sa skladá do funkčného celku v priebehu aktivácie fagocytu z membránových (gp91^{phox} a p22^{phox}) a cytosólických podjednotiek (p47^{phox}, p40^{phox} a p67^{phox}) (Celli and Zahrt 2013). Avšak ako mnohé iné patogény si *F. tularensis* vyvinula obranné mechanizmy proti pôsobeniu NADPH oxidázy. Jedným z nich je blokácia jej správneho zloženia prostredníctvom kyslej fosfatázy AcpA (Mohapatra et al. 2010) alebo priama detoxikácia ROS sprostredkovaná buď bakteriálnou katalázou alebo superoxid dismutázou (Bakshi et al. 2006; Lindgren et al. 2007).

1.1.6.3 Cytosólický osud

V priebehu svojej replikácie v cytosóle je *F. tularensis* nútená prispôsobiť svoje nutričné potreby dostupným zdrojom živín. V myších embryonálnych fibroblastoch *F.*

tularensis indukuje ATG5-nezávislú formu autofágie, ktorá jej zabezpečuje dostatočný prísun aminokyselín potrebných pre proteínovú syntézu alebo jej slúži ako zdroj uhlíka. Napriek tomu, že sa *F. tularensis* v priebehu tohto deja nachádza v tesnej blízkosti autofagozómov, nepodlieha degradácii xenofágiou. Jej prítomnosť v LC3pozitívnych vakuolách s dvojitou membránou bola zaznamenaná len v prípade narušenia jej replikácie (Chong et al. 2012). Štúdie ukazujú, že *F. tularensis,* ako aj iné intracelulárne patogény, ovplyvňuje proces autofágie za účelom udržania bakteriálnej proliferácie a prežitia v cytosóle (Chong et al. 2012; Steele et al. 2013; Case et al.
2014).

1.1.6.4 Sekundárna infekcia hostiteľských buniek

Po úniku *F. tularensis* do cytosólu dochádza k výraznej bakteriálnej proliferácii a následnej indukcii apoptickej alebo pyroptickej bunkovej smrti (Lai et al. 2001; Henry et al. 2007). *F. tularensis* je po rozrušení membrány hostiteľskej bunky uvoľnená do extracelulárneho priestoru a následne infikuje okolité bunky. Nedávne štúdie však odhalili, že *F. tularensis* sa je schopná šíriť aj bez narušenia celistvosti a životnosti hostiteľských buniek. V priebehu tohto procesu podobnému trogocytóze, baktéria využíva pre svoj transfer vzájomnú výmenu cytoplazmy hostiteľskými bunkami (Steele et al. 2016; Pizarro-Cerdá et al. 2016).

1.2 Bunková signalizácia vedúca k zápalovej odpovedi

Vrodená imunitná odpoveď predstavuje prvú líniu hostiteľskej obrany proti invadujúcim patogénom. V priebehu infekcie je zodpovedná za rozlíšenie mikrobiálneho pôvodcu prostredníctvom tzv. pattern recognition receptors (PRR), ktorých hlavnou úlohou je detekcia evolučne zachovaných štruktúr patogénov, tzv. pathogen-associated molecular patterns (PAMPs) a molekúl pochádzajúcich z poškodených buniek, tzv. damage-associated molecular patterns. Po rozlíšení týchto stimulov dochádza ku kaskádovitej aktivácii signálnych dráh, vrátane transkripčných faktorov tzv. nuclear factor-kappa B (NF-κB) a tzv. IFN regulatory factor (IRF), vedúcej ku produkcii prozápalových cytokínov, IFN typu I alebo ďalších mediátorov. Výsledným efektom týchto procesov je skorá hostiteľská imunitná odpoveď vedúca k eliminácii patogéna ako aj formovaniu rozvíjajúcej sa adaptívnej imunity (Mogensen 2009; Kawasaki and Kawai 2014).

1.2.1 TLR

Hlavnú rodinu receptorov PRR predstavujú TLR, ktoré sú u myší zastúpené 12 (TLR1 - TLR9, TLR11 - TLR13) a u ľudí 10 členmi (TLR1 - TLR10) (Newton and Dixit 2012; Kawasaki and Kawai 2014)). Každý TLR sa skladá z tzv. leucine-rich repeat (LRR) domény zodpovednej za detekciu PAMPs a tzv. Toll/interleukin 1 receptor (TIR) domény zabezpečujúcej následnú transdukciu signálu a aktiváciu prozápalovej alebo IFN odpovede typu I (Botos et al. 2011). TLR sú exprimované najmä na antigén prezentujúcich bunkách, ako sú dendritické bunky alebo makrofágy, ale taktiež na fibroblastoch a epiteliálnych bunkách. Na základe bunkovej lokalizácie je možné TLR rozdeliť do 2 podrodín, a to na TLR vyskytujúce sa na bunkovom povrchu (TLR1 - TLR2, TLR4 - TLR6 a TLR10) alebo v intracelulárnych endolyzozómoch (TLR3, TLR7 - TLR9, TLR11 - TLR13) **(Tab. 1-2)** (Kawasaki and Kawai 2014).

Povrchové TLR rozlišujú celú radu mikrobiálnych komponent **(Tab. 1-2)**. TLR2 deteguje v podobe heterodiméru s TLR1 alebo TLR6 tri- alebo diacylované lipoproteíny, peptidoglykán, kyselinu lipoteichoovú, zymosan alebo manan (Mogensen 2009; Kawasaki and Kawai 2014). Okrem toho TLR2 vytvára komplex aj spolu s TLR10, ktorý rozlišuje PAMPs pochádzajúce z listérií (Regan et al. 2013). TLR4 rozlišuje bakteriálny LPS za spoluúčasti tzv. myeloid differentiation factor 2 (MD2) a ko-receptoru CD14 (Kim et al. 2007; Park et al. 2009). Okrem toho sa tento receptor podieľa aj na detekcii F proteínu respiračného syncyciálneho vírusu (RSV) alebo proteínov pochádzajúcich z vírusu myšieho mammárneho karcinómu (MMTV) (KurtJones et al. 2000; Rassa et al. 2002). Za rozlíšenie flagelínu z bičíkatých baktérií zodpovedá TLR5, ktorý je významne exprimovaný najmä na dendritických bunkách v tenkom čreve (Pandey et al. 2015).

Tab. 1-2: TLR a ich ligandy

TLR	Ligand	Pôvod ligandu
2/1, 2/6	triacylované a diacylované lipoproteíny, manan, kyselina lipoteichoová, peptidoglykán, zymosan	Baktérie, huby
3	dsRNA, siRNA	RNA vírusy
4	LPS, fúzny proteín RSV a MMTV	Gram- baktérie, RNA vírusy
5	Flagelín	Baktérie

7, 8	ssRNA, krátke úseky dsRNA	Baktérie, RNA vírusy
9	Nemetylované CpG DNA, hemozoín	Baktérie, DNA vírusy, prvoky
10[a]	Neznámy	Baktérie
11[b]	Flagelín, profilín	Baktérie, prvoky
12[b]	Profilín	Prvoky
13[b]	23S rRNA	Gram - a Gram+ baktérie

[a] exprimovaný len u ľudí; [b] exprimovaný len u myší

Prevzaté a upravené z: (Mogensen 2009; Broz and Monack 2013; Pandey et al. 2015).

Ligandy intracelulárnych TLR sú najmä nukleové kyseliny **(Tab. 1-2)**. TLR3 rozpoznáva vírusovú dvojvláknovú (ds) RNA, ale taktiež tzv. small interfering RNA (siRNA). TLR7 spolu s TLR8 zodpovedajú za rozlíšenie jednovláknovej (ss) RNA. Nemetylovanú DNA bohatú na motívy CpG, ale aj hemozoín rozoznáva TLR9. Ďalší detektor flagelínu predstavuje TLR11, ktorý interaguje aj s PAMPs uropatogénnych baktérií. Navyše, TLR11 vytvára s TLR12 heterodimér zodpovedný za detekciu profilínu z *Toxoplasma gondii*. TLR13 zabezpečuje rozlišovanie zložiek vírusu vezikulárnej stomatitídy (VSV) a 23S ribozomálnej RNA (Mogensen 2009; Kawasaki and Kawai 2014).

1.2.1.1 Signalizácia riadená TLR

Charakter bunkovej signalizácie zahájenej prostredníctvom TLR sa líši v závislosti od účastniacich sa adaptorových proteínov. Okrem TLR3, takmer všetky TLR využívajú pre prenos signálu tzv. myeloid differentiation factor 88 (MyD88) buď priamo (TLR5, TLR8 - TLR11) alebo v kombinácii s TIRAP/Mal (TLR1/2, TLR2/6, TLR4) (Kawasaki and Kawai 2014). MyD88 obsahuje okrem TIR domény aj tzv. death domain (DD), ktorá mu umožňuje väzbu na DD tzv. IL-1 receptor-associated kinase (IRAK) (Lin et al. 2010). Adaptorový proteín tzv. TIR domain-containing adaptor-inducing IFN-β (TRIF; známy aj ako TICAM1) sa účastní signalizácie riadenej TLR3 a TLR4. Avšak v prípade endocytovaného TLR4 dochádza k využitiu aj tzv. TRIF-related adaptor molecule (TRAM; známy aj ako TICAM2). Prenos signálu prostredníctvom TRIF je zabezpečený okrem TIR domény aj s tzv. receptor-interacting protein (RIP) kinase homotypic interaction motif (Newton and Dixit 2012).

Po stimulácii TLR dochádza k vytvoreniu signalizačného komplexu nazývaného „myddosome", ktorý obsahuje okrem MyD88 aj členov rodiny IRAK **(Obr. 1-2)**. V

priebehu jeho vzniku dochádza k autofosforylácii IRAK4, ktorá je dôležitá pre následnú aktiváciu IRAK2 alebo IRAK1 a ich interakciu s tzv. TNF receptorassociated factor 6 (TRAF6) (Lin et al. 2010). Táto E3 ubikvitín-ligáza spoločne s E2 ubikvitín-konjugujúcimi enzýmami Ubc13 a Uev1A katalyzuje vznik polyubikvitínových reťazcov prepojených cez lyzín 63 (K63). Ich detekcia tzv. TGF-ßactivated kinase 1 (TAK1) binding protein (TAB) 2 a TAB3 zohráva kľúčovú ú1ohu v aktivácii TAK1 (Adhikari et al. 2007; Yin et al. 2009; Ajibade et al. 2013). Táto kináza umožňuje fosforyláciu tzv. inhibitor of NF-κB (IκB) kinase (IKK)-ß a tzv. mitogen-activated protein kinases (MAPKs). IKK-ß tvorí spolu s IKK-α a tzv. IKKγ (známy aj ako NEMO) komplex IKK, ktorý je zodpovedný za fosforyláciu inhibítora NF-κB, IκBα. Ten následne podlieha degradácii v proteazóme a uvoľnený NF-κB je translokovaný do jadra, kde stimuluje prozápalovú odpoveď (Newton and Dixit 2012; Kawasaki and Kawai 2014). Stimulácia členov rodiny MAPKs (ERK1/2, p38 a JNK) vedie k aktivácii transkripčného faktora tzv. activator protein 1 (AP-1), ktorý sa taktiež podieľa na regulácii expresie cytokínov (Kawasaki and Kawai 2014; Pandey et al. 2015).

V plazmacytoidných dendritických bunkách vedie aktivácia signalizačného komplexu MyD88-IRAK4-IRAK1-TRAF6 prostredníctvom TLR7 alebo TLR9 aj k IFN odpovedi typu I. Pre tento proces je dôležitá prítomnosť aj E3 ubikvitín-ligázy, TRAF3, ktorá sa účastní spoločne s IKK-α aktivácie IRF7 alebo IRF1 (Mancuso et al. 2009; Takeuchi and Akira 2010; Kawasaki and Kawai 2014).

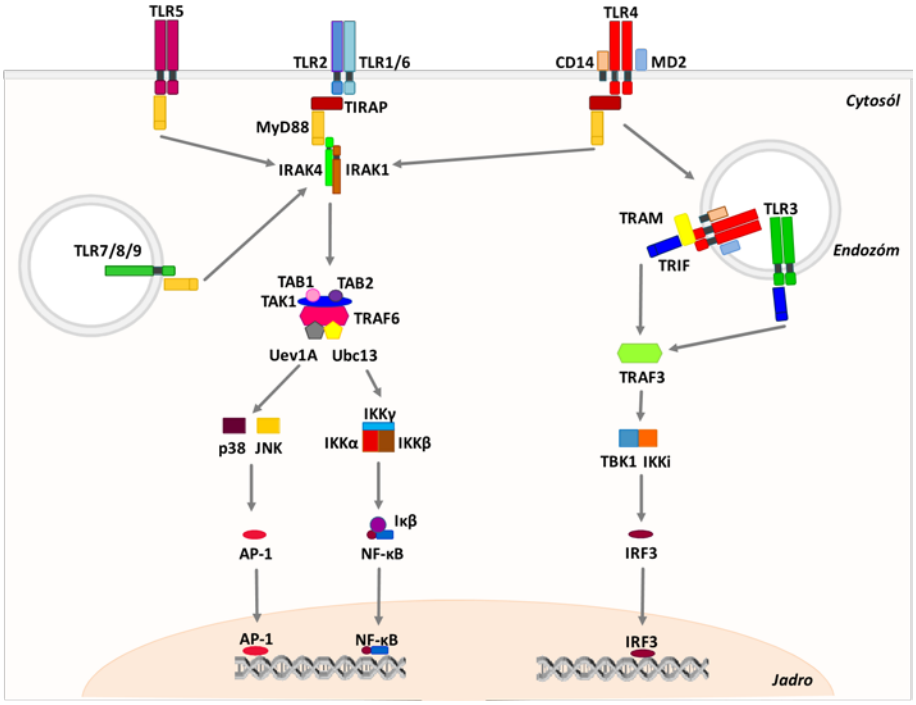

Obr. 1-2: TLR a ich signalizačné dráhy. Po rozlíšení ligandu receptorom TLR dochádza k aktivácii adaptorového proteínu MyD88 alebo TRIF a indukcii prozápalovej alebo IFN odpovede typu I. Prevzaté a upravené z: (Feng and Chao 2011; Patel et al. 2012).

V prípade stimulácie receptora TLR3 alebo TLR4 je signál transdukovaný cez adaptorový proteín TRIF, ktorý sa spolupodieľa s jeho interakčnými partnermi RIP1 a TRAF6 na indukcii NF-κB alebo AP-1 **(Obr. 1-2)**. TRIF interaguje aj s TRAF3, ktorý je nepostrádateľný pre indukciu tzv. TANK-binding kinase 1 (TBK1) a IKK*i* (známy aj ako IKKε). Podobne ako u TRAF6, TRAF3 spolupracuje s E2 ubikvitínkonjugujúcimi enzýmami Ubc13 alebo Ubc5 a katalyzuje K63-polyubikvitináciu TBK1 a IKKi. Tieto signalizačné molekuly následne spoločne s IKKγ aktivujú IRF3 alebo IRF7, ktoré sú v podobe homodimérov alebo heterodimérov translokované do jadra, kde regulujú expresiu génov IFN typu I alebo indukovateľných IFN (Xie 2013; Ullah et al. 2016).

1.2.2 RLR

Tzv. retinoic acid-inducible gene-I (RIG-I)-like receptors (RLR) predstavujú skupinu RNA helikáz dôležitých pre detekciu vírusových a bakteriálnych nukleových kyselín (Newton and Dixit 2012). Tieto cytosólické receptory obsahujú na N-konci dve tzv. caspase activation and recruitment domains (CARD), v centrálnej časti DExD/Hbox helikázovú doménu a na C-konci tzv. carboxy-terminal domain (CTD) vyväzujúcu

dsRNA (Pandey et al. 2015). Medzi zástupcov RLR patrí RIG-I (známy aj ako DDX58) rozlišujúci krátke úseky dsRNA (do 1 kb) obsahujúce na konci 5´trifosfát. Tieto ligandy pochádzajú najčastejšie z vírusov alebo vznikajú prepisom mikrobiálnej dsDNA bohatej na AT-oblasti pomocou tzv. cytosolic DNA sensor (CDS) RNA polymerázy III (RNA Pol III) (Takeuchi and Akira 2010; Newton and Dixit 2012; Dempsey and Bowie 2015). Za detekciu dlhých úsekov dsRNA (viac ako 2 kb) zodpovedá tzv. melanoma differentiation-associated protein 5 (MDA5) (Takeuchi and Akira 2010). Tzv. laboratory of genetics and physiology 2 (LGP2) postráda CARD doménu a slúži skôr ako regulátor signalizácie riadenej RIG-I a MDA5 **(Tab. 1-3)** (Takeuchi and Akira 2010; Pandey et al. 2015).

Tab. 1-3: RLR a ich ligandy

RLR	Ligand	Pôvod ligandu
LGP2	Neznámy	RNA vírusy
MDA5	Dlhé úseky dsRNA	RNA vírusy
RIG-I	Krátke úseky dsRNA obsahujúce 5´trifosfát	Baktérie, DNA a RNA vírusy

Prevzaté a upravené z: (Takeuchi and Akira 2010; Pandey et al. 2015).

1.2.2.1 Signalizácia riadená RLR

Po rozlíšení dsRNA podliehajú senzory RIG-I a MDA-5 konformačnej zmene, ktorá im umožňuje defosforylovať ich CARD domény pomocou PP1α fosfatázy **(Obr. 1-3)**. RIG-I je v tejto a CTD doméne polyubikvitinovaný E3 ubikvitín-ligázami TRIM25 a RIPLET (známy aj ako RNF135), čo umožňuje interakciu s tzv. IFN-β promoter stimulator 1 (IPS1; známy aj ako MAVS; VISA alebo CARDIF). Tento adaptorový proteín je lokalizovaný na mitochondriách, membránach asociovaných s mitochondriami alebo peroxizómoch. Po oligomerizácii formuje IPS1 spolu s TRAF, TBK1, IKKi alebo IKKα-IKKβ-IKKγ komplexy, ktoré aktivujú transkripčné faktory IRF3, IRF7, NF-κB alebo AP-1 a produkciu prozápalovej ako aj IFN odpovede typu I (Loo and Gale 2011; Chan and Gack 2016; Hu and Sun 2016).

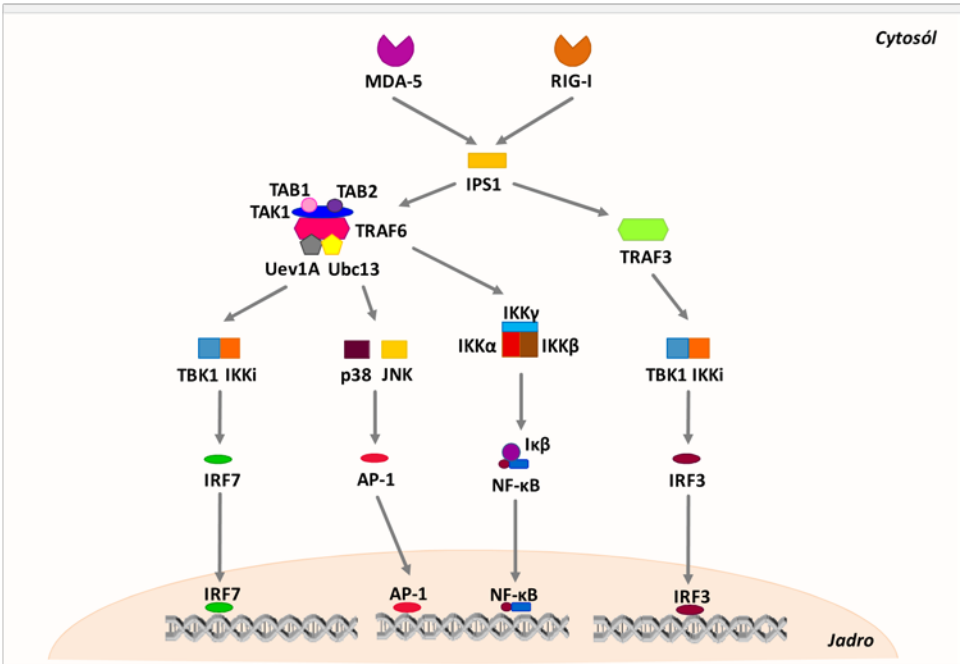

Obr. 1-3: RLR a ich signalizačné dráhy. Po rozlíšení ligandu MDA-5 alebo RIG-I dochádza k aktivácii adaptorového proteínu IPS1 a indukcii prozápalovej alebo IFN odpovede typu I. Prevzaté a upravené z: (Xie 2013; Hu and Sun 2016).

1.2.3 NLR

Ďalšiu rozsiahlu rodinu cytoplazmatických PRR tvoria tzv. nucleotide-binding oligomerization domain (NOD)-like receptors (NLR), ktoré sú u ľudí zastúpené až 22 členmi (Chan and Gack 2016). Tieto senzory pozostávajú z C-terminálnej LRR a centrálnej NOD domény. Okrem toho obsahujú na N-konci aj variabilnú interakčnú doménu, ktorá sa vyskytuje v štyroch formách a je použitá pre klasifikáciu NLR do týchto podrodín: tzv. acidic transactivation domain (NLRA), tzv. baculoviral inhibitory repeat-like domain (NLRB), CARD (NLRC) a tzv. pyrin domain (PYD) (NLRP) **(Tab. 1-4)**. Na základe funkcie NLR je možné túto rodinu rozdeliť aj na receptory účastniace sa tvorby inflamazómu, signálnej transdukcie, transkripčnej aktivácie a autofágie (Kim et al. 2016). Významných zástupcov zodpovedných za detekciu muramyl dipeptidu (MDP) predstavujú NOD2 a NLRP1. NOD1 rozlišuje kyselinu meso-diaminopimelovú (DAP), tzv. NLR family CARD domain containing protein 4 (NLRC4) je zodpovedný za rozpoznanie flagelínu a NLRP3 za RNA vírusového ako aj bakteriálneho pôvodu (Franchi et al. 2009; Takeuchi and Akira 2010).

Tab. 1-4: NLR a ich ligandy

NLR	Podrodina	Ligand	Pôvod ligandu
CIITA	NLRA	-	-
NAIP5	NLRB	Flagelín	Baktérie
NOD1	NLRC	DAP	Baktérie
NOD2		MDP, ssRNA s 5-PPP	Baktérie, RNA vírusy
NLRC4		Flagelín	Baktérie
NLRP1	NLRP	MDP	Baktérie
NLRP3		LPS, MDP, RNA	Baktérie, RNA vírusy

Prevzaté a upravené z: (Franchi et al. 2009; Takeuchi and Akira 2010; Moreira and Zamboni 2012).

1.2.3.1 Signalizácia riadená NLR

U zástupcov podrodiny NLRC, NOD1 a NOD2, dochádza po rozlíšení PAMPs k ich oligomerizácii a následnej CARD-CARD doménovej interakcii s RIP2 (známy aj ako RICK) **(Obr. 1-4)**. Nastáva sformovanie signalizačného komplexu pozostávajúceho z TRAF2, TRAF5, TRAF6 a Ubc13/Uev1A, ktorý umožňuje K63-polyubikvitináciu tohto adaptorového proteínu. Regulácia NF-κB je následne sprostredkovaná aktiváciou komplexu TAK1. Mechanizmus spúšťania IFN odpovede typu I je medzi týmito senzormi odlišný. NOD1 stimuluje signalizačnú dráhu zahrňujúcu TRAF3-TBK1-IKKiIRF7 prostredníctvom RIP2, avšak v prípade aktivácie NOD2 ssRNA je prítomný IPS1 (Newton and Dixit 2012; Xie 2013; Kim et al. 2016).

Po aktivácii členov rodiny NLRB (NAIP), NLRC (NLRC4) alebo NLRP (NLRP1, NLRP2, NLRP3, NLRP6, NLRP7 a NLRP12) dochádza ku tvorbe mnohoproteínového signalizačného komplexu tzv. inflamazómu (Kim et al. 2016). Tento celok pozostáva zvyčajne z príslušného receptoru, adaptorového proteínu tzv. apoptosis-associated speck-like protein containing CARD (ASC) a prozápalovej kaspázy-1. V priebehu vzniku inflamazómu dochádza k PYD-PYD doménovej interakcii NLR s ASC, na ktorý sa následne vyväzuje pro-kaspáza-1 pomocou domény CARD. Táto cysteínová proteáza je podrobená aktivácii autoproteolytickým štiepením na 2 aktívne podjednotky p20 a p10, ktoré zodpovedajú za reguláciu sekrécie prozápalových cytokínov IL-1β a IL-18 ako aj indukciu naprogramovanej bunkovej smrti nazývanej pyroptóza (Franchi et al. 2009; Kim et al. 2016; Sharma and Kanneganti 2016).

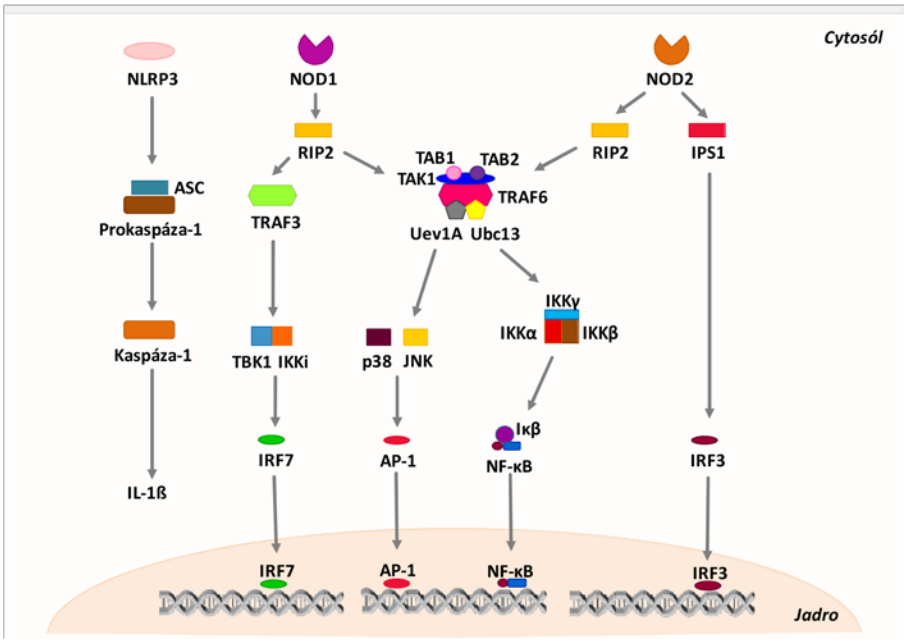

Obr. 1-4: NLR a ich signalizačné dráhy. Po rozlíšení ligandu NOD1 alebo NOD2 dochádza k aktivácii adaptorového proteínu RIP2 alebo IPS1 a indukcii prozápalovej alebo IFN odpovede typu I. Prevzaté a upravené z: (Xie 2013).

1.2.4 CDS

Za detekciu mikrobiálnej alebo priamo hostiteľskej DNA zodpovedá okrem TLR9 celá rada CDS **(Tab. 1-5)**. Medzi významných zástupcov tejto rodiny patria tzv. DNA-dependent activator of IRFs (DAI; známy aj ako ZBP-1), tzv. LRR Binding FLII Interacting Protein 1 (LRRFIP1), tzv. meiotic recombination 11 (MRE11) alebo tzv. DExD/H box helikázy (DDX41, DHX9 a DHX36) (Pandey et al. 2015). Jedným z kľúčových receptorov je aj tzv. cyclic GMP-AMP (cGAMP) synthase (cGAS; známa aj ako MB21D1), ktorá je zodpovedná za detekciu okrem dsDNA aj ssDNA, jej vlásenkových foriem ako aj hybridov DNA:RNA (Tao et al. 2016). Po rozlíšení cytosólickej DNA cGAS katalyzuje cyklizáciu ATP a GTP za vzniku 2'3'-cGAMP, ktorý zohráva dôležitú úlohu pri aktivácii tzv. stimulator of IFN genes (STING; známy aj ako MITA, ERIS, MPYS alebo TMEM173) (Takeuchi and Akira 2010; Dempsey and Bowie 2015; Marinho et al. 2017). Tento transmembránový proteín je zodpovedný za priamu detekciu cyklických dinukleotidov, ale okrem toho funguje aj ako adaptorový proteín mnohých DNA senzorov (Burdette et al. 2011). Taktiež sa predpokladá, že sa STING účastní signalizačných procesov aktivovaných pomocou RNA, avšak presný mechanizmus jeho pôsobenia nie je zatiaľ známy (Liu et al. 2017). Pomerne nedávno bola

objasnená aj úloha tzv. IFN-γ inducible protein 16 (IFI16; u myší nazývaného p204). Tento cytosólický a nukleárny proteín je zodpovedný za rozpoznanie vírusovej ako aj bakteriálnej ssDNA a dsDNA (Jønsson et al. 2017). Predpokladá sa, že v cytosóle IFI16 predstavuje dôležitého spoluhráča cGAS pri produkcii cGAMP a následnej aktivácii STING (Jønsson et al. 2017). V jadre rozlišuje IFI16 epizomálnu dsDNA a vedie ku spusteniu cytosólického inflamazómu (Marinho et al. 2017). Spoločne s DNA senzorom tzv. absent in melanoma 2 (AIM2) patrí do rodiny tzv. PYHIN proteínov, ktoré sú zároveň radené medzi tzv. AIM2-like receptors (Unterholzner et al. 2010). Tieto proteíny obsahujú C-terminálnu doménu tzv. hematopoetic interferoninducible nuclear proteins with a 200-amino-acid repeat (HIN200) prostredníctvom ktorej rozlišujú DNA. Na N-konci obsahujú ALRs tzv. PYD doménu zabezpečujúcu proteín-proteínové interakcie (Xiao 2015).

Tab. 1-5: CDS a ich ligandy

CDS	Ligand	Pôvod ligandu
AIM2	dsDNA	Baktérie, DNA vírusy, vlastné
cGAS	ssDNA, dsDNA, Y-forma DNA, hybrid DNA:RNA	Baktérie, DNA a RNA vírusy, vlastné
DAI	dsDNA	DNA vírusy
DDX41	dsDNA, c-di-AMP, c-di-GMP	DNA vírusy
DHX9	CpG-B DNA	DNA vírusy
DHX36	CpG-A DNA	DNA vírusy
IFI16	ssDNA, dsDNA	Baktérie, DNA a RNA vírusy
LRRFIP1	dsDNA, dsRNA	Baktérie, RNA vírusy
MRE11	dsDNA	Vlastné
RNA Pol III	dsDNA bohatá na AT-oblasti	DNA vírusy
STING	c-di-AMP, c-di-GMP, 3'3'-cGAMP 2'3'-cGAMP	Baktérie Vlastné

Prevzaté a upravené z: (Peng et al. 2011; Atianand and Fitzgerald 2013; Pandey et al. 2015; Xiao 2015; Tao et al. 2016).

1.2.4.1 Signalizácia riadená CDS

V prípade signalizácie sprostredkovanej cytosólickými DNA senzormi cGAS, IFI16, DAI, MRE11 alebo DDX41 je dôležitým interakčným partnerom STING **(Obr. 1-5)**. Po obdržaní signálu migruje tento adaptorový proteín z endoplazmatického retikula do perinukleárnych mikrozomálnych útvarov. V priebehu tohto presunu vytvára spoločne s TBK1 signalizačný komplex zodpovedný za aktiváciu transkripčných faktorov NF-κB alebo IRF3 a následnú produkciu prozápalovej alebo IFN odpovede typu I (Abe and Barber 2014; Jønsson et al. 2017; Sokolowska and Nowis 2018).

Receptory DHX9 alebo DHX36 využívajú pre prenos signálu adaptorový proteín MyD88 podieľajúci sa na aktivácii transkripčných faktorov IRF7 alebo NF-κB (Atianand and Fitzgerald 2013). Aktivácia LRRFIPI vedie k fosforylácii β-katenínu, ktorý je následne translokovaný do jadra, kde sa viaže na IRF3. Tento krok má za následok zvýšené vyviazanie acetyltransferázy p300 zodpovednej za nárast transkripcie génu *Ifnb1* (Yang et al. 2010).

AIM2 spoločne s nukleárnym IFI16 podliehajú po rozlíšení DNA oligomerizácii a PYD-PYD doménovej interakcii s ASC. Ich aktivácia vedie obdobne ako u niektorých zástupcov rodiny NLR k formácii inflamazómu spojenou s produkciou IL-1β a IL-18 (Kerur et al. 2011; Xiao 2015).

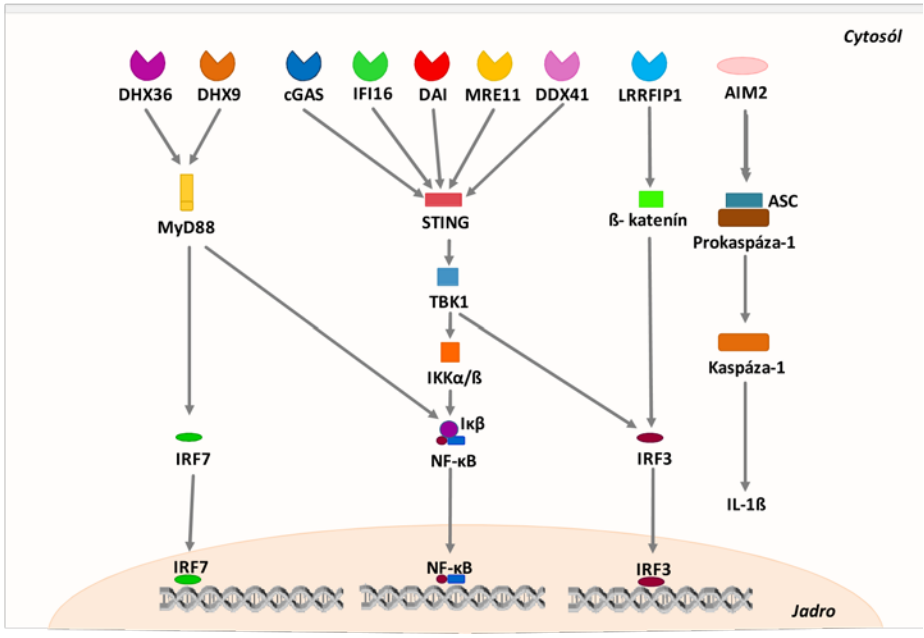

Obr. 1-5: CDS a ich signalizačné dráhy. Po rozlíšení DNA cytosólickými DNA senzormi dochádza k aktivácii príslušných adaptorových proteínov a indukcii prozápalovej alebo IFN odpovede typu I. Prevzaté a upravené z: (Pandey et al. 2015; Dempsey and Bowie 2015).

1.3 Modulácia zápalovej odpovede *F. tularensis*

F. tularensis ako aj iné invadujúce intracelulárne patogény čelí v priebehu svojho života celej rade obranných mechanizmov hostiteľskej imunity. Modulácia antimikrobiálnej odpovede proti *F. tularensis* začína už v mieste infekcie, kde baktéria vzdoruje pôsobeniu komplementu, protilátok alebo antimikrobiálnych peptidov. Jej následný vstup do hostiteľskej bunky je aj preto považovaný za jeden z možných mechanizmov obídenia extracelulárnej obrany.

V priebehu jednotlivých fáz intracelulárneho života zdoláva *F. tularensis* mnohé prekážky. Na úrovni bunkového povrchu, fagozómu alebo v cytosóle prichádza do kontaktu s rôznymi zástupcami PRR hrajúcimi dôležitú úlohu v aktivácii hostiteľskej obrany, ako aj zápalovej odpovede. Obídenie alebo manipulácia týchto procesov v skorej fáze infekcie predstavuje jednu z najdôležitejších vlastností úspešného patogéna (Bosio 2011; Jones et al. 2012a).

1.3.1 Interakcia s povrchovými TLR

F. tularensis si v priebehu evolúcie vyvinula celú radu mechanizmov, ktoré jej umožňujú vyhnúť sa alebo rozvrátiť priebeh vrodenej imunitnej odpovede. Jedným z nich je aj schopnosť baktérie obísť aktiváciu bunkovej signalizácie sprostredkovanej TLR4. Zástupcovia čeľade *Francisellaceae* patria medzi gram-negatívne baktérie známe prítomnosťou LPS v ich vonkajšej membráne (Wallet et al. 2016). Tento ligand predstavuje významného agonistu TLR4, ale v prípade *F. tularensis* má nízky stimulačný charakter (Ancuta et al. 1996; Hajjar et al. 2006; Okan and Kasper 2013). Pre optimálnu aktiváciu tohto senzora je totižto vyžadovaná prítomnosť hexaacylovaného lipidu A s reťazcami dlhými 12 až 14 uhlíkov a 2 fosfátových skupín v polohe 1' a 4' (Phillips et al. 2004). V prípade *F. tularensis* sú ale prítomné len 4 acylové (14 až 18 uhlíkov dlhé) a jedna fosfátová skupina, ktorá je navyše modifikovaná galaktozamínom (Jones et al. 2012a; Okan and Kasper 2013).

Za prvoradý senzor TLR účastniaci sa aktivácie zápalovej odpovede počas infekcie *F. tularensis* je považovaný receptor TLR2 (Abplanalp et al. 2009). Po rozlíšení bakteriálnych povrchových lipoproteínov, ako napríklad Tul4 a FTT_1103, dochádza k jej endocytóze a stimulácii adaptorového proteínu MyD88 a následnej NFκB-dependentnej prozápalovej odpovede **(Obr. 1-6)** (Katz et al. 2006; Cole et al. 2007;

Thakran et al. 2008). Avšak napriek predpokladanej biologickej dostupnosti oboch týchto agonistov, *F. tularensis* nestimuluje v infikovaných bunkách silnú prozápalovú odpoveď (Bosio 2011). Jedným z možných vysvetlení je relatívne nízka schopnosť týchto ligandov aktivovať TLR2 ich zamaskovaním prítomnou kapsulou alebo reguláciou ich produkcie pomocou systému CRISPR/Cas, či špecifických proteínov (Zarrella et al. 2011; Jones et al. 2012b; Sampson et al. 2013).

Taktiež bolo preukázané, že *F. tularensis* nielenže masívne uniká detekčným systémom hostiteľa, ale je schopná aj aktívne inhibovať priebeh bunkovej signalizácie regulovanej PRR, vrátane TLR (Telepnev et al. 2003, 2005; Bosio et al. 2007; Butchar et al. 2008; Crane et al. 2013). Nedávne štúdie ukázali, že lipidy pochádzajúce z virulentnej *F. tularensis*, ale nie z *F. novicida*, zodpovedajú za útlm následnej aktivácie prozápalovej odpovede agonistami TLR (Ireland et al. 2013; Crane et al. 2013). Okrem toho bol popísaný aj inhibičný charakter bakteriálneho proteínu FTT_0831c na translokáciu NF-kB podjednotky p65 do jadra (Mahawar et al. 2012). Navyše, fagocytóza opsonizovanej *F. tularensis* C3 zložkou komplementu viedla k potlačeniu TLR2-dependentnej aktivácie MAPKs a NF-κB (Dai et al. 2013). V priebehu infekcie *F. tularensis* dochádzalo aj ku stimulácii fosfatázy SHIP, ktorá negatívne regulovala PI3K/Akt - signalizačnú dráhu, a tým aj aktiváciu NF-κB (Parsa et al. 2006).

1.3.2 Cytosólická obrana zapojená v boji proti *F. tularensis*

Hostiteľské obranné mechanizmy proti invadujúcim patogénom nie sú sústredené len na povrchu bunky alebo vo fagozóme. Po úniku do cytosólu čelí *F. tularensis* celej rade intracelulárnych PRR, ktorých hlavným cieľom je zabrániť bakteriálnej replikácii a spustiť účinnú imunitnú odpoveď **(Obr. 1-6)**. *Francisella* je v tomto prostredí rozlišovaná cytosólickými DNA senzormi cGAS a Ifi204, ktoré využívajú pre prenos signálu STING. Tento adaptorový proteín sa podieľa na aktivácii transkripčného faktora IRF3 a následnej produkcii IFN typu I (Henry et al. 2007; Jin et al. 2011; Storek et al. 2015; Wallet et al. 2016). Pôvod bakteriálnej DNA spúšťajúcej túto odpoveď nie je zatiaľ objasnený. Predpokladá sa, že sa môže uvoľňovať z poškodených fagozómov po úteku *F. tularensis* do cytosólu alebo dochádza ku zvýšeniu jej množstva počas bakteriálnej replikácie (Jones et al. 2012a).

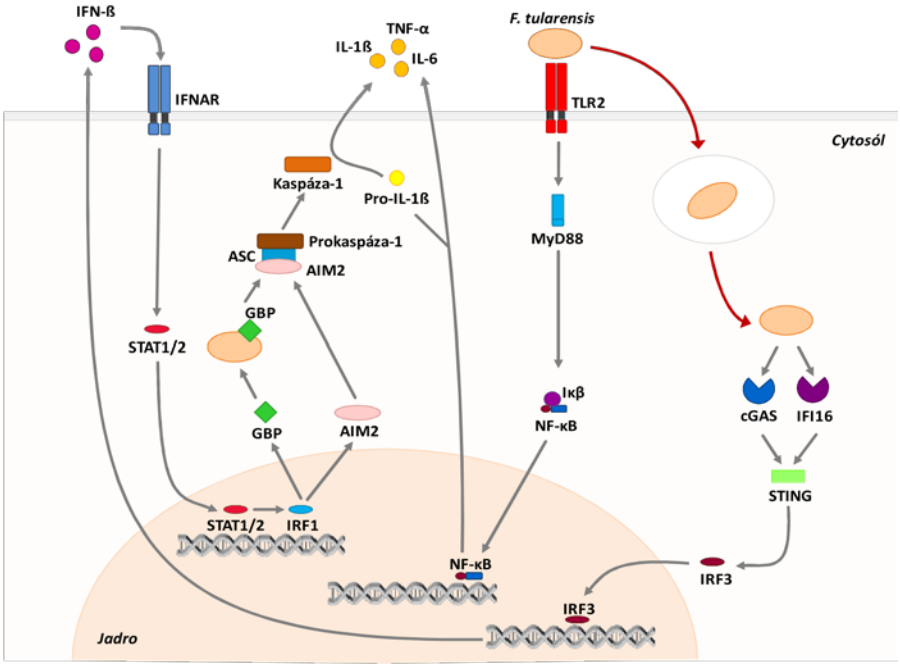

Obr. 1-6: Bunková signalizácia riadená PRR v priebehu infekcie *F. tularensis*. Stimulácia povrchového TLR2 *F. tularensis* vedie k indukcii NF-κB-dependentnej prozápalovej odpovede. Po rozlíšení bakteriálnej DNA cGAS a IFI16 dochádza k expresii IFN-ß, ktorá umocňuje aktiváciu AIM2 inflamazómu vedúceho ku produkcii IL-1ß. Prevzaté a upravené z: (Jones et al. 2011; Man et al. 2016).

Autokrínna alebo parakrínna signalizácia IFN typu I cez transmembránový receptor IFNAR vedie následne k fosforylácii tzv. signal transducer and activator of transcription 1 (STAT1) a STAT2. Tie sú v podobe heterodiméru translokované do jadra, kde spoločne s IRF9 vytvárajú komplex tzv. IFN-stimulated gene (ISG) factor 3 (ISGF3) regulujúci transkripciu ISG (McNab et al. 2015; Man et al. 2016). Medzi dôležité ISG exprimované v priebehu infekcie *F. tularensis* patria transkripčný faktor IRF1 a cytosólický DNA senzor AIM2. IRF1 je dôležitý z pohľadu regulácie expresie tzv. guanylate-binding protein 2 (GBP2), GBP5 a tzv. immunity related GTPase family member b10 (IRGB10). Tieto GTPázy zodpovedajú za bakteriálnu lýzu a s tým spojený nárast PAMPs v cytosóle (Man et al. 2015, 2016; Meunier et al. 2015). AIM2 zabezpečuje detekciu uvoľnenej DNA a vedie k aktivácii inflamazómu umožňujúceho sekréciu IL-1ß a IL-18, ako aj indukciu pyroptózy (Fernandes-Alnemri et al. 2010; Rathinam et al. 2010; Jones et al. 2010). Prozápalová funkcia tohto signalizačného komplexu je spojená so stimuláciou TLR2-závislej expresie pro-IL-1ß a pro-IL-18, indukcie IFN odpovede typu I, ako aj fagozomálneho úteku *F. tularensis* do cytósolu (Jones et al. 2011; Wallet et al. 2016).

Avšak napriek tomu, že AIM2 inflamazóm predstavuje kľúčový receptor vrodenej imunitnej anti-tularemickej obrany, virulentné kmene *F. tularensis* ho nestimulujú vo veľkej miere (Wallet et al. 2016). Jeho účinná aktivácia môže byť ovplyvnená schopnosťou baktérie potlačovať priebeh bunkovej signalizácie regulovanej TLR (pozri vyššie) alebo IFNAR (Jones et al. 2012a). Ako príklad je možné uviesť zvýšenú expresiu tzv. suppressor of cytokine signaling 3 (SOCS3) v priebehu infekcie, ktorý je zodpovedný za inhibíciu fosforylácie STAT1 (Parsa et al. 2008). Taktiež bol preukázaný inhibičný charakter lipidov pochádzajúcich z *F. tularensis* na translokáciu transkripčného faktora IRF1 do jadra (Ireland et al. 2013). Navyše bola v nedávnej štúdii popísaná aj obmedzená aktivácia kaspázy-1 a následnej produkcie IL-18 vplyvom fagocytózy *F. tularensis* cez CR3 (Hoang et al. 2018). Ďalším vysvetlením zníženej aktivácie AIM2 inflamazómu môže byť aj schopnosť zachovania štrukturálnej integrity baktérie, ktorá zabraňuje uvoľňovaniu PAMPs a následnej indukcii inflamazómu (Peng et al. 2011; Jones et al. 2012a; Crane et al. 2014).

2 Ciele práce

V tejto dizertačnej práci boli stanovené nasledujúce ciele:

- charakterizovať priebeh vrodenej imunitnej odpovede regulovanej PRR počas infekcie makrofágov *F. tularensis* subsp. *holarctica* LVS
- stanoviť rozdiely v stimulácii makrofágov infikovaných plne virulentným a atenuovanými kmeňmi *F. tularensis* subsp. *holarctica* LVS
- objasniť signalizačné deje spojené s moduláciou zápalovej odpovede virulentným kmeňom

3 Experimentálna časť

3.1 Materiál

3.1.1 Chemikálie

Aminokyseliny (pre prípravu Chamberlainovho média)	Sigma-Aldrich, USA		
ß-Merkaptoetanol	Serva, Nemecko		
Brain Heart Infusion médium/ agar	Becton Dickinson, USA		
Bromfenolová modrá	Sigma-Aldrich, USA		
BSA	Sigma-Aldrich, USA	c-di-GMP	InvivoGen, USA
DAPI	Invitrogen, Thermo Fisher Scientific, USA		
Difco GC medium báze	Becton Dickinson, USA		
DTT	Bio-Rad, USA		
EDTA	Sigma-Aldrich, USA	$FeSO_4.7H_2O$	Sigma-Aldrich, USA
Gentamycín	Sigma-Aldrich, USA	Glukóza	Sigma-Aldrich, USA
Glycerol	Sigma-Aldrich, USA		
Glycín	Sigma-Aldrich, USA		
Hemoglobín, hovädzí	Becton Dickinson, USA	IsoVitalex™	Becton Dickinson, USA
KH_2PO_4	Sigma-Aldrich, USA		
K_2HPO_4	Sigma-Aldrich, USA	LPS	InvivoGen, USA
L-tiamín-HCl	Sigma-Aldrich, USA	LyoVec™	InvivoGen, USA
Metanol	Sigma-Aldrich, USA	$MgSO_4.7H_2O$	Sigma-Aldrich, USA
Mlieko, odtučnené, sušené	Bio-Rad, USA		
Močovina	Sigma-Aldrich, USA	NaCl	Sigma-Aldrich, USA
NaF	Sigma-Aldrich, USA		
NaOH	Sigma-Aldrich, USA		

N-etylmaleimid	Sigma-Aldrich, USA
NH_4Cl	Sigma-Aldrich, USA NP-40 Sigma-Aldrich, USA
Oligo $(dT)_{12-18}$	Invitrogen, Thermo Fisher Scientific,USA
Ortovanadečnan sodný	Sigma-Aldrich, USA Pam_3CSK_4 InvivoGen, USA
Pantotenát vápenatý	Sigma-Aldrich, USA
PBS	Sigma-Aldrich, USA
Paraformaldehyd	Sigma-Aldrich, USA Penicilín Sigma-Aldrich, USA
PMSF	Roche, Švajčiarsko
Pyrofosfát sodný	Sigma-Aldrich, USA
SDS	Sigma-Aldrich, USA
Spermíntetrahydrochlorid	Sigma-Aldrich, USA Streptomycín Sigma-Aldrich, USA
Tris-base	Sigma-Aldrich, USA
Tris-HCl pufer; 1,5 M; pH 8,8	Bio-Rad, USA
Triton X-100	Amersham, Veľká Británia
Tween 20	Sigma-Aldrich, USA

3.1.2 Komerčné kity

CytoTox-ONE™ Homogenous Membrane Integrity Assay	Promega, USA
ECL Western Blotting Detection Kit	Thermo Fisher Scientific, USA
ELISA kit (myšací; TNF-α, IL-6)	R&D Systems, USA
Luciferase AssaySystem	Promega, USA
Protease Inhibitor Cocktail	Roche, Švajčiarsko
RNeasy Mini Kit	Qiagen, Nemecko
TaqMan™ Universal PCR Master Mix	Applied Biosystems, Thermo Fisher Scientific, USA

3.1.3 Enzýmy

Benzonase® Nuclease	Sigma-Aldrich, USA
Dnáza I	New England Biolabs, USA

3.1.4 Primery

FAM-značené Taqman™ primery *Ifnb1* (Mm00439552_s1), *Ifnα4* (Mm00833969_s1), *Il1b* (Mm00434228_m1), *Rn18s* (Mm03928990_g1) a *Tnfα* (Mm00443258_m1) boli objednané od firmy Applied Biosystems, Thermo Fisher Scientific, USA.

3.1.5 Protilátky

AlexaFluor™ 488 kozí anti-králičí IgG	Becton Dickinson, USA
Anti-IKKα/ß	Cell Signaling Technology, Holandsko
Anti-IRF3	Cell Signaling Technology, Holandsko
Anti-K48-polyubikvitínovým reťazcom	Genentech, USA
Anti-K63-polyubikvitínovým reťazcom	Cell Signaling Technology, Holandsko
Anti-p38	Cell Signaling Technology, Holandsko
Anti-p-IKKα/ß	Cell Signaling Technology, Holandsko
Anti-p-IRF3	Cell Signaling Technology, Holandsko
Anti-p-p38	Cell Signaling Technology, Holandsko
Anti-TAB2	Santa Cruz Biotechnology, USA
Anti-TAB3	Santa Cruz Biotechnology, USA
Anti-TAK1	Cell Signaling Technology, Holandsko
Anti-TBK1	Abcam, Veľká Británia

Anti-TRAF3 Santa Cruz Biotechnology, USA

Anti-TRAF6 Santa Cruz Biotechnology, USA Anti-α-tubulín Abcam, Veľká Británia

HRP-konjugovaný kozí anti-králičí IgG Santa Cruz Biotechnology, USA HRP-konjugovaný kozí anti-myšací IgG Santa Cruz Biotechnology, USA

3.2 Kultivačné médiá

3.2.1 Bakteriálne kultivačné médiá

Brain Heart Infusion médium/ agar

Brain Heart Infusion (BHI) médium (37 g) alebo BHI agar (52 g) boli pripravené rozpustením navážky v 1 l deionizovanej H_2O a následne sterilizované autoklávovaním (121 °C, 15 min).

Kompletné Chamberlainovo médium

Roztok 1

L-arginín-HCl (0,8 g)
L-cysteín-HCl (0,4 g)
L-histidín-HCl (0,4 g)
L-izoleucín (0,8 g)
L-leucín (0,8 g)
L-lyzín-HCl (0,8 g)
DL-prolín (4 g)
DL-serín (0,8 g)
DL-treonín (4 g)
DL-valín (0,8 g)
DL-metionín (0,8 g)

Roztok 2

Glukóza (8 g)

Roztok 3

NaCl (20 g)
KH_2PO_4 (2 g)
K_2HPO_4 (2 g)

Roztok 4

L-kyselina asparágová (0,8 g)
L-tyrozín (0,8 g)

Doplnok roztoku 1

L-tiamín-HCl (0,02 g/10 ml, 4 ml roztoku pridané do 2 l média)
Spermín tetrahydrochlorid (0,08 g/10 ml, 10 ml roztoku pridané do 2 l média)

Pantotenát vápenatý (0,01 g/10 ml, 4 ml roztoku pridané do 2 l média)

Doplnok roztoku 2

$MgSO_4.7H_2O$ (0,675 g/10 ml, 4 ml roztoku pridané do 2 l média)
$FeSO_4.7H_2O$ (0,01 g/10 ml, 4 ml roztoku pridané do 2 l média)

Médium bolo pripravené podľa Chamberlaina (Chamberlain 1965). Navážky chemikálií jednotlivých roztokov boli rozpustené v 0,2 l deionizovanej H_2O, pričom roztok 4 bol pripravený za pridávania 3 M NaOH. V ďalšom kroku boli roztoky postupne zmiešané a pH média bolo upravené na 6,3. Objem bol doplnený na 2 l a médium bolo prefiltrované cez jednorazový 0,22 μm filter.

McLeod agar

Pracovný roztok I	Pracovný roztok II
Difco GC medium base (72 g)	Hovädzí hemoglobín (20 g)

Navážky chemikálií jednotlivých roztokov boli rozpustené v 1 l deionizovanej H_2O a zmiešané v pomere 1:1. Po následnej sterilizácii autoklávovaním (121 °C, 20 min) a vychladnutí na 50 °C bol pridaný IsoVitalex™ (20 ml).

3.2.2 Bunkové kultivačné médiá

Bunkové kultivačné médium obsahovalo Iscove's Modified Dulbecco's Medium (IMDM) (Gibco, Thermo Fisher Scientific, USA), 10% tepelne inaktivované fetálne hovädzie sérum (FBS) (Gibco, Thermo Fisher Scientific, USA) a 100 U/ml penicilínu (Sigma-Aldrich, USA) a 100 g/ml streptomycínu (Sigma-Aldrich, USA). V prípade kultivácie infikovaných buniek vírusmi bolo využité médium Opti-MEM (Gibco, Thermo Fisher Scientific, USA).

3.3 Bakteriálne a vírusové kultúry

3.3.1 Kmene a podmienky kultivácie

Bakteriálne a vírusové kmene použité v tejto práci sú uvedené v **Tab. 3-1**. Atenuovaný vakcinačný kmeň *F. tularensis* LVS a jej mutantné kmene *ΔdsbA*/LVS a *ΔiglC*/LVS boli kultivované na McLeod agarových miskách obohatených o hovädzí hemoglobín a IsoVitalex™ alebo v kompletnom Chamberlainovom médiu pri 37 °C a 5 % CO_2. Kmene *L. monocytogenes* rástli pri rovnakých podmienkach ako *F. tularensis* LVS, ale na BHI agarových miskách alebo v BHI médiu. Všetky bakteriálne kmene boli inkubované do OD_{600} = 0,4. Kultivácia VSV-AV2 bola popísaná v práci Stojdla et al. (Stojdl et al. 2003).

Tab. 3-1:Použité bakteriálne a vírusové kmene

Baktérie/Vírusy	Kmene	Zdroj/ Referencia
F. tularensis	subsp. *holarctica*; Live Vaccine Strain; LVS; ATCC29684	Americká zbierka typov kultúr, Rockville, MD, USA
	ΔdsbA/LVS	(Straskova et al. 2009)
	ΔiglC/LVS	(Golovliov et al. 2003)
L. monocytogenes	EGD-e	(Bron et al. 2006)
	EGD-e::pPL2/ *lux* pHELP	(Bron et al. 2006)
	EGD-e-cGFP	(Fortinea et al. 2000)
VSV	VSV-AV2	(Stojdl et al. 2003)

3.3.2 Spôsoby zabitia *F. tularensis* LVS

Bakteriálna suspenzia *F. tularensis* LVS bola podrobená lýze sonikáciou (8 x 15 s, stupeň 4), tepelnej inaktivácii pri 95 °C počas 10 min alebo zabitiu pôsobením UV-žiarenia (cez noc). Okrem toho bola sonikovaná baktéria taktiež ošetrená 2,5 U/µl Benzonase® Nuclease pri 37 °C počas 45 min alebo bola tepelne inaktivovaná pri 95 °C počas 10 min. Miera úspešnosti zabitia baktérie bola overená stanovením CFU po vysiatí bakteriálneho lyzátu na McLeod agarové misky.

3.4 Použité bunky

Makrofágy odvodené z buniek kostnej drene (bone marrow-derived macrophages - BMDMs) boli izolované zo stehennej a holennej kosti 6 až 8 týždnov starých myší. Jednalo sa o inbredný kmeň C57BL/6J: *Ifnb*$^{+/\beta luc}$, *Ips1*$^{-/-}$*Ifnb*$^{+/\beta luc}$, *Myd88*$^{-/}$*Ifnb*$^{+/\beta luc}$, *Sting*$^{-/-}$*Ifnb*$^{+/\beta luc}$, *Ticam1*$^{-/-}$*Ifnb*$^{+/\beta luc}$, *Ticam*$^{-/-}$*Ips1*$^{-/-}$ a *Ips1*$^{-/-}$, ktoré boli pripravené v Umeå Transgene Core Facility. Pôvodné myšacie kmene boli poskytnuté: *Ifnb*$^{+/\beta luc}$ (Lienenklaus et al. 2009) pánom S.Weissom, *Sting*$^{-/-}$ (C57BL/6J-Tmem173gt/J) (Sauer et al. 2011) a *Ticam1*$^{-/-}$ (C57BL/6J-Ticam1Lps2/J) (Hoebe et al. 2003) Jacksonovým laboratóriom a *Myd88*$^{-/-}$ (Adachi et al. 1998) a *Ips1*$^{-/-}$ pánom S. Akirom.

3.5 Roztoky a pufry

3.5.1 Izolácia BMDMs

RBC lyzačný pufer (10x), pH 7,3

EDTA	1 mM
$NaHCO_3$	142 mM
NH_4Cl	1,55 M

3.5.2 Imunofluorescenčné farbenie

Blokovací pufer

BSA	3%
PBS	100 ml

Permeabilizačný pufer

Triton X-100	0,2%
PBS	100 ml

3.5.3 Imunoprecipitácia

Lyzačný pufer

Koktail inhibítorov proteáz	1 x

NaCl	150 mM
NaF	1 mM
NP-40	1%
Ortovanadečnan sodný	1 mM
PMSF	2 mM
Pyrofosfát sodný	10 mM Tris-HCl;
pH 7,5	50 mM

TDS pufer

DTT	5 mM
SDS	1%
Tris-HCl; pH 7,5	50 mM

TNN pufer

EDTA	5 mM
NaCl	250 mM
NP 40	0,5%
Tris-HCl; pH 7,5	50 mM

Ubikvitinačný lyzačný pufer

EDTA	5 mM
Koktail inhibítorov proteáz	1 x
Močovina	8 M
NaCl	25 mM
N-etylmaleimid	2 mM
Tris-HCl; pH 7,5	50 mM

3.5.4 SDS-PAGE

Tris-glycínový pufer, pH 8,5

Glycín	384 mM

SDS	0,1%
Tris-base	50 mM

Vzorkový pufer pre SDS-PAGE (2x koncentrovaný)

Bromfenolová modrá (0,5%)	0,002%
Glycerol	20% ß-Merkaptoetanol
10%	
SDS	4,6%
Tris-HCl, pH 6,8 (0,5 M)	125 mM

3.5.5 Western blot

Blokovací pufer

Mlieko, odtučnené, sušené	5%
TBS s 0,1% Tween 20	100ml

Blotovací pufer

Glycín	192 mM
Metanol	20%
Tris-base	25 mM

TBS s 0,1% Tween 20

NaCl	14 mM
Tris-base	20 mM
Tween 20	0,1%

3.6 Prístrojové vybavenie

Blotovací systém

Transblot semi-dry transfer cell	Bio-Rad, USA

Centrifúgy

5430R	Eppendorf, Veľká Británia
IEC CL31R Multispeed centrifuge	Thermo Fisher Scientific, USA
MiniSpin Plus Microcentrifuge	Eppendorf, Veľká Británia

CO_2 inkubátor

MCO-5	Sanyo, Japonsko

Kvantitatívna real-time PCR

ABI Prism 7500 Fast Real-Time PCR System	Thermo Fisher Scientific, USA

Laboratórny vodný kúpeľ

TW12	Julabo, Nemecko

Laminárne boxy

BioUltra 3	Telstar, Španielsko
Safeflow 1.2, BioAi	EuroClone, Taliansko

Mikroskopy

Eclipse Ti-S/ TS 100	Nikon Instruments Europe B.V., Holandsko

Prístroj na vyvolávanie RTG filmov

Curix 60/ CP1000	Agfa, Belgicko

Sonikátory

Sonicator UP50H/UP100H	Hielsher Ultrasonics, Nemecko
Ultrasound sonicator	Hielsher Ultrasonics, Nemecko

Spektrofotometre

NanoPhotometer	Implen, Nemecko

Paradigm detection platform	Beckman Coulter, USA Infinite
M1000 PRO multi-mode microplate reader	Tecan, Švajčiarsko

Termomixér

Comfort	Eppendorf, Veľká Británia

Vertikálny elektroforetický aparát

Mini-Protean Tetra-Cell	Bio-Rad, USA

Zdroje

PowerPac 200	Bio-Rad, USA

3.7 Programové vybavenie

Adobe Illustrator CC 2017	Adobe Systems Incorporated, USA
GraphPad Prism v6.05	Graphpad Software Inc., USA

3.8 Metódy

3.8.1 Izolácia a kultivácia BMDMs

BMDMs boli získané vypláchnutím kostnej drene z holennej a stehennej kosti myší. Po ošetrení 1x RBC lyzačným pufrom a premytí IMDM médiom boli bunky diferencované v danom médiu obohatenom o 10% FBS, 20% L929-bunkový supernatant (obsahujúci tzv. macrophage colony-stimulating factor; M-CSF), 100 U/ml penicilín a 100 g/ml streptomycín. BMDMs boli kultivované počas 5 dní pri 37 °C a 5 % CO_2.

3.8.2 Infekcia BMDMs

Multiplicita infekcie (MOI) pre *F. tularensis* LVS a jej mutantné kmene bola zvolená 50:1 a pre *L. monocytogenes* 10:1. Synchronizovaná fagocytóza baktérií bola zabezpečená centrifugáciou (400g, 5 min) s následnou 30 min kultiváciou pri 37 °C a 5 % CO_2. Extracelulárne baktérie boli odstránené premytím predhriatym PBS a inkubáciou v médiu s 50 μg/ml gentamycínom počas 30 min. Po 1 h kultivácii boli infikované

BMDMs ponechané v kultivačnom médiu bez antibiotika a v príslušných časových intervaloch boli bunky premyté a zlyzované. V prípade infekcie mŕtvou *F. tularensis* LVS (MOI 50) alebo VSV-AV2 (MOI 0,01), boli patogény pridané ku scentrifugovaným BMDMs. VSV-AV2 bol 3 h po infekcii odmytý a Opti-MEM bol nahradený kultivačným médiom obsahujúcim IMDM.

3.8.3 Stimulácia a ko-infekcia BMDMs

BMDMs boli stimulované 100 ng/ml Pam_3CSK_4, 20 µg/ml c-di-GMP alebo 10 ng/ml LPS v daných časových intervaloch. V prípade ko-stimulačných alebo koinfekčných experimentov boli ligandy alebo patogény pridané k bunkám 3 h po zahájení predošlej infekcie.

3.8.4 Stanovenie luciferázovej aktivity *in vitro*

BMDMs boli nasadené do 24- alebo 48-jamkovej kultivačnej doštičky pre tkanivové kultúry o hustote 3,5 x 10^5 alebo 1,5 x 10^5 buniek na jamku. Po prevedení infekcie alebo stimulácie boli premyté predhriatym PBS a zlyzované v 30 µl lyzačného pufru (Luciferase Cell Culture Lysis Reagent), ktorý je súčasťou komerčného kitu Luciferase Assay Systems. Luciferázová aktivita bola zmeraná v 25 µl bunkového lyzátu zmiešaného s 50 µl substrátu (Luciferase Assay Reagent) na prístroji Infinite M1000 PRO. Miera luminiscencie vyjadrená v relatívnych svetelných jednotkách (RLU) bola normovaná na koncentráciu proteínov a znázornená ako násobok získaných hodnôt nestimulovaných WT BMDMs.

3.8.5 Kvantitatívna real-time PCR

Pre izoláciu mRNA z infikovaných BMDMs (7,5 x 10^5/ jamka) bol využitý RNeasy Mini Kit. Následne bol 1 µg mRNA ošetrený Dnázou I počas 30 min pri 37 °C a reverzne prepísaný na cDNA za použitia Oligo $(dT)_{12-18}$. Reakčná zmes pre qRT-PCR obsahovala 10 µl 2x TaqMan™ Universal PCR Master Mixu, 2 µl cDNA, 7 µl H_2O bez Rnáz a 1µl FAM-značeného Taqman™ primeru pre *Ifnb1*, *Ifnα4, Il1b, Rn18s* alebo *Tnfα*. Podmienky priebehu testov expresie génov TaqMan boli zvolené podľa odporúčania výrobcu. Hladiny mRNA boli merané v triplikátoch na prístroji ABI Prism 7500 Fast Real-Time PCR System. Výsledky boli normalizované na hladiny mRNA referenčného

génu 18S rRNA a vyjadrené ako násobok hodnôt mRNA kontrolných vzoriek pomocou porovnávacej Ct metódy ($_{\Delta\Delta}$Ct).

3.8.6 ELISA

Koncentrácie cytokínov TNF-α a IL-6 boli stanovené v bunkových supernatantoch odobratých po infekcii BMDMs *F. tularensis* LVS, *ΔiglC*/LVS alebo *L. monocytogenes* pomocou ELISA kitu. Metóda bola prevedená podľa inštrukcií výrobcu, pričom absorbancia vzoriek bola zmeraná na prístroji Infinite M1000 PRO.

3.8.7 Imunofluorescenčné farbenie

Bunky boli nasadené na hodinové sklíčka do 24-jamkovej kultivačnej doštičky (2,5 x 10^5/ jamka) a ponechané adhézii do druhého dňa. Po následnej 8 h infekcii *F. tularensis* LVS (MOI 50) alebo *L. monocytogenes* EGD-e-cGFP (MOI 10) boli bunky fixované 4% paraformaldehydom počas 30 min a následne neutralizované 50 mM NH_4Cl. Po premytí buniek PBS, nasledovala permeabilizácia buniek infikovaných *F. tularensis* LVS 0,2% Triton X-100 počas 15 min a blokácia buniek v 3% BSA po dobu 45 min. Baktérie boli detegované pomocou polyklonálneho králičieho séra namiereného proti *F. tularensis* (riedené 1:3000) (Plzakova et al. 2015) a kozej anti-králičej AlexaFluor™ 488 IgG (riedená 1:500). V poslednom kroku boli bunky nafarbené DAPI a analyzované pomocou fluorescenčnej mikroskopie.

3.8.8 Imunoprecipitácia vzoriek

Bunky (1,5 x 10^6/ jamka) boli po pridaní lyzačného pufru denaturované pomocou roztoku TDS. Následne boli lyzáty scentrifugované pri 13 000 rpm počas 5 min a pelety boli rozpustené v TNN pufru. Izolácia signálnych komplexov pomocou agarózových guličiek s naviazaným proteínom A/G bola prevedená po inkubácii vzoriek so špecifickou protilátkou pri 4 °C cez noc. Po premytí boli komplexy uvoľnené do 2 x koncentrovaného vzorkového pufru pre SDS-PAGE. V prípade ubikvitinačných štúdii bol ku BMDMs pridaný ubikvitinačný lyzačný pufer. Vzorky boli podrobené sonikácii a po centrifugácii pri 14000 rpm počas 2 min boli pelety rozpustené v 2 x koncentrovanom vzorkovom pufri pre SDS-PAGE.

3.8.9 Western blot

BMDMs nasadené do 6-jamkovej kultivačnej doštičky pre tkanivové kultúry (1,5 x 10^6/ jamka) boli zlyzované v 2 x koncentrovanom vzorkovom pufri pre SDSPAGE. Vzorky boli rozseparované pomocou 10% SDS PAGE a preblotované na polyvinyliden difluoridové membrány (GE Healthcare, USA). Po 1 h blokácii membrán v roztoku 5% mlieka v TBS s 0,1% Tween 20 nasledovala inkubácia s príslušnou primárnou protilátkou pri 4 °C cez noc. Po premytí bola membrána inkubovaná počas 1 h so sekundárnou protilátkou, HRP-konjugovaným IgG.

Imunoreaktívne proteíny boli detegované pomocou ECL Western Blotting Detection Kit a RTG filmom (Kodak, USA).

3.8.10 Test cytotoxicity

Pre stanovenie cytotoxického vplyvu *F. tularensis* LVS, *ΔdsbA*/LVS, *ΔiglC*/LVS alebo *L. monocytogenes* na BMDMs bol využitý kit CytoTox-ONE™ Homogenous Membrane Integrity Assay. Bunkové supernatanty boli odobraté po infekcii v určených časových intervaloch (3, 6, 8 a 12 h) a bola v nich stanovená hladina uvoľnenej laktátdehydrogenázy (LDH) podľa inštrukcií výrobcu. Ako pozitívna kontrola boli použité neinfikované BMDMs, ktoré boli lyzované pomocou Lysis solution. Vzorky boli zmerané na prístroji Infinite M1000 PRO. Fluorescencia vzoriek bola vyjadrená percentuálne a bola vztiahnutá ku hladine LDH stanovenej v neinfikovaných BMDMs.

3.8.11 Stanovenie relatívneho vstupu *L. monocytogenes* do BMDMs

Po ko-infekcii BMDMs (7,5 x 10^5/jamka) *F. tularensis* LVS (MOI 25) alebo *ΔiglC*/LVS (MOI 25) s *L. monocytogenes* EGD-e::pPL2/*lux* pHELP (MOI 5) boli bunky zlyzované v 50 ul lyzačného pufru obsahujúceho 0,2% Triton X-100, 10% glycerol a PBS. Následne bola zmeraná luminiscencia vzoriek na prístroji Infinite M1000 PRO, ktorá bola vyjadrená v RLU a predstavovala relatívny vstup *L. monocytogenes* do buniek.

3.9 Štatistická analýza dát

Dáta sú vyjadrené ako priemer so štandardnou chybou merania (±SEM). Štatistická analýza bola prevedená pomocou dvojfaktorového ANOVA testu s Bonferroniho testom alebo nepárovým Studentovým t-testom za použitiaGraphPad
Prism v6.05 Software.

4 Výsledky

4.1 Aktivácia signalizačných dráh riadených PRR *F. tularensis* LVS

4.1.1 Signálne dráhy receptorov PRR

Pre charakterizáciu signalizačných kaskád zapojených v stimulácii IFN odpovede typu I v priebehu skorej vrodenej imunitnej odpovede voči *F. tularensis* LVS boli prevedené *in vitro* experimenty. BMDMs pochádzali z myší nesúcich IFN-ß luciferázový reportérový systém a zároveň boli deficientné pre nasledujúce adaptorové proteíny: MyD88 (*Myd88*$^{-/-}$*Ifnß*$^{+/\Delta\beta luc}$), TRIF (*Ticam1*$^{-/-}$*Ifnß*$^{+/\Delta\beta luc}$), STING (*Sting*$^{-/}$*Ifnß*$^{+/\Delta\beta luc}$) alebo IPS1 (*Ips1*$^{-/-}$*Ifnß*$^{+/\Delta\beta luc}$). IFN-ß luciferázová aktivita bola stanovovaná v zlyzovaných bunkách v časových intervaloch 0, 6, 9 a 12 h po infekcii *F. tularensis*
LVS. Najvyššie hladiny IFN odpovede typu I boli stimulované vo WT *Ifnß*$^{+/\Delta\beta luc}$ BMDMs v 9 h. V prípade buniek postrádajúcich proteíny MyD88 alebo IPS1 bola pozorovaná znížená aktivácia IFN-ß luciferázovej aktivity v porovnaní s BMDMs získanými z WT *Ifnß*$^{+/\Delta\beta luc}$ myší v priebehu celého merania **(Obr. 4-1A, D)**. *Sting*$^{-/}$*Ifnß*$^{+/\Delta\beta luc}$ BMDMs vykazovali na rozdiel od *Ticam1*$^{-/-}$*Ifnß*$^{+/\Delta\beta luc}$ buniek pokles IFN odpovede typu I aj v 9 h **(Obr. 4-1B, C)**. Pozorovaný nárast IFN-ß luciferázovej aktivity v skorších časových intervaloch mohol byť v *Sting*$^{-/-}$*Ifnß*$^{+/\Delta\beta luc}$ BMDMs vyvolaný v dôsledku negatívnej regulácie TLR týmto adaptorovým proteínom (Sharma et al. 2015). Získané výsledky poukazujú na to, že vznik zápalovej odpovede v priebehu infekcie *F. tularensis* LVS zahŕňa koordinovanú aktiváciu signálnych dráh riadených receptormi TLR, CDS a RLR.

4.1.2 Aktivácia prozápalovej odpovede

Pre ďalšie štúdium modulácie vrodenej imunitnej odpovede *F. tularensis*, boli BMDMs infikované *L. monocytogenes,* intracelulárnym patogénom stimulujúcim

expresiu IFN-ß prostredníctvom signálnych dráh riadených TLR, RLR a hlavne cez adaptorový proteín STING **(Obr. 4-2A-B)** (Sauer et al. 2011; Witte et al. 2012; Abdullah et al. 2012). Stanovenie IFN-ß luciferázovej aktivity vo WT *Ifnβ*$^{+/\Delta\beta luc}$ BMDMs v 9 h odhalilo výrazne nižšiu schopnosť *F. tularensis* LVS (až približne 200krát) stimulovať IFN odpoveď typu I v porovnaní s *L. monocytogenes* **(Obr. 4-2A)**.
Navyše *F. tularensis* LVS indukovala taktiež výrazne nižšie hladiny mRNA *Ifnb1*, ale aj prozápalového génu *Tnfa* **(Obr. 4-3)**.

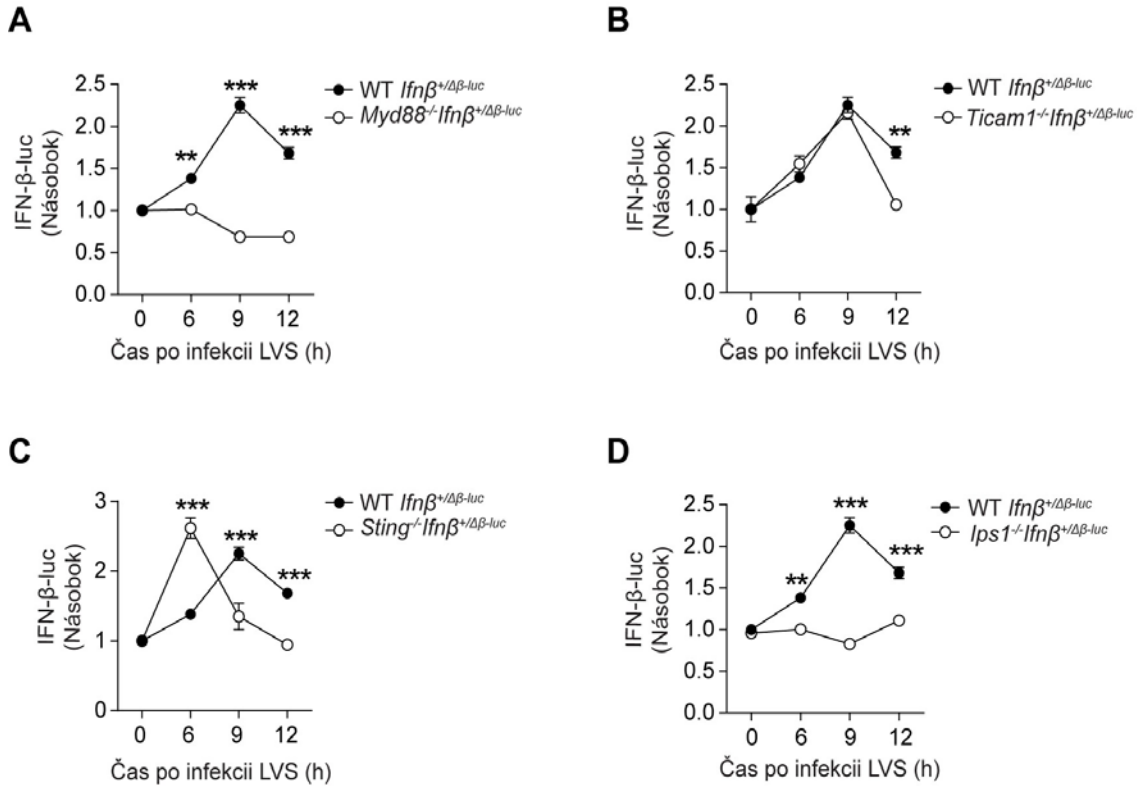

Obr. 4-1: *F. tularensis* LVS stimuluje zápalovú odpoveď prostredníctvom signalizačných dráh regulovaných TLR, CDS a RLR. (A-D) IFN-ß luciferázová aktivita nameraná vo WT *Ifnβ*$^{+/\Delta\beta luc}$, *Myd88*$^{-/-}$*Ifnβ*$^{+/\Delta\beta luc}$ **(A)**, *Ticam1*$^{-/-}$*Ifnβ*$^{+/\Delta\beta luc}$ **(B)**, *Sting*$^{-/-}$*Ifnβ*$^{+/\Delta\beta luc}$ **(C)** alebo *Ips1*$^{-/-}$*Ifnβ*$^{+/\Delta\beta luc}$ **(D)** BMDMs infikovaných *F. tularensis* LVS (MOI 50) v časových intervaloch 0, 6, 9 a 12 h. Výsledky predstavujú reprezentatívne dáta z 2 nezávislých experimentov a sú vyjadrené v ±SEM. Štatistická významnosť bola určená pomocou dvojfaktorového ANOVA testu s využitím Bonferroniho testu, **P≤ 0,01; ***P≤ 0,001.

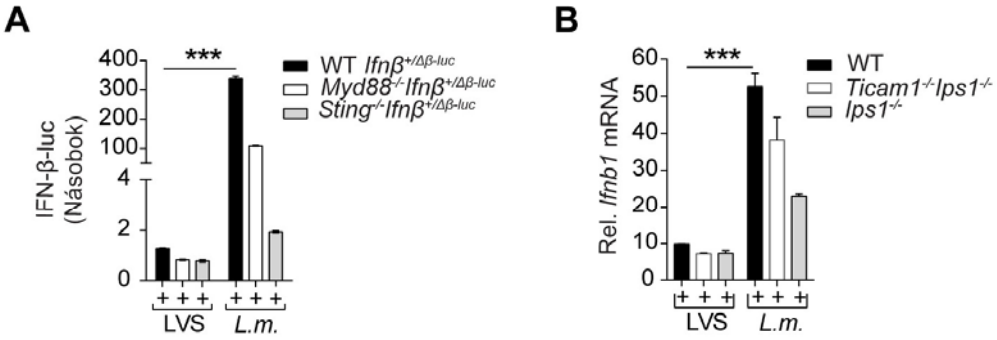

Obr. 4-2: *L. monocytogenes* stimuluje IFN odpoveď typu I cez signalizačné dráhy kontrolované TLR, CDS a RLR. (A) IFN-ß luciferázová aktivita analyzovaná vo WT *Ifnβ*$^{+/\Delta\beta luc}$, *Myd88*$^{-/-}$*Ifnβ*$^{+/\Delta\beta luc}$ alebo *Sting*$^{-/-}$*Ifnβ*$^{+/\Delta\beta luc}$ BMDMs infikovaných *F. tularensis* LVS (MOI 50) alebo *L. monocytogenes* (MOI 10) 9 h po infekcii. Výsledky predstavujú reprezentatívne dáta z 3 nezávislých experimentov a sú vyjadrené v ±SEM. **(B)** Stanovenie hladín mRNA *Ifnb1* vo WT, *Ticam1*$^{-/-}$*Ips1*$^{-/-}$ alebo *Ips1*$^{-/-}$ infikovaných *F. tularensis* LVS (MOI 50) alebo *L. monocytogenes* (MOI 10). Výsledky sú vyjadrené v ±SEM. Štatistická významnosť bola určená pomocou Studentovho t-testu, ***P≤ 0,001.

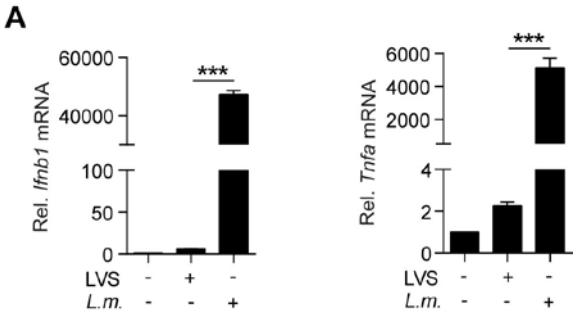

Obr. 4-3: *F. tularensis* LVS stimuluje slabú prozápalovú odpoveď. qRT-PCR analýza mRNA *Ifnb1* a prozápalového génu *Tnfa* vo WT BMDMs infikovaných *F. tularensis* LVS (MOI 50) alebo *L. monocytogenes* (MOI 10) 8 h po infekcii. Výsledky predstavujú reprezentatívne dáta z 2 nezávislých experimentov a sú vyjadrené v ±SEM. Štatistická významnosť bola určená pomocou Studentovho t-testu, ***P≤ 0,001.

4.1.3 Vplyv bakteriálnej cytopatogenity na prozápalovú odpoveď

Cieľom testu bakteriálnej cytopatogenity bolo vyvrátenie vplyvu zvýšenej úmrtnosti buniek infikovaných *F. tularensis* LVS na aktiváciu IFN odpovede typu I **(Obr. 4-4A)**. Detekcia množstva LDH bola prevedená v 3, 6, 8 a v 12 h po infekcii. Hodnoty LDH vo WT *Ifnβ*$^{+/\Delta\beta luc}$ BMDMs infikovaných *F. tularensis* LVS dosahovali porovnateľných hodnôt až na 12 h interval, kde hladina LDH mierne narástla na 5,7 %. V

prípade infekcie WT *Ifnβ*$^{+/\Delta\beta luc}$ BMDMs *L. monocytogenes* bolo množstvo LDH výrazne zvýšené len v 12 h (32,7 %) **(Obr. 4-4B)**. Získané výsledky potvrdili zníženú schopnosť *F. tularensis* LVS aktivovať prozápalovú odpoveď.

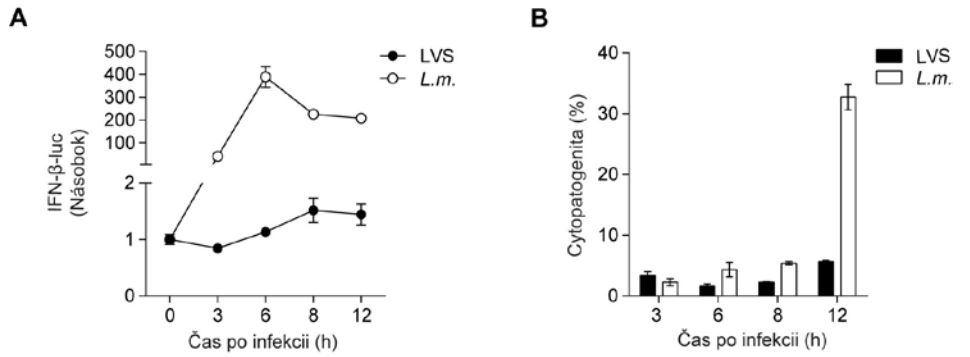

Obr. 4-4: Za nízku aktiváciu zápalovej odpovede *F. tularensis* LVS nezodpovedá zvýšená úmrtnosť BMDMs. (A) Časový priebeh (0, 3, 6, 8 a 12 h) aktivácie IFN odpovede typu I počas infekcie WT *Ifnβ*$^{+/\Delta\beta luc}$ BMDMs *F. tularensis* LVS (MOI 50) alebo *L. monocytogenes* (MOI 10). **(B)** Cytopatogenita WT *Ifnβ*$^{+/\Delta\beta luc}$ BMDMs v priebehu infekcie *F. tularensis*LVS (MOI 50) alebo *L. monocytogenes* (MOI 10). Aktivita LDH je vyjadrená percentuálne a je vztiahnutá ku hladine LDH stanovenej v neinfikovaných BMDMs. Výsledky predstavujú reprezentatívne dáta z 2 nezávislých experimentov a sú vyjadrené v ±SEM.

4.1.4 Infektivita BMDMs

Miera schopnosti baktérií infikovať hostiteľské bunky bola stanovovaná na základe rozdielnej stimulácie prozápalovej odpovede v predošlých experimentoch. WT BMDMs infikované *F. tularensis* LVS alebo *L. monocytogenes* GFP boli po 8 h analyzované pomocou imunofluorescenčnej mikroskopie **(Obr. 4-5A)**. Množstvo infikovaných buniek *F. tularensis* LVS alebo *L. monocytogenes* nebolo signifikantne rozdielne **(Obr. 4-5B)**.

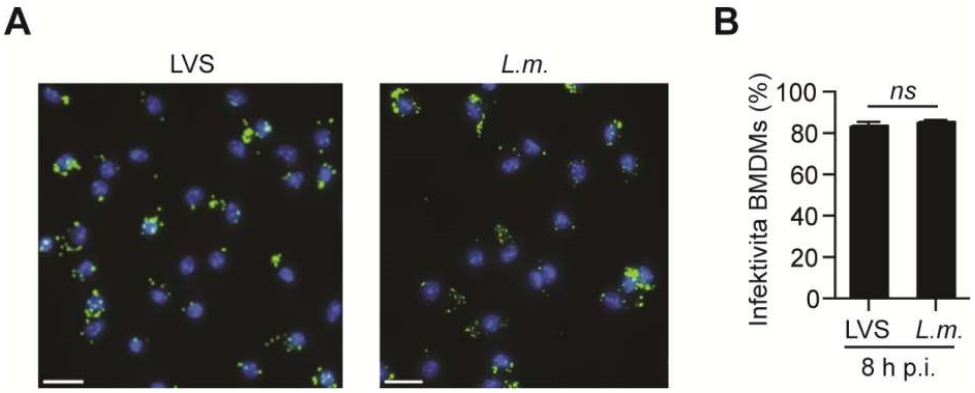

Obr. 4-5: *F. tularensis* LVS infikuje WT BMDMs v rovnakej miere ako *L. monocytogenes*. (A) Imunofluorescenčná detekcia *F. tularensis* LVS pomocou králičej anti-LVS protilátky

(zelená) a *L. monocytogenes* GFP (zelená) vo WT BMDMs. Jadrá sú označené pomocou DAPI (modrá). Stupnica: 20 µm. **(B)** Kvantifikácia *F. tularensis* LVS a *L. monocytogenes* GFP vo WT BMDMs. Výsledky predstavujú dáta z 2 nezávislých experimentov (n > 600 počítaných buniek). Štatistická významnosť bola určená pomocou Studentovho t-testu, ns P> 0,05.

4.2 Aktívna supresia signalizačných dráh riadených TLR, CDS a RLR

Medzi nepostrádateľné vlastnosti úspešného patogéna patrí schopnosť vyhnúť sa aktivácii hostiteľskej imunitnej odpovede alebo ju aspoň eliminovať. V priebehu infekcie WT BMDMs *F. tularensis* LVS stimuluje pomerne nízku zápalovú odpoveď **(Obr. 4-2, 4-3, 4-4A)**. Cieľom nasledujúcich experimentov bolo preukázať, či za jej slabou aktiváciou stojí nedostatočná indukcia signalizačných dráh regulovaných receptormi PRR alebo ich aktívna bakteriálna inhibícia.

Schopnosť *F. tularensis* LVS potlačovať aktiváciu signalizačných dráh regulovaných receptormi PRR bola skúmaná v prítomnosti *L. monocytogenes* **(Obr. 46A)**, atenuovaného kmeňa vírusu vezikulárnej stomatitídy (VSV-AV2) **(Obr. 4-6B)** alebo mŕtvej *F. tularensis* LVS **(Obr. 4-7)**. Analýza IFN-ß luciferázovej aktivity vo WT *Ifnß*$^{+/\Delta\beta luc}$ BMDMs potvrdila supresívny efekt *F. tularensis* LVS na aktivovanú odpoveď buniek vyvolanú *L. monocytogenes* **(Obr. 4-6A)**. V prípade ko-infekčného experimentu s VSV-AV2 stimulujúcim IFN odpoveď typu I cez receptor RIG-I (Kato et al. 2006; Dietrich et al. 2010) bola pozorovaná výrazne znížená aktivácia tejto odpovede **(Obr. 46B)**. *F. tularensis* LVS aktívne suprimovala expresiu IFN-ß aj v prítomnosti zlyzovanej baktérie **(Obr. 4-7A-B)**. Získané výsledky poukazujú na schopnosť *F. tularensis* LVS aktívne potlačovať signalizáciu kontrolovanú TLR, CDS a RLR.

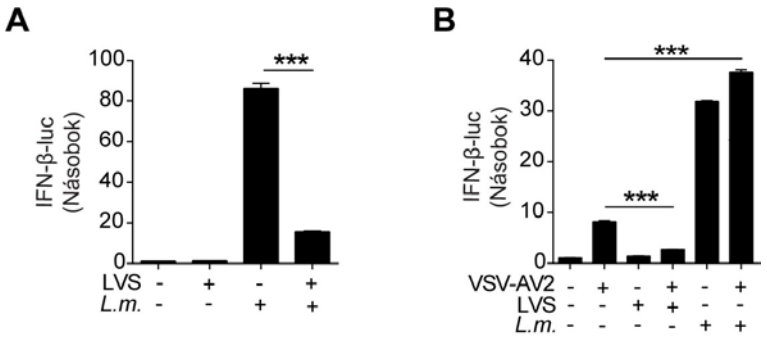

Obr. 4-6: Aktívna supresia signalizačných dráh regulovaných TLR, CDS a RLR *F. tularensis* LVS. (A-B) IFN-ß luciferázová aktivita vo WT *Ifnß*$^{+/\Delta\beta luc}$ BMDMs infikovaných

F. tularensis LVS (MOI 50) 3 h pred stimuláciou *L. monocytogenes* (MOI 10) **(A)** alebo VSVAV2 (MOI 0,01) **(B)** a následnou 5 h alebo 3 h inkubáciou. Výsledky predstavujú reprezentatívne dáta z 2 nezávislých experimentov a sú vyjadrené v ±SEM. Štatistická významnosť bola určená pomocou Studentovho t-testu, ***P≤ 0,001.

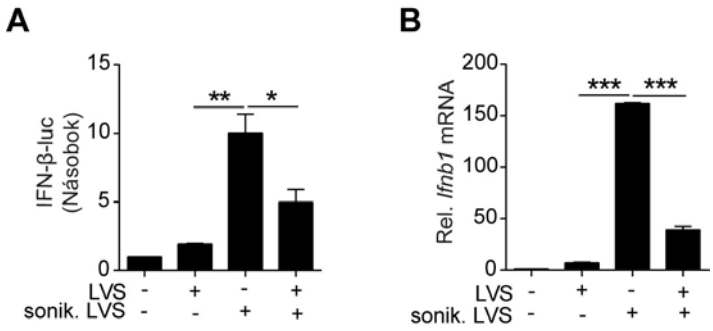

Obr. 4-7: *F. tularensis* LVS aktívne oslabuje IFN odpoveď typu I v prítomnosti mŕtvej baktérie. (A-B) IFN-ß luciferázová aktivita **(A)** a miera expresie mRNA *Ifnb1* **(B)** vo WT *Ifnβ*$^{+/\Delta\beta luc}$ BMDMs infikovaných počas 8 h živou alebo mŕtvou (sonikovanou) *F. tularensis* LVS (MOI 50) alebo stimulovaných po 3 h infekcii *F. tularensis* LVS mŕtvou baktériou (MOI 50) a ponechaných následnej 5 h inkubácii. Výsledky predstavujú reprezentatívne dáta z 2 nezávislých experimentov a sú vyjadrené v ±SEM. Štatistická významnosť bola určená pomocou Studentovho t-testu, *P≤ 0,05; **P≤ 0,01; ***P≤ 0,001.

Ďalej bol skúmaný supresívny efekt *F. tularensis* LVS na aktiváciu signalizačných dráh regulovaných TLR2, TLR4 a STING. WT *Ifnβ*$^{+/\Delta\beta luc}$ BMDMs boli infikované *F. tularensis* LVS alebo *L. monocytogenes* a po 3 h stimulované príslušnými ligandmi. Pre aktiváciu receptora TLR2 bol zvolený triacylovaný lipopeptid, Pam_3CSK_4 **(Obr. 4-8A, 4-9A)**, pre TLR4 LPS **(Obr. 4-8B, 4-9B)** a pre stimuláciu signalizačnej dráhy regulovanej senzorom STING bol vybratý c-di-GMP **(Obr. 4-8C,4-9C)** (Fitzgerald et al. 2003; Dietrich et al. 2010; Burdette et al. 2011). Stanovenie IFN-ß luciferázovej aktivity **(Obr. 4-8A-C)** a analýza hladín mRNA *Ifnb1* a *Tnfa* pomocou qRT-PCR **(Obr. 4-9A-C)** odhalila, že *F. tularensis* LVS je na rozdiel od *L. monocytogenes* schopná tieto stimuly aktívne suprimovať.

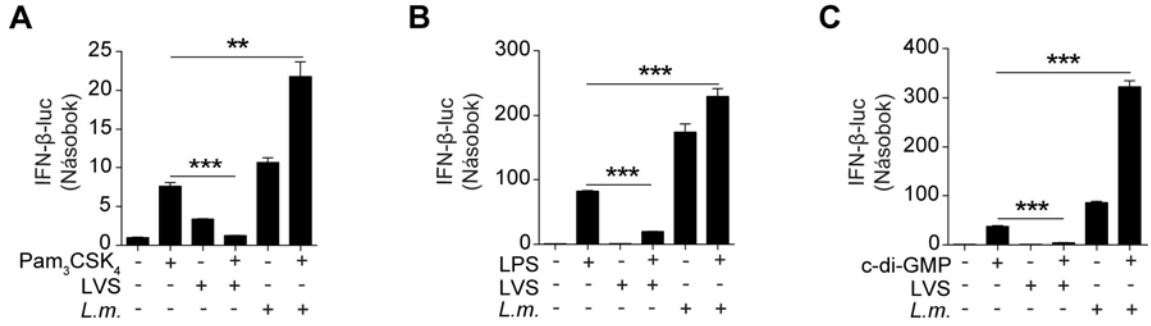

Obr. 4-8: *F. tularensis* LVS blokuje TLR2-, TLR4- a STING-dependentnú aktiváciu zápalovej odpovede. (A-C) WT *Ifnβ*$^{+/\Delta\beta luc}$ BMDMs boli infikované *F. tularensis* LVS (MOI 50) alebo *L. monocytogenes* (MOI 10) 3 h pred zahájením stimulácie 100 ng/ml Pam_3CSK_4 **(A)**, 10 ng/ml LPS **(B)** alebo 20 µg/ml c-di-GMP **(C)**. IFN-ß luciferázová aktivita bola detegovaná po následnej 5 h inkubácii stimulovaných buniek. Výsledky predstavujú reprezentatívne dáta z 3 nezávislých experimentov a sú vyjadrené v ±SEM. Štatistická významnosť bola určená pomocou Studentovho t-testu, **P≤ 0,01; ***P≤ 0,001.

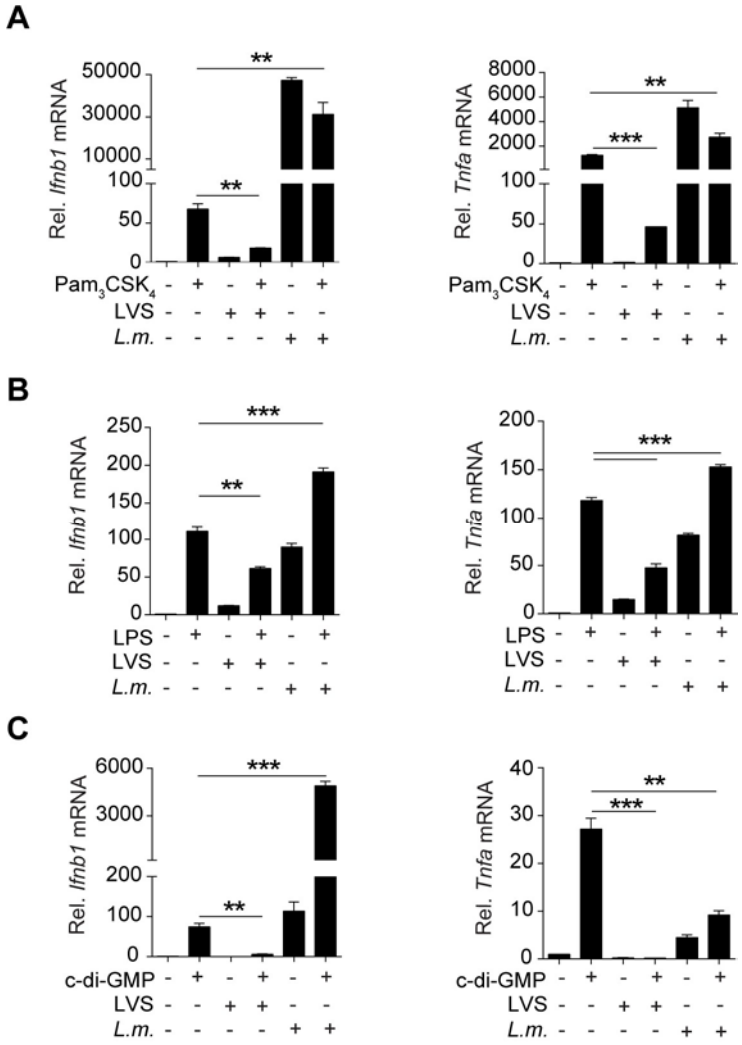

Obr. 4-9: V inhibícii expresie génov *Ifnb1* a *Tnfa F. tularensis* LVS sú zahrnuté signalizačné dráhy TLR2, TLR4 a STING. (A-C) Expresia mRNA *Ifnb1* alebo *Tnfa* bola analyzovaná prostredníctvom qRT-PCR vo WT *Ifnβ*$^{+/\Delta\beta luc}$ BMDMs infikovaných *F. tularensis* LVS (MOI 50) alebo *L. monocytogenes* (MOI 10) 3 h pred zahájením stimulácie 100 ng/ml Pam_3CSK_4 **(A)**, 10 ng/ml LPS **(B)** alebo 20 µg/ml c-di-GMP **(C)** trvajúcej nasledujúcich 5 h. Výsledky sú vyjadrené v ±SEM. Štatistická významnosť bola určená pomocou Studentovho ttestu, **P≤ 0,01; ***P≤ 0,001.

4.3 Úloha fagozomálneho úteku *F. tularensis* LVS v supresii signálnych dráh riadených PRR

Fagozomálny útek *F. tularensis* LVS do cytosólu a jej následná replikácia v ňom predstavuje pre baktériu dôležitú fázu jej intracelulárneho života. Avšak aj v tejto časti cyklu musí *F. tularensis* LVS čeliť rôznym nástrahám imunitného systému hostiteľskej bunky. Pre štúdium podielu funkčného T6SS alebo cytosólického výskytu *F. tularensis* LVS na aktivácii alebo potlačení signalizácie riadenej PRR boli použité mutantné kmene s narušenou schopnosťou fagozomálneho úniku, *ΔiglC*/LVS a *ΔdsbA*/LVS. Stanovenie

IFN-ß luciferázovej aktivity, hladín mRNA a cytokínov bolo prevedené 8 h po infekcii WT BMDMs. Na rozdiel od divokého kmeňa *F. tularensis* LVS, *ΔiglC*/LVS aj *ΔdsbA*/LVS vykazovali zvýšenú schopnosť stimulovať prozápalovú **(Obr. 4-10B-C)** a IFN odpoveď typu I **(Obr. 4-10A, 4-13, 4-14)**. V prípade mutantného kmeňa *ΔdsbA*/LVS dosahovali namerané hladiny IFN-ß luciferázovej aktivity aj mRNA *Ifnb1* a *Tnfa* v porovnaní s *ΔiglC*/LVS vyšších hodnôt **(Obr. 4-13, 4-14)**.

Cieľom nasledujúcich experimentov bolo porovnanie supresívneho efektu *F. tularensis* LVS a jej mutantného kmeňa *ΔiglC*/LVS na vrodenú imunitnú odpoveď v prítomnosti *L. monocytogenes*. Infikované WT BMDMs boli podrobené analýze pomocou qRT-PCR alebo metódy ELISA. *F. tularensis* LVS v porovnaní s *ΔiglC*/LVS bola schopná suprimovať stimuláciu génov IFN odpovede typu I (mRNA *Ifnb1* a *Ifna4*) **(Obr. 4-10A)**, prozápalovej odpovede (mRNA *Tnfa* a *Il1b*) **(Obr. 4-10B)** a produkciu TNF-α a IL-6 **(Obr. 4-10C)** v prítomnosti *L. monocytogenes* vo väčšej miere. Získané dáta poukazujú na dôležitosť fagozomálneho úteku *F. tularensis* LVS z pohľadu supresie signalizačných kaskád regulovaných TLR, CDS a RLR.

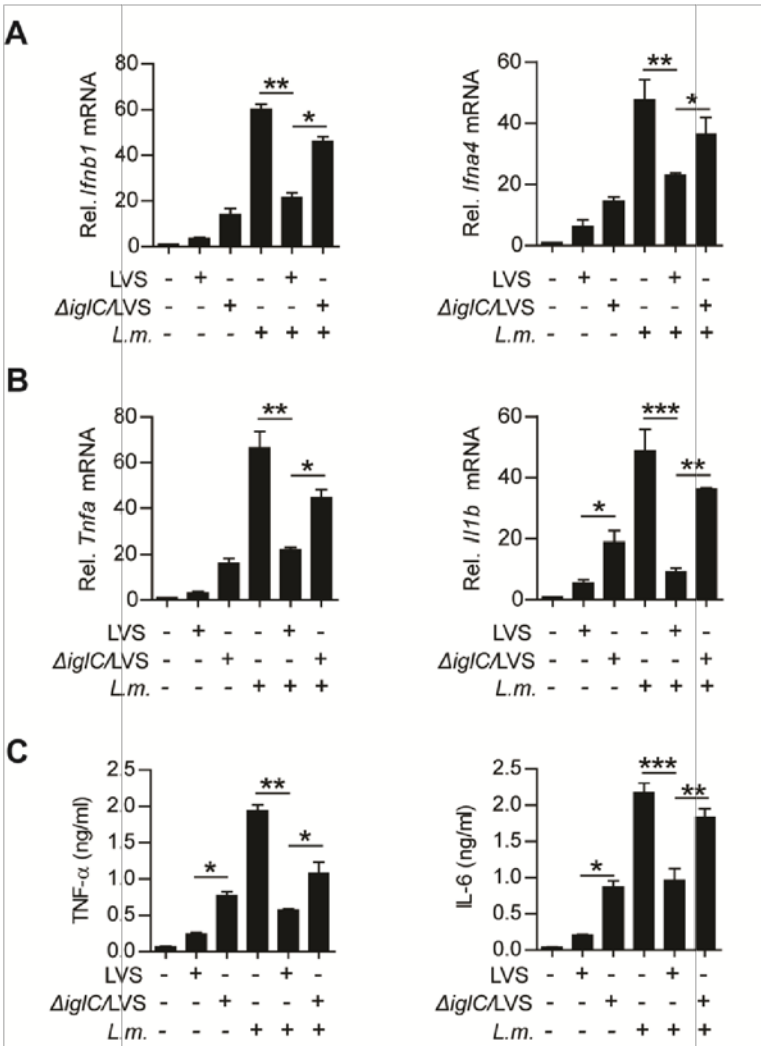

Obr. 4-10: Fagozomálny útek *F. tularensis* LVS do cytosólu je dôležitý pre bakteriálnu inhibíciu signalizačných kaskád regulovaných PRR. (A-C) WT BMDMs boli infikované počas 8 h *F. tularensis* LVS (MOI 50), *ΔiglC*/LVS (MOI 50) alebo *L. monocytogenes* (MOI 10), prípadne boli 3 h pred stimuláciou *L. monocytogenes* (MOI 10) infikované *F. tularensis* LVS (MOI 50) alebo *ΔiglC*/LVS (MOI 50) a inkubované počas ďalších 5 h. Vo vzorkách boli následne analyzované hladiny mRNA *Ifnb1* a *Ifna4* **(A)**, *Tnfa* a *Il1b* **(B)** a produkcia TNF-α a IL-6 **(C)**. Výsledky predstavujú reprezentatívne dáta z 2 nezávislých experimentov a sú vyjadrené v ±SEM. Štatistická významnosť bola určená pomocou Studentovho t-testu, *P≤ 0,05; **P≤ 0,01; ***P≤ 0,001.

4.3.1 Miera sekundárnej fagocytózy BMDMs

Analýza relatívneho vstupu baktérií do buniek bola prevedená z dôvodu vylúčenia nedostatočnej fagocytózy *L. monocytogenes* infikovanými bunkami, a tým aj zníženej stimulácie vrodenej imunitnej odpovede. WT BMDMs boli stimulované buď samotnou luminiscenčnou *L. monocytogenes* (EDGe::pPL2/*lux*pHELP) alebo boli najskôr podrobené infekcii *F. tularensis* LVS, prípadne *ΔiglC*/LVS, a až následne koinfekcii *L. monocytogenes* (EDGe::pPL2/*lux*pHELP). Schopnosť WT BMDMs fagocytovať

primárne alebo až sekundárne *L. monocytogenes* sa signifikantne nelíšila. Okrem toho neboli pozorované ani rozdiely medzi bunkami, ktoré boli najskôr infikované *F. tularensis* LVS alebo *ΔiglC*/LVS **(Obr. 4-11)**.

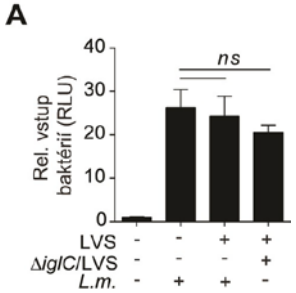

Obr. 4-11: Znížená prozápalová a IFN odpoveď typu I nie je vyvolaná narušenou fagocytózou *L. monocytogenes* už infikovanými BMDMs. Miera luminiscencie *L. monocytogenes* (EGDe::pPL2/*lux*pHELP) (MOI 5) fagocytovanej predbežne infikovanými BMDMs *F. tularensis* LVS (MOI 25) alebo *ΔiglC*/LVS (MOI 25) bola vyjadrená v RLU a predstavovala relatívny vstup baktérií. Výsledky predstavujú priemer z dát zo 4 nezávislých experimentov a sú vyjadrené v ±SEM. Štatistická významnosť bola určená pomocou Studentovho t-testu, ns P> 0,05.

4.3.2 Indukcia bunkovej cytopatogenity

Test cytopatogenity bol prevedený za účelom odhalenia, či za zníženú stimuláciu zápalovej odpovede v priebehu ko-infekcie *F. tularensis* LVS a *L. monocytogenes* nezodpovedá zvýšená úmrtnosť buniek. Detekcia množstva LDH bola prevedená 8 h po infekcii. Hodnoty LDH vo WT BMDMs ko-infikovaných *F. tularensis* LVS alebo *ΔiglC*/LVS a *L. monocytogenes* dosahovali porovnateľných hodnôt (9,54 a 8,84 %) **(Obr. 4-12)**.

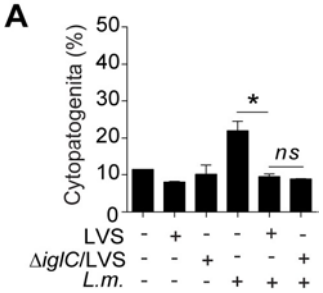

Obr. 4-12: Znížená aktivácia zápalovej odpovede nie je ovplyvnená životnosťou BMDMs. Cytopatogenita WT BMDMs infikovaných *F. tularensis* LVS (MOI 25) alebo *ΔiglC*/LVS (MOI 25) a po 3 h podrobených stimulácii *L. monocytogenes* (MOI 5) počas nasledujúcich 5 h. Aktivita LDH je vyjadrená percentuálne a je vztiahnutá ku hladine LDH stanovenej v neinfikovaných

BMDMs. Výsledky predstavujú reprezentatívne dáta z 2 nezávislých experimentov a sú vyjadrené v ±SEM. Štatistická významnosť bola určená pomocou Studentovho t-testu, *P≤ 0,05; **P≤ 0,01; ***P≤ 0,001.

Taktiež bol skúmaný inhibičný efekt mutantných kmeňov na signalizáciu aktivovanú prostredníctvom TLR2, TLR4 a STING. WT *Ifnβ*$^{+/\Delta\beta luc}$ BMDMs boli infikované buď *F. tularensis* LVS, *ΔiglC*/LVS alebo *ΔdsbA*/LVS a po 3 h inkubácii stimulované ligandmi Pam_3CSK_4 **(Obr. 4-13A, 4-14A)**, LPS **(Obr. 4-14B)** alebo c-diGMP **(Obr. 4-13B, 4-14C)**. Analýza IFN-ß luciferázovej aktivity a qRT-PCR odhalila, že divoký kmeň *F. tularensis* LVS vykazoval v porovnaní s atenuovanými kmeňmi zvýšenú schopnosť oslabovať navodenú hostiteľskú imunitnú odpoveď regulovanú prostredníctvom TLR2, TLR4 a STING.

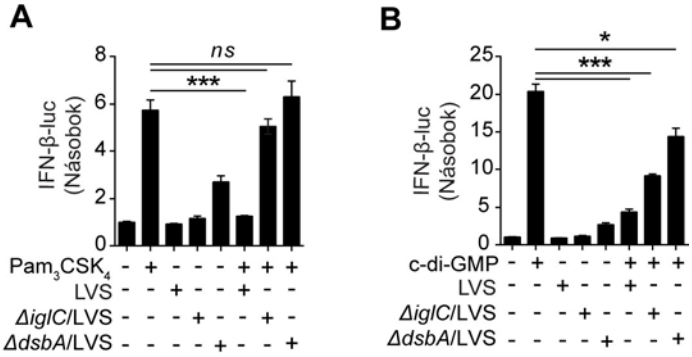

Obr. 4-13: Úloha fagozomálneho úniku *F. tularensis* LVS v blokácii signalizácie regulovanej TLR2 a STING. (A-B) IFN-ß luciferázová aktivita bola meraná vo WT *Ifnβ*$^{+/\Delta\beta luc}$ BMDMs infikovaných *F. tularensis* LVS, *ΔiglC*/LVS alebo *ΔdsbA*/LVS 3 h pred stimuláciou 100 ng/ml Pam_3CSK_4 **(A)** alebo 20 µg/ml c-di-GMP **(B)** počas nasledujúcich 5 h. Výsledky predstavujú reprezentatívne dáta z 2 nezávislých experimentov a sú vyjadrené v ±SEM. Štatistická významnosť bola určená pomocou Studentovho t-testu, ns P> 0,05; *P≤ 0,05; ***P≤ 0,001.

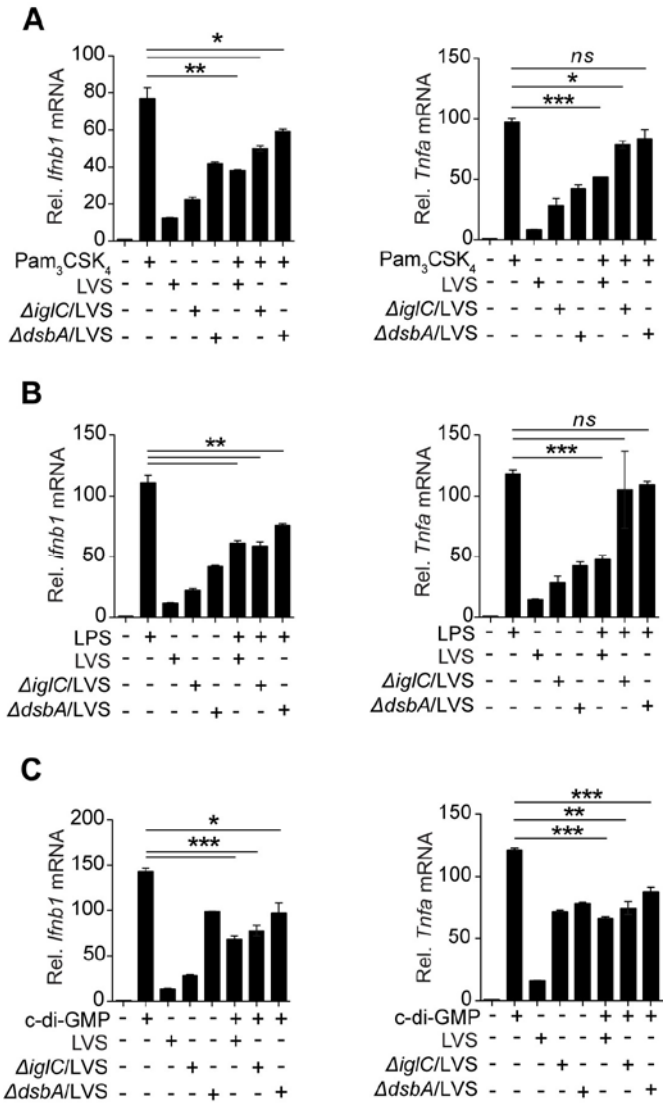

Obr. 4-14: Blokácia TLR- , CDS- a RLR-dependentnej signalizácie je podmienená výskytom *F. tularensis* LVS v cytosóle. (A-C) Hladiny mRNA *Ifnb1* alebo *Tnfa* boli analyzované pomocou qRT-PCR vo WT *Ifnβ*$^{+/\Delta\beta luc}$ BMDMs infikovaných buď *F. tularensis* LVS, *ΔiglC*/LVS alebo *ΔdsbA*/LVS 3 h pred zahájením 5 h stimulácie 100 ng/ml Pam_3CSK_4 **(A)**, 10 ng/ml LPS **(B)** alebo 20 µg/ml c-di-GMP **(C)**. Výsledky predstavujú reprezentatívne dáta z 2 nezávislých experimentov a sú vyjadrené v ±SEM. Štatistická významnosť bola určená pomocou Studentovho t-testu, ns P> 0,05; *P≤ 0,05; **P≤ 0,01; ***P≤ 0,001.

4.4 Vplyv bakteriálnej životaschopnosti na supresiu signalizačných dráh riadených PRR

Hostiteľská vrodená imunitná odpoveď namierená voči *F. tularensis* LVS zahŕňa koordináciu mnohých signalizačných dráh. V nasledujúcich experimentoch bol študovaný vplyv životaschopnosti baktérie na aktiváciu, ale aj inhibíciu bunkovej signalizácie regulovanej receptormi PRR. Zároveň bola skúmaná aj povaha tzv. PAMPs molekúl *F. tularensis* LVS, ktoré by mohli túto odpoveď ovplyvňovať.

4.4.1 Inhibícia zápalovej odpovede závisí na vitalite *F. tularensis* LVS

Cieľom tejto štúdie bolo zistiť, či je nutná prítomnosť živej baktérie pre supresiu zápalovej odpovede. *F. tularensis* LVS bola preto usmrtená pomocou sonikácie, tepelnej inaktivácie alebo pôsobenia UV-žiarenia. WT *Ifnβ*$^{+/\Delta\beta luc}$ BMDMs boli následne infikované živou alebo mŕtvou *F. tularensis* LVS a po 8 h bola zmeraná IFN-ß luciferázová aktivita. Stimulácia IFN odpovede typu I bola u všetkých foriem zabitia *F. tularensis* LVS v porovnaní so živou baktériou vyššia **(Obr. 4-15)**.

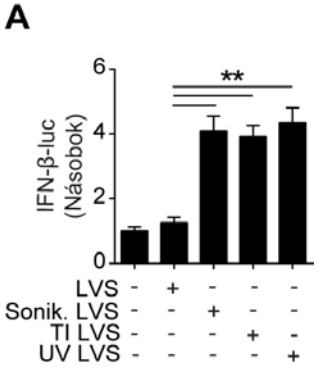

Obr. 4-15: Mŕtva *F. tularensis* LVS neblokuje aktiváciu IFN odpovede typu I. IFN-ß luciferázová aktivita analyzovaná vo WT *Ifnβ*$^{+/\Delta\beta luc}$ BMDMs 8 h po infekcii živou, tepelne inaktivovanou (TI) *F. tularensis* LVS alebo zabitou pôsobením UV-žiarenia. Výsledky predstavujú reprezentatívne dáta z 2 nezávislých experimentov a sú vyjadrené v ±SEM. Štatistická významnosť bola určená pomocou Studentovho t-testu, **P≤ 0,01.

Následne bol testovaný vplyv mŕtvej *F. tularensis* LVS na priebeh signalizačnej kaskády regulovanej receptorom TLR2. WT *Ifnβ*$^{+/\Delta\beta luc}$ BMDMs boli infikované živou alebo sonikovanou formou *F. tularensis* LVS a po 3 h nasledovala stimulácia pomocou ligandu Pam_3CSK_4. Stanovenie IFN-ß luciferázovej aktivity **(Obr. 4-16A)** a hladín mRNA *Ifnb1* a *Tnfa* pomocou qRT-PCR **(Obr. 4-16B**) ukázalo, že sonikovaná forma *F. tularensis* LVS oproti živej baktérii aktivovala zvýšenú prozápalovú aj IFN odpoveď typu I v prítomnosti Pam_3CSK_4. Mŕtva baktéria mala na rozdiel od živej *F. tularensis* LVS oslabenú schopnosť potlačovať signalizáciu kontrolovanú receptorom TLR2 **(Obr. 4-16A-B)**.

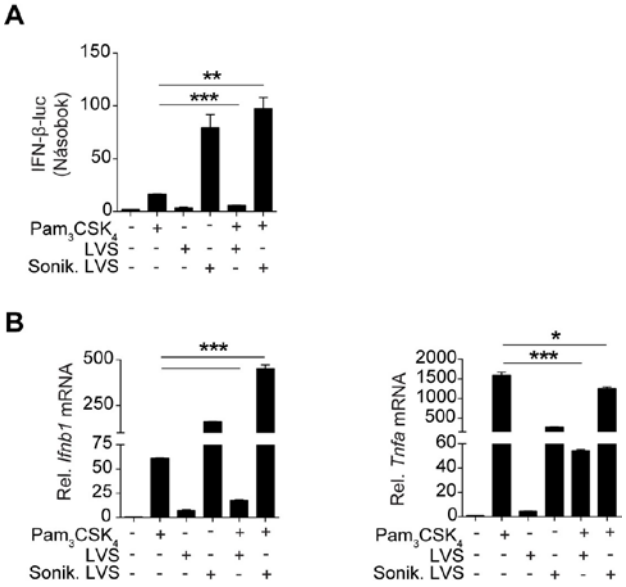

Obr. 4-16: Inhibičný efekt sonikovanej *F. tularensis* LVS na signalizáciu regulovanú receptorom TLR2. (A-B) IFN-ß luciferázová aktivita **(A)** a hladiny mRNA *Ifnb1* a *Tnfa* **(B)** namerané vo WT *Ifnβ*$^{+/\Delta\beta luc}$ BMDMs infikovaných živou alebo sonikovanou *F. tularensis* LVS, prípadne stimulovaných 100 ng/ml Pam_3CSK_4 po 3 h infekcii. Výsledky predstavujú reprezentatívne dáta z 2 nezávislých experimentov a sú vyjadrené v ±SEM. Štatistická významnosť bola určená pomocou Studentovho t-testu, *P≤ 0,05; **P≤ 0,01; ***P≤ 0,001.

Obdobne predošlému experimentu bol skúmaný vplyv aj tepelnej inaktivácie na supresívne vlastnosti *F. tularensis* LVS. WT *Ifnβ*$^{+/\Delta\beta luc}$ BMDMs boli po infekcii živou alebo mŕtvou baktériou stimulované buď agonistom TLR2 **(Obr. 4-17A)** alebo senzora STING **(Obr. 4-17B)**. Oproti stimulácii c-di-GMP, tepelne inaktivovaná *F. tularensis* LVS potlačovala IFN-ß luciferázovú aktivitu vyvolanú pôsobením Pam_3CSK_4.

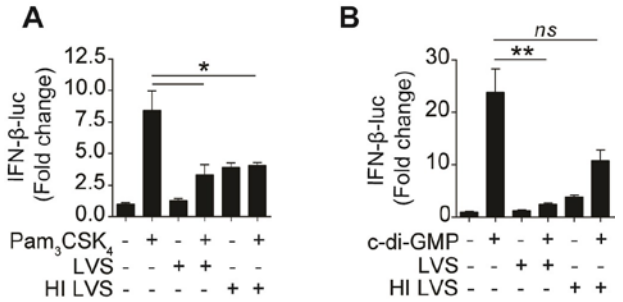

Obr. 4-17: Tepelne inaktivovaná *F. tularensis* LVS suprimuje signalizáciu regulovanú TLR a CDS. (A-B) IFN-ß luciferázová aktivita vo WT *Ifnβ*$^{+/\Delta\beta luc}$ BMDMs infikovaných živou alebo TI *F. tularensis* LVS analyzovaná v 8 h alebo najskôr infikovaných a v 3 h po infekcii stimulovaných 100 ng/ml Pam_3CSK_4 **(A)** alebo 20 µg/ml c-di-GMP **(B)**. Výsledky predstavujú reprezentatívne

dáta z 2 nezávislých experimentov a sú vyjadrené v ±SEM. Štatistická významnosť bola určená pomocou Studentovho t-testu, ns P> 0,05; **P≤ 0,01.

4.4.2 Povaha PAMPs

Pre charakterizáciu molekúl PAMPs stimulujúcich zápalovú odpoveď bola *F. tularensis* LVS podrobená lýze pomocou sonikácie. WT *Ifnß*$^{+/\Delta\beta luc}$ BMDMs boli infikované živou alebo mŕtvou baktériou a po 8 h v nich bola analyzovaná IFN-ß luciferázová aktivita. Získané dáta ukázali výrazne vyššiu stimuláciu produkcie IFN-ß v prítomnosti sonikovanej *F. tularensis* LVS. Avšak v prípade jej ošetrenia tepelnou inaktiváciou bol zaznamenaný výrazný pokles tejto odpovede, zrejme v dôsledku tepelnej denaturácie molekúl proteínovej povahy alebo nukleových kyselín. Pri vystavení bakteriálneho lyzátu pôsobeniu benzonázy, endonukleázy štiepiacej nukleové kyseliny, bol pozorovaný rovnaký trend **(Obr. 4-18)**.

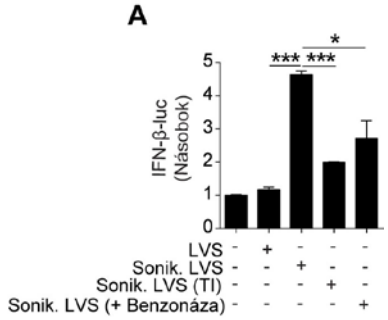

Obr. 4-18: *F. tularensis* LVS aktivuje IFN odpoveď typu I prostredníctvom ligandov proteínovej povahy a nukleových kyselín. IFN-ß luciferázová aktivita bola analyzovaná 8 h po infekcii WT *Ifnß*$^{+/\Delta\beta luc}$ BMDMs *F. tularensis* LVS (MOI 50), sonikovanou baktériou, ale taktiež zlyzovanou *F. tularensis* LVS podrobenou tepelnej inaktivácii (TI), či pôsobeniu benzonázy. Výsledky predstavujú reprezentatívne dáta z 2 nezávislých experimentov a sú vyjadrené v ±SEM. Štatistická významnosť bola určená pomocou Studentovho t-testu, *P≤ 0,05; ***P≤ 0,001.

Sonikovaná *F. tularensis* LVS indukovala znížené hladiny IFN-ß luciferázovej aktivity aj počas infekcie *Myd88*$^{-/-}$*Ifnß*$^{+/\Delta\beta luc}$ alebo *Sting*$^{-/-}$*Ifnß*$^{+/\Delta\beta luc}$ BMDMs **(Obr. 419A)**. Pokles v expresii génov *Ifnb1* a *Tnfa* bol taktiež zaznamenaný v prípade infekcie buniek pochádzajúcich z *Ticam1*$^{-/-}$*Ips1*$^{-/-}$ alebo *Ips1*$^{-/-}$ myší **(Obr. 4-19B, C)**. Výsledky potvrdzujú predchádzajúce zistenie, že *F. tularensis* LVS stimuluje signalizáciu regulovanú TLR (adaptorové molekuly MyD88 a TRIF) prostredníctvom molekúl lipoproteínového charakteru a receptorov CDS a RLR pomocou nukleových kyselín (adaptorové proteíny STING a IPS1).

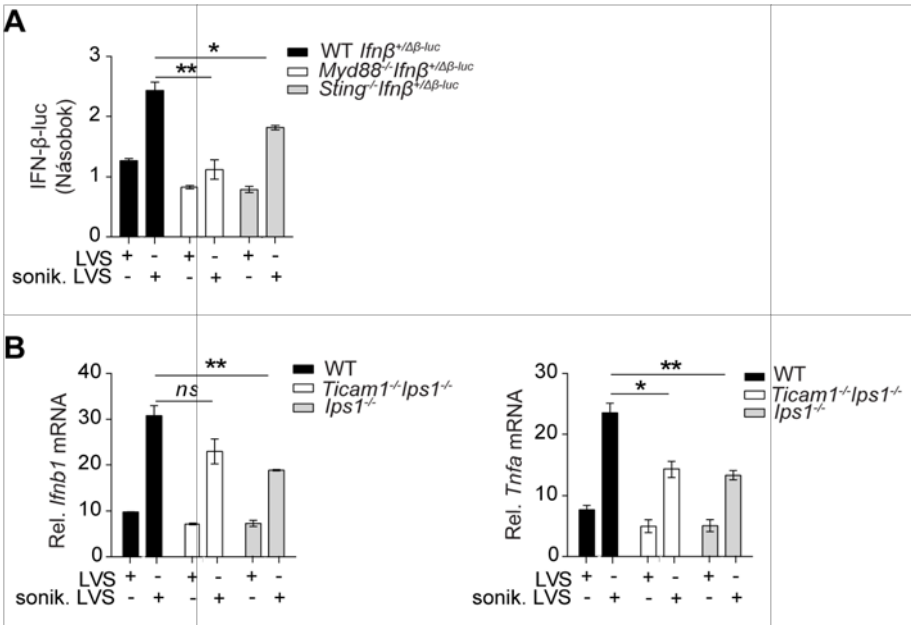

Obr. 4-19: Stimulácia IFN odpovede typu I sonikovanou *F. tularensis* LVS. (A) IFN-ß luciferázová aktivita vo WT *Ifnβ*$^{+/\Delta\beta luc}$, *Myd88*$^{-/-}$*Ifnβ*$^{+/\Delta\beta luc}$ alebo *Sting*$^{-/-}$*Ifnβ*$^{+/\Delta\beta luc}$ BMDMs vyvolaná 8 h po infekcii živou alebo sonikovanou *F. tularensis* LVS (MOI 50). Výsledky predstavujú reprezentatívne dáta z 3 nezávislých experimentov a sú vyjadrené v ±SEM. **(B)** qRT-PCR analýza transkriptov mRNA *Ifnb1* a *Tnfa* po 8 h infekcii WT, *Ticam1*$^{-/-}$*Ips1*$^{-/-}$ alebo *Ips1*$^{-/-}$ BMDMs živou alebo sonikovanou *F. tularensis* LVS (MOI 50). Výsledky sú vyjadrené v ±SEM. Štatistická významnosť bola určená pomocou Studentovho t-testu, ns P> 0,05; *P≤ 0.05, **P≤ 0.01.

4.5 Inhibícia signalizačných dejov *F. tularensis* LVS

Dôležitým aspektom úspešného prežívania intracelulárnych patogénov je aj ovládnutie bunkovej signalizácie a jej následné presmerovanie podľa vlastných potrieb. Preto niet divu, že sa u patogénov vyvinula v priebehu evolúcie celá rada nástrojov, ktoré im umožňujú zasahovať do jednotlivých signalizačných krokov, vrátane procesov fosforylácie a ubikvitinácie. Cieľom nasledujúcich štúdií bolo zistiť, do ktorých týchto dejov zasahuje aj *F. tularensis* LVS.

4.5.1 Supresia fosforylačných a polyubikvitinačných dejov

Vzhľadom na preukázanú schopnosť *F. tularensis* LVS zvrátiť priebeh bunkovej signalizácie riadenej receptormi PRR boli ďalšie experimenty zamerané na detekciu zasiahnutých signalizačných molekúl. WT BMDMs boli infikované buď *F. tularensis* LVS, *ΔiglC*/LVS alebo *ΔdsbA*/LVS počas 15, 30 alebo 60 min. Bunkové lyzáty boli

podrobené Western blotovej analýze. Prítomnosť fosforylovaných foriem TAK1, IKKα/ß, p38 MAPK, TBK1, IRF3 a nahromadenie K63-polyubikvitínových reťazcov bolo detegované vo väčšej miere len vo vzorkách infikovaných mutantnými kmeňmi *F. tularensis* LVS **(Obr. 4-20A, 4-21A)**.

V ďalšom bode štúdie bol skúmaný inhibičný efekt *F. tularensis* LVS na aktiváciu vyššie spomínaných molekúl v prítomnosti *L. monocytogenes* **(Obr. 420B)** alebo ligandu Pam_3CSK_4 **(Obr. 4-21B)**. V oboch prípadoch bola pozorovaná výraznejšia fosforylácia signalizačných molekúl a akumulácia K63-polyubikvitínových reťazcov v priebehu infekcie mutantnými kmeňmi *ΔiglC*/LVS alebo *ΔdsbA*/LVS **(Obr. 4-20B, 4-21B)**. Hoci oproti *L. monocytogenes* vyvolávala *F. tularensis* LVS nižšiu akumuláciu K48-poylubikvitínových reťazcov, ich tvorbu pri ko-infekčných experimentoch nepotlačovala **(Obr. 4-22)**. Získané dáta poukazujú na schopnosť *F. tularensis* LVS inhibovať signalizačné dráhy regulované receptormi PRR a dôležitosť zachovania schopnosti bakteriálneho úteku do cytosólu.

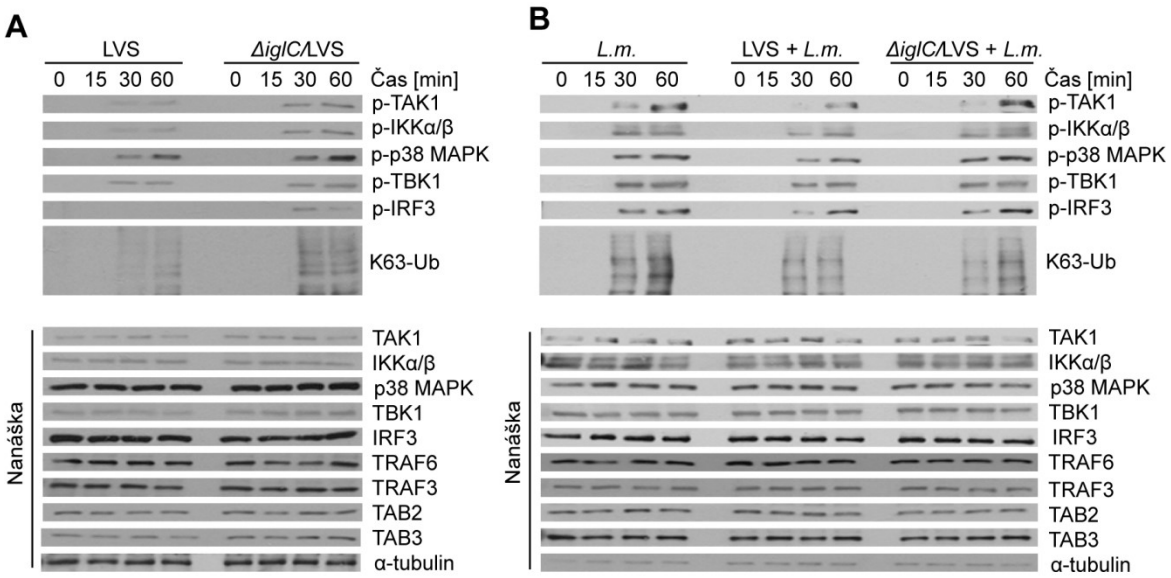

Obr. 4-20: *F. tularensis* LVS blokuje fosforylačné a polyubikvitinačné procesy v signalizačných dráhach riadených PRR. (A-B) WT BMDMs infikované *F. tularensis* LVS alebo *ΔiglC*/LVS **(A)**, prípadne najskôr infikované *F. tularensis* LVS alebo *ΔiglC*/LVS a po 3 h stimulované *L. monocytogenes* **(B)** boli analyzované v časových intervaloch 0, 15, 30, 60 min alebo 3 h + 15, 30 a 60 min pomocou Western blotu na prítomnosť buď fosforylovaných foriem TAK1, IKKα/ß, p38, TBK1, IRF3 alebo nahromadenia K63-polyubikvitínových reťazcov. Ako kontroly hladiny celkového množstva proteínu boli detegované TAK1, IKKα/ß, p38, TBK1, IRF3, TRAF6, TRAF3, TAB2, TAB3 alebo α-tubulín. Výsledky predstavujú reprezentatívne dáta z 2 nezávislých experimentov.

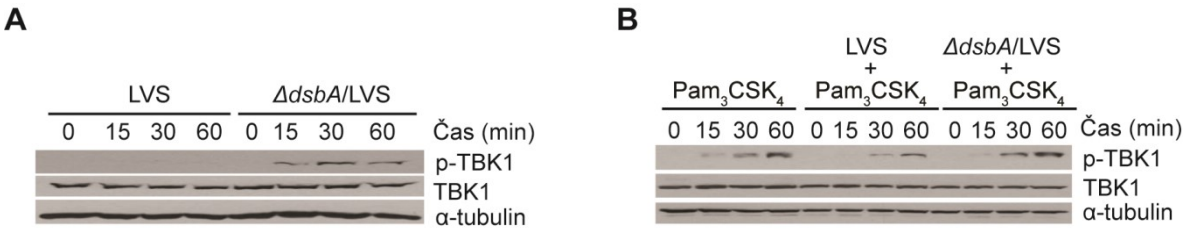

Obr. 4-21: Vplyv fagozomálneho úniku *F. tularensis* LVS na aktiváciu TBK1 indukovanú receptorom TLR2. (A-B) Western blot analýza WT BMDMs infikovaných buď *F. tularensis* LVS alebo *ΔdsbA*/LVS **(A)**, prípadne infikovaných *F. tularensis* LVS alebo *ΔdsbA*/LVS a po 3 h stimulovaných 100 ng/ml Pam_3CSK_4 **(B)** v časových intervaloch 0, 15, 30, 60 min alebo 3 h + 15, 30 a 60 min na prítomnosť fosforylovanej formy TBK1. Ako kontroly hladiny celkového množstva proteínu boli detegované TBK1 a α-tubulín. Výsledky predstavujú reprezentatívne dáta z 3 nezávislých experimentov.

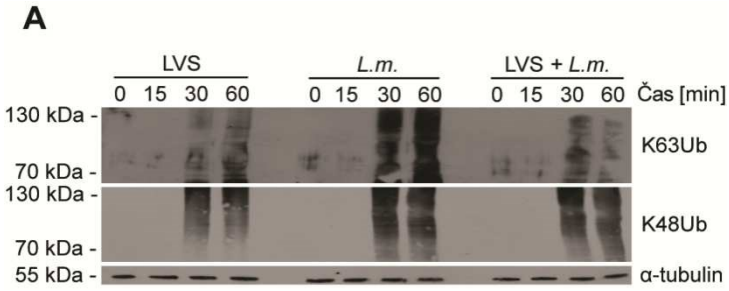

Obr. 4-22: *F. tularensis* LVS potlačuje nahromadenie K63-polyubikvitínových reťazcov. Western blot analýza WT BMDMs infikovaných buď *F. tularensis* LVS alebo *L. monocytogenes*, prípadne infikovaných *F. tularensis* LVS a po 3 h stimulovaných *L. monocytogenes* v časových intervaloch 0, 15, 30, 60 min alebo 3 h + 15, 30 a 60 min na prítomnosť K63- alebo K48-polyubikvitínových reťazcov. Ako kontrola hladiny celkového množstva proteínu bol detegovaný α-tubulín. Výsledky predstavujú reprezentatívne dáta z 2 nezávislých experimentov.

4.5.2 Inhibícia vzniku signálnych komplexov TRAF6 a TRAF3

Pre overenie vplyvu supresívneho efektu *F. tularensis* LVS na zloženie dôležitých prozápalových signalizačných komplexov TRAF6 a TRAF3, boli WT BMDMs podrobené infekcii *F. tularensis* LVS, *ΔiglC*/LVS alebo následnej ko-infekcii s *L. monocytogenes*. Vzorky imunoprecipitované na príslušný TRAF proteín boli potom analyzované pomocou Western blotu na prítomnosť TAK1, IKKα/ß, TKB1, IRF3, TAB2, TAB3, TRAF6, TRAF3 alebo K63-polyubikvitínových reťazcov. V porovnaní s *ΔiglC*/LVS, *F. tularensis* LVS aktivovala zníženú tvorbu K63-polyubikvitínových reťazcov a menšie zoskupenie sa TAK1, TAB2 a TAB3 v komplexe TRAF6 **(Obr. 423A)** alebo TBK1 v TRAF3 **(Obr. 4-23C)**. V prípade ko-infekčných experimentov vykazovala

F. tularensis LVS oproti *ΔiglC*/LVS zvýšenú schopnosť suprimovať tvorbu komplexu TRAF6 **(Obr. 4-23B)** alebo TRAF3 **(Obr. 4-23D)** aktivovanú prostredníctvom *L. monocytogenes*. Nadobudnuté dáta nasvedčujú tomu, že *F. tularensis* LVS ovplyvňuje priebeh signalizácie indukovanej receptormi PRR prostredníctvom inhibície vzniku týchto komplexov.

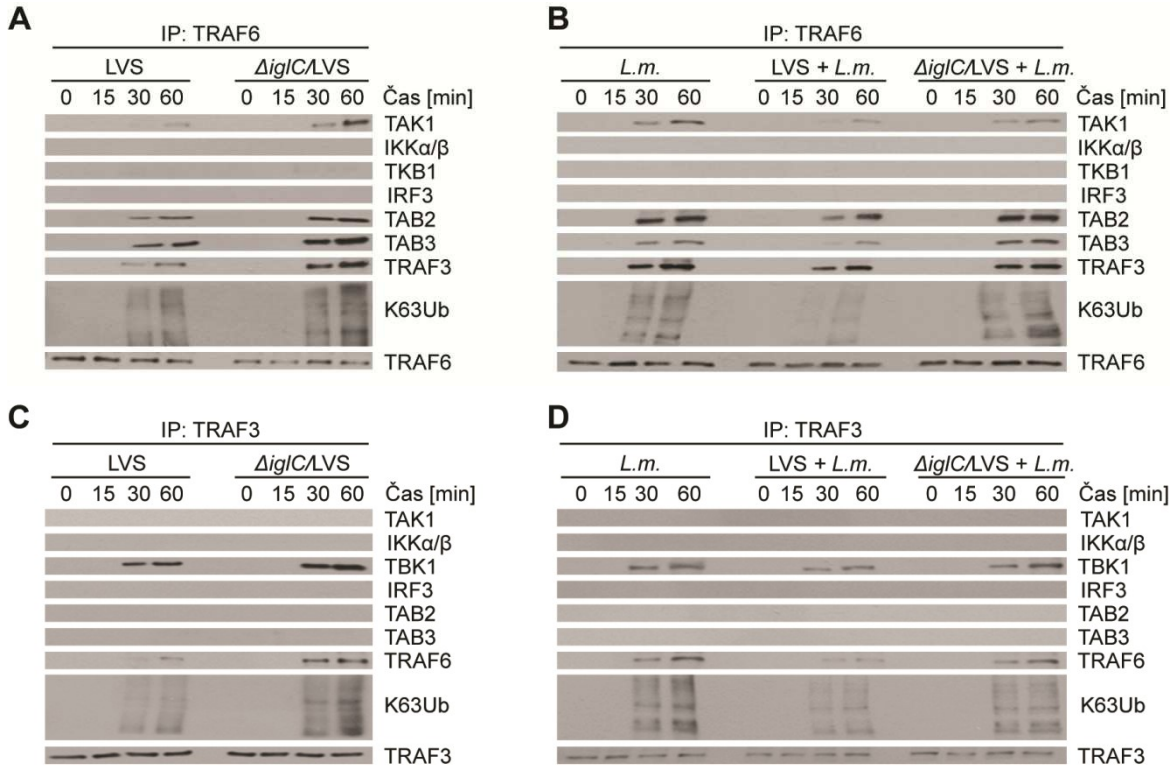

Obr. 4-23: *F. tularensis* LVS potlačuje vytvorenie signalizačných komplexov TRAF6 a TRAF3. (A-D) Western blot analýza imunoprecipitovaných signálnych komplexov TRAF6 **(A, B)** a TRAF3 **(C, D)** v časových intervaloch 0, 15, 30, 60 min alebo 3 h + 15, 30 a 60 min na prítomnosť TAK1, IKKα/ß, TBK1, IRF3, TAB2, TAB3, TRAF3, TRAF6 alebo K63polyubikvitínových reťazcov. Vzorky pochádzali z WT BMDMs infikovaných *F. tularensis* LVS alebo *ΔiglC*/LVS, prípadne najskôr infikovaných *F. tularensis* LVS alebo *ΔiglC*/LVS a po 3 h ko-infikovnaých *L. monocytogenes.* Výsledky predstavujú reprezentatívne dáta z 2 nezávislých experimentov.

5 Diskusia

Vysoká virulencia *F. tularensis* je z časti pripisovaná schopnosti tohto patogéna úspešne prežívať v hostiteľských bunkách bez spustenia výraznej imunitnej odpovede (Butchar et al. 2008; Chase et al. 2009; Huang et al. 2010; Walters et al. 2015). V priebehu zložitého životného cyklu čelí *F. tularensis* celej rade hostiteľských obranných mechanizmov, vrátane možnej aktivácie signalizačných kaskád riadených rôznymi PRR. Predpokladá sa, že svoju úlohu v ich obídení môže zohrávať schopnosť tejto baktérie

pozmeniť biologickú dostupnosť, ako aj štruktúru svojich povrchových molekúl alebo inhibovať niektoré signalizačné deje (Telepnev et al. 2003; Phillips et al. 2004; Jones et al. 2012b; Ireland et al. 2013). Dôležitých zástupcov PRR účastniacich sa stimulácie prozápalovej odpovede predstavujú senzory z rodín TLR, RLR a CDS. Spôsob akým *F. tularensis* aktivuje alebo moduluje priebeh bunkovej signalizácie sprostredkovanej týmito receptormi nie je ale zatiaľ úplne objasnený.

Pre charakterizáciu signálnych kaskád regulovaných vyššie spomínanými receptormi boli použité primárne kostne-dreňové makrofágy deficientné pre rôzne adaptorové proteíny. Konkrétne bola sledovaná IFN odpoveď typu I, ktorá zohráva vo vrodenej imunitnej obrane proti *F. tularensis* kľúčovú úlohu (Henry et al. 2007; Cole et al. 2008). Získané výsledky ukázali, že *F. tularensis* subsp. *holarctica* LVS (*F. tularensis* LVS) stimuluje pomerne nízku prozápalovú odpoveď prostredníctvom MyD88, TRIF, STING a IPS1 **(Obr. 4-1; 4-2)**. MyD88-dependentná signalizácia bola pravdepodobne sprostredkovaná aktiváciou TLR9 bakteriálnou DNA alebo TLR2 povrchovými lipoproteínmi *F. tularensis* LVS **(Obr. 4-18; 4-19)** (Cole et al. 2007; Abplanalp et al. 2009; Dietrich et al. 2010). Produkcia IFN typu I prostredníctvom STING bola potvrdená už v predchádzajúcich štúdiách (Jones et al. 2010; Jin et al. 2011). Tento adaptorový proteín mohol byť stimulovaný po rozlíšení cytoplazmatickej
DNA pochádzajúcej z *F. tularensis* LVS cytosólickým DNA senzorom cGAS **(Obr. 418; 4-19)** (Storek et al. 2015). V prípade TLR3- a TLR4-regulovanej signalizácie zohráva významnú úlohu TRIF, ktorý je ale nevyhnutný aj pre optimálnu aktiváciu TLR2-MyD88- a cGAS-STING-signalizačných dráh (Petnicki-Ocwieja et al. 2013; Wang et al. 2016). Adaptorový proteín IPS1 je známy svojou účasťou v RLR-závislej signalizácii, ale taktiež môže umocňovať aktiváciu cGAS-STING signalizácie vďaka detekcii RNA vzniknutej *de novo* po prepise mikrobiálnej dsDNA RNA-polymerázou III (Chiu et al. 2009). Avšak, či prozápalová odpoveď indukovaná prostredníctvom TRIF a IPS1 v priebehu infekcie *F. tularensis* LVS vzniká len v dôsledku ich pomocnej úlohy v aktivácii MyD88- a STING-závislej signalizácie zostáva nejasné. V priebehu infekcie *F. novicida* totižto nebola účasť týchto adaptorových proteínov spoločne s MyD88 v aktivácii IFN odpovede typu I potvrdená (Henry et al. 2007). Napriek tomu je zrejmé, že signálne kaskády regulované PRR sú funkčne prepojené, a že vznik prozápalovej odpovede po

infekcii *F. tularensis* LVS je výsledkom simultánnej alebo sekvenčnej aktivácie mnohých týchto dráh.

Pre dobre adaptovaný patogén je najefektívnejším nástrojom na prekonanie hostiteľskej imunitnej obrany viacstupňový útok na signalizačné dráhy riadené PRR. Výsledky tejto dizertačnej práce odhalili, že *F. tularensis* LVS stimuluje, ale zároveň aktívne blokuje signalizačné dráhy riadené TLR, CDS a RLR **(Obr. 4-6; 4-7; 4-8; 4-9)**. Za túto inhibíciu môže byť zodpovedná schopnosť *F. tularensis* LVS interferovať s regulačnými bodmi signalizácie riadenej PRR, a to komplexmi TRAF6 a TRAF3. Tieto E3 ubikvitín-ligázy sa po aktivácii spomínaných receptorov účastnia K63polyubikvitinačných procesov, čím zabezpečujú chod signalizačných dejov vedúcich až k expresii prozápalových cytokínov (Panda et al. 2015). No, v prípade *F. tularensis* dochádza k inhibícii akumulácie týchto polyubikvitínových reťazcov ako aj zoskupenia TAB2, TAB3 a TAK1 v komplexe TRAF6 alebo TBK1 v TRAF3 **(Obr. 4-23)**. Tieto dáta boli potvrdené aj zníženou aktiváciou signalizačných molekúl p-TAK1, p-p38 MAPK, p-IKKα/ß, p-TBK1 a p-IRF3 **(Obr. 4-20B; 4-21B)**. Schopnosť *F. tularensis* zasahovať do týchto dôležitých centier bunkovej signalizácie môže vysvetľovať súčasnú inhibíciu viacerých signalizačných dráh riadených PRR. Presný mechanizmus supresie týchto komplexov zostáva ale zatiaľ nejasný. Jeden z potenciálnych inhibítorov TRAF6 a TRAF3 môže predstavovať SOCS3, ktorého expresia je v priebehu infekcie významne zvýšená (Parsa et al. 2008). Okrem toho, že tento hostiteľský proteín reguluje proteazomálnu degradáciu TBK1, inhibuje aj aktiváciu týchto signalizačných komplexov (Frobøse et al. 2006; Inagaki-Ohara et al. 2013; Liu et al. 2015). *F. tularensis* je avšak schopná zasahovať aj do ďalších signalizačných krokov. Okrem zníženej aktivácie receptorov ovplyvňuje aj bunkovú signalizáciu na transkripčnej úrovni, či už potlačením aktivácie IRF1, IRF8, NF-κB alebo degradáciou hostiteľskej mRNA (Hajjar et al. 2006; Zarrella et al. 2011; Jones et al. 2012b; Ireland et al. 2013; Crane et al. 2013; Bauler et al. 2014; Walters et al. 2015).

Avšak zostáva otázne, či za schopnosťou *F. tularensis* LVS aktivovať, ale následne utlmovať vnútrobunkovú signalizáciu nestojí pozmenená virulencia baktérie. Predchádzajúce štúdie poukazujú na fakt, že výsledný fenotyp baktérie môže byť výrazne ovplyvnený zvolenými rastovými podmienkami (Golovliov et al. 1997; Loegering et al. 2006; Zarrella et al. 2011; Singh et al. 2013; Steiner et al. 2014). *F. tularensis* kultivovaná

v Mueller-Hintonovom médiu vykazovala na rozdiel od baktérií adaptovaných na hostiteľské prostredie schopnosť stimulovať prozápalovú odpoveď (Singh et al. 2013). Tieto rozdiely by mohli vysvetľovať, prečo *F. tularensis* vykazuje v priebehu infekcie imunostimulačný, ale vzápätí aj imunosupresívny charakter.

Špecifické bakteriálne efektorové proteíny zodpovedné za rozvrátenie vrodenej imunity nie sú zatiaľ známe. IglC a DsbA (FipB) predstavujú významné virulenčné faktory, ktorých prítomnosť je nevyhnutná pre správne fungovanie T6SS a taktiež bakteriálny vstup do cytoplazmy (Lindgren et al. 2004a; Qin et al. 2009, 2016). Výsledky tejto dizertačnej práce poukazujú na fakt, že strata týchto proteínov závažne narušuje schopnosť *F. tularensis* LVS blokovať signalizačné kaskády riadené PRR **(Obr. 4-10; 4-13; 4-14)**. Zvýšená stimulácia prozápalovej odpovede atenuovanými kmeňmi by mohla byť vyvolaná neprerušovanou stimuláciou TLR v dôsledku ich predĺženého zadržiavania vo fagozóme a zároveň ich neschopnosťou aktívne inhibovať signalizáciu riadenú PRR (Cole et al. 2010). Avšak v priebehu infekcie *ΔiglC*/LVS bolo v porovnaní s *ΔdsbA*/LVS pozorované mierne potlačenie prozápalovej odpovede po stimulácii *L. monocytogenes* alebo exogénnymi ligandmi. To naznačuje, že napriek hlavnej úlohe T6SS v supresii signalizačných dráh PRR, môžu hrať svoju úlohu síce v menšej miere aj ďalšie faktory, ktoré sú nezávislé od prítomnosti *F. tularensis* LVS v cytosóle. Navyše je možné, že strata proteínu DsbA zodpovedného za správne zloženie niektorých komponent T6SS a potenciálnych supresorových molekúl môže viesť ku zníženej inhibičnej schopnosti tohto mutanta (Qin et al. 2016). Získané dáta poukazujú na to, že inhibícia vrodenej imunitnej odpovede *F. tularensis* LVS súvisí s bakteriálnou lokalizáciou v cytoplazme a/alebo že je táto inhibícia sprostredkovaná efektorovými proteínmi T6SS.

Výsledky dizertačnej práce taktiež ukázali, že inhibícia signalizačných kaskád riadených PRR závisí od životaschopnosti *F. tularensis* LVS **(Obr. 4-15; 4-16; 4-17)**. Tieto dáta sú v súlade s prácou skupiny Dr. Bosio, ktorá uvádza, že stimulácia prozápalovej odpovede exogénnymi ligandmi je blokovaná len v prítomnosti živej baktérie (Telepnev et al. 2003; Bosio and Dow 2005; Chase et al. 2009). To znamená, že za supresiu je zodpovedná buď metabolicky aktívna baktéria, molekula citlivá na proces bakteriálneho zabitia alebo komponenty ktorá by mohla byť odmytá v priebehu prípravy bakteriálnej suspenzie. V štúdii Telepnev et al. bolo zistené, že tento jav je nezávislý od *de novo* proteínovej syntézy *F. tularensis* (Telepnev et al. 2003). Okrem toho,

nadobudnuté výsledky poukazujú na možnú prítomnosť supresorových molekúl, ako sú napríklad bakteriálne lipidy (Ireland et al. 2013; Crane et al. 2013). V prípade zabitia *F. tularensis* LVS tepelnou inaktiváciou nebolo totižto preukázané úplné vymiznutie inhibičného efektu baktérie **(Obr. 4-17)**. To naznačuje, že na supresii vrodenej imunitnej odpovede sa môžu účastniť aj ďalšie faktory, ktorých funkcia nie je závislá od životaschopnosti *F. tularensis* LVS.

Špecifické virulenčné mechanizmy podieľajúce sa na rozvrátení signalizačných kaskád riadených PRR zostávajú aj naďalej neobjasnené. Avšak táto dizertačná práca odhalila prítomnosť bakteriálnych faktorov umožňujúcich *F. tularensis* LVS manipulovať hostiteľský ubikvitínový systém. Okrem toho výsledky naznačujú, že schopnosť *F. tularensis* LVS blokovať priebeh bunkovej signalizácie riadenej PRR úzko súvisí s prítomnosťou virulenčných faktorov dôležitých pre fagozomálny únik baktérie do cytoplazmy. Tento vnútrobunkový priestor predstavuje vyhľadávané útočisko mnohých patogénov najmä kvôli bohatému prísunu živín. Zároveň ale tvorí aj domov hostiteľskej imunitnej obrany, vrátane mnohých PRR, ktorých aktivácia znamená potenciálnu hrozbu pre nedostatočne „ozbrojené“ baktérie. Preto môže byť schopnosť *F. tularensis* zosynchronizovať jej útek do cytoplazmy s aktívnym rozvrátením signalizačných dráh PRR považovaná za významnú bakteriálnu stratégiu, ktorá umožňuje *F. tularensis* úspešne prežívať v hostiteľovi.

6 Záver

Cieľom dizertačnej práce bolo objasniť priebeh bunkovej signalizácie riadenej PRR počas skorej fáze infekcie BMDMs *F. tularensis* subsp. *holarctica* LVS (*F. tularensis* LVS). Získané výsledky je možné zhrnúť do nasledujúcich záverov:

- *F. tularensis* LVS je schopná stimulovať, ale zároveň aj aktívne inhibovať signalizačné kaskády riadené TLR, RLR a CDS.
- Za inhibíciu týchto signalizačných dráh je zodpovedná schopnosť *F. tularensis* LVS potlačovať vznik K63-polyubikvitínových reťazcov a následne aj komplexov TRAF6 a TRAF3 **(Obr. 6-1)**.
- Tento inhibičný efekt je závislý od fagozomálneho úteku *F. tularensis* LVS do cytosólu a/alebo prítomnosti funkčného T6SS.
- Pre inhibíciu signálnych kaskád PRR je vyžadovaná prítomnosť životaschopnej baktérie.

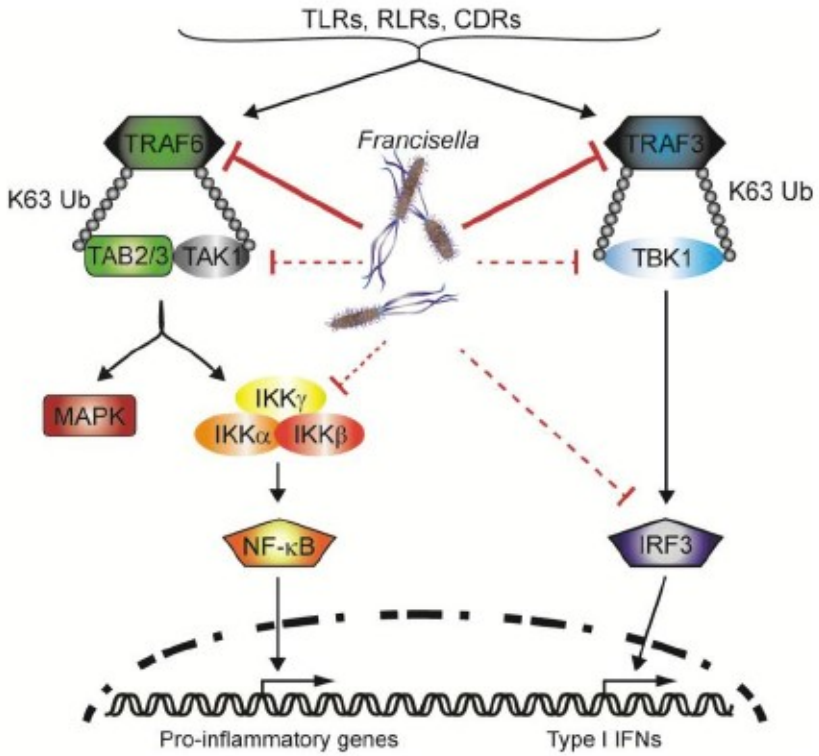

Obr. 6-1: Model bunkovej signalizácie riadenej PRR v makrofágoch infikovaných *F. tularensis* subsp. *holarctica* LVS.

7 Zoznam použitej literatúry

Abdullah Z, Schlee M, Roth S, et al (2012) RIG-I detects infection with live *Listeria* by sensing secreted bacterial nucleic acids. EMBO J 31:4153–4164. doi: 10.1038/emboj.2012.274

Abe T, Barber GN (2014) Cytosolic-DNA-mediated, STING-dependent proinflammatory gene induction necessitates canonical NF-κB activation through TBK1. J Virol 88:5328–5341. doi: 10.1128/JVI.00037-14

Abplanalp AL, Morris IR, Parida BK, et al (2009) TLR–Dependent Control of *Francisella tularensis* Infection and Host Inflammatory Responses. PLoS ONE 4:e7920. doi: 10.1371/journal.pone.0007920

Adachi O, Kawai T, Takeda K, et al (1998) Targeted disruption of the MyD88 gene results in loss of IL-1- and IL-18-mediated function. Immunity 9:143–150

Adhikari A, Xu M, Chen ZJ (2007) Ubiquitin-mediated activation of TAK1 and IKK. Oncogene 26:3214–3226. doi: 10.1038/sj.onc.1210413

Ajibade AA, Wang HY, Wang R-F (2013) Cell type-specific function of TAK1 in innate immune signaling. Trends Immunol 34:307–316. doi: 10.1016/j.it.2013.03.007

Ancuta P, Pedron T, Girard R, et al (1996) Inability of the *Francisella tularensis* lipopolysaccharide to mimic or to antagonize the induction of cell activation by endotoxins. Infect Immun 64:2041–2046

Anthony LS, Morrissey PJ, Nano FE (1992) Growth inhibition of *Francisella tularensis* live vaccine strain by IFN-gamma-activated macrophages is mediated by reactive nitrogen intermediates derived from L-arginine metabolism. J Immunol 148:1829–1834

Atianand MK, Fitzgerald KA (2013) Molecular Basis of DNA Recognition in the Immune System. J Immunol 190:1911–1918. doi: 10.4049/jimmunol.1203162

Bakshi CS, Malik M, Regan K, et al (2006) Superoxide Dismutase B Gene (sodB)Deficient Mutants of *Francisella tularensis* Demonstrate Hypersensitivity to Oxidative

Stress and Attenuated Virulence. J Bacteriol 188:6443–6448. doi: 10.1128/JB.00266-06

Balagopal A, MacFarlane AS, Mohapatra N, et al (2006) Characterization of the receptor-ligand pathways important for entry and survival of *Francisella tularensis* in human macrophages. Infect Immun 74:5114–5125. doi: 10.1128/IAI.00795-06

Barel M, Hovanessian AG, Meibom K, et al (2008) A novel receptor - ligand pathway for entry of *Francisella tularensis* in monocyte-like THP-1 cells: interaction between surface nucleolin and bacterial elongation factor Tu. BMC Microbiol 8:145. doi: 10.1186/1471-2180-8-145

Barker JR, Chong A, Wehrly TD, et al (2009) The *Francisella tularensis* pathogenicity island encodes a secretion system that is required for phagosome escape and virulence. Mol Microbiol 74:1459–1470

Baron GS, Nano FE (1998) MglA and MglB are required for the intramacrophage growth of *Francisella novicida*. Mol Microbiol 29:247–259. doi: 10.1046/j.1365-2958.1998.00926.x

Bauler TJ, Chase JC, Wehrly TD, Bosio CM (2014) Virulent *Francisella tularensis* Destabilize Host mRNA to Rapidly Suppress Inflammation. J Innate Immun 6:793–805. doi: 10.1159/000363243

Bosio CM (2011) The subversion of the immune system by *Francisella tularensis*. Front Microbiol 2:9. doi: 10.3389/fmicb.2011.00009

Bosio CM, Bielefeldt-Ohmann H, Belisle JT (2007) Active suppression of the pulmonary immune response by *Francisella tularensis* Schu4. J Immunol Baltim Md 1950 178:4538–4547

Bosio CM, Dow SW (2005) *Francisella tularensis* induces aberrant activation of pulmonary dendritic cells. J Immunol Baltim Md 1950 175:6792–6801

Botos I, Segal DM, Davies DR (2011) The structural biology of Toll-like receptors. Struct Lond Engl 1993 19:447–459. doi: 10.1016/j.str.2011.02.004

Brodmann M, Dreier RF, Broz P, Basler M (2017) *Francisella* requires dynamic type VI secretion system and ClpB to deliver effectors for phagosomal escape. Nat Commun 8:15853. doi: 10.1038/ncomms15853

Bron PA, Monk IR, Corr SC, et al (2006) Novel luciferase reporter system for in vitro and organ-specific monitoring of differential gene expression in *Listeria monocytogenes*. Appl Environ Microbiol 72:2876–2884. doi: 10.1128/AEM.72.4.2876-2884.2006

Brotcke A, Monack DM (2008) Identification of fevR, a Novel Regulator of Virulence Gene Expression in *Francisella novicida*. Infect Immun 76:3473–3480. doi: 10.1128/IAI.00430-08

Broz P, Monack DM (2013) Newly described pattern recognition receptors team up against intracellular pathogens. Nat Rev Immunol 13:551–565. doi: 10.1038/nri3479

Burdette DL, Monroe KM, Sotelo-Troha K, et al (2011) STING is a direct innate immune sensor of cyclic di-GMP. Nature 478:515–518. doi: 10.1038/nature10429

Butchar JP, Cremer TJ, Clay CD, et al (2008) Microarray Analysis of Human Monocytes Infected with *Francisella tularensis* Identifies New Targets of Host Response Subversion. PLoS ONE 3:e2924. doi: 10.1371/journal.pone.0002924

Carvalho CL, Lopes de Carvalho I, Zé-Zé L, et al (2014) Tularaemia: A challenging zoonosis. Comp Immunol Microbiol Infect Dis 37:85–96. doi: 10.1016/j.cimid.2014.01.002

Case EDR, Chong A, Wehrly TD, et al (2014) The *Francisella* O-antigen mediates survival in the macrophage cytosol via autophagy avoidance. Cell Microbiol 16:862–877. doi: 10.1111/cmi.12246

Celli J, Zahrt TC (2013) Mechanisms of *Francisella tularensis* Intracellular Pathogenesis. Cold Spring Harb Perspect Med 3:. doi: 10.1101/cshperspect.a010314

Centers for Disease Control and Prevention. (2000) Biological and chemical terrorism: strategic plan for preparedness and response: recommendations of the CDC Strategic Planning Workgroup.

Chamberlain RE (1965) Evaluation of Live Tularemia Vaccine Prepared in a Chemically Defined Medium. Appl Microbiol 13:232–235

Chan YK, Gack MU (2016) Viral evasion of intracellular DNA and RNA sensing. Nat Rev Microbiol 14:360–373. doi: 10.1038/nrmicro.2016.45

Chase JC, Celli J, Bosio CM (2009) Direct and Indirect Impairment of Human Dendritic Cell Function by Virulent *Francisella tularensis* Schu S4. Infect Immun 77:180–195. doi: 10.1128/IAI.00879-08

Chiu Y-H, Macmillan JB, Chen ZJ (2009) RNA polymerase III detects cytosolic DNA and induces type I interferons through the RIG-I pathway. Cell 138:576–591. doi: 10.1016/j.cell.2009.06.015

Chong A, Wehrly TD, Child R, et al (2012) Cytosolic clearance of replication-deficient mutants reveals *Francisella tularensis* interactions with the autophagic pathway. Autophagy 8:1342–1356. doi: 10.4161/auto.20808

Clemens DL, Ge P, Lee B-Y, et al (2015) Atomic structure of T6SS reveals interlaced array essential to function. Cell 160:940–951. doi: 10.1016/j.cell.2015.02.005

Clemens DL, Lee B-Y, Horwitz MA (2005) *Francisella tularensis* enters macrophages via a novel process involving pseudopod loops. Infect Immun 73:5892–5902. doi: 10.1128/IAI.73.9.5892-5902.2005

Cole LE, Laird MHW, Seekatz A, et al (2010) Phagosomal retention of *Francisella tularensis* results in TIRAP/Mal-independent TLR2 signaling. J Leukoc Biol 87:275–281. doi: 10.1189/jlb.0909619

Cole LE, Mann BJ, Shirey KA, et al (2011) Role of TLR signaling in *Francisella tularensis*-LPS-induced, antibody-mediated protection against *Francisella tularensis* challenge. J Leukoc Biol 90:787–797. doi: 10.1189/jlb.0111014

Cole LE, Santiago A, Barry E, et al (2008) Macrophage Proinflammatory Response to *Francisella tularensis* Live Vaccine Strain Requires Coordination of Multiple Signaling Pathways. J Immunol 180:6885–6891

Cole LE, Shirey KA, Barry E, et al (2007) Toll-Like Receptor 2-Mediated Signaling Requirements for *Francisella tularensis* Live Vaccine Strain Infection of Murine Macrophages. Infect Immun 75:4127–4137. doi: 10.1128/IAI.01868-06

Cowley SC, Elkins KL (2011) Immunity to *Francisella*. Front Microbiol 2:. doi: 10.3389/fmicb.2011.00026

Crane DD, Bauler TJ, Wehrly TD, Bosio CM (2014) Mitochondrial ROS potentiates indirect activation of the AIM2 inflammasome. Front Microbiol 5:. doi: 10.3389/fmicb.2014.00438

Crane DD, Ireland R, Alinger JB, et al (2013) Lipids Derived from Virulent *Francisella tularensis* Broadly Inhibit Pulmonary Inflammation via Toll-Like Receptor 2 and Peroxisome Proliferator-Activated Receptor α. Clin Vaccine Immunol CVI 20:1531–1540. doi: 10.1128/CVI.00319-13

Dai S, Rajaram MVS, Curry HM, et al (2013) Fine Tuning Inflammation at the Front Door: Macrophage Complement Receptor 3-mediates Phagocytosis and Immune Suppression for *Francisella tularensis*. PLoS Pathog 9:. doi: 10.1371/journal.ppat.1003114

De Pascalis R, Taylor BC, Elkins KL (2008) Diverse Myeloid and Lymphoid Cell Subpopulations Produce Gamma Interferon during Early Innate Immune Responses to *Francisella tularensis* Live Vaccine Strain. Infect Immun 76:4311–4321. doi: 10.1128/IAI.00514-08

Dempsey A, Bowie AG (2015) Innate immune recognition of DNA: A recent history. Virology 479–480:146–152. doi: 10.1016/j.virol.2015.03.013

Dennis DT, Inglesby TV, Henderson DA, et al (2001) Tularemia as a biological weapon: medical and public health management. JAMA 285:2763–2773

Dietrich N, Lienenklaus S, Weiss S, Gekara NO (2010) Murine toll-like receptor 2 activation induces type I interferon responses from endolysosomal compartments. PloS One 5:e10250. doi: 10.1371/journal.pone.0010250

Eigelsbach HT, Downs CM (1961) Prophylactic Effectiveness of Live and Killed Tularemia Vaccines I. Production of Vaccine and Evaluation in the White Mouse and Guinea Pig. J Immunol 87:415–425

Eliasson H, Lindbäck J, Nuorti JP, et al (2002) The 2000 Tularemia Outbreak: A CaseControl Study of Risk Factors in Disease-Endemic and Emergent Areas, Sweden. Emerg Infect Dis 8:956–960. doi: 10.3201/eid0809.020051

Elkins KL, Cooper A, Colombini SM, et al (2002) In vivo clearance of an intracellular bacterium, *Francisella tularensi*s LVS, is dependent on the p40 subunit of interleukin-12 (IL-12) but not on IL-12 p70. Infect Immun 70:1936–1948

Ellis J, Oyston PCF, Green M, Titball RW (2002) Tularemia. Clin Microbiol Rev 15:631–646. doi: 10.1128/CMR.15.4.631-646.2002

Ericsson M, Kroca M, Johansson T, et al (2001) Long-lasting recall response of CD4+ and CD8+ alphabeta T cells, but not gammadelta T cells, to heat shock proteins of *Francisella tularensis*. Scand J Infect Dis 33:145–152

Feng Y, Chao W (2011) Toll-like receptors and myocardial inflammation. Int J Inflamm 2011:170352. doi: 10.4061/2011/170352

Fernandes-Alnemri T, Yu J-W, Juliana C, et al (2010) The AIM2 inflammasome is critical for innate immunity to *Francisella tularensis*. Nat Immunol 11:385–393. doi: 10.1038/ni.1859

Fitzgerald KA, Rowe DC, Barnes BJ, et al (2003) LPS-TLR4 signaling to IRF-3/7 and NF-kappaB involves the toll adapters TRAM and TRIF. J Exp Med 198:1043–1055. doi: 10.1084/jem.20031023

Forsman M, Sandström G, Sjöstedt A (1994) Analysis of 16S ribosomal DNA sequences of *Francisella* strains and utilization for determination of the phylogeny of the genus and for identification of strains by PCR. Int J Syst Bacteriol 44:38–46. doi: 10.1099/00207713-44-1-38

Fortinea N, Trieu-Cuot P, Gaillot O, et al (2000) Optimization of green fluorescent protein expression vectors for in vitro and in vivo detection of *Listeria monocytogenes*.

Res Microbiol 151:353–360
Franchi L, Warner N, Viani K, Nuñez G (2009) Function of Nod-like Receptors in Microbial Recognition and Host Defense. Immunol Rev 227:106–128. doi: 10.1111/j.1600-065X.2008.00734.x

Francis E (1921) The occurence of tularaemia in man. Public Health Rep 36:1731–1738

Frobøse H, Rønn SG, Heding PE, et al (2006) Suppressor of cytokine Signaling-3 inhibits interleukin-1 signaling by targeting the TRAF-6/TAK1 complex. Mol Endocrinol Baltim Md 20:1587–1596. doi: 10.1210/me.2005-0301

Geier H, Celli J (2011) Phagocytic receptors dictate phagosomal escape and intracellular proliferation of *Francisella tularensis*. Infect Immun 79:2204–2214. doi: 10.1128/IAI.01382-10

Golovliov I, Ericsson M, Sandström G, et al (1997) Identification of proteins of *Francisella tularensis* induced during growth in macrophages and cloning of the gene encoding a prominently induced 23-kilodalton protein. Infect Immun 65:2183–2189

Golovliov I, Sjöstedt A, Mokrievich A, Pavlov V (2003) A method for allelic replacement in *Francisella tularensis*. FEMS Microbiol Lett 222:273–280. doi: 10.1016/S0378-1097(03)00313-6

Hajjar AM, Harvey MD, Shaffer SA, et al (2006) Lack of in vitro and in vivo recognition of *Francisella tularensis* subspecies lipopolysaccharide by Toll-like receptors. Infect Immun 74:6730–6738. doi: 10.1128/IAI.00934-06

Hall JD, Woolard MD, Gunn BM, et al (2008) Infected-Host-Cell Repertoire and Cellular Response in the Lung following Inhalation of *Francisella tularensis* Schu S4, LVS, or U112. Infect Immun 76:5843–5852. doi: 10.1128/IAI.01176-08

Hartley G, Taylor R, Prior J, et al (2006) Grey variants of the live vaccine strain of *Francisella tularensis* lack lipopolysaccharide O-antigen, show reduced ability to survive in macrophages and do not induce protective immunity in mice. Vaccine 24:989–996. doi: 10.1016/j.vaccine.2005.08.075

Henry T, Brotcke A, Weiss DS, et al (2007) Type I interferon signaling is required for activation of the inflammasome during *Francisella* infection. J Exp Med 204:987–994. doi: 10.1084/jem.20062665

Hoang KV, Rajaram MVS, Curry HM, et al (2018) Complement Receptor 3-Mediated Inhibition of Inflammasome Priming by Ras GTPase-Activating Protein During *Francisella tularensis* Phagocytosis by Human Mononuclear Phagocytes. Front Immunol 9:. doi: 10.3389/fimmu.2018.00561

Hoebe K, Janssen EM, Kim SO, et al (2003) Upregulation of costimulatory molecules induced by lipopolysaccharide and double-stranded RNA occurs by Trif-dependent and Trif-independent pathways. Nat Immunol 4:1223–1229. doi: 10.1038/ni1010

Hornick RB, Eigelsbach HT (1966) Aerogenic immunization of man with live Tularemia vaccine. Bacteriol Rev 30:532–538

Hu H, Sun S-C (2016) Ubiquitin signaling in immune responses. Cell Res 26:457–483. doi: 10.1038/cr.2016.40

Huang MT-H, Mortensen BL, Taxman DJ, et al (2010) Deletion of ripA Alleviates Suppression of the Inflammasome and MAPK by *Francisella tularensis*. J Immunol 185:5476–5485. doi: 10.4049/jimmunol.1002154

Inagaki-Ohara K, Kondo T, Ito M, Yoshimura A (2013) SOCS, inflammation, and cancer. JAK-STAT 2:. doi: 10.4161/jkst.24053

Ireland R, Wang R, Alinger JB, et al (2013) *Francisella tularensis* SchuS4 and SchuS4 lipids inhibit IL-12p40 in primary human dendritic cells by inhibition of IRF1 and IRF8. J Immunol Baltim Md 1950 191:1276–1286. doi: 10.4049/jimmunol.1300867

Jin L, Hill KK, Filak H, et al (2011) MPYS is required for IRF3 activation and type I IFN production in the response of cultured phagocytes to bacterial second messengers c-di-AMP and c-di-GMP. J Immunol Baltim Md 1950 187:2595–2601. doi: 10.4049/jimmunol.1100088

Johansson A, Berglund L, Sjöstedt A, Tärnvik A (2001) Ciprofloxacin for Treatment of

Tularemia. Clin Infect Dis 33:267–268. doi: 10.1086/321825

Johansson A, Farlow J, Larsson P, et al (2004) Worldwide Genetic Relationships among *Francisella tularensis* Isolates Determined by Multiple-Locus Variable-Number Tandem Repeat Analysis. J Bacteriol 186:5808–5818. doi: 10.1128/JB.186.17.5808-5818.2004

Jones CL, Napier BA, Sampson TR, et al (2012a) Subversion of Host Recognition and Defense Systems by *Francisella* spp. Microbiol Mol Biol Rev MMBR 76:383–404. doi: 10.1128/MMBR.05027-11

Jones CL, Sampson TR, Nakaya HI, et al (2012b) Repression of bacterial lipoprotein production by *Francisella novicida* facilitates evasion of innate immune recognition. Cell Microbiol 14:1531–1543. doi: 10.1111/j.1462-5822.2012.01816.x

Jones JW, Broz P, Monack DM (2011) Innate Immune Recognition of *Francisella Tularensis*: Activation of Type-I Interferons and the Inflammasome. Front Microbiol 2:. doi: 10.3389/fmicb.2011.00016

Jones JW, Kayagaki N, Broz P, et al (2010) Absent in melanoma 2 is required for innate immune recognition of *Francisella tularensis*. Proc Natl Acad Sci 107:9771–9776. doi: 10.1073/pnas.1003738107

Jønsson KL, Laustsen A, Krapp C, et al (2017) IFI16 is required for DNA sensing in human macrophages by promoting production and function of cGAMP. Nat Commun 8:ncomms14391. doi: 10.1038/ncomms14391

Karttunen R, Surcel HM, Andersson G, et al (1991) *Francisella tularensis*-induced in vitro gamma interferon, tumor necrosis factor alpha, and interleukin 2 responses appear within 2 weeks of tularemia vaccination in human beings. J Clin Microbiol 29:753–756

Kato H, Takeuchi O, Sato S, et al (2006) Differential roles of MDA5 and RIG-I helicases in the recognition of RNA viruses. Nature 441:101–105. doi: 10.1038/nature04734

Katz J, Zhang P, Martin M, et al (2006) Toll-like receptor 2 is required for inflammatory responses to *Francisella tularensis* LVS. Infect Immun 74:2809–2816. doi: 10.1128/IAI.74.5.2809-2816.2006

Kawasaki T, Kawai T (2014) Toll-like receptor signaling pathways. Front Immunol 5:461. doi: 10.3389/fimmu.2014.00461

Kerur N, Veettil MV, Sharma-Walia N, et al (2011) IFI16 acts as a nuclear pathogen sensor to induce the inflammasome in response to Kaposi sarcoma associated herpesvirus infection. Cell Host Microbe 9:363–375. doi: 10.1016/j.chom.2011.04.008

Ketavarapu JM, Rodriguez AR, Yu J-J, et al (2008) Mast cells inhibit intramacrophage *Francisella tularensis* replication via contact and secreted products including IL-4. Proc Natl Acad Sci 105:9313–9318. doi: 10.1073/pnas.0707636105

Kim HM, Park BS, Kim J-I, et al (2007) Crystal structure of the TLR4-MD-2 complex with bound endotoxin antagonist Eritoran. Cell 130:906–917. doi: 10.1016/j.cell.2007.08.002

Kim YK, Shin J-S, Nahm MH (2016) NOD-Like Receptors in Infection, Immunity, and Diseases. Yonsei Med J 57:5–14. doi: 10.3349/ymj.2016.57.1.5

Kingry LC, Petersen JM (2014) Comparative review of *Francisella tularensis* and *Francisella novicida*. Front Cell Infect Microbiol 4:. doi: 10.3389/fcimb.2014.00035

Kirimanjeswara GS, Olmos S, Bakshi CS, Metzger DW (2008) Humoral and cellmediated immunity to the intracellular pathogen *Francisella tularensis*. Immunol Rev 225:244–255. doi: 10.1111/j.1600-065X.2008.00689.x

Koskela P, Herva E (1982) Cell-mediated and humoral immunity induced by a live *Francisella tularensis* vaccine. Infect Immun 36:983–989

Koskela P, Salminen A (1985) Humoral immunity against *Francisella tularensis* after natural infection. J Clin Microbiol 22:973–979

Kroca M, Tärnvik A, Sjöstedt A (2000) The proportion of circulating γδ T cells increases after the first week of onset of tularaemia and remains elevated for more than a year. Clin Exp Immunol 120:280–284. doi: 10.1046/j.1365-2249.2000.01215.x Kubelkova K, Krocova Z, Balonova L, et al (2012) Specific antibodies protect gammairradiated mice

against *Francisella tularensis* infection. Microb Pathog 53:259–268. doi: 10.1016/j.micpath.2012.07.006

Kurt-Jones EA, Popova L, Kwinn L, et al (2000) Pattern recognition receptors TLR4 and CD14 mediate response to respiratory syncytial virus. Nat Immunol 1:398–401. doi: 10.1038/80833

Lai XH, Golovliov I, Sjöstedt A (2001) *Francisella tularensis* induces cytopathogenicity and apoptosis in murine macrophages via a mechanism that requires intracellular bacterial multiplication. Infect Immun 69:4691–4694. doi: 10.1128/IAI.69.7.4691-4694.2001

Larsson P, Elfsmark D, Svensson K, et al (2009) Molecular Evolutionary Consequences of Niche Restriction in *Francisella tularensis*, a Facultative Intracellular Pathogen. PLoS Pathog 5:. doi: 10.1371/journal.ppat.1000472

Lavine CL, Clinton SR, Angelova-Fischer I, et al (2007) Immunization with heat-killed *Francisella tularensis* LVS elicits protective antibody-mediated immunity. Eur J Immunol 37:3007–3020. doi: 10.1002/eji.200737620

Lienenklaus S, Cornitescu M, Zietara N, et al (2009) Novel reporter mouse reveals constitutive and inflammatory expression of IFN-beta in vivo. J Immunol Baltim Md 1950 183:3229–3236. doi: 10.4049/jimmunol.0804277

Lin S-C, Lo Y-C, Wu H (2010) Helical assembly in the MyD88-IRAK4-IRAK2 complex in TLR/IL-1R signalling. Nature 465:885–890. doi: 10.1038/nature09121

Lin Y, Ritchea S, Logar A, et al (2009) Interleukin-17 is required for T helper 1 cell immunity and host resistance to the intracellular pathogen *Francisella tularensis*. Immunity 31:799–810. doi: 10.1016/j.immuni.2009.08.025

Lindgren H, Golovliov I, Baranov V, et al (2004a) Factors affecting the escape of *Francisella tularensis* from the phagolysosome. J Med Microbiol 53:953–958. doi: 10.1099/jmm.0.45685-0

Lindgren H, Shen H, Zingmark C, et al (2007) Resistance of *Francisella tularensis* Strains against Reactive Nitrogen and Oxygen Species with Special Reference to the Role of KatG. Infect Immun 75:1303–1309. doi: 10.1128/IAI.01717-06

Lindgren H, Stenmark S, Chen W, et al (2004b) Distinct roles of reactive nitrogen and oxygen species to control infection with the facultative intracellular bacterium *Francisella tularensis*. Infect Immun 72:7172–7182. doi: 10.1128/IAI.72.12.7172-7182.2004

Liu D, Sheng C, Gao S, et al (2015) SOCS3 Drives Proteasomal Degradation of TBK1 and Negatively Regulates Antiviral Innate Immunity. Mol Cell Biol 35:2400–2413. doi: 10.1128/MCB.00090-15

Liu Y, Lin R, Olagnier D (2017) RIGulation of STING expression: at the crossroads of viral RNA and DNA sensing pathways. Inflamm Cell Signal 4:e1491. doi: 10.14800/ics.1491

Loegering DJ, Drake JR, Banas JA, et al (2006) *Francisella tularensis* LVS GROWN IN MACROPHAGES HAS REDUCED ABILITY TO STIMULATE THE SECRETION OF INFLAMMATORY CYTOKINES BY MACROPHAGES in vitro. Microb Pathog 41:218–225. doi: 10.1016/j.micpath.2006.07.007

Loo Y-M, Gale M (2011) Immune signaling by RIG-I-like receptors. Immunity 34:680–692. doi: 10.1016/j.immuni.2011.05.003

Mahawar M, Atianand MK, Dotson RJ, et al (2012) Identification of a novel *Francisella tularensis* factor required for intramacrophage survival and subversion of innate immune response. J Biol Chem jbc.M112.367672. doi: 10.1074/jbc.M112.367672

Man SM, Karki R, Malireddi RKS, et al (2015) The transcription factor IRF1 and guanylate-binding proteins target activation of the AIM2 inflammasome by *Francisella* infection. Nat Immunol 16:467–475. doi: 10.1038/ni.3118

Man SM, Karki R, Sasai M, et al (2016) IRGB10 Liberates Bacterial Ligands for Sensing by the AIM2 and Caspase-11-NLRP3 Inflammasomes. Cell 167:382-396.e17. doi: 10.1016/j.cell.2016.09.012

Mancuso G, Gambuzza M, Midiri A, et al (2009) Bacterial recognition by TLR7 in the lysosomes of conventional dendritic cells. Nat Immunol 10:587–594. doi: 10.1038/ni.1733

Marinho FV, Benmerzoug S, Oliveira SC, et al (2017) The Emerging Roles of STING in Bacterial Infections. Trends Microbiol. doi: 10.1016/j.tim.2017.05.008

Mccoy GW, Chapin CW (1912) Further Observations on a Plague-Like Disease of Rodents with a Preliminary Note on the Causative Agent, Bacterium Tularense. J Infect Dis 10:61–72. doi: 10.1093/infdis/10.1.61

McCrumb FR (1961) AEROSOL INFECTION OF MAN WITH PASTEURELLA TULARENSIS. Bacteriol Rev 25:262–267

McLendon MK, Apicella MA, Allen L-AH (2006) *Francisella tularensis*: Taxonomy, Genetics, and Immunopathogenesis of a Potential Agent of Biowarfare. Annu Rev Microbiol 60:167–185. doi: 10.1146/annurev.micro.60.080805.142126

McNab F, Mayer-Barber K, Sher A, et al (2015) Type I interferons in infectious disease. Nat Rev Immunol 15:87–103. doi: 10.1038/nri3787

Meunier E, Wallet P, Dreier RF, et al (2015) Guanylate-binding proteins promote activation of the AIM2 inflammasome during infection with *Francisella novicida*. Nat Immunol 16:476–484. doi: 10.1038/ni.3119

Mogensen TH (2009) Pathogen recognition and inflammatory signaling in innate immune defenses. Clin Microbiol Rev 22:240–273, Table of Contents. doi: 10.1128/CMR.00046-08

Mohapatra NP, Soni S, Rajaram MVS, et al (2010) *Francisella* Acid Phosphatases Inactivate the NADPH Oxidase in Human Phagocytes. J Immunol Baltim Md 1950 184:5141–5150. doi: 10.4049/jimmunol.0903413

Moreau GB, Mann BJ (2013) Adherence and uptake of *Francisella* into host cells. Virulence 4:826–832. doi: 10.4161/viru.25629

Moreira LO, Zamboni DS (2012) NOD1 and NOD2 Signaling in Infection and

Inflammation. Front Immunol 3:. doi: 10.3389/fimmu.2012.00328

Mörner T (1992) The ecology of tularaemia. Rev Sci Tech Int Off Epizoot 11:1123–1130

Nano FE, Schmerk C (2007) The *Francisella* pathogenicity island. Ann N Y Acad Sci 1105:122–137. doi: 10.1196/annals.1409.000

Newton K, Dixit VM (2012) Signaling in Innate Immunity and Inflammation. Cold Spring Harb Perspect Biol 4:a006049. doi: 10.1101/cshperspect.a006049

Ohara Y, Sato T, Fujita H, et al (1991) Clinical manifestations of tularemia in Japan-analysis of 1,355 cases observed between 1924 and 1987. Infection 19:14–17

Okan NA, Kasper DL (2013) The atypical lipopolysaccharide of *Francisella*. Carbohydr Res 378:79–83. doi: 10.1016/j.carres.2013.06.015

Oyston PCF (2008) *Francisella tularensis*: unravelling the secrets of an intracellular pathogen. J Med Microbiol 57:921–930. doi: 10.1099/jmm.0.2008/000653-0

Panda S, Nilsson JA, Gekara NO (2015) Deubiquitinase MYSM1 Regulates Innate Immunity through Inactivation of TRAF3 and TRAF6 Complexes. Immunity 43:647–659. doi: 10.1016/j.immuni.2015.09.010

Pandey S, Kawai T, Akira S (2015) Microbial Sensing by Toll-Like Receptors and Intracellular Nucleic Acid Sensors. Cold Spring Harb Perspect Biol 7:. doi: 10.1101/cshperspect.a016246

Park BS, Song DH, Kim HM, et al (2009) The structural basis of lipopolysaccharide recognition by the TLR4-MD-2 complex. Nature 458:1191–1195. doi: 10.1038/nature07830

Parsa KVL, Butchar JP, Rajaram MVS, et al (2008) *Francisella* gains a survival advantage within mononuclear phagocytes by suppressing the host IFNgamma response. Mol Immunol 45:3428–3437. doi: 10.1016/j.molimm.2008.04.006

Parsa KVL, Ganesan LP, Rajaram MVS, et al (2006) Macrophage Pro-Inflammatory Response to *Francisella novicida* Infection Is Regulated by SHIP. PLoS Pathog 2:e71. doi: 10.1371/journal.ppat.0020071

Patel H, Shaw SG, Shi-Wen X, et al (2012) Toll-Like Receptors in Ischaemia and Its Potential Role in the Pathophysiology of Muscle Damage in Critical Limb Ischaemia. Cardiol Res Pract 2012:. doi: 10.1155/2012/121237

Pechous RD, McCarthy TR, Zahrt TC (2009) Working toward the Future: Insights into *Francisella tularensis* Pathogenesis and Vaccine Development. Microbiol Mol Biol Rev MMBR 73:684–711. doi: 10.1128/MMBR.00028-09

Peng K, Broz P, Jones J, et al (2011) Elevated AIM2-mediated pyroptosis triggered by hypercytotoxic *Francisella* mutant strains is attributed to increased intracellular bacteriolysis. Cell Microbiol 13:1586–1600. doi: 10.1111/j.1462-5822.2011.01643.x

Petnicki-Ocwieja T, Chung E, Acosta DI, et al (2013) TRIF mediates Toll-like receptor 2-dependent inflammatory responses to *Borrelia burgdorferi*. Infect Immun 81:402–410. doi: 10.1128/IAI.00890-12

Petrosino JF, Xiang Q, Karpathy SE, et al (2006) Chromosome Rearrangement and Diversification of *Francisella tularensis* Revealed by the Type B (OSU18) Genome Sequence. J Bacteriol 188:6977–6985. doi: 10.1128/JB.00506-06

Phillips NJ, Schilling B, McLendon MK, et al (2004) Novel modification of lipid A of *Francisella tularensis*. Infect Immun 72:5340–5348. doi: 10.1128/IAI.72.9.5340-5348.2004

Pierini LM (2006) Uptake of serum-opsonized *Francisella tularensis* by macrophages can be mediated by class A scavenger receptors. Cell Microbiol 8:1361–1370. doi: 10.1111/j.1462-5822.2006.00719.x

Pizarro-Cerdá J, Charbit A, Enninga J, et al (2016) Manipulation of host membranes by the bacterial pathogens *Listeria*, *Francisella*, *Shigella* and *Yersinia*. Semin Cell Dev Biol 60:155–167. doi: 10.1016/j.semcdb.2016.07.019

Plzakova L, Krocova Z, Kubelkova K, Macela A (2015) Entry of *Francisella tularensis* into Murine B Cells: The Role of B Cell Receptors and Complement Receptors. PLOS ONE 10:e0132571. doi: 10.1371/journal.pone.0132571

Poquet Y, Kroca M, Halary F, et al (1998) Expansion of Vγ9Vδ2 T Cells Is Triggered by *Francisella tularensis*-Derived Phosphoantigens in Tularemia but Not after Tularemia Vaccination. Infect Immun 66:2107–2114

Qin A, Scott DW, Thompson JA, Mann BJ (2009) Identification of an Essential *Francisella tularensis* subsp. tularensis Virulence Factor. Infect Immun 77:152–161. doi: 10.1128/IAI.01113-08

Qin A, Zhang Y, Clark ME, et al (2016) Components of the type six secretion system are substrates of *Francisella tularensis* Schu S4 DsbA-like FipB protein. Virulence 0:1–13. doi: 10.1080/21505594.2016.1168550

Rassa JC, Meyers JL, Zhang Y, et al (2002) Murine retroviruses activate B cells via interaction with toll-like receptor 4. Proc Natl Acad Sci U S A 99:2281–2286. doi: 10.1073/pnas.042355399

Rathinam VAK, Jiang Z, Waggoner SN, et al (2010) The AIM2 inflammasome is essential for host-defense against cytosolic bacteria and DNA viruses. Nat Immunol 11:395–402. doi: 10.1038/ni.1864

Regan T, Nally K, Carmody R, et al (2013) Identification of TLR10 as a key mediator of the inflammatory response to *Listeria monocytogenes* in intestinal epithelial cells and macrophages. J Immunol Baltim Md 1950 191:6084–6092. doi: 10.4049/jimmunol.1203245

Sampson TR, Saroj SD, Llewellyn AC, et al (2013) A CRISPR-CAS System Mediates Bacterial Innate Immune Evasion and Virulence. Nature 497:254–257. doi: 10.1038/nature12048

Santic M, Al-Khodor S, Abu Kwaik Y (2010) Cell biology and molecular ecology of *Francisella tularensis*. Cell Microbiol 12:129–139. doi: 10.1111/j.1462-5822.2009.01400.x

Santic M, Molmeret M, Klose KE, et al (2005) The *Francisella tularensis* pathogenicity island protein IglC and its regulator MglA are essential for modulating phagosome biogenesis and subsequent bacterial escape into the cytoplasm. Cell Microbiol 7:969–979. doi: 10.1111/j.1462-5822.2005.00526.x

Sauer J-D, Sotelo-Troha K, von Moltke J, et al (2011) The N-ethyl-N-nitrosoureainduced Goldenticket mouse mutant reveals an essential function of Sting in the in vivo interferon response to *Listeria monocytogenes* and cyclic dinucleotides. Infect Immun 79:688–694. doi: 10.1128/IAI.00999-10

Schulert GS, Allen L-AH (2006) Differential infection of mononuclear phagocytes by *Francisella tularensis*: role of the macrophage mannose receptor. J Leukoc Biol 80:563–571. doi: 10.1189/jlb.0306219

Sharma D, Kanneganti T-D (2016) The cell biology of inflammasomes: Mechanisms of inflammasome activation and regulation. J Cell Biol 213:617–629. doi: 10.1083/jcb.201602089

Sharma S, Campbell AM, Chan J, et al (2015) Suppression of systemic autoimmunity by the innate immune adaptor STING. Proc Natl Acad Sci U S A 112:E710-717. doi: 10.1073/pnas.1420217112

Singh A, Rahman T, Malik M, et al (2013) Discordant results obtained with *Francisella tularensis* during in vitro and in vivo immunological studies are attributable to compromised bacterial structural integrity. PloS One 8:e58513. doi: 10.1371/journal.pone.0058513

Sjöstedt A, Eriksson M, Sandström G, Tärnvik A (1992) Various membrane proteins of *Francisella tularensis* induce interferon-gamma production in both CD4+ and CD8+ T cells of primed humans. Immunology 76:584–592

Sokolowska O, Nowis D (2018) STING Signaling in Cancer Cells: Important or Not? Arch Immunol Ther Exp (Warsz) 66:125–132. doi: 10.1007/s00005-017-0481-7

Spidlova P, Stulik J (2017) *Francisella tularensis* type VI secretion system comes of age. Virulence 0:1–4. doi: 10.1080/21505594.2016.1278336

Steele S, Brunton J, Ziehr B, et al (2013) *Francisella tularensis* harvests nutrients derived via ATG5-independent autophagy to support intracellular growth. PLoS Pathog 9:e1003562. doi: 10.1371/journal.ppat.1003562

Steele S, Radlinski L, Taft-Benz S, et al (2016) Trogocytosis-associated cell to cell spread of intracellular bacterial pathogens. eLife 5:e10625. doi: 10.7554/eLife.10625

Steiner DJ, Furuya Y, Metzger DW (2014) Host-pathogen interactions and immune evasion strategies in *Francisella tularensis* pathogenicity. Infect Drug Resist 7:239–251. doi: 10.2147/IDR.S53700

Stojdl DF, Lichty BD, tenOever BR, et al (2003) VSV strains with defects in their ability to shutdown innate immunity are potent systemic anti-cancer agents. Cancer Cell 4:263–275

Storek KM, Gertsvolf NA, Ohlson MB, Monack DM (2015) cGAS and Ifi204 cooperate to produce type I IFNs in response to *Francisella* infection. J Immunol Baltim Md 1950 194:3236–3245. doi: 10.4049/jimmunol.1402764

Straskova A, Pavkova I, Link M, et al (2009) Proteome analysis of an attenuated *Francisella tularensis* dsbA mutant: identification of potential DsbA substrate proteins. J Proteome Res 8:5336–5346. doi: 10.1021/pr900570b

Sundaresh S, Randall A, Unal B, et al (2007) From protein microarrays to diagnostic antigen discovery: a study of the pathogen *Francisella tularensis*. Bioinforma Oxf Engl 23:i508-518. doi: 10.1093/bioinformatics/btm207

Surcel HM, Syrjälä H, Karttunen R, et al (1991) Development of *Francisella tularensis* antigen responses measured as T-lymphocyte proliferation and cytokine production (tumor necrosis factor alpha, gamma interferon, and interleukin-2 and -4) during human tularemia. Infect Immun 59:1948–1953

Takeuchi O, Akira S (2010) Pattern Recognition Receptors and Inflammation. Cell 140:805–820. doi: 10.1016/j.cell.2010.01.022

Tao J, Zhou X, Jiang Z (2016) cGAS-cGAMP-STING: The three musketeers of cytosolic DNA sensing and signaling. IUBMB Life 68:858–870. doi: 10.1002/iub.1566

Tärnvik A, Berglund L (2003) Tularaemia. Eur Respir J 21:361–373. doi: 10.1183/09031936.03.00088903

Telepnev M, Golovliov I, Grundström T, et al (2003) *Francisella tularensis* inhibits Toll-like receptor-mediated activation of intracellular signalling and secretion of TNF-α and IL-1 from murine macrophages. Cell Microbiol 5:41–51. doi: 10.1046/j.1462-5822.2003.00251.x

Telepnev M, Golovliov I, Sjöstedt A (2005) *Francisella tularensis* LVS initially activates but subsequently down-regulates intracellular signaling and cytokine secretion in mouse monocytic and human peripheral blood mononuclear cells. Microb Pathog 38:239–247. doi: 10.1016/j.micpath.2005.02.003

Thakran S, Li H, Lavine CL, et al (2008) Identification of *Francisella tularensis* lipoproteins that stimulate the toll-like receptor (TLR) 2/TLR1 heterodimer. J Biol Chem 283:3751–3760. doi: 10.1074/jbc.M706854200

Trevisanato SI (2007) The 'Hittite plague', an epidemic of tularemia and the first record of biological warfare. Med Hypotheses 69:1371–1374. doi: 10.1016/j.mehy.2007.03.012

Ullah MO, Sweet MJ, Mansell A, et al (2016) TRIF-dependent TLR signaling, its functions in host defense and inflammation, and its potential as a therapeutic target. J Leukoc Biol 100:27–45. doi: 10.1189/jlb.2RI1115-531R

Unterholzner L, Keating SE, Baran M, et al (2010) IFI16 is an innate immune sensor for intracellular DNA. Nat Immunol 11:997–1004. doi: 10.1038/ni.1932

Wallet P, Lagrange B, Henry T (2016) *Francisella* Inflammasomes: Integrated Responses to a Cytosolic Stealth Bacterium. Curr Top Microbiol Immunol 397:229–256. doi: 10.1007/978-3-319-41171-2_12

Walters K-A, Olsufka R, Kuestner RE, et al (2015) Prior infection with Type A *Francisella tularensis* antagonizes the pulmonary transcriptional response to an aerosolized Toll-like receptor 4 agonist. BMC Genomics 16:874. doi: 10.1186/s12864-015-2022-2

Wang X, Majumdar T, Kessler P, et al (2016) STING Requires the Adaptor TRIF to Trigger Innate Immune Responses to Microbial Infection. Cell Host Microbe 20:329–341. doi: 10.1016/j.chom.2016.08.002

Wherry WB, Lamb BH (1914) Infection of Man with *Bacterium Tularense*. J Infect Dis 15:331–340. doi: 10.1093/infdis/15.2.331

Witte CE, Archer KA, Rae CS, et al (2012) Innate immune pathways triggered by *Listeria monocytogenes* and their role in the induction of cell-mediated immunity. Adv Immunol 113:135–156. doi: 10.1016/B978-0-12-394590-7.00002-6

World Health Organization (1970) Health aspects of chemical and biological weapons. Geneva, Switzerland

Xiao TS (2015) The nucleic acid-sensing inflammasomes. Immunol Rev 265:103–111. doi: 10.1111/imr.12281

Xie P (2013) TRAF molecules in cell signaling and in human diseases. J Mol Signal 8:7. doi: 10.1186/1750-2187-8-7

Yang P, An H, Liu X, et al (2010) The cytosolic nucleic acid sensor LRRFIP1 mediates the production of type I interferon via a beta-catenin-dependent pathway. Nat Immunol 11:487–494. doi: 10.1038/ni.1876

Yin Q, Lin S-C, Lamothe B, et al (2009) E2 interaction and dimerization in the crystal structure of TRAF6. Nat Struct Mol Biol 16:658–666. doi: 10.1038/nsmb.1605

Zarrella TM, Singh A, Bitsaktsis C, et al (2011) Host-adaptation of *Francisella tularensis* alters the bacterium's surface-carbohydrates to hinder effectors of innate and adaptive immunity. PloS One 6:e22335. doi: 10.1371/journal.pone.0022335

Biological Weapons – UNODA. https://www.un.org/disarmament/wmd/bio/. Accessed 20 Jun 2017a

Treaties, States parties, and Commentaries - Convention on the Prohibition of Biological Weapons, 1972. https://ihl-databases.icrc.org/ihl/INTRO/450?OpenDocument. Accessed 20 Jun 2017b

8 Súhrn

Francisella tularensis je vysoko infekčný intracelulárny patogén a pôvodca ochorenia nazývaného tularémia. Predpokladá sa, že dôležitým aspektom jej virulencie je schopnosť rozvrátiť imunitnú odpoveď hostiteľa utlmením alebo narušením funkcií buniek vrodenej imunity. Počiatočné štádium infekcie je charakterizované výraznou bakteriálnou replikáciou bez spustenia signifikantnej prozápalovej odpovede, ktorá hrá kľúčovú úlohu v rozvoji efektívnej hostiteľskej obrany voči invadujúcemu patogénu.

Cieľom predloženej dizertačnej práce bolo popísať priebeh bunkovej signalizácie sprostredkovanej tzv. pattern recognition receptors (PRR) počas skorej fáze infekcie primárnych kostne-dreňových makrofágov baktériou *Francisella tularensis* subsp. *holarctica* LVS (*F. tularensis* LVS). Získané dáta preukázali schopnosť *F. tularensis* LVS aktivovať, ale aj súčasne blokovať signalizačné dráhy riadené tzv. Toll-like receptors, RIG-I-like receptors a tzv. cytosolic DNA sensors. *F. tularensis* LVS ovplyvňuje tieto kaskády inhibíciou K63-polyubikvitinačných procesov ako aj tvorby signalizačných komplexov obsahujúcich TRAF6 a TRAF3. Závislosť supresívneho efektu *F. tularensis* LVS na prítomnosti funkčného sekrečného systému typu 6 a/alebo životaschopnej baktérie v cytoplazme hostiteľskej bunky bola preukázaná použitím mutantných kmeňov s narušenou schopnosťou fagozomálneho úniku *ΔiglC*/LVS a *ΔdsbA*/LVS.

Výsledky dizertačnej práce poukazujú na schopnosť *F. tularensis* LVS unikať do cytoplazmy a zároveň inhibovať viaceré signalizačné dráhy riadené PRR, čo umožňuje baktérii proliferovať v hostiteľskej bunke bez spustenia výraznej vrodenej imunitnej odpovede.

Kľúčové slová: *Francisella tularensis*, pattern recognition receptors, inhibícia,

S

komplexy TRAF6 a TRAF3

9 ummary

Francisella tularensis is a highly infectious intracellular pathogen and the causative agent of the disease called tularemia. An important aspect of *Francisella tularensis* virulence represents the capacity to subvert the host immune response by inhibiting or disrupting of the innate immune cell functions. The initial stage of infection is characterized by the massive bacterial replication without apparent inflammatory response, which is crucial for the development of effective host defense against invading pathogen.

The aim of this Ph.D. thesis was to describe the early pattern recognition receptors (PRR) signaling response to *Francisella tularensis* subsp. *holarctica* LVS (*F. tularensis* LVS) in primary bone marrow-derived macrophages. The obtained data show the capacity of *F. tularensis* LVS to simultaneously activate and suppress Tolllike receptors, RIG-I-like receptors, and cytosolic DNA sensors signaling pathways. *F. tularensis* LVS modulates these PRR pathways by the suppression of K63-linked polyubiquitination events and by the inhibition of the assembly of TRAF6 and TRAF3 signaling complexes. The use of the mutant strains with the impaired phagosomal escape (*ΔiglC*/LVS and *ΔdsbA*/LVS) showed that the suppressive effect of *F. tularensis* LVS was dependent on the functional type 6 secretion system and/or on the presence of viable bacteria in the host cytoplasm.

The results of this Ph.D. thesis demonstrate that the ability of *F. tularensis* LVS to escape into the cytoplasm and, concurrently, to inhibit multiple PRR signaling pathways accounts for the capability of the bacterium to proliferate in the host cell without triggering of the self-limiting innate immune response.

S

Key words: *Francisella tularensis*, pattern recognition receptors, inhibition, TRAF6 and TRAF3 complexes

10 ouhrn

Francisella tularensis je vysoce infekční intracelulární patogen a původce onemocnění nazývaného tularémie. Předpokládá se, že důležitým aspektem virulence je schopnost rozvrátit imunitní odpověď hostitele utlumením nebo narušením funkcí buněk vrozené imunity. Počáteční stádium infekce je charakterizováno masivní bakteriální replikací bez stimulace signifikantní prozánětlivé odpovědi, která hraje klíčovou roli v rozvoji efektivní hostitelské obrany namířené proti patogenu.

Cílem předložené disertační práce bylo popsat průběh buněčné signalizace zprostředkované tzv. pattern recognition receptors (PRR) během časné fáze infekce primárních kostně-dřeňových makrofágů bakterií *Francisella tularensis* subsp. *holarctica* LVS (*F. tularensis* LVS). Získaná data prokázala schopnost *F. tularensis* LVS aktivovat, ale také současně blokovat signalizační dráhy řízené tzv. Toll-like receptors, RIG-I-like receptors a tzv. cytosolic DNA sensors. *F. tularensis* LVS ovlivňuje tyto kaskády inhibicí K63-polyubikvitinačních procesů a tvorby signalizačních komplexů obsahujících TRAF6 a TRAF3. Závislost supresivního efektu *F. tularensis* LVS na sekrečním systému typu 6 a/nebo na viabilitě bakterie v cytoplazmě hostitelské buňky byla prokázaná pomocí mutantních kmenů *ΔiglC*/LVS a *ΔdsbA*/LVS s narušenou schopností fagozomálního úniku.

Výsledky disertační práce ukazují na schopnost *F. tularensis* LVS unikat do cytoplazmy a zároveň inhibovat několik signalizačních drah řízených PRR, což umožňuje bakterii proliferovat v hostitelské buňce bez spuštění výrazné vrozené imunitní odpovědi.

S

Klíčová slova: *Francisella tularensis*, pattern recognition receptors, inhibice, komplexy TRAF6 a TRAF3

11 Prehľad publikačnej činnosti

Publikácie vzťahujúce sa k téme dizertačnej práce

- **Putzova D**, Senitkova I, Stulik J (2016) Tularemia vaccines. *Folia Microbiologica* **61**: 495–504.
- **Putzova D**, Panda S, Härtlova A, Stulík J, Gekara NO (2017) Subversion of innate immune responses by *Francisella* involves the disruption of TRAF3 and TRAF6 signalling complexes. *Cellular Microbiology* **19**.

Ostatné publikácie v recenzovaných časopisoch

- Drastíková M, Beránek M, Hegerová J, **Putzová D** (2012) Význam DNA vyšetření mutací C282Y, H63D a S65C v HFE genu. *Časopis lékařů českých* **151**: 428–431.
- Dankova V, Balonova L, Straskova A, Spidlova P, **Putzova D**, Kijek T, Bozue J,Cote C, Mou S, Worsham P, Szotakova B, Cerveny L, Stulik J (2014) Characterization of tetratricopeptide repeat-likeproteins in *Francisella tularensis* and identification of a novel locus required for virulence. *Infection and Immunity* **82**: 5035–5048.
- Straskova A, Spidlova P, Mou S, Worsham P, **Putzova D**, Pavkova I, Stulik J (2015) *Francisella tularensis* type B *ΔdsbA* mutant protects against type A strain and induces strong inflammatory cytokine and Th1-like antibody response *in vivo*. *Pathogens and Disease* **73**.
- Fabrik I, Link M, **Putzova D**, Plzakova L, Lubovska Z, Philimonenko V, Pavkova I, Rehulka P, Krocova Z, Hozak P, et al. (2018) The Early Dendritic Cell Signaling Induced by Virulent *Francisella tularensis* Strain Occurs in Phases and Involves the Activation of Extracellular Signal-Regulated Kinases (ERKs) and p38 In the Later Stage. *Molecular & Cellular Proteomics* **17**: 81–94.

Prílohy

Publikácie vzťahujúce sa k téme dizertačnej práce

Putzova D, Senitkova I, Stulik J (2016) Tularemia vaccines. *Folia Microbiologica* **61**: 495–504.

doi: 10.1007/s12223-016-0461-z

DOI 10.1007/s12223-016-0461-z

Tularemia vaccines

Daniela Putzova[1] & Iva Senitkova[1] & Jiri Stulik[1]

Received: 9 November 2015 /Accepted: 1 May 2016

Abstract Francisella tularensis is the causative agent of the potentially lethal disease tularemia. Due to a low infectious dose and ease of airborne transmission, Francisella is classified as a category A biological agent. Despite the possible risk to public health, there is no safe and fully licensed vaccine. A potential vaccine candidate, an attenuated live vaccine strain, does not fulfil the criteria for general use. In this review, we will summarize existing and new candidates for live attenuated and subunit vaccines.

Introduction—Francisella tularensis

Francisella tularensis (F. tularensis) is a non-motile, gramnegative, facultative intracellular pathogen that is the etiological agent of the potentially lethal disease tularemia in both humans and animals. This species is considered a biological weapon and classified as a category A bioterrorism agent by the US Centers for Disease Control and Prevention (Khan et al. 2000) due to its high infectivity, potential airborne transmission and ability to cause severe disease. During the Cold War, F. tularensis belonged to the group of agents produced and stockpiled by the former Soviet Union and the USA (reviewed in Dennis et al. 2001). In 1970, the World Health Organization committee categorized F. tularensis as a biological threat and estimated that the dispersal of 50 kg of its aerosolized virulent form over an urban area with five million inhabitants would result in 250,000 incapacitating causalities and 19,000 deaths(World Health Organization1970).Today′s major concerns are the misuse of F. tularensis during possible terrorist attacks.

F. tularensis belongs to the class γ-Proteobacteria, family Francisellaceae and genus Francisella (Forsman et al. 1994; World Health Organization 2007). The species F. tularensis is divided into three subspecies: tularensis, holarctica and mediasiatica, which vary in their pathogenicity and geographic distribution (Oyston 2008). F. tularensis subsp. tularensis (classified as type A) is found predominantly in North America and consists of two different genetic sub-populations, AI and AII (Johansson et al. 2004), which are characterized by the extreme virulence, as less than 10 bacteria can lead to lethal disease (reviewed in Tärnvik and Berglund 2003). F. tularensis subsp. holarctica (type B) occurs primarily in the Northern Hemisphere and causes a milder form of tularemia. F. tularensis subsp. mediasiatica was detected in Central Asia, and its virulence resembles the holarctica subspecies. The species novicida, isolated in North America and Australia, is rarely responsible for human tularemia (reviewed

jiri.stulik@unob.cz

* Jiri Stulik

Published online: 19 May 2016

[1] Department of Molecular Pathology and Biology, Faculty of Military Health Sciences, University of Defense, Trebesska 1575, 500 01 Hradec Kralove, Czech Republic

in Pechous et al. 2009).

Natural hosts for F. tularensis include lagomorphs, rodents, carnivores, ungulates, marsupials, amphibians, birds, fish and invertebrates (Mörner 1992). However, despite the wide distribution of Francisella in numerous wildlife species, its primary reservoirs remain unknown. Natural infection can be transmitted to humans through arthropod vectors, such as ticks, flies or mosquitoes, or by direct contact during handling of infected animals, drinking of contaminated water or inhaling of aerosols (Mörner 1992; Tärnvik and Berglund 2003).

Tularemia

Tularemia is an acute febrile disease whose severity depends on the route of infection and virulence of the strain (Ellis et al. 2002). The incubation period normally ranges from 3 to 5 days; however, the period may be extended to up to 21 days. In the early phase of infection, tularemia is frequently misdiagnosed because disease symptoms resemble flu symptoms, such as high fever, body aches, and swollen lymph nodes.Themost commonformoftularemia isulceroglandular tularemia, which is usually spread through vector-borne transmission (reviewed by Tärnvik and Berglund 2003). A painless ulcer develops at the site of inoculation followed by enlargement of regional lymph nodes (Ohara et al. 1991). The infrequent clinical form, oculoglandular tularemia, occurs after direct contact of the eye with the bacteria. Oropharyngeal tularemia, which is accompanied by stomatitis and pharyngitis, results from contaminated food or water intake (reviewed by Tärnvik and Berglund 2003; World Health Organization 2007). The most severe form is respiratory tularemia, which is caused by the inhalation of aerosolized F. tularensis subsp. tularensis. The mortality rate for respiratory tularemia ranges from 30 to 60 % without effective antibiotic therapy (reviewed by Tärnvik and Berglund 2003). Treatment successfully resolves infection when administered in the early phase of infection. Antibiotics of choice are aminoglycosides, tetracyclines, chloramphenicol and quinolones (reviewed by Dennis et al. 2001).

The human immune response to tularemia was described in naturally infected patients or live vaccine strain (LVS) vaccinated volunteers (Koskela and Herva 1982; Koskela and Salminen 1985; Surcel et al. 1991; Sjöstedt et al. 1992a; Poquet et al. 1998; Ericsson et al. 1994). Considering that F. tularensis is an intracellular pathogen, it was thought that a cell-mediated immune response is required to clear infection. $CD4^+$ and $CD8^+$ T cells are detectable 2 weeks postinfection, as well as proinflammatory cytokines, including interferon-γ (IFN-γ), TNF-α and interleukin 2 (IL-2) (Koskela and Herva 1982; Surcel et al. 1991; Sjöstedt et al. 1992a). The cell-mediated response is long-lasting and even inducible 30 years after the onset of disease (Ericsson et al. 2001). In naturally infected individuals, phosphoantigendirected Vγ9/Vδ2 T cells arise during the first week after infection (Poquet et al. 1998). Human peripheral blood cells show increased expression of IFN-γ-regulated genes within 2–3 days post-infection (Andersson et al. 2006). In respect to humoral immunity, the production of specific IgM, IgA and IgG antibodies reaches its highest levels at 1–2 months and persists 0.5 to 11 years post-infection (Koskela and Salminen 1985). Recent studies in the murine model of tularemia showed that both components of adaptive immunity are critical for the induction of full protection against tularemia (Lavine et al. 2007; Cole et al. 2011; Kubelkova et al. 2012).

The current problem in tularemia prophylaxis is the lack of a vaccine. The only available prophylactic tool is LVS, which is not intended for public use due to its attenuation background. It is therefore vital to develop a new vaccine that will be safe and effective in inducing protective long-lasting immune response against respiratory challenge with the most virulent strain of F. tularensis. Currently, F. tularensis vaccine development has focused on developing live attenuated (Table 1) and subunit vaccines (Table 2).

Killed whole-cell vaccines

Killed whole-cell vaccines are composed of non-infectious modified bacterial suspensions. The earliest tularemia vaccine was developed using acetone extraction or phenolization by Foshay et al. (1942). The vaccine protected non-human primates against challenge with 740 CFU of F. tularensis subsp. tularensis Schu S4 (Schu S4); however, it caused symptoms of disease (Coriell et al. 1948) and was not efficient to protect against highly virulent strains in animal models (Foshay et al. 1942; Pechous et al. 2009).

Recent studies showed that protection induced by killed whole-cell vaccines are enhanced through the use of boosters and adjuvants. Eyles et al. (2008) found that intramuscular (i.m.)-delivered, inactivated LVS vaccination in conjunction with immune-stimulating complexes and immunostimulatory CpG oligonucleotides had a protective effect against aerosol challenge with F. tularensis subsp. holarctica, but not against low-dose aerosol challenge with Schu S4. Baron and co-workers (2007) determined that inactivated LVS administered via the intranasal (i.n.) route protected mice against i.n. infection with LVS, although only in combination with IL-12 administration.

Live attenuated vaccines

The first anti-Francisella live attenuated vaccine was generated from F. tularensis subsp. holarctica, which was isolated in the former Soviet Union (Tigertt 1962). A sample of the vaccine was provided to the US where multiple passages of the strain led to the preparation of LVS (Eigelsbach and Downs 1961). The results obtained from vaccine trials in humans showed that LVS induced protective immunity against a low-dose aerosol challenge with Schu S4 (McCrumb 1961). However, LVS has not been officially licensed by the Food and Drug Administration as a human vaccine due to an unknown mechanism of

attenuation, the instability of colony phenotype and the partial virulence after vaccination via the aerosol route (Hornick and Eigelsbach 1966; Hartley et al. 2006; Petrosino et al. 2006).

Table 1 *Francisella* live attenuated vaccines

Gene	Species or subspecies	Vaccination dose (route)	Boost	Challenge dose and strain (route)	Survival in mice	Reference
guaA *guaB*	LVS	2.2×10^7 CFU (i.p.) 3.6×10^7 CFU (i.p.)	No	2.8×10^5 CFU of LVS (i.p.)	100 % in BALB/c	(Santiago et al. 2009)
purMCD	LVS	5×10^6 CFU (i.p.)	No	5×10^3 CFU LVS (i.p.)	100 % in BALB/c	(Pechous et al. 2006)
	LVS Schu S4	10^6 CFU (i.n.) 10^4 CFU (i.n.)	10^6 CFU (i.n.) 10^6 CFU (i.n.)	100 CFU Schu S4 (i.n.)	100 % in BALB/c 71 % in BALB/c	(Pechous et al. 2008)
capB	LVS	1×10^5 CFU (i.n.)	No	$10 \times LD_{50}$ of Schu S4 (aerosol)	100 % in BALB/c	(Jia et al. 2010)
FTT_1103	Schu S4	1.3×10^8 CFU (i.n.) 2.6×10^8 CFU (i.n.) 1×10^8 CFU (i.n.)	No	37 CFU of Schu S4 (i.n.) 68 CFU of Schu S4 (i.n.) 95 CFU of Schu S4 (i.n.)	100 % in C57BL/6 50 % in C57BL/6 75 % in BALB/c	(Qin et al. 2009)
clpB	Schu S4	10^7 CFU (i.d.)	No	105 CFU of Schu S4 (i.n.)	100 % in BALB/c	(Golovliov et al. 2013)
iglB	*F. novicida*	10^6 CFU (i.n.) 10^3 CFU (orally)	No	3×10^4 CFU of LVS (i.n.) 25 CFU of Schu S4 (i.n.)	100 % in BALB/c 67 % in C57BL/6	(Cong et al. 2009)
iglC	Schu S4	10^6 CFU (i.d.) 10^7 CFU (i.d.)	No	500 CFU of FSC033 (i.d.) 10 CFU of FSC033 (aerosol)	0 % in BALB/c	(Twine et al. 2005)
iglH	FSC200	3×10^7 CFU (s.c.)	No	3×10^2 CFU of FSC200 (s.c.)	100 % in BALB/c	(Straskova et al. 2012)
mglA	*F. novicida*	1×10^5 CFU (aerosol)	No	6×10^2 CFU of *F. novicida* (aerosol)	0 % in BALB/c	(West et al. 2008)
wbtA	LVS	10^5 CFU (i. p.)	No	10^4 CFU of LVS (i.p.)	100 % in BALB/c	(Raynaud et al. 2007)
wbtI	LVS	10^5 CFU (i.d.) 5×10^4 CFU (i.p.)	10^5 CFU (i.d.) 5×10^4 CFU (i.p.)	$25 \times LD_{50}$ of LVS (i.p.) $250 \times LD_{50}$ of LVS (i.p.)	100 % in BALB/c 60 % in BALB/c	(Li et al. 2007)
wzy	LVS	1.5×10^7 CFU (i.n.) 3.5×10^6 CFU (i.n.)	2.4×10^7 CFU (i.n.) 3×10^7 and 3.2×10^7 CFU (i.n.)	1.2×10^5 CFU of LVS (i.n.) 8 CFU of Schu S4 (i.n.)	100 % in BALB/cByJ 84 % in BALB/cByJ	(Kim et al. 2012)
acpA *acpB* *acpC* *hapA*	*F. novicida*	10^6 CFU (i.n.)	No	10^6 CFU of *F. novicida* (i.n.)	100 % in BALB/c	(Mohapatra et al. 2008)
sodB	LVS	5.27×10^3 CFU (i.n.) 5.16×10^2 CFU (i.n.)	No 1.21×10^3 CFU (i.n.)	14 CFU of Schu S4 (i.n.) 10^3 CFU of Schu S4 (i.n.)	40 % in C57BL/6 42 % in C57BL/6	(Bakshi et al. 2008)
FTT_1676	Schu S4	50 CFU (i.d.)	No	50 CFU of Schu S4 (i.d.) 10 CFU of Schu S4 (i.n.)	100 % in BALB/c	(Rockx-Brouwer et al. 2012)
FTT_0369c	Schu S4	50 CFU (i.d.)	No	50 CFU of Schu S4 (i.d.) 10 CFU of Schu S4 (i.n.)	100 % in BALB/c 90 % in BALB/c	

Table2 Francisella subunitvaccines

AntigenName	AdjuvantDelivery	systemVaccinationdose(r oute)Boost	Challengedoseand strain(route)	SurvivalinmiceReference
LPSLipopolysaccharideNoNo		ng(i.d. No	10^4 ofLVS(i.p.)100%inBABL/cByJ(Dreisbachetal. 2000)	
		100 50 μg(i.p.) 10^6 CFUofLVS(i.p.)	CFUofSchuS) i.p. %inBALB/c(Fulopetal. 2001)	
			%inBALB/c	
			%inC57BL/6(Ashtekaretal.	
DnaKChaperoneproteinGPI-0100No		20 μgofDnaK,together 1 20 μgofDnaK,togetherwith 100	1.5×10^6 CFUofLVS	2012)
		with10 μgofTul4(i.n.) 10^5 PFUofAd-opt-	(CFUofLVS(i.p.)80%inBALB/c(Kauretal.	
Tul4MembraneproteinNoAd-opt1×10		× Tul4(i.m.)-twice		2012)
		1 10^6 CFUof rLm/IglC(i.d.)4400CFUofLVS(i.n.)87.5%inBALB/c(Jiaetal.		
IglCIntracellulargrowth locus,subunitC	No rLm	×) 1 i.d.	1 10^7 CFUof rLm/IglC(i.d.)1×LD $_{100}$ 85.5 SchuS4	2009)
		(×) i.d.		%inBALB/c
		1	aerosol	
FopAOutermembrane protein	$Al(OH)_3$ Liposomes10 IL-12	(μgofliposomal rFopA(i.p.)	20 μgofliposomal rFopA—twice ×LD_{50} ofLVS(i.n.)100%survivalin C57BL/6	Hickeyetal. 2011)
			1	
			(	

Currently, live attenuated vaccines are prepared from live organisms and take into account the balance between attenuation and immunogenicity. Namely, over-attenuation could lead to the loss of partial bacterial virulence and an insufficient protective immune response. These types of vaccines are constructedby deletinggenes involved in metabolic and virulence pathways, which are also necessary for F. tularensis intracellular replication and in vivo survival.

Mutations in genes involved in Francisella metabolic pathways

Screening for genes involved in purine biosynthetic pathways in the Schu S4 strain revealed novel candidates for live attenuated vaccines (Prior et al. 2001). F. novicida mutants ΔpurA, ΔpurCD and ΔpurM were attenuated in mice; protection against challenge with a homologous wild-type strain was not observed (Tempel et al. 2006; Quarry et al. 2007). Mutant ΔpurF protected mice against intraperitoneal (i.p.) challenge with F. novicida, but not against the virulent Schu S4 strain (Quarry et al. 2007). In another study, an attenuated LVS mutant lacking the purine biosynthetic locus ΔpurMCD protected against LVS lethal challenge (Pechous et al. 2006); however, a single dose of this vaccine did not demonstrate a protective effect against i.n. or intradermal (i.d.) Schu S4 infection. In contrast, i.n. immunization with the Schu S4 mutant ΔpurMCD protected against i.n. challenge with a parental strain; however, the challenge′s outcome was influenced by the side effects of immunization (Pechous et al. 2008). Targeted deletion of the genes guaA and guaB in LVS leads to the attenuation in mice and to the stimulation of a protective immune response to i.p. challenge with a lethal dose of the parental strain (Santiago et al. 2009). However, Schu S4 mutants were not able to protect against the wild-type strain (Santiago et al. 2015).

The capsule synthesis gene (capB) encodes an ATPdependent ligase that is involved in capsule polysaccharide biosynthesis (Larsson et al. 2005). An LVS mutant with a targeted deletion in capB is significantly attenuated in mice, and its protective effect against i.n. challenge with a dose 10fold greater than the LD_{50} of Schu S4 was 100 % (Jia et al. 2010). Jia and colleagues prepared a vaccine regimen from a highly attenuated LVS mutant, ΔcapB, which served as a primary immunogen, and rLm/iglC, which is an attenuated recombinant Listeria monocytogenes expressing F. tularensis protein IglC, which was used as a booster. Mice vaccinated with ΔcapB and rLm/iglC exhibited prolonged survival and mean time to death with a challenge dose 10 times the LD_{50} of aerosolized

Mutations in genes from the Francisella pathogenicity island

The Francisella pathogenicity island (FPI) is a ⊡30 kb region ofthe Francisella genome(Nano etal. 2004) thatis duplicated in all F. tularensis subspecies except F. novicida (Larsson et al. 2009). The FPI contains the IglABCD operon, as well as pdpABC, that is essential for virulence. The majority of FPI proteins forms the type VI-like secretion system and is required for phagosomal escape following intracellular replication (Nano et al. 2004; Straskova et al. 2012).

In LVS, deletion of the iglC gene, which encodes a 23 kDa intracellular growth locus protein, led to an intracellular macrophage growth defect and attenuation in mice (Golovliov et al. 2003). The same mutation in F. novicida provided protection against i.n. infection with the parental strain. These effects were mediated by induction of Th1-type cytokine and antibody response (Pammit et al. 2006). In contrary, ΔiglC of Schu S4 origin did not protect mice against aerosol exposure to type A F. tularensis (Twine et al. 2005). Cong and colleagues (2009) prepared the ΔiglB mutant of F. novicida U112, which protected mice against pulmonary challenge with the virulent Schu S4 strain. In a recent study, the F. novicida mutant ΔiglB, which expresses the D1 domain of FljB flagellin from Salmonella typhimurium (S. typhimurium) and is a potent Toll-like receptor 5 (TLR5) agonist, was constructed. Oral vaccination with the construct protected rats against pulmonary challenge with Schu S4 (Cunningham et al. 2014). In addition, the deletion of another FPI gene, iglH, in the FSC200 strain established an attenuated phenotype that protected mice against subcutaneous challenge with a fully virulent, homologous wild-type strain (Straskova et al. 2012); thus, these studies underline the potential of FPI genes in the development of live attenuated vaccines.

To survive, Francisella reacts to stimuli from its surroundings and, in response, regulates virulence factor production. Several factors were identified to regulate FPI gene expression and include the following: FevR, MglA, PmrA and SspA (Charity et al. 2007; Mohapatra et al. 2007). Deletion of either the mglA or pmrA genes in F. novicida led to the attenuation of virulence in mice (Lauriano et al. 2004; Mohapatra et al. 2007), although only the ΔpmrA mutant protected against challenge with the parental strain but not the Schu S4 strain (Mohapatra et al. 2007).

Schu S4 compared to immunization by ΔcapB or parental strain alone. The use of a booster also invoked increased T cell immunity and enhanced IFN-γ secretion (Jia et al. 2013).

Mutations in various Francisella genes

Lipopolysaccharide (LPS), which consists of lipid A, core oligosaccharide and O-polysaccharide (O-PS) are the outer membrane components of a majority of gram-negative bacteria. In case of Francisella, these components are designed to support the pathogenicbehaviourofbacteria(OkanandKasper2013).Duet othe unusual tetraacylated structure of lipid A (Vinogradov et al. 2002), Francisella is able to evade detection by TLR4 (Dueñas et al. 2006). Attempts to mutate the LVS genes wbtA and wbtI, which are responsible for biosynthesis of O-PS, led to loss of OPS and the attenuation of the strain's virulence in mice. Moreover, mutants were able to protect against i.p. challenge with the parental strain (Raynaud et al. 2007; Li et al. 2007). Consistent with previous studies, the deletion of the gene wzy, which encodes O-PS polymerase, in LVS caused the strain to be highly attenuated in mice and demonstrated the protective effect of i.n. vaccination against i.n. challenge with the parental strain and virulent strain Schu S4 (Kim et al. 2012).

Acid phosphatases are the enzymes required for hydrolysis of phosphomonoesters, and they are the major virulence factors because of their connection to intracellular survival through repression of the oxidative burst in phagosomes (Reilly et al. 1996). Mohapatra and colleagues (2008) observed that the F. novicida quadrupole mutant, which lacks genes acpA, acpB, acpC and hapA, showed impaired phosphatase activity, phagosomal escape and intracellular survival in vitro and in mice, and its attenuated phenotype provided protection against F. novicida challenge.

Another bacterial protein involved in elimination of reactive oxygen intermediates is iron superoxide dismutase, which is encoded by the gene sodB. An LVS mutant, sodB, led to a significant attenuation of virulence in mice (Bakshi et al. 2006) and provided greater protection when compared to LVS administration after i.n. challenge with a lethal dose of Schu S4 (Bakshi et al. 2008).

The role of KatG is to catalyze bactericidal molecules, including H_2O_2 and $ONOO^-$. Intracellular growth of LVS or the Schu S4 mutant ΔkatG was not affected, although mutants showed enhanced susceptibility to H_2O_2 during in vitro analysis. The results from the i.d. immunization study demonstrated attenuation of the LVS mutant ΔkatG compared to the homologous wild-type strain. However, no differences were detected between the Schu S4 mutant

ΔkatG and corresponding wild-type strain (Lindgren et al. 2007).

The typeIV pili (Tfp) are multifunctional,flexible adhesive fibres expressed in many gram-negative bacteria (Chakraborty et al. 2008). Genome analysis of Francisella revealed genes required for the expression of Tfp system (Larsson et al. 2005). The pilin PilA is considered a critical virulence factor for the type B strain in the mouse model, as its deletion results in attenuation and an inability of bacteria to spread from the original site of infection (Forslund et al. 2006). Consistent with this finding, the mutation of other Tfp components, such as PilF, PilT, PilE5 and PilE6 in the LVS strain, led to the virulence attenuation (Chakraborty et al. 2008; Ark and Mann 2011). Moreover, Forslund et al. (2010) observed that mice infected with in-frame deletion mutants of the genes pilA, pilCand pilQin Schu S4strainexperienced a moderately delayed time to death.

In gram-negative bacteria, the formation of disulphide bonds in many proteins (including virulence factors) depends on the DsbA protein (Senitkova et al. 2011). A mutant lacking the gene FTT_1103, which encodes a dsbA homologue in Schu S4, was unable to escape phagosomes. The strain was attenuated in mice and showed a protective effect against i.n. Schu S4 challenge in BALB/c or C57BL/6 mice (Qin et al. 2009). Similar results were obtained for BALB/c mice infected with the ΔdsbA mutant on the FSC200 background
(Straskova et al. 2015).

Intradermal immunization with the deletion mutant of chaperone ClpB in Schu S4 protected BALB/c mice against respiratory challenge with a homologous wild-type strain (Twine et al. 2012). Moreover, Golovliov et al. (2013) observed that a Schu S4 mutant exhibited anenhanced protective effect when compared to a mutant in F. tularensis subsp. holarctica FSC200 (FSC200).

During the Francisella intracellular life cycle, the expression of FTT_1676 and FTT_0369c genes is upregulated (Wehrly et al. 2009). The genes encode a glycosylated membrane lipoprotein (Balonova et al. 2012) and the Sel1-family tetratricopeptide repeat-containing protein, respectively. Inactivation of both genes led to attenuation in mice (Wehrly et al. 2009). Rockx-Brouwer et al. found that i.d. inoculation with a low concentration of both mutants were protective against i.n. or i.d. challenge with Schu S4. However, the degree of protection correlated with the replication ability of mutants in the host (Rockx-Brouwer et al. 2012). In a recent study, F. novicida lacking an orthologue of FTT_1676, transposon mutant FTN_0109, displayed impaired intracellular growth. Authors observed a complete protective effect against pulmonary infection with 10 LD_{50} of LVS in BALB/c mice, whereas intratracheal challenge with 25 LD_{50} of Schu S4 provided partial protection of Fisher 344 rats against the same dose of LVS (Cunningham et al. 2015).

Subunit vaccines

Subunit vaccines are considered a safe vaccine because of their composition, which consists of synthesized or isolated microbial antigens. Inthe caseof Francisella, there are several bacterial structures that are considered potential subunit vaccines. One bacterial structure is Francisella LPS, which was able to induce some degree of protective immune response. Intradermal treatment of mice with LPS isolated from LVS provided protection against lethal challenge with a homologous strain (Dreisbach et al. 2000), but not against Schu S4 (Fulop et al. 2001). LPS purified from Schu S4 was able to extend the time to death in mice, but it was not able to protect against challenge with the parental strain (Prior et al. 2003). The failure of LPS to evoke a fully protective immune response probably results from its inability to stimulate robust cell-mediated immunity. In theory, the poor protection ability of LPS may be improved by adjuvant systems that induce T cell immunity. Richard et al. explored the immunogenic properties of synthetic nanoparticles prepared from catanionic surfactant vesicles that were activated by the incorporation of Francisella components. Adjuvant-associated LPS from LVS was used as a vaccine. Treated mice were protected against i.p. challenge with LVS yet remained vulnerable to i.n. infection with Schu S4. Authors enhanced effectiveness by incorporating components from LVS or Schu S4 whole bacterial lysates. However, they reached only partial protection against i.n. challenge with Schu S4 (Richard et al. 2014).

The weak proinflammatory nature of LPS turned our attention to Francisella immunogenic proteins. The partial protective effect against lethal respiratory challenge with LVS in mice was induced by Francisella heat shock protein DnaK and surface lipoprotein Tul4 with co-administration of GPI0100 i.n. as an adjuvant (Ashtekar et al. 2012). Recently, Banik et al. prepared a multivalent subunit vaccine by using tobacco mosaic virus as delivery system in combination with Francisella proteins, Tul4, DnaK and OmpA. Treated mice were protected against lethal LVS infection (Banik et al. 2015). Tul4 served as a basis for a subunit vaccine constructed from a replication-incompetent adenovirus carrying a codonoptimized gene for its expression, Ad-opt/Tul4. As a result, 60 % of mice were protected against i.p. infection with LVS following an i.m. immunization with a construct and two boosters (Kaur et al.

2012). In another report, authors vaccinated using a construct from an attenuated Δasd Δcya Δcrp S. typhimurium mutant carrying Tul4. The construct provided partial protection against intravenous challenge with LVS (Sjöstedt et al. 1992b). Similar results were obtained by Golovliov et al. (1995) who tested Tul4 in combination with immunostimulating complexes.

Jia et al. used an approach which employed attenuated rLm as a delivery vehicle that stably expressed various Francisella proteins, including AcpA, Bfr, DnaK, GroEL, KatG, Pld or IglC. However, only i.d. immunization with IglC-producing rLm evoked sufficient protection against i.n. lethal challenge with LVS or aerosolized Schu S4 (Jia et al. 2009).

Another candidate for a potential subunit vaccine, outer membrane protein A (FopA), was utilized as a recombinant protein incorporated into liposomes. Immunized mice showed a specific antibody response, and they were protected against a lethal i.n. and i.d. challenge with LVS, but not with the type A strain. Passively transferred FopA-immune serum to the naive mice protected against LVS infection (Hickey et al. 2011).

Conclusions

A tularemia vaccine has to fulfil various criteria; it must be safe and should be able to induce complete long-lasting protective immunity in individuals of all ages and with diverse levels of immunocompetence. The vaccine should protect against respiratory tularemia invoked not only by the most virulent type A strain Schu S4 but also by other less virulent strains. Despite intensive research in this area, there are still serious hurdles that impede the significant progress in tularemia vaccine development. Currently, LVS strain represent the most extensively studied vaccine candidate; however, as it was already mentioned, it does not provide sufficient protection against respiratory infection with Francisella type A strains and the molecular basis of its attenuation has not been clarified, as well. On the other side, a plethora of new promising candidates for live attenuated vaccines with defined gene deletion and good protective efficacy against type A strains have been prepared. Nevertheless, their experimental and clinical testing is in its infancy. Additionally, they usually exhibit high variability in their protective effects that is associated with the selection of the vaccination strain, dose and route of administration. The selection of proper animal model represents another weak point in a vaccine development. Mice are generally used for vaccination studies, but they are more sensitive to primary pulmonary infection with Francisella tularensis than humans; therefore, their usage for evaluation of basic mechanisms of Francisella pathogenesis and immune response to this microbe is not sufficient. It is necessary to combine several animal models in order to confirm the potential benefit of experimental vaccine for humans. Last but not the least, the mechanism of vaccine-elicited immune response has not been elucidated in a sufficient way up to now. This knowledge is a prerequisite for the identification of reliable correlates of post-vaccination protection.

Although live attenuated vaccines show promising protective effects, current trends in prophylaxis development, due to safety reasons, favour subunit vaccines rather than the live attenuated strains. Because Francisella is an intracellular pathogen, a Francisella subunit vaccine needs to induce cell-based response. However, the identification of Tcell specific epitopes is not trivial. One of the most promising approaches is whole genome immunoinformatic analysis, which detects immunogenic Francisella peptides that bind to MHCI (Rotem et al. 2014; Zvi et al. 2011). Alternatively, a protein array-based approach can identify epitopes from MHCII complexes from various serological targets (Valentino et al. 2011). It is expected that these new Bomics^ approaches can provide novel peptides epitopes for the development of the effective subunit vaccines.

Acknowledgments This work was supported by the Specific Research grant of Ministry of Education, Youth and Sports of Czech Republic (SV/ FVZ201202) and by a long-term organization development plan 1011.

Compliance with ethical standards

Conflict of interest The authors declare no conflict of interest.

References

Andersson H, Hartmanova B, Bäck E et al (2006) Transcriptional profiling of the peripheral blood response during tularemia. Genes Immun 7:503–513. doi:10.1038/sj.gene.6364321

Ark NM, Mann BJ (2011) Impact of Francisella tularensis pilin homologs on pilus formation and virulence. Microbial Pathogenesis 51:110– 120. doi:10.1016/j.micpath.2011.05.001

Ashtekar AR, Katz J, Xu Q, Michalek SM (2012) A mucosal subunit vaccine protects against lethal respiratory infection with Francisella tularensis LVS. PLoS ONE 7, e50460. doi:10.1371/journal.pone. 0050460

Bakshi CS, Malik M, Regan K et al (2006) Superoxide dismutase B gene (sodB)-deficient mutants of Francisella tularensis demonstrate hypersensitivity to oxidative stress and attenuated virulence. J Bacteriol 188:6443–6448. doi:10.1128/JB.00266-06

Bakshi CS, Malik M, Mahawar M et al (2008) An improved vaccine for prevention of respiratory tularemia caused by Francisella tularensis SchuS4 strain. Vaccine 26:5276–5288. doi:10.1016/j.vaccine.2008. 07.051

Balonova L, Mann BF, Cerveny L, et al (2012) Characterization of protein glycosylation in Francisella tularensis subsp. holarctica. Mol Cell Proteomics. doi: 10.1074/mcp.M111.015016

Banik S, Mansour AA, Suresh RVet al (2015) Development of a multivalent subunit vaccine against tularemia using tobacco mosaic virus (TMV) based delivery system. PLoS One. doi:10.1371/journal. pone.0130858

Baron SD, Singh R, Metzger DW (2007) Inactivated Francisella tularensis live vaccine strain protects against respiratory tularemia by intranasal vaccination in an immunoglobulin A-dependent fashion. Infect Immun 75:2152–2162. doi:10.1128/IAI.01606-06

Chakraborty S, Monfett M, Maier TM et al (2008) Type IV pili in Francisella tularensis: roles of pilF and pilT in fiber assembly, host cell adherence, and virulence. Infect Immun 76:2852–2861. doi:10. 1128/IAI.01726-07

Charity JC, Costante-Hamm MM, Balon EL et al (2007) Twin RNA polymerase-associated proteins control virulence gene expression in Francisella tularensis. PLoS Pathog. doi:10.1371/journal.ppat. 0030084

Cole LE, Mann BJ, Shirey KA et al (2011) Role of TLR signaling in Francisella tularensis-LPS-induced, antibody-mediated protection against Francisella tularensis challenge. J Leukoc Biol 90:787– 797. doi:10.1189/jlb.0111014

Cong Y, Yu J-J, Guentzel MN et al (2009) Vaccination with a defined Francisella tularensis subsp. novicida pathogenicity island mutant (ΔiglB) induces protective immunity against homotypic and heterotypic challenge. Vaccine 27:5554–5561. doi:10.1016/j.vaccine. 2009.07.034

Coriell LL, King EO, Smith MG (1948) Studies on tularemia; observations on tularemia in normal and vaccinated monkeys. J Immunol 58:183–202

Cunningham AL, Dang KM, Yu J-J et al (2014) Enhancement of vaccine efficacy by expression of a TLR5 ligand in the defined live attenuated Francisella tularensis subsp. novicida strain U112ΔiglB::fljB. Vaccine 32:5234–5240. doi:10.1016/j.vaccine.2014.07.038

Cunningham AL, Guentzel MN, Yu J-J et al (2015) Vaccination with the live attenuated Francisella novicida mutant FTN0109 protects against pulmonary tularemia. World J Vaccines 05:25–36. doi:10.4236/wjv.2015.51004

Dennis DT, Inglesby TV, Henderson DA et al (2001) Tularemia as a biological weapon: medical and public health management. JAMA 285:2763–2773

Dreisbach VC, Cowley S, Elkins KL (2000) Purified lipopolysaccharide from Francisella tularensis live vaccine strain (LVS) induces protective immunity against LVS infection that requires B cells and gamma interferon. Infect Immun 68:1988–1996

Dueñas AI, Aceves M, Orduña A et al (2006) Francisella tularensis LPS induces the production of cytokines in human monocytes and signals via Toll-like receptor 4 with much lower potency than E. coli LPS. Int Immunol 18:785–795. doi:10.1093/intimm/dxl015

Eigelsbach HT, Downs CM (1961) Prophylactic effectiveness of live and killed tularemia vaccines I. Production of vaccine and evaluation in the white mouse and guinea pig. J Immunol 87:415–425

Ellis J, Oyston PCF, Green M, Titball RW (2002) Tularemia. Clin Microbiol Rev 15:631–646. doi:10.1128/CMR.15.4.631-646.2002

Ericsson M, Sandström G, Sjöstedt A, Tärnvik A (1994) Persistence of cell-mediated immunity and decline of humoral immunity to the intracellular bacterium Francisella tularensis 25 years after natural infection. J Infect Dis 170:110–114

Ericsson M, Kroca M, Johansson T et al (2001) Long-lasting recall response of CD4+ and CD8+ alphabeta Tcells, but not gammadelta T cells, to heat shock proteins of Francisella tularensis. Scand J Infect Dis 33:145–152

Eyles JE, Hartley MG, Laws TR et al (2008) Protection afforded against aerosol challenge by systemic immunisation with inactivated Francisella tularensis live vaccine strain (LVS). Microbial Pathogenesis 44:164–168. doi:10.1016/j.micpath.2007.08.009

Forslund A-L,Kuoppa K,SvenssonK et al(2006)Direct repeat-mediated deletion of a type IV pilin gene results in major virulence attenuation of Francisella tularensis. Mol Microbiol 59:1818–1830. doi:10. 1111/j.1365-2958.2006.05061.x

Forslund A-L, Salomonsson EN, Golovliov I et al (2010) The type IV pilin, PilA, is required for full virulence of Francisella tularensis subspecies tularensis. BMC Microbiology 10:227. doi:10.1186/1471-2180-10-227

Forsman M, Sandström G, Sjöstedt A (1994) Analysis of 16S ribosomal DNA sequences of Francisella strains and utilization for determination of the phylogeny of the genus and for identification of strains by PCR. Int J Syst Bacteriol 44:38–46. doi:10.1099/00207713-44-1-38

Foshay L, Hesselbrock WH, Wittenberg HJ, Rodenberg AH (1942) Vaccine prophylaxis against tularemia in man. Am J Public Health Nations Health 32:1131–1145

Fulop M, Mastroeni P, Green M, Titball RW (2001) Role of antibody to lipopolysaccharide in protection against low- and high-virulence strains of Francisella tularensis. Vaccine 19:4465–4472. doi:10. 1016/S0264-410X(01)00189-X

Golovliov I, Ericsson M, Åkerblom L et al (1995) Adjuvanticity of ISCOMs incorporating a Tcell-reactive lipoprotein of the facultative intracellular pathogen Francisella tularensis. Vaccine 13:261–267. doi:10.1016/0264-410X(95)93311-V

Golovliov I, Sjöstedt A, Mokrievich A, Pavlov V (2003) A method for allelic replacement in Francisella tularensis. FEMS Microbiology Letters 222:273–280. doi:10.1016/S0378-1097(03)00313-6

Golovliov I, Twine SM, Shen H et al (2013) A ΔclpB mutant of Francisella tularensissubspecies holarcticastrain, FSC200,isa more effective live vaccine than F. tularensis LVS in a mouse respiratory challenge model of tularemia. PLoS One doi. doi:10.1371/journal. pone.0078671

Hartley G, Taylor R, Prior J et al (2006) Grey variants of the live vaccine strain of Francisella tularensis lack lipopolysaccharide O-antigen, show reduced ability to survive in macrophages and do not induce protective immunity in mice. Vaccine 24:989–996. doi:10.1016/j. vaccine.2005.08.075

Hickey AJ, Hazlett KRO, Kirimanjeswara GS, Metzger DW (2011) Identification of Francisella tularensis outer membrane protein A (FopA) as a protective antigen for tularemia. Vaccine 29:6941–6947. doi:10.1016/j.vaccine.2011.07.075

Hornick RB, EigelsbachHT (1966)Aerogenic immunizationofmanwith live tularemia vaccine. Bacteriol Rev 30:532–538

Jia Q, Lee B-Y, Clemens DL et al (2009) Recombinant attenuated Listeria monocytogenes vaccine expressing Francisella tularensis IglC induces protection in mice against aerosolized type A F. tularensis. Vaccine 27:1216–1229. doi:10.1016/j.vaccine.2008.12.014

Jia Q, Lee B-Y, BowenR et al (2010) A Francisella tularensis live vaccine strain (LVS) mutant with a deletion in capB, encoding a putative capsular biosynthesis protein, is significantly more attenuated than LVS yet induces potent protective immunity in

mice against F. tularensis challenge. Infect Immun 78:4341–4355. doi:10.1128/ IAI.00192-10

Jia Q, Bowen R, Sahakian J et al (2013) A heterologous prime-boost vaccination strategy comprising the Francisella tularensis live vaccine strain capB mutant and recombinant attenuated Listeria monocytogenes expressing F. tularensis IglC induces potent protective immunity in mice against virulent F. tularensis aerosol challenge. Infect Immun 81:1550–1561. doi:10.1128/IAI.01013-12

Johansson A, Farlow J, Larsson P et al (2004) Worldwide genetic relationships among Francisella tularensis isolates determined by multiple-locus variable-number tandem repeat analysis. J Bacteriol 186:5808–5818. doi:10.1128/JB.186.17.5808-5818.2004

Kaur R, Chen S, Arévalo MT et al (2012) Protective immunity against tularemia provided by an adenovirus-vectored vaccine expressing Tul4 of Francisella tularensis. Clin Vaccine Immunol 19:359–364. doi:10.1128/CVI.05384-11

Khan AS, Levitt AM, Sage MJ et al (2000) Biological and chemical terrorism: strategic plan for preparedness and response: recommendations of the CDC Strategic Planning Workgroup. http://www.cdc. gov/mmwr/preview/mmwrhtml/rr4904a1.htm. Accessed 20 January 2015

Kim T-H, Pinkham JT, Heninger SJ et al (2012) Genetic modification of the O-polysaccharide of Francisella tularensis results in an avirulent live attenuated vaccine. J Infect Dis 205:1056–1065. doi:10.1093/ infdis/jir620

Koskela P, Herva E (1982) Cell-mediated and humoral immunity induced by a live Francisella tularensis vaccine. Infect Immun 36:983–989

Koskela P, Salminen A (1985) Humoral immunity against Francisella tularensis after natural infection. J Clin Microbiol 22:973–979

Kubelkova K, Krocova Z, Balonova L et al (2012) Specific antibodies protect gamma-irradiated mice against Francisella tularensis infection. Microbial Pathogenesis 53:259–268. doi:10.1016/j.micpath. 2012.07.006

Larsson P, Oyston PCF, Chain P et al (2005) The complete genome sequence of Francisella tularensis, the causative agent of tularemia. Nat Genet 37:153–159. doi:10.1038/ng1499

Larsson P, Elfsmark D, Svensson K et al (2009) Molecular evolutionary consequences of niche restriction in Francisella tularensis, a facultative intracellular pathogen. PLoS Pathog. doi:10.1371/journal.ppat. 1000472

Lauriano CM, Barker JR, Yoon S-S et al (2004) MglA regulates transcription of virulence factors necessary for Francisella tularensis intraamoebae and intramacrophage survival. PNAS 101:4246– 4249. doi:10.1073/pnas.0307690101

Lavine CL, Clinton SR, Angelova-Fischer I et al (2007) Immunization with heat-killed Francisella tularensis LVS elicits protective antibody-mediated immunity. Eur J Immunol 37:3007–3020. doi:10.1002/eji.200737620

Li J, Ryder C, Mandal M et al (2007) Attenuation and protective efficacy of an O-antigen-deficient mutant of Francisella tularensis LVS. Microbiology 153:3141–3153. doi:10.1099/mic.0.2007/006460-0

Lindgren H, Shen H, Zingmark C et al (2007) Resistance of Francisella tularensis strains against reactive nitrogen and oxygen species with special reference to the role of KatG. Infect Immun 75:1303–1309. doi:10.1128/IAI.01717-06

McCrumb FR (1961) Aerosol infection of man with Pasteurella tularensis. Bacteriol Rev 25:262–267

Mohapatra NP, Soni S, Bell BL et al (2007) Identification of an orphan response regulator required for the virulence of Francisella spp. and transcription of pathogenicity island genes. Infect Immun 75:3305– 3314. doi:10.1128/IAI.00351-07

Mohapatra NP, Soni S, Reilly TJ et al (2008) Combined deletion of four Francisella novicida acid phosphatases attenuates virulence and macrophage vacuolar escape. Infect Immun 76:3690–3699. doi:10. 1128/IAI.00262-08

Mörner T (1992) The ecology of tularaemia. Rev - Off Int Epizoot 11: 1123–1130

Nano FE, Zhang N, Cowley SC et al (2004) A Francisella tularensis pathogenicity island required for intramacrophage growth. J Bacteriol 186:6430–6436. doi:10.1128/JB.186.19.6430-6436.2004

Ohara Y, Sato T, Fujita H et al (1991) Clinical manifestations of tularemia in Japan—analysis of 1,355 cases observed between 1924 and 1987. Infection 19:14–17

Okan NA, Kasper DL (2013) The atypical lipopolysaccharide of Francisella. Carbohydr Res 378:79–83. doi:10.1016/j.carres.2013. 06.015

Oyston PCF (2008) Francisella tularensis: unravelling the secrets of an intracellular pathogen. J Med Microbiol 57:921–930. doi:10.1099/ jmm.0.2008/000653-0

Pammit MA, Raulie EK, Lauriano CM et al (2006) Intranasal vaccination with a defined attenuated Francisella novicida strain induces gamma interferon-dependent antibody-mediated protection against tularemia. Infect Immun 74:2063–2071. doi:10.1128/IAI.74.4.20632071.2006

Pechous RD, Celli J, Penoske R et al (2006) Construction and characterization of an attenuated purine auxotroph in a Francisella tularensis live vaccine strain. Infect Immun 74:4452–4461. doi:10.1128/IAI. 00666-06

Pechous RD, McCarthy TR, Mohapatra NP et al (2008) A Francisella tularensis Schu S4 purine auxotroph is highly attenuated in mice but offers limited protection against homologous intranasal challenge. PLoS ONE. doi:10.1371/journal.pone.0002487

Pechous RD, McCarthy TR, Zahrt TC (2009) Working toward the future: insights into Francisella tularensis pathogenesis and vaccine development. Microbiol Mol Biol Rev 73:684–711.doi:10.1128/MMBR. 00028-09

Petrosino JF, Xiang Q, Karpathy SE et al (2006) Chromosome rearrangement and diversification of Francisella tularensis revealed by the type B (OSU18) genome sequence. J Bacteriol 188:6977–6985. doi:10.1128/JB.00506-06

Poquet Y, Kroca M, Halary F et al (1998) Expansion of Vgamma9 Vdelta2 T cells is triggered by Francisella tularensis-derived phosphoantigens in tularemia but not after tularemia vaccination. Infect Immun 66:2107–2114

Prior RG, Klasson L, Larsson P et al (2001) Preliminary analysis and annotation of the partial genome sequence of Francisella tularensis strain Schu 4. J Applied Microbiology 91:614–620. doi:10.1046/j. 1365-2672.2001.01499.x

Prior JL, Prior RG, Hitchen PG et al (2003) Characterization of the O antigen gene cluster and structural analysis of the O antigen of Francisella tularensis subsp. tularensis. J Med Microbiol 52:845–851. doi:10.1099/jmm.0.05184-0

Qin A, Scott DW, Thompson JA, Mann BJ (2009) Identification of an essential Francisella tularensis subsp. tularensis virulence factor. Infect Immun 77:152–161. doi:10.1128/IAI.01113-08

Quarry JE, Isherwood KE, Michell SL et al (2007) A Francisella tularensis subspecies novicida purF mutant, but not a purA

mutant, induces protective immunity to tularemia in mice. Vaccine 25:2011– 2018. doi:10.1016/j.vaccine.2006.11.054

Raynaud C, Meibom KL, Lety M-A et al (2007) Role of the wbt locus of Francisella tularensis in lipopolysaccharide O-antigen biogenesis and pathogenicity. Infect Immun 75:536–541. doi:10.1128/IAI. 01429-06

Reilly TJ, Baron GS, Nano FE, Kuhlenschmidt MS (1996) Characterization and sequencing of a respiratory burst-inhibiting acid phosphatase from Francisella tularensis. J Biol Chem 271: 10973–10983. doi:10.1074/jbc.271.18.10973

Richard K, Mann BJ, Stocker L et al (2014) Novel catanionic surfactant vesicle vaccines protect against Francisella tularensis LVS and confer significant partial protection against F. tularensis Schu S4 strain. Clin Vaccine Immunol 21:212–226. doi:10.1128/CVI.00738-13

Rockx-Brouwer D, Chong A, Wehrly TD et al (2012) Low dose vaccination with attenuated Francisella tularensis strain SchuS4 mutants protects against tularemia independent of the route of vaccination. PLoS ONE 7, e37752. doi:10.1371/journal.pone.0037752

Rotem S, Cohen O, Bar-Haim E, et al (2014) Protective immunity against lethal F. tularensis holarctica LVS provided by vaccination with selected novel CD8+ T cell epitopes. PLoS ONE 9:e85215. doi: 10.1371/journal.pone.0085215

Santiago AE, Cole LE, Franco A et al (2009) Characterization of rationally attenuated Francisella tularensis vaccine strains that harbor deletions in the guaA and guaB genes. Vaccine 27:2426–2436. doi:10.1016/j.vaccine.2009.02.073

Santiago AE, Mann BJ, Qin A, et al (2015) Characterization of Francisella tularensis Schu S4 defined mutants as live-attenuated vaccine candidates. Pathog Dis 73:ftv036. doi: 10.1093/femspd/ftv036

Senitkova I, Spidlova P, Hernychova L, Stulik J (2011) The disulfide bond formation and its relationship to bacterial pathogenicity of three important gram-negative bacteria. Mil Med Sci Lett 80:118–128

Sjöstedt A, Eriksson M, Sandström G, Tärnvik A (1992a) Various membrane proteins of Francisella tularensis induce interferon-gamma production in both CD4+ and CD8+ T cells of primed humans. Immunology 76:584–592

Sjöstedt A, Sandström G, Tärnvik A (1992b) Humoral and cell-mediated immunity in mice to a 17-kilodalton lipoprotein of Francisella tularensis expressed by Salmonella typhimurium. Infect Immun 60:2855–2862

Straskova A, Cerveny L, Spidlova P et al (2012) Deletion of IglH in virulent Francisella tularensis subsp. holarctica FSC200 strain results in attenuation and provides protection against the challenge with the parental strain. Microbes and Infection 14:177–187. doi: 10.1016/j.micinf.2011.08.017

Straskova A, Spidlova P, Mou S et al (2015) Francisella tularensis type B ΔdsbA mutant protects against type A strain and induces strong inflammatory cytokine and Th1-like antibody response in vivo. Pathog Dis. doi:10.1093/femspd/ftv058

Surcel HM, Syrjälä H, Karttunen R et al (1991) Development of Francisella tularensis antigen responses measured as T-lymphocyte proliferation and cytokine production (tumor necrosis factor alpha, gamma interferon, and interleukin-2 and -4) during human tularemia. Infect Immun 59:1948–1953

Tärnvik A, Berglund L (2003) Tularaemia. Eur Respir J 21:361–373. doi: 10.1183/09031936.03.00088903

Tempel R, Lai X-H, Crosa L et al (2006) Attenuated Francisella novicida transposon mutants protect mice against wild-type challenge. Infect Immun 74:5095–5105. doi:10.1128/IAI.00598-06

Tigertt WD (1962) Soviet viable Pasteurella tularensis vaccines a review of selected articles. Bacteriol Rev 26:354–373

Twine S, Byström M, Chen W et al (2005) A mutant of Francisella tularensis strain SCHU S4 lacking the ability to express a 58kilodalton protein is attenuated for virulence and is an effective live vaccine. Infect Immun 73:8345–8352. doi:10.1128/IAI.73.12.83458352.2005

Twine S, Shen H, Harris G et al (2012) BALB/c mice, but not C57BL/6 mice immunized with a ΔclpB mutant of Francisella tularensis subspecies tularensis are protected against respiratory challenge with wild-type bacteria: association of protection with post-vaccination and post-challenge immune responses. Vaccine 30:3634–3645. doi: 10.1016/j.vaccine.2012.03.036

Valentino MD, Maben ZJ, Hensley LL et al (2011) Identification of T-cell epitopes in Francisella tularensis using an ordered protein array of serological targets. Immunology 132:348–60. doi:10.1111/j.13652567.2010.03387.x

Vinogradov E, Perry MB, Conlan JW (2002) Structural analysis of Francisella tularensis lipopolysaccharide. Eur J Biochem 269:6112– 6118

Wehrly TD, Chong A, Virtaneva K et al (2009) Intracellular biology and virulence determinants of Francisella tularensis revealed by transcriptional profiling inside macrophages. Cell Microbiol 11:1128– 1150. doi:10.1111/j.1462-5822.2009.01316.x

West TE, Pelletier MR, Majure MC et al (2008) Inhalation of Francisella novicida ΔmglA causes replicative infection that elicits innate and adaptive responses but is not protective against invasive pneumonic tularemia. Microbes and Infection 10:773–780. doi:10.1016/j. micinf.2008.04.008

World Health Organization (1970) Health aspects of chemical and biological weapons. http://apps.who.int/iris/bitstream/10665/39444/1/ 24039.pdf. Accessed 20 January 2015

World Health Organization (2007) WHO guidelines on Tularaemia. http://www.cdc.gov/tularemia/resources/whotularemiamanual.pdf. Accessed 20 January 2015

Zvi A, Rotem S, Bar-Haim E, et al (2011) Whole-genome immunoinformatic analysis of F. tularensis: predicted CTL epitopes clustered in hotspots are prone to elicit a T-cell response. PLoS ONE 6:e20050. doi: 10.1371/journal.pone.0020050

Putzova D, Panda S, Härtlova A, Stulík J, Gekara NO (2017) Subversion of innate immune responses by *Francisella* involves the disruption of TRAF3 and TRAF6 signalling complexes. *Cellular Microbiology* **19**.

doi: 10.1111/cmi.12769

Received: 15 August 2016 | Revised: 20 July 2017 | Accepted: 21 July 2017

DOI: 10.1111/cmi.12769

WILEY

RESEARCH ARTICLE

Subversion of innate immune responses by Francisella involves the disruption of TRAF3 and TRAF6 signalling complexes

Daniela Putzova[1,2†] | Swarupa Panda[1†] | Anetta Härtlova[1†] | Jiří Stulík[2] | Nelson O. Gekara[1]

[1]Department of Molecular Biology, The Laboratory for Molecular Infection Medicine Sweden (MIMS), Umeå Centre for Microbial Research (UCMR), Umeå University, Umeå, Sweden

[2]Department of Molecular Pathology and Biology, Faculty of Military Health Sciences, University of Defense, Hradec Králové, Czech Republic

Correspondence
Nelson O. Gekara, Department of Molecular Biology, The Laboratory for Molecular Infection Medicine Sweden (MIMS), Umeå Centre for Microbial Research (UCMR), Umeå University, Umeå, Sweden
Email: nelson.gekara@mims.umu.se

Funding information
The Swedish Reserach Council (Vetenskapsrådet), Grant/Award Number: 2013-8621 and 2015-02857; organisation development plan 1011

Abstract

The success of pathogens depends on their ability to circumvent immune defences. Francisella tularensis is one of the most infectious bacteria known. The remarkable virulence of Francisella is believed to be due to its capacity to evade or subvert the immune system, but how remains obscure. Here, we show that Francisella triggers but concomitantly inhibits the Toll-like receptor, RIG-I-like receptor, and cytoplasmic DNA pathways. Francisella subverts these pathways at least in part by inhibiting K63-linked polyubiquitination and assembly of TRAF6 and TRAF3 complexes that control the transcriptional responses of pattern recognition receptors. We show that this mode of inhibition requires a functional type VI secretion system and/or the presence of live bacteria in the cytoplasm. The ability of Francisella to enter the cytosol while simultaneously inhibiting multiple pattern recognition receptor pathways may account for the notable capacity of this bacterium to invade and proliferate in the host without evoking a self-limiting innate immune response.

1 | INTRODUCTION

The success of pathogens depends on their ability to elude the immune system. Francisella tularensis, the etiological agent of the debilitating illness tularaemia, is one of the most infectious bacteria known and is among the top six potential bioterrorism agents, so-called Category A agents (Darling, Catlett, Huebner, & Jarrett, 2002). The remarkable virulence of Francisella is believed to be due to its capacity to invade and proliferate in the host without evoking a self-limiting immune reaction (Bosio, 2011; Pechous, McCarthy, & Zahrt, 2009; Steiner, Furuya, & Metzger, 2014).

The innate immune detection of and responsiveness to microbes is mediated by pattern recognition receptors (PRRs) that recognise conserved microbe-associated molecular patterns (MAMPs). PRRs include the cell surface or endosomal membrane-localised Toll-like receptors (TLRs) and the cytoplasmic PRRs such as RIG-I-like receptors (RLRs) and cytosolic DNA receptors (CDRs). Triggering of PRRs culminates in the transcriptional induction of proinflammatory cytokines and type I interferons (IFNs) that together coordinate antimicrobial immune defences (Kumar, Kawai, and Akira, 2011).

In order to overcome the host barrier to infection, Francisella has been shown to employ several mechanisms to evade detection by the innate immune system. For example, Francisella expresses lipopolysaccharide (LPS) with an atypical structure poorly recognised by TLR4 (Ancuta, Pedron, Girard, Sandstrom, & Chaby, 1996; Huang et al., 2010; Phillips, Schilling, McLendon, Apicella, & Gibson, 2004). Recently, Francisella has been demonstrated to evadeTLR2-mediated inflammatory responses by repressing the production of the TLR2 agonist lipoprotein (Jones, Sampson, Nakaya, Pulendran, & Weiss, 2012; Okan et al., 2013; Sampson, Saroj, Llewellyn, Tzeng, & Weiss, 2013). Moreover, in the cytoplasm, Francisella has been suggested to limit the accessibility of microbeassociated molecular patterns to cytosolic PRRs, which may explain the propensity of cytotoxic bacterial mutants to elicit a higher innate immune response (Peng, Broz, Jones, Joubert, & Monack, 2011).

In addition to these avoidance strategies, the ability of Francisella to colonise the host without stirring a strong inflammatory response is in part due to subversion of innate immune pathways. Active inhibition of innate immune signalling events including activation of the

† These authors contributed equally to this work.

Cellular Microbiology. 2017;19:e12769. https://doi.org/10.1111/cmi.12769 wileyonlinelibrary.com/journal/cmi

nuclear factor kappa B, signal transducers of transcription factor 1, IFN regulatory factors 1 and 8 (IRF1 and IRF8), mitogen-activated protein kinase (MAPK), and phosphatidylinositol 3-kinase/Akt pathways has been reported (Cremer, Butchar, & Tridandapani, 2011; Ireland, Wang, Alinger, Small, & Bosio, 2013; Roth, Gunn, Lafuse, & Satoskar, 2009; Telepnev, Golovliov, Grundstrom, Tarnvik, & Sjostedt, 2003; Telepnev, Golovliov, & Sjostedt, 2005). In spite of these insights, which PRR pathways are activated or inhibited upon Francisella infection and how remain poorly understood.

Ubiquitination is a critical posttranslational modification that regulates diverse cellular processes, including inflammatory responses. Ubiquitination involves the conjugation of a single or multiple ubiquitins by ubiquitin ligases onto proteins, that is, monoubiquitination and polyubiquitination, respectively. During polyubiquitination, ubiquitins can be attached onto each other either via the N terminal methionine or any of its seven internal lysine residues (K6, K11, K27, K29, K33, K48, and K63). This results in polyubiquitin chains of diverse structures that control the signalling activity or stability of proteins. The best characterised are the K63-linked polyubiquitin chains that control signal complex formation and the K48-linked chains that target proteins for proteasomal degradation (Kulathu & Komander, 2012).

Many pathogens well adapted to their host are known to activate PRR signalling cascades and subsequently suppress them. In fact, increasing evidence indicate that many pathogens do hijack the host ubiquitin system to their advantage (Ashida, Kim, & Sasakawa, 2014). Here, we show that F. tularensis live vaccine strain (LVS) triggers but concomitantly blocks the TLR, RLR, and CDR pathways. The E3 ligases TRAF6 and TRAF3 complexes are critical points of regulation for PRR pathways (Hacker et al., 2006; Panda, Nilsson, & Gekara, 2015). Our data show that LVS inhibits K63-linked polyubiquitination and assembly of TRAF6 and TRAF3 signalling complexes. Analysis of LVS mutants suggests a role for the Francisella type VI secretion system (T6SS) and/or cytoplasmic localization of bacteria in such inhibition. The ability of Francisella to inactivate these key proximal PRR complexes may account for the ability of this bacterium to inhibit multiple PRR pathways simultaneously and hence infect host cells without eliciting strong innate immune responses.

2 | RESULTS

2.1 | LVS weakly induces inflammatory responses via TLR, RLR, and CDR pathways

Francisella has a complicated life cycle involving transition from the cell surface to the endosomal compartment and finally into the cytosol. Therefore, in theory, Francisella should be sensed by multiple PRR families. TLRs, RLRs, and CDRs are the major PRR pathways for transcriptional induction of innate immune mediators. How Francisella activates or manipulates these PRR pathways is not well understood. Type I IFNs play a key role in innate immune defences against Francisella (Henry, Brotcke, Weiss, Thompson, & Monack, 2007). To study type I IFN induction upon Francisella infection and the specific PRR pathways involved, bone marrow-derived macrophages (BMDMs) from IFN-β luciferase reporter mice ($Ifn\beta^{+/\Delta\beta\text{-luc}}$; Lienenklaus et al., 2009) that are proficient or deficient in adaptor molecules for different PRR pathways including MYD88 ($Myd88^{-/-}Ifn\beta^{+/\Delta\beta\text{-luc}}$) for TLRs, IPS1 (MAVS; $Ips1^{-/-}Ifn\beta^{+/\Delta\beta\text{-luc}}$) for RLRs, STING ($Sting^{-/-}Ifn\beta^{+/\Delta\beta\text{-luc}}$) for CDRs, and TRIF ($Ticam1^{-/-}Ifn\beta^{+/\Delta\beta\text{-luc}}$) for TLRs and CDRs (Wang et al., 2016) were infected with F. tularensis LVS. IFN-β luciferase measurements and quantitative real time polymerase chain reaction (qRT-PCR) analysis of Ifnβ1 and Ifnα4 activation in these knockout cells revealed a reduced response in $Myd88^{-/-}$, $Ips1^{-/-}$, and $Ticam1^{-/-}$ (Figures 1 and S1A,B).

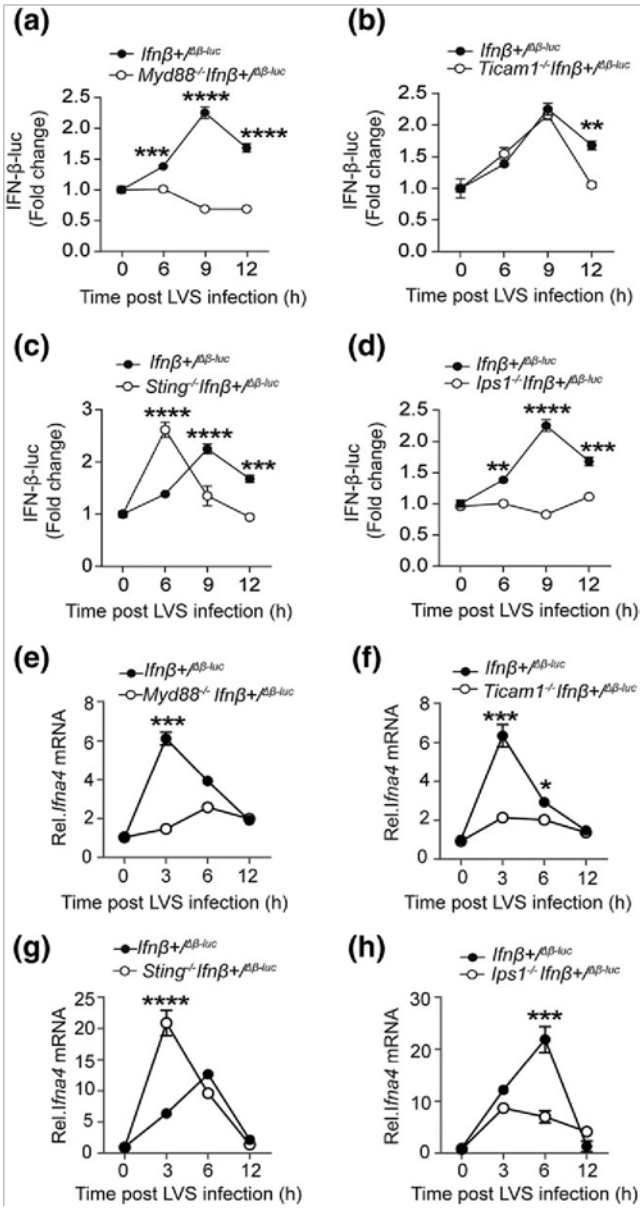

FIGURE 1 Infection of macrophages by Francisella results in a weak activation of Toll-like receptor, RIG-I-like receptor, and cytoplasmic DNA receptor pathways. (a–d) Bone marrow-derived macrophages

(BMDMs) from IFN-β luciferase reporter ($Ifnb^{+/\Delta ß\text{-}luc}$) or $Myd88^{-/-}Ifnb^{+/\Delta ß\text{-}luc}$. (a) $Ticam1^{-/-}Ifnb^{+/\Delta ß\text{-}luc}$, (b) $Sting^{-/-}Ifnb^{+/\Delta ß\text{-}luc}$, (c) and $Ips1^{-/-}Ifn\beta^{+/\Delta ß\text{-}luc}$, (d) mice infected with Francisella tularensis live vaccine strain (LVS; multiplicity of infection 50) for indicated durations then analysed for IFN-β luciferase response or by RT-PCR for Ifnα4 transcripts (e–h). Results are representative of two independent experiments. Data are shown as mean ± SEM. **P < .01; ***P < .001
(two-way analysis of variance with Bonferroni posttest)

Notably, for Sting$^{-/-}$ cells, reduced IFN-β response was mainly at late time points (8–12 hr postinfection), whereas at earlier time points, elevated IFN-β response was observed in such cells (Figure 1c). The enhanced response is probably due to a role for STING in negative regulation of TLRs (Sharma et al., 2015). In brief, these findings illustrated that inflammatory response to Francisella involves a coordinated activation of TLR, RLR, and CDR pathways. This is consistent with previous observations (Cole et al., 2008).

To further investigate how Francisella modulates innate immune responses, we compared LVS-induced responses with those by Listeria monocytogenes (L. monocytogenes). L. monocytogenes is a facultative intracellular bacterium that similarly activates TLR and RLR pathways but mainly induces type I IFNs via the STING pathway (Abdullah et al., 2012; Sauer et al., 2011; Witte et al., 2012). LVSinduced innate immune responses were found to be very modest; at least 10-fold lower to that by L. monocytogenes as determined by IFN-β luciferase and qRT-PCR assays (Figures 2a–f and S1C,D). Viability assay and immunofluorescence microscopy of infected BMDMs showed that the low LVS-induced response was neither due to enhanced death (Figure 2b) nor low bacteria uptake by LVSpreinfected BMDMs (Figure 2e–f).

2.2 | LVS blocks the TLR, RLR, and CDR pathways

Next, we wondered whether the repressed LVS-induced innate immune response was due to two opposing effects: the low activation or the active subversion of PRR pathways by Francisella. To test the latter, wild type or Ifnβ$^{+/\Delta\beta\text{-luc}}$ BMDMs were preexposed to LVS or L. monocytogenes for 3 hr before stimulation with defined ligands for different PRR pathways including, Pam_3CSK_4 (TLR2-MYD88 pathway; Dietrich et al., 2010), LPS (TLR4-TICAM1 pathway; Fitzgerald et al., 2003; Hoebe et al., 2003) and cyclic-di-GMP (STING pathway; Burdette et al., 2011). IFN-β luciferase and qRT-PCR analysis revealed that LVS severely blocks the activation of all such pathways. This was in contrasts to L. monocytogenes that led to an enhanced activation of these pathways (Figure 3a–e). As noted above, similar to LVS, L. monocytogenes activates TLR, RLR, and CDRs pathways (Figures 2c and S1). To further study the inhibitory effects of Francisella on these pathways, next we asked whether LVS could also attenuate the induction of innate immune responses by

L. monocytogenes. Accordingly, preinfection of Ifnβ$^{+/\Delta\beta\text{-luc}}$ BMDMs with LVS impaired L. monocytogenes-induced IFN-β luciferase response (Figure 3f). Similarly, qRT-PCR analysis confirmed that LVS could inhibit the induction of Ifnb1 and Tnfa genes by LPS or L. monocytogenes (Figure S2A,B).

Vesicular stomatitis virus (VSV) is a model viral pathogen known to both activate and suppress the induction of innate immune responses. VSV-AV2 is a natural VSV strain with a mutation in the M protein and hence can mount a strong innate immune response mainly via the activation of the RLR pathway (Kato et al., 2006; Stojdl et al., 2003). To further test the inhibitory effects of LVS on the RLR pathway, Ifnβ$^{+/\Delta\beta\text{-luc}}$ BMDMs preinfected with LVS were stimulated with VSV-AV2. LVS severely blocked VSV-AV2-induced IFN-β luciferase response. This was in clear contrast to L. monocytogenes that promoted VSVAV2-induced responses (Figure 3g). Together, these findings demonstrate that during infection, LVS actively inhibits the TLR, RLR, and CDR pathways and that this phenomenon may account for the restrained innate immune response elicited by LVS.

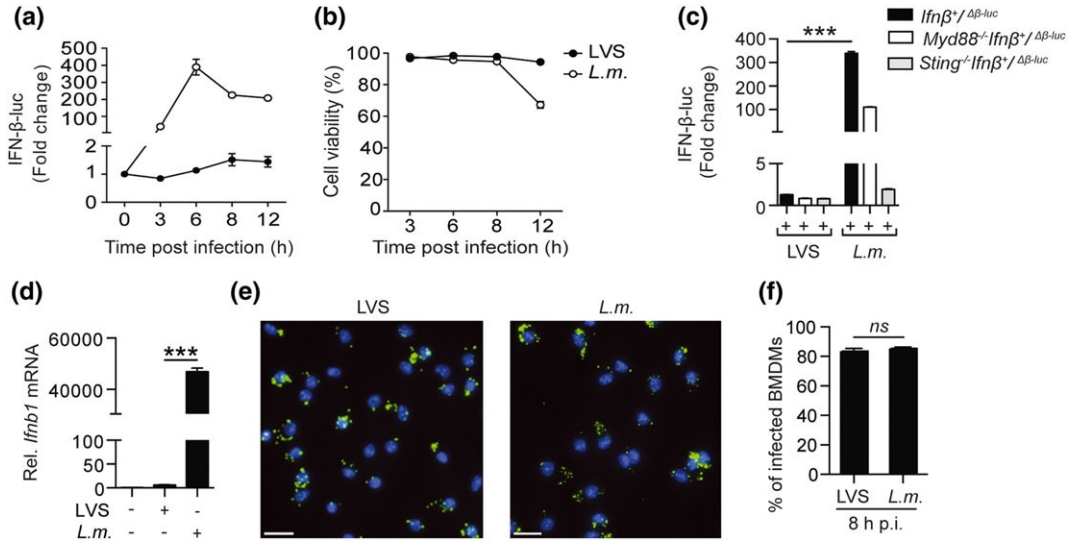

FIGURE 2 Francisella actively subverts activation of Toll-like receptor, RIG-I-like receptor, and cytoplasmic DNA receptor pathways. (a,b) Ifnb$^{+/\Delta\beta\text{-luc}}$ were infected with live vaccine strain (LVS; multiplicity of infection [MOI] 50), or Listeria monocytogenes (L.m.; MOI 10) for indicated durations were analysed for (a) IFN-β luciferase response and (b) cell viability (expressed as % relative to the untreated control). (c) IFN-β luciferase response in Ifnb$^{+/\Delta\beta\text{-luc}}$, Myd88$^{-/-}$Ifnb$^{+/\Delta\beta\text{-luc}}$, and Sting$^{-/-}$Ifnb$^{+/\Delta\beta\text{-luc}}$ bone marrow-derived macrophages (BMDMs) 8 hr after infection with LVS (MOI 50) or L. m. (MOI 10). (d–f) wild-type BMDMs infected with LVS or L.m.-green fluorescent protein (GFP) for 8 hr then analysed for Ifnb1 transcripts by quantitative reverse transcription polymerase chain reaction (d) or for intracellular bacteria by fluorescence microscopy (e). Bacteria were detected by immunostaining with rabbit anti-LVS

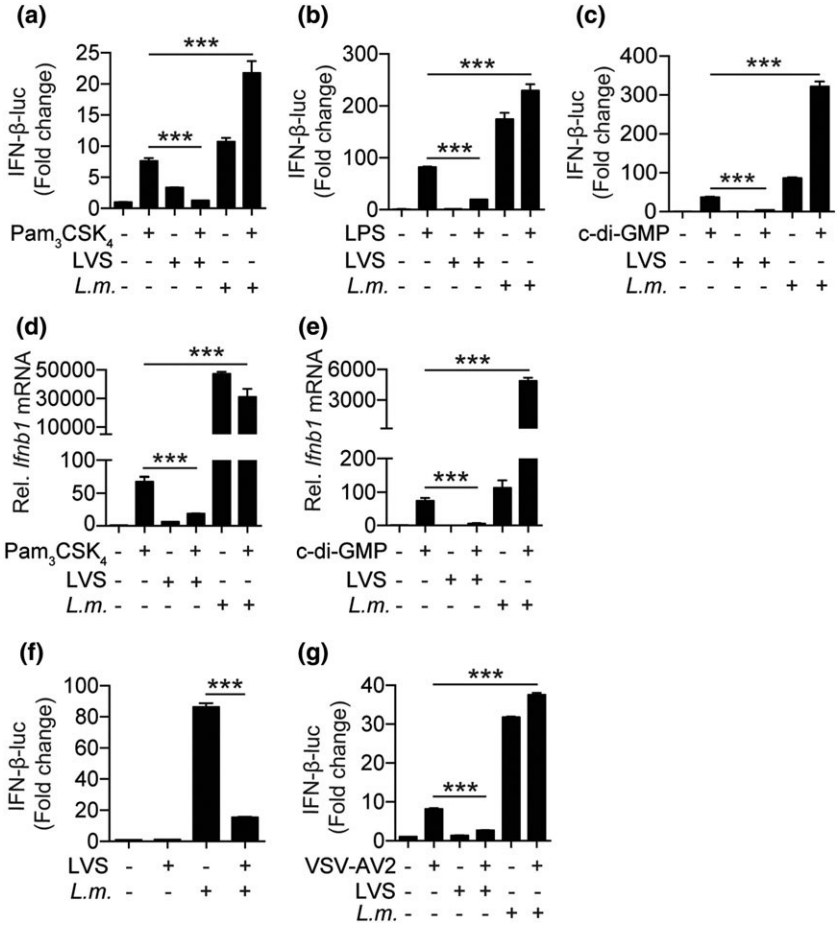

(green) or GFP (L.m.); nuclear staining (DAPI) is depicted in blue. Scale bar: 20 μm. (f) Quantification of bacterial loads in fluorescence micrographs depicted in (e). Graph shows pooled data from two independent experiments (n > 600 of counted cells). Results are representative at least of two independent experiments. Data are shown as mean ± SEM. ***P < .001 (Student's t test)

FIGURE 3 Francisella actively subverts activation of Toll-like receptor, RIG-I-like receptor, and cytoplasmic DNA receptor pathways. (a–c) IFN-β luciferase response in $Ifnb^{+/\Delta\beta\text{-luc}}$ bone marrow-derived macrophages (BMDMs) preinfected with live vaccine strain (LVS) or Listeria monocytogenes (L.m.) for 3 hr then stimulated with Pam_3CSK_4 (a), lipopolysaccharide (b), or c-di-GMP (c) for additional 5 hr. (d,e) Ifnb1 transcripts in wildtype BMDMs preinfected for 3 hr with LVS and then stimulated with Pam_3CSK_4 (d) or cdi-GMP (e) for an additional 5 hr. (f,g) IFN-β luciferase response in $Ifnb^{+/\Delta\beta\text{-luc}}$ BMDMs preinfected with LVS for 3 hr then stimulated with (f) L.m. or (g) vesicular stomatitis virus (VSV-AV2) for the next 5 hr. Results are representative of three independent experiments. Data are shown as mean ± SEM. ***P < .001 (one-way analysis of variance with Bonferroni posttest)

2.3 | Bacterial viability is essential for Francisellamediated inhibition of innate immune pathways

The above data indicate that the innate immune response elicited by Francisella must be the net outcome of the simultaneous activation and inhibition of PRR pathways. To gain more insights into how these distinct effects counterbalance each other, we sought to understand the following: (a) whether the viability of Francisella was essential for the activation or inhibition of PRR signalling and (b) the nature of bacterial products responsible for these two opposing effects. Compared to live LVS, heat-inactivated, ultraviolet-inactivated LVS elicited a higher IFN-β luciferase response (Figure S3A). Similarly, LVS lysed by sonication elicited a more robust response compared to live LVS (Figure S3B). The enhanced stimulatory potency of sonicated LVS was however sensitive to heat inactivation or treatment with benzonase, an endonuclease that digests both DNA and RNA (Figure S3B). This suggests that nucleic acids or heat-sensitive TLR ligands such as lipoproteins (TLR2; Cole et al., 2007) are likely the major PRR ligands via which extracellular LVS activates this response. In support of this idea, sonicated LVS were found not to elicit any response in $Myd88^{-/-}Ifn\beta^{+/\Delta\beta\text{-luc}}$ BMDMs (Figure S3C). Next, we tested the effect of sonicated LVS on TLR2, a major pathway known to be involved in innate immune responsiveness to Francisella (Cole et al., 2007; Katz, Zhang, Martin, Vogel, & Michalek, 2006). In contrast to the inhibitory effects of live LVS, sonicated LVS was found to promote the induction of IFN-β luciferase response by the TLR2 ligand Pam_3CSK_4 (Figure S3D). The enhanced response elicited by sonicated bacteria is in part due to the bioavailability of TLR ligands. Therefore, we tested structurally intact heat-inactivated LVS (HI-LVS). Compared to live LVS, HI-LVS provoked a stronger IFN-β luciferase response. Curiously, HI-LVS attenuated IFN-β luciferase upon TLR2 stimulation (Figure S3E). This suggests that although bacterial viability is important for Francisella-mediated subversion of PRR pathways, other factors that do not depend on bacterial viability such as bacteriaderived lipids (Crane, Ireland, Alinger, Small, & Bosio, 2013) may contribute to observed innate immune suppression.

2.4 | Francisella-mediated inhibition of PRR pathways is associated with T6SS and/or bacterial localization in the cytoplasm

Entry into the cytoplasm is an important hallmark for Francisella virulence. The Francisella T6SS is essential for the intracellular bacterial growth (de Bruin et al., 2011). IglC and DsbA (FipB), key virulence factors of Francisella, are essential for a functional T6SS (Qin et al., 2016; Ren, Champion, & Huntley, 2014). Hence, defects in these proteins impair entry into and replication of Francisella in the cytoplasm (Lindgren et al., 2004; Qin, Scott, Thompson, & Mann, 2009; Straskova et al., 2009). To investigate the role of the T6SS or entry into the cytoplasm on Francisella-mediated modulation of PRR pathways, we tested ΔiglC/LVS and ΔdsbA/LVS mutants. Compared to wild-type LVS, both ΔdsbA/LVS and ΔiglC/LVS strains elicited a higher induction of inflammatory response (Figures 4 and S4). Enhanced inflammatory response to these LVS mutants could be due to prolonged retention in phagosome resulting in sustained triggering of TLRs (Cole et al., 2010) and/or their inability to actively subvert PRRs signalling. To test the latter, we asked whether ΔdsbA/LVS and ΔiglC/LVS could also inhibit induction of inflammatory responses under costimulation settings. In contrast to wild-type LVS, ΔdsbA/LVS and ΔiglC/LVS strains did not robustly inhibit L. monocytogenes (Figure 4a–c), Pam_3CSK_4 (Figures 4d and S4A) or c-di-GMP (Figures 4eand S4B). However we observed that ΔiglC/LVS-infected BMDMs also exhibited slightly attenuated inflammatory induction by L. monocytogenes, Pam3CSK4 or c-di-GMP. This indicates that although the T6SS plays a major role in the suppression of innate immune pathways by Francisella, other factors not dependent on bacterial presence in the cytoplasm also contribute, albeit to a lesser extent.

To investigate whether observed subversion of innate immune responses was due to reduced bacterial uptake in cells upon preexposure to LVS, we monitored the intracellular load of bioluminescent L. monocyogenes (L.m.-lux) in such cells. No significant loss of cell viability was detected in LVS- and ΔiglC/LVS-infected cells. Importantly, in spite of the repressed inflammatory response, the intracellular load of L.m.-lux in such cells was comparable to those in control cells not preexposed to LVS (Figure S5A,B). Together these data demonstrate that the T6SS and/or entry into the cytoplasm play a major role in Francisella-mediated subversion of PRR pathways and that such effects are not due to cell death or diminished phagocytosis.

2.5 | LVS blocks proximal polyubiquitination and phosphorylation events in PRR pathways

Next, we sought to elucidate the signalling steps affected in Francisellamediated subversion of PRR pathways. TRAF6 and TRAF3 are critical points of convergence for many PRR pathways that control the transcriptional induction of innate immune mediators. In response to PRR triggering, TRAF6 and TRAF3 undergo K63-linked polyubiquitinaton, enabling these molecules to act as scaffolds for the recruitment and subsequent proximity-dependent activation of "downstream" signalling molecules (Hacker et al., 2006; Panda et al., 2015). The molecules recruited to the TRAF6 complex include the TAB2 and TAB3 adaptors and the TGF-beta activated kinase 1 (TAK1) that controls the activation of MAPKs and IKKα/β (inhibitor of nuclear factor kappa B kinase alpha or beta subunits) leading to the induction of proinflammatory genes. TheTRAF3 complex on the other hand recruits theTBK1 kinase that controls IRF3-driven induction of type I IFN genes (schematically summarised in Figure 6a). To investigate how Francisella modulates these signalling steps, BMDMs were infected with wild-type LVS, ΔiglC/LVS or ΔdsbA/LVS then analysed for activated (phosphorylated) forms of TAK1, p38 MAPK, IKKα/β, TBK1, IRF3, and the accumulation of K63- and K48-linked polyubiquitin chains. Consistent with the inhibitory effects (Figures 4; S4; S5; S6A,B; and S7), LVS, ΔiglC/LVS, or ΔdsbA/LVS were found to elicit an enhanced accumulation of these signalling molecules (Figures 5a and S6C). This demonstrates that Francisella infection results in simultaneous activation and inhibition of proximal PRR signalling events. These results are consistent with previous reports showing that Francisella initially activates but

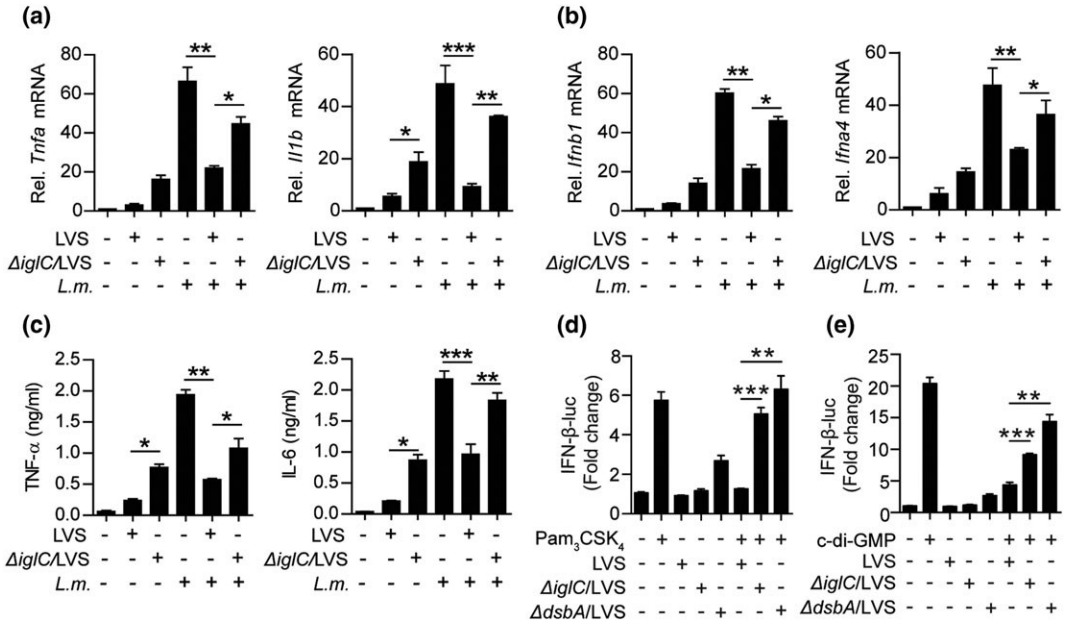

FIGURE 4 Subversion of PRR-mediated induction of inflammatory responses by Francisella requires T6SS and/or bacterial localization of the cytosol. (a–c) Wild-type bone marrow-derived macrophages (BMDMs) either infected with live vaccine strain (LVS) or ΔiglC/LVS or Listeria monocytogenes (L.m.) for 8 hr or first preinfected with LVS or ΔiglC/LVS for 3 hr then stimulated with L.m. for an additional 5 hr were analysed by quantitative reverse transcription polymerase chain reaction for the induction of proinflammatory cytokine genes Tnfa and Il1b (a) or IFN-I genes Ifnb1 and Ifna4 (b), or by ELISA for secreted TNF-α or IL-6 (c). (d,e) IFN-β luciferase response in $Ifnb^{+/\Delta\beta\text{-luc}}$ BMDMs infected for 8 hr with LVS or ΔdsbA/LVS or ΔiglC/LVS or preinfected with LVS or ΔdsbA/LVS or ΔiglC/LVS for 3 hr then stimulated with Pam_3CSK_4 (d) or c-di-GMP (e) for an additional 5 hr. Results are representative of three independent experiments. Data are shown as mean ± SEM. *P < .05; **P < .01; ***P < .001 (Student's t test)

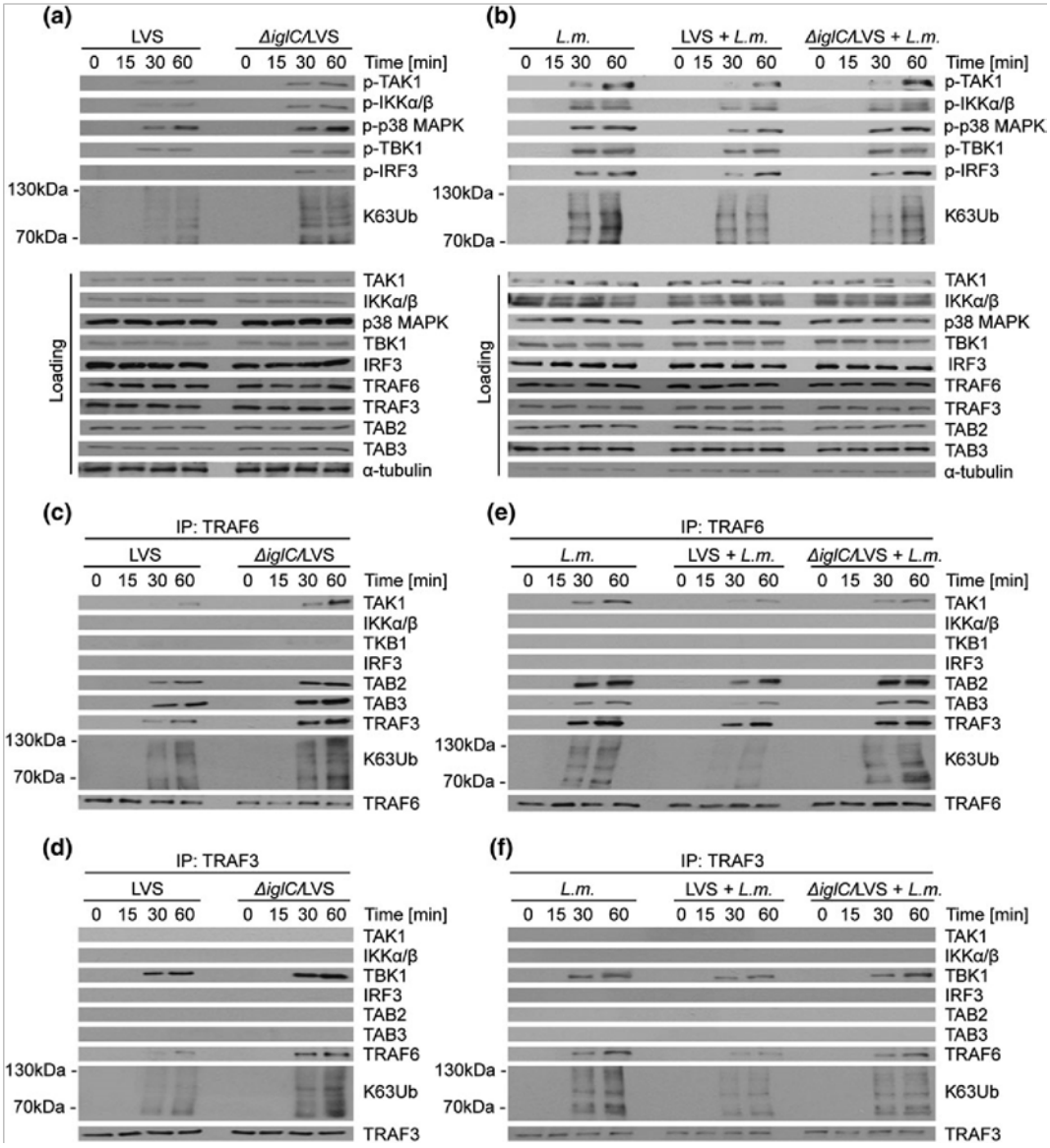

FIGURE 5 Francisella attenuates K63-linked polyubiquitination and assembly of TRAF6 and TRAF3 complexes. (a,b) wild-type (WT) bone marrowderived macrophages (BMDMs) infected with live vaccine strain (LVS) or ΔiglC/LVS for indicated durations (a) or WT BMDMs preinfected with LVS or ΔiglC/LVS for 3 hr then stimulated with Listeria monocytogenes (L.m.) for indicated durations (b) then analysed by Western blotting for the phosphorylation of TAK1, IKKα/β, p38 MAPK, TBK1, and IRF3 and accumulation of K63-linked polyubiquitin chains. As controls, total levels of TAK1, IKKα/β, p38 MAPK, TBK1, IRF3, TRAF6, TRAF3, TAB2, TAB3, and α-tubulin were analysed. (c–f) TRAF6 and TRAF3 complexes were immunoprecipitated from WT BMDMs infected with LVS or ΔiglC/LVS for indicated durations (c,d) or from WT BMDMs preinfected with LVS or ΔiglC/LVS for 3 hr then stimulated with L.m. for indicated durations (e,f). Complexes were analysed by Western blotting for the presence of TAK1, IKKα/β, TBK1, IRF3, TAB2, TAB3, TRAF3, TRAF6, and K63-linked polyubiquitin chains. Quantification of K63 polyubiquitination of TRAF6 and

TRAF3 are depicted in Figure S7. Results are representative of at least two independent experiments

subsequently downregulates intracellular signalling (Telepnev et al., 2003; Telepnev et al., 2005).

To more directly test Francisella-mediated inhibition of PRR pathways, these signalling events were also monitored under coinfection/costimulation settings. Indeed LVS inhibited L. monocytogenes-

and Pam_3CSK_4-induced activation of TAK1, p38 MAPK, IKKα/β, TBK1, and IRF3 as well as the accumulation of K63-polyubiquitin chains in BMDMs. This was in contrast with the ΔiglC/LVS or ΔdsbA/LVS strains that failed to or modestly exerted such inhibitory effects (Figures 5b, S6D, and 6b). In sum, these data demonstrate that LVS is an inhibitor of proximal PRR signalling events and its suppressive effects are largely dependent on a functional T6SS and/or entry of bacteria into the cytosol.

2.6 | LVS affects the polyubiquitination and assembly of TRAF6 and TRAF3 complexes

Given the central importance of TRAF6 and TRAF3 in the propagation of signals from multiple PRRs, next we evaluated whether Francisellamediated subversion of PRR pathways involved blockage in the assembly of TRAF6 and TRAF3 complexes. Compared to wild-type LVS, ΔiglC/LVS induced higher K63-linked polyubiquitination and recruitment of TAB2, TAB3, and TAK1 into the TRAF6 complex (Figure 5c) or TBK1 into the TRAF3 complex (Figure 5d). Notably, when analysed under coinfection settings, LVS was found to inhibit L. monocytogenes-induced K63-linked polyubiquitination and recruitment of TAB2, TAB3 and TAK1 into the TRAF6 complex or TBK1 into the TRAF3 complex (Figures 5e,f and S7), in a manner dependent on IglC. These results demonstrate that LVS is an inhibitor of the TRAF6 and TRAF3 complex assembly and that this may account for its ability to simultaneously block multiple PRR pathways.

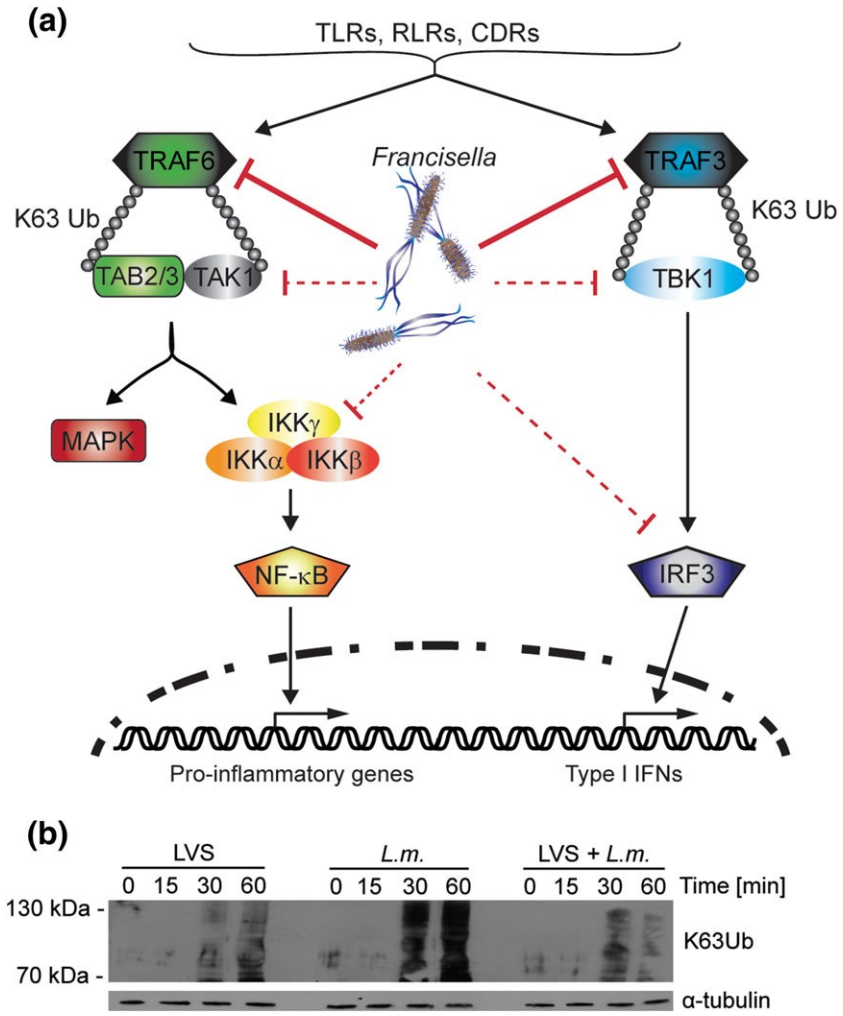

FIGURE 6 Francisella subverts multiple PRR pathways for proinflammatory and type I IFN responses. (a) Proposed model for subversion of PRRs by Francisella. (b) Francisella attenuates K63 polyubiquitination events in macrophages: Western blot analysis of K63 polyubiquitination in wild-type bone marrowderived macrophages that were infected with LVS or L.m. for indicated durations or preinfected with LVS for 3 hr then stimulated with L.m. for indicated durations. Results are representative of two independent experiments. PRR = pattern recognition receptor; LVS = live vaccine strain; L.m. = Listeria monocytogenes; TLR = Toll-like receptor; RLR = RIG-I-like receptor; CDR = cytoplasmic DNA receptor

3 | DISCUSSION

In this study, we investigated how Francisella modulates the TLR, RLR, and CDR pathways. By analysing macrophages from a variety of knockout mice, we show that Francisella elicits weak induction of innate immune pathways in a manner dependent on the presence of the MYD88, TRIF, IPS1, and MAVS adaptors.

What are the mechanisms or Francisella ligands involved in the activation of these pathways? Activation of MYD88-dependent responses is possibly due to the activation of TLR2 by lipoproteins (Abplanalp, Morris, Parida, Teale, & Berton, 2009) or TLR9 by DNA, whereas the STING-dependent responses could be due to the recognition of bacterial DNA in the cytoplasm by cGAS (Storek, Gertsvolf, Ohlson, & Monack, 2015). The TRIF adaptor is traditionally known for its role in TLR3 and TLR4 signalling. However, TRIF is also essential for optimal activation of the TLR2-MYD88 (Petnicki-Ocwieja et al., 2013) and cGAS-STING (Wang et al., 2016) pathways. Similarly, in addition to its primary role in RNA-mediated activation RLRs, it is conceivable that IPS1 adaptor could potentiate the

activation of cGAS-STING pathways via RNA polymerase III-dependent sensing of cytoplasmic DNA (Chiu, Macmillan, & Chen, 2009).

Although it remains unclear whether the TRIF- and IPS1-dependent inflammatory responses elicited by Francisella are due to the auxiliary role of these adaptors in the MYD88 and STING pathways, it is apparent that many PRR pathways are functionally interconnected and that the net inflammatory response upon Francisella infection is the product of a simultaneous or sequential activation of multiple PRR pathways. Thus, for a pathogen well adapted to its host, the most effective means to overcome the innate immune defences is a multipronged attack on diverse PRR pathways. The data herein show that although able to trigger the TLR, RLR, and CDR pathways, Francisella also actively blocks these pathways, and this could be due to its ability to target focal points of regulation for PRR pathways, the TRAF3 and TRAF6 complexes. In addition to these complexes, Francisella possibly also impedes other signalling steps, for example, upstream adaptors or receptors (Crane et al., 2013) or downstream at the transcription level (Bauler, Chase, Wehrly, & Bosio, 2014; Ireland et al., 2013; Walters et al., 2015). Hence, in spite of the productive infection and high replication in macrophages, Francisella evokes only a weak innate immune response much to its advantage.

The specific bacterial effectors responsible for innate immune subversion are not clear. IglC and DsbA are essential for the T6SS (Qin et al., 2016) and are required for bacterial entry into the cytoplasm (Lindgren et al., 2004; Qin et al., 2009). The fact that loss of IglC or DsbA severely impairs the capacity of Francisella to block innate immune pathways suggests that innate immune suppression by Francisella is dependent on bacterial localization in the cytoplasm and/or that such inhibition is mediated by T6SS effectors.

Although the specific virulence mechanisms involved in subversion on immune pathways remain unclear, the present study demonstrates for the first time that Francisella possesses factors that manipulate the host ubiquitin system. Further, the results support the concept that the ability of Francisella to block immune pathways may have occurred hand in hand with the evolution of virulence factors that allow the bacteria to invade the cytoplasm. The cytoplasm, a nutrient-rich milieu, is the ultimate target for many pathogens. However, entry into the cytosol does not come without additional risks for the pathogen; the cytoplasm is home to many PRRs whose activation may spell doom for the invasive pathogens. Therefore, in the absence of immune subversion, access to the cytoplasm can in fact be counterintuitive to the pathogen. The capacity of Francisella to synchronise its entry into the cytosol and the active subversion of innate immune pathways may account for the notable success of Francisella as a pathogen.

4 | EXPERIMENTAL PROCEDURES

4.1 | Animals

The use of experimental animals was carried out according to the guidelines set out by the Regional Animal Ethic Committee approval no. A107-11 or A53-14. Sting$^{-/-}$(C57BL/6J-Tmem173gt/J; Sauer et al., 2011) and Ticam1$^{-/-}$(C57BL/6J-Ticam1Lps2/J; Hoebe et al., 2003) were from Jackson Laboratory. Ifnb$^{+/\Delta\beta\text{-luc}}$ (Lienenklaus et al., 2009) mice were provided by S. Weiss. Myd88$^{-/-}$ (Adachi et al., 1998) and Ips-1$^{-/-}$ mice were from S. Akira's laboratory. Above mice were crossed with each other at the Umeå Transgene Core Facility to generate the following mouse lines: Myd88$^{-/-\text{Ifnb}+/\Delta\beta\text{-luc}}$, Ticam1$^{-/-\text{Ifnb}+/\Delta\beta\text{-luc}}$, Sting$^{-/-\text{Ifnb}+/\Delta\beta\text{-luc}}$, and Ips-1$^{-/-\text{Ifnb}+/\Delta\beta\text{-luc}}$ as recently described (Hartlova et al., 2015).

4.2 | Antibodies and chemicals

Anti-IKKα/β, anti-p38 MAPK, anti-TAK1, anti-IRF3, anti-p-IRF3, and anti-K63-linkage specific-polyubiquitin antibody were from Cell Signaling Technology. Anti-TRAF3, anti-TRAF6, anti-TAB2, anti-TAB3, Horseradish peroxidase (HRP)-conjugated goat antimouse IgG, and goat antirabbit IgG were from Santa Cruz. Anti-TBK1 and anti-pTBK1 antibodies were from Abcam. Ultrapure LPS, cyclic diguanylate monophosphate (c-di-GMP), and Pam_3CSK_4 were from InvivoGen.

4.3 | Bacterial and viral pathogens

Wild-type, ΔdsbA/LVS and ΔiglC/LVS, mutant strains of F. tularensis LVS were grown in Chamberlain's medium; L. monocytogenes EGD-e, pPL2 lux/pHELP (Bron, Monk, Corr, Hill, & Gahan, 2006), and GFP (Fortinea et al., 2000) strains were cultured in brain–heart infusion medium at 37 °C in 5% CO_2 atmosphere. For infections, all bacterial strains were grown to exponential phase in a given bacterial medium corresponding to OD = 0.4 at 37 °C. Francisella was inactivated by heating at 95 °C for 10 min, by sonication (8× for 15 s at Grade 4) or by overnight ultraviolet inactivation. The efficiency of bacterial lysis was confirmed by lack of growth on McLeod's agar plate. Bacterial lysate was treated by 2.5 U/μl benzonase® nuclease (Sigma-Aldrich) at 37 °C for 45 min.

VSV-AV2 has been described before (Stojdl et al., 2003).

4.4 | Preparation of BMDMs

To prepare BMDMs, bone marrow cells were isolated from mouse femurs and tibias and cultivated in Iscove's modified Dulbecco's medium (Life Technologies) supplemented with 10% fetal bovine serum (Thermo Fisher Scientific), 1% penicillin–streptomycin, and 20% (v/v) L929 cell-conditioned medium at 37 °C in 5% CO_2 atmosphere for 5 days.

4.5 | Infection of bone marrow-derived macrophages

BMDMs seeded into 6-, 12-, 24-, or 96-well plates at a density of 1.5×10^6, 7.5×10^5, 2.5×10^5, or 5×10^4 per well, were infected with wild-type LVS, ΔdsbA/LVS or ΔiglC/LVS, at a multiplicity of infection (MOI) of 50 and with L. monocytogenes at MOI of 10. To synchronise entry of the bacteria to the cells, plates were centrifuged at 400× g for 5 min. Thirty minutes postinfection, cells were washed once with phosphate-buffered saline (PBS) and cultured further in 50 μg/ml of gentamicin (Sigma-Aldrich) to kill extracellular bacteria. After 60 min postinfection, the medium was replaced and cells were cultured further in antibiotic-free Iscove's modified Dulbecco's medium. BMDMs were stimulated with either c-di-GMP (20

μg/ml), LPS (10 or 100 ng/ ml), Pam_3CSK_4 (100 ng/ml), L. monocytogenes (MOI 10), VSV-AV2 (MOI 0.01) or F. tularensis LVS (MOI 50).

4.6 | Immunofluorescence staining

BMDMs seeded on glass coverslips at a density of 2.5×10^5 cells per well were infected with F. tularensis LVS (MOI 50) or

L. monocytogenes-GFP (MOI 10) as described above for 8 hr. Following infection, cells were washed with PBS and fixed with 4% paraformaldehyde. Fixed cells were permeabilized with 0.2% Triton X-100, blocked with 3% BSA/PBS and incubated with polyclonal rabbit antiF. tularensis serum and antirabbit Alexa Fluor 488 antibody. Cells were stained with DAPI, washed with PBS, and mounted onto microscope slides and imaged by fluorescence microscopy.

4.7 | In vitro luciferase assay

Cells were lysed in 30-μl lysis buffer containing 0.2% (v/v) Triton-X100 and 10% (v/v) glycerol in PBS. Twenty-five microlitres of each lysate was mixed with 50 μl of Luciferase Assay Reagent (Promega), and luciferase activity was measured using TECAN Infinite M1000 PRO multimode microplate reader. Relative luminescence units were normalised to protein concentration and expressed as fold change in relation to unstimulated wild-type values.

4.8 | Bacterial uptake

Cells were lysed in 50-μl lysis buffer containing 0.2% (v/v) Triton-X100 and 10% (v/v) glycerol in PBS. Luminescence was measured using TECAN Infinite M1000 PRO multimode microplate reader. Relative luminescence units were expressed as fold change in relation to unstimulated wild-type values.

4.9 | Immunoblot analysis

Samples were separated by 10% SDS-PAGE and transferred onto Polyvinylidene difluoride (PVDF) or nitrocellulose membranes (GE Healthcare). Membranes were blocked for 1 hr with 1X RotiBlock (Roth) and subsequently incubated with different primary antibodies overnight. After incubation with HRP-labelled secondary antibodies, proteins were detected using Enhanced chemiluminescence (ECL) reagents and X-ray films. Immunoprecipitation and immunoblot analyses were performed as detailed in our recent study (Panda et al., 2015).

4.10 | Quantitative real-time polymerase chain reaction

RNA was isolated from cells using RNeasy kit from Qiagen. One microgram of total RNA was reverse transcribed using oligo (dT) primers (New England Biolabs). qRT-PCR analysis was performed and analysed using ABI Prism 7500 Fast RT-PCR System (Applied Biosystems). The results were normalised to the housekeeping genes and expressed as fold change relative to RNA samples from control or mock-treated cells/mice using the comparative CT method ($\Delta\Delta_{CT}$). All Taqman gene expression data are presented as the expression relative to 18S rRNA reference gene (RN18S1). The following TaqMan Gene Expression Assays were used (Applied Biosystems): Ifnb1 (Mm00439552_s1), Ifnα4 (Mm00833969_s1), Tnfa (Mm00443258_m1), Il1b (Mm 00434228_m1), and Rn18S1 (Mm03928990_g1).

4.11 | Cell viability assay

Cell viability was tested by CytoTox-ONE Homogenous Membrane Integrity Assay (Promega). Fluorescence was measured using TECAN Infinite M1000 PRO multimode microplate reader. Cell viability (%) was expressed as a percentage relative to the untreated control.

4.12 | Statistical analysis

The data are presented as mean with standard error of the mean (±SEM). Statistical analysis was performed using one-way analysis of variance with Bonferroni posttest or Mann–Whitney test using GraphPad Prism 5 software.

ACKNOWLEDGEMENTS

We thank Prof. Anders Sjostedt, Umeå University, Sweden, for the ΔiglC/LVS strain and Dr Siegfried Weiss, Helmholtz Centre for Infection Research, Germany, for the $Ifnb^{+/\Delta ß\text{-}luc}$ mice. We thank Saskia Erttmann for critical reading of the manuscript and for help with schematic illustration. This work was supported by funding from the Laboratory for Molecular Infection Medicine Sweden (MIMS), to N.O.G, and the Swedish Research Council (grants 2013-8621 and 2015-02857). This work was supported by a long-term organisation development plan 1011 to D.P and J.S.

ORCID

Nelson O. Gekara http://orcid.org/0000-0002-1269-8288

REFERENCES

Abdullah, Z., Schlee, M., Roth, S., Mraheil, M. A., Barchet, W., Bottcher, J., … Knolle, P. A. (2012). RIG-I detects infection with live Listeria by sensing secreted bacterial nucleic acids. The EMBO Journal., 31, 4153–4164.

Abplanalp, A. L., Morris, I. R., Parida, B. K., Teale, J. M., & Berton, M. T. (2009). TLR-dependent control of Francisella tularensis infection and host inflammatory responses. PloS One, 4, e7920.

Adachi, O., Kawai, T., Takeda, K., Matsumoto, M., Tsutsui, H., Sakagami, M., … Akira, S. (1998). Targeted disruption of the MyD88 gene results in loss of IL-1- and IL-18-mediated function. Immunity, 9, 143–150.

Ancuta, P., Pedron, T., Girard, R., Sandstrom, G., & Chaby, R. (1996). Inability of the Francisella tularensis lipopolysaccharide to mimic or to antagonize the induction of cell activation by endotoxins. Infection and Immunity., 64, 2041–2046.

Ashida, H., Kim, M., & Sasakawa, C. (2014). Exploitation of the host ubiquitin system by human bacterial pathogens. Nature Reviews. Microbiology, 12, 399–413.

Bauler, T. J., Chase, J. C., Wehrly, T. D., & Bosio, C. M. (2014). Virulent Francisella tularensis destabilize host mRNA to rapidly suppress inflammation. Journal of Innate Immunity, 6, 793–805.

Bosio, C. M. (2011). The subversion of the immune system by Francisella tularensis. Frontiers in Microbiology., 2, 9.

Bron, P. A., Monk, I. R., Corr, S. C., Hill, C., & Gahan, C. G. (2006). Novel luciferase reporter system for in vitro and organ-specific monitoring of differential gene expression in Listeria monocytogenes. Applied and Environmental Microbiology, 72, 2876–2884.

de Bruin, O. M., Duplantis, B. N., Ludu, J. S., Hare, R. F., Nix, E. B., Schmerk, C. L., … Nano, F. E. (2011). The biochemical properties of the Francisella pathogenicity island (FPI)-encoded proteins IglA, IglB, IglC, PdpB and DotU suggest roles in type VI secretion. Microbiology, 157, 3483–3491.

Burdette, D. L., Monroe, K. M., Sotelo-Troha, K., Iwig, J. S., Eckert, B., Hyodo, M., … Vance, R. E. (2011). STING is a direct innate immune sensor of cyclic di-GMP. Nature, 478, 515–518.

Chiu, Y. H., Macmillan, J. B., & Chen, Z. J. (2009). RNA polymerase III detects cytosolic DNA and induces type I interferons through the RIG-I pathway. Cell, 138, 576–591.

Cole, L. E., Laird, M. H., Seekatz, A., Santiago, A., Jiang, Z., Barry, E., … Vogel, S. N. (2010). Phagosomal retention of Francisella tularensis results in TIRAP/Mal-independent TLR2 signaling. Journal of Leukocyte Biology, 87, 275–281.

Cole, L. E., Santiago, A., Barry, E., Kang, T. J., Shirey, K. A., Roberts, Z. J., … Vogel, S. N. (2008). Macrophage proinflammatory response to

Francisella tularensis live vaccine strain requires coordination of multiple signaling pathways. Journal of Immunology., 180, 6885–6891. Cole, L. E., Shirey, K. A., Barry, E., Santiago, A., Rallabhandi, P., Elkins, K. L., … Vogel, S. N. (2007). Toll-like receptor 2-mediated signaling requirements for Francisella tularensis live vaccine strain infection of murine macrophages. Infection and Immunity., 75, 4127–4137.

Crane, D. D., Ireland, R., Alinger, J. B., Small, P., & Bosio, C. M. (2013). Lipids derived from virulent Francisella tularensis broadly inhibit pulmonary inflammation via Toll-like receptor 2 and peroxisome proliferator-activated receptor alpha. Clinical and Vaccine Immunology, 20, 1531–1540.

Cremer, T. J., Butchar, J. P., & Tridandapani, S. (2011). Francisella subverts innate immune signaling: Focus on PI3K/Akt. Frontiers in Microbiology., 5, 13.

Darling, R. G., Catlett, C. L., Huebner, K. D., & Jarrett, D. G. (2002). Threats in bioterrorism I: CDC category A agents. Emergency Medicine Clinics of North America, 20, 273–309.

Dietrich, N., Lienenklaus, S., Weiss, S., Gekara, N. O. (2010). Murine toll-like receptor 2 activation induces type I interferon responses from endolysosomal compartments. PLoS One, 5, e10250.

Fitzgerald, K. A., Rowe, D. C., Barnes, B. J., Caffrey, D. R., Visintin, A., Latz, E., … Golenbock, D. T. (2003). LPS-TLR4 signaling to IRF-3/7 and NFkappaB involves the toll adapters TRAM and TRIF. The Journal of Experimental Medicine., 198, 1043–1055.

Fortinea, N., Trieu-Cuot, P., Gaillot, O., Pellegrini, E., Berche, P., & Gaillard, J. L. (2000). Optimization of green fluorescent protein expression vectors for in vitro and in vivo detection of Listeria monocytogenes. Research in Microbiology, 151, 353–360.

Hacker, H., Redecke, V., Blagoev, B., Kratchmarova, I., Hsu, L. C., Wang, G. G., … Karin, M. (2006). Specificity inToll-like receptor signalling through distinct effector functions of TRAF3 and TRAF6. Nature, 439, 204–207.

Hartlova, A., Erttmann, S. F., Raffi, F. A., Schmalz, A. M., Resch, U., Anugula, S., … Gekara, N. O. (2015). DNA damage primes the type I interferon system via the cytosolic DNA sensor STING to promote anti-microbial innate immunity. Immunity, 42, 332–343.

Henry, T., Brotcke, A., Weiss, D. S., Thompson, L. J., & Monack, D. M. (2007). Type I interferon signaling is required for activation of the inflammasome during Francisella infection. The Journal of Experimental Medicine, 204, 987–994.

Hoebe, K., Janssen, E. M., Kim, S. O., Alexopoulou, L., Flavell, R. A., Han, J., & Beutler, B. (2003). Upregulation of costimulatory molecules induced by lipopolysaccharide and double-stranded RNA occurs by Trif-dependent and Trif-independent pathways. Nature Immunology, 4, 1223–1229.

Huang, M. T., Mortensen, B. L., Taxman, D. J., Craven, R. R., Taft-Benz, S., Kijek, T. M., … Ting, J. P. (2010). Deletion of ripA alleviates suppression of the inflammasome and MAPK by Francisella tularensis. Journal of Immunology, 185, 5476–5485.

Ireland, R., Wang, R., Alinger, J. B., Small, P., & Bosio, C. M. (2013). Francisella tularensis SchuS4 and SchuS4 lipids inhibit IL-12p40 in primary human dendritic cells by inhibition of IRF1 and IRF8. Journal of Immunology., 191, 1276–1286.

Jones, C. L., Sampson, T. R., Nakaya, H. I., Pulendran, B., & Weiss, D. S. (2012). Repression of bacterial lipoprotein production by Francisella novicida facilitates evasion of innate immune recognition. Cellular Microbiology., 14, 1531–1543.

Kato, H., Takeuchi, O., Sato, S., Yoneyama, M., Yamamoto, M., Matsui, K., … Akira, S. (2006). Differential roles of MDA5 and RIG-I helicases in the recognition of RNA viruses. Nature, 441, 101–105. Katz, J., Zhang, P., Martin, M., Vogel, S. N., & Michalek, S. M. (2006). Tolllike receptor 2 is required for inflammatory responses to Francisella tularensis LVS. Infection and Immunity., 74, 2809–2816.

Kulathu, Y., & Komander, D. (2012). Atypical ubiquitylation—The unexplored world of polyubiquitin beyond Lys48 and Lys63 linkages. Nature Reviews. Molecular Cell Biology., 13, 508–523.

Kumar, H., Kawai, T., & Akira, S. (2011). Pathogen recognition by the innate immune system. International Reviews of Immunology, 30, 16–34.

Lienenklaus, S., Cornitescu, M., Zietara, N., Lyszkiewicz, M., Gekara, N., Jablonska, J., … Weiss, S. (2009). Novel reporter mouse reveals constitutive and inflammatory expression of IFN-beta in vivo. Journal of Immunology., 183, 3229–3236.

Lindgren, H., Golovliov, I., Baranov, V., Ernst, R. K., Telepnev, M., & Sjostedt, A. (2004). Factors affecting the escape of Francisella tularensis from the phagolysosome. Journal of Medical Microbiology, 53, 953–958.

Okan, N. A., Chalabaev, S., Kim, T. H., Fink, A., Ross, R. A., & Kasper, D. L. (2013). Kdo hydrolase is required for Francisella tularensis virulence and evasion of TLR2-mediated innate immunity. mBio, 4. https://doi. org/e00638-00612

Panda, S., Nilsson, J. A., & Gekara, N. O. (2015). Deubiquitinase MYSM1 regulates innate immunity through inactivation of TRAF3 and TRAF6 complexes. Immunity, 43, 647–659.

Pechous, R. D., McCarthy, T. R., & Zahrt, T. C. (2009). Working toward the future: Insights into Francisella tularensis pathogenesis and vaccine development. Microbiology and Molecular Biology Reviews, 73, 684–711.

Peng, K., Broz, P., Jones, J., Joubert, L. M., & Monack, D. (2011). Elevated AIM2-mediated pyroptosis triggered by hypercytotoxic Francisella mutant strains is attributed to increased intracellular bacteriolysis. Cellular Microbiology, 13, 1586–1600.

Petnicki-Ocwieja, T., Chung, E., Acosta, D. I., Ramos, L. T., Shin, O. S., Ghosh, S., … Hu, L. T. (2013). TRIF mediates Toll-like receptor 2-dependent inflammatory responses to Borrelia burgdorferi. Infection and Immunity., 81, 402–410.

Phillips, N. J., Schilling, B., McLendon, M. K., Apicella, M. A., & Gibson, B. W. (2004). Novel modification of lipid A of Francisella tularensis. Infection and Immunity., 72, 5340–5348.

Qin, A., Scott, D. W., Thompson, J. A., & Mann, B. J. (2009). Identification of an essential Francisella tularensis subsp. tularensis virulence factor. Infection and Immunity., 77, 152–161.

Qin, A., Zhang, Y., Clark, M. E., Moore, E. A., Rabideau, M. M., Moreau, G. B., & Mann, B. J. (2016). Components of the type six secretion system are substrates of Francisella tularensis Schu S4 DsbA-like FipB protein. Virulence, 7, 882–894.

Ren, G., Champion, M. M., & Huntley, J. F. (2014). Identification of disulfide bond isomerase substrates reveals bacterial virulence factors. Molecular Microbiology, 94, 926–944.

Roth, K. M., Gunn, J. S., Lafuse, W., & Satoskar, A. R. (2009). Francisella inhibits STAT1-mediated signaling in macrophages and prevents activation of antigen-specific T cells. International Immunology, 21, 19–28.

Sampson, T. R., Saroj, S. D., Llewellyn, A. C., Tzeng, Y. L., & Weiss, D. S. (2013). A CRISPR/Cas system mediates bacterial innate immune evasion and virulence. Nature, 497, 254–257.

Sauer, J. D., Sotelo-Troha, K., von Moltke, J., Monroe, K. M., Rae, C. S., Brubaker, S. W., … Vance, R. E. (2011). The N-ethyl-N-nitrosoureainduced Goldenticket mouse mutant reveals an essential function of Sting in the in vivo interferon response to Listeria monocytogenes and cyclic dinucleotides. Infection and Immunity., 79, 688–694.

Sharma, S., Campbell, A. M., Chan, J., Schattgen, S. A., Orlowski, G. M., Nayar, R., … Fitzgerald, K. A. (2015). Suppression of systemic autoimmunity by the innate immune adaptor STING. Proceedings of the National Academy of Sciences of the United States of America., 112, E710–E717.

Steiner, D. J., Furuya, Y., & Metzger, D. W. (2014). Host–pathogen interactions and immune evasion strategies in Francisella tularensis pathogenicity. Infect Drug Resist., 7, 239–251.

Stojdl, D. F., Lichty, B. D., tenOever, B. R., Paterson, J. M., Power, A. T., Knowles, S., … Bell, J. C. (2003). VSV strains with defects in their ability to shutdown

innate immunity are potent systemic anti-cancer agents. Cancer Cell, 4, 263–275.

Storek, K. M., Gertsvolf, N. A., Ohlson, M. B., & Monack, D. M. (2015). cGAS and Ifi204 cooperate to produce type I IFNs in response to Francisella infection. Journal of Immunology., 194, 3236–3245. Straskova, A., Pavkova, I., Link, M., Forslund, A. L., Kuoppa, K., Noppa, L., … Stulik, J. (2009). Proteome analysis of an attenuated Francisella tularensis dsbA mutant: Identification of potential DsbA substrate proteins. Journal of Proteome Research, 8, 5336–5346.

Telepnev, M., Golovliov, I., Grundstrom, T., Tarnvik, A., & Sjostedt, A. (2003). Francisella tularensis inhibits Toll-like receptor-mediated activation of intracellular signalling and secretion of TNF-alpha and IL-1 from murine macrophages. Cellular Microbiology., 5, 41–51.

Telepnev, M., Golovliov, I., & Sjostedt, A. (2005). Francisella tularensis LVS initially activates but subsequently down-regulates intracellular signaling and cytokine secretion in mouse monocytic and human peripheral blood mononuclear cells. Microbial pathogenesis., 38, 239–247.

Walters, K. A., Olsufka, R., Kuestner, R. E., Wu, X., Wang, K., Skerrett, S. J., & Ozinsky, A. (2015). Prior infection with type A Francisella tularensis antagonizes the pulmonary transcriptional response to an aerosolized Toll-like receptor 4 agonist. BMC Genomics, 16, 874.

Wang, X., Majumdar, T., Kessler, P., Ozhegov, E., Zhang, Y., Chattopadhyay, S., … Sen, G. C. (2016). STING requires the adaptor TRIF to trigger innate immune responses to microbial infection. Cell Host & Microbe., 20, 329–341.

Witte, C. E., Archer, K. A., Rae, C. S., Sauer, J. D., Woodward, J. J., & Portnoy, D. A. (2012). Innate immune pathways triggered by Listeria monocytogenes and their role in the induction of cell-mediated immunity. Advances in Immunology., 113, 135–156.

SUPPORTING INFORMATION

Additional Supporting Information may be found online in the supporting information tab for this article.

How to cite this article: Putzova D, Panda S, Härtlova A, Stulík J, Gekara NO. Subversion of innate immune responses by Francisella involves the disruption of TRAF3 and TRAF6 signalling complexes. Cellular Microbiology. 2017;19:e12769.
https://doi.org/10.1111/cmi.12769

Prílohy

Ostatné publikácie v recenzovaných časopisoch

Drastíková M, Beránek M, Hegerová J, **Putzová D** (2012) Význam DNA vyšetření mutací C282Y, H63D a S65C v HFE genu. *Časopis lékařů českých* **151**: 428–431.

V˘znam DNA vy‰etfiení mutací C282Y, H63D a S65C v *HFE* genu

Monika Drastíková, Martin Beránek, Jaroslava Hegerová, Daniela Putzová

Univerzita Karlova v Praze, Lékafiská fakulta Hradec Králové, Ústav klinické biochemie a diagnostiky FN

SOUHRN

V˘chodisko. Hereditární hemochromatóza je pomûrnû ãasté dûdiãné onemocnûní, pro které je charakteristické zv˘‰ené vstfiebávání Ïeleza a jeho následné ukládání do dÛleÏit˘ch orgánÛ tûla. Cílem práce je urãit v˘skyt mutací C282Y, H63D a S65C ve skupinû pacientÛ s podezfiením na hereditární hemochromatózu a získané v˘sledky porovnat se zdravou ãeskou populací.

Metody. Soubor pacientÛ se skládal z 95 muÏÛ a 45 Ïen (medián vûku 55 rokÛ, rozsah 20–83 rokÛ). Soubor zdrav˘ch osob (kontrolní skupina) tvofiilo 167 dobrovolníkÛ (65 muÏÛ a 102 Ïen, medián vûku 25 rokÛ, rozsah 18–62 rokÛ). Genetická anal˘za mutací v *HFE* genu byla provedena pomocí metody PCR/RFLP.

V˘sledky. Frekvence rizikov˘ch alel v souboru pacientÛ byly: 18,2 % pro mutaci C282Y; 17,5 % pro H63D a 1,8 % pro S65C. Frekvence rizikov˘ch alel v kontrolním souboru byly: 5,7 % pro mutaci C282Y; 12,3 % pro H63D a 0,6 % pro S65C.

Závûry. V˘sledky svûdãí o trojnásobnû vy‰‰ím v˘skytu mutace C282Y ve skupinû pacientÛ s podezfiením na hereditární hemochromatózu oproti kontrolní skupinû (18,2 % vs. 5,7 %). V˘skyt mutací H63D a S65C se v obou porovnávan˘ch souborech statisticky neli‰il. **Klíãová slova:** hemochromatóza, *HFE* gen, C282Y, H63D, S65C, PCR/RFLP.

SUMMARY

Drastíková M, Beránek M, Hegerová J, Putzová D. The importance of DNA analysis of C282Y, H63D and S65C mutations in the *HFE* gene

Background. Hereditary hemochromatosis is a relatively common genetic disease characterized by increased iron absorption and deposition in major organs of the body. The aim of this study was to determine the prevalence of C282Y, H63D and S65C mutations in the *HFE* gene in patients suspected of hereditary hemochromatosis and to compare it with healthy subjects (control group).

Methods. The group of patients consisted of 95 males and 45 females (median age 55 years, range 20 to 83 years). The control group was represented by 167 volunteers of Caucasian origin (65 males and 102 females, median age 25 years, range 18 to 62 years). The PCR/RFLP genetic analysis was used to detect mutations in the *HFE* gene.

Results. Allelic frequencies of C282Y, H63D, and S65C in the patients group were 18.2 %, 17.5 %, and 1.8 %, respectively. The frequencies of the alleles in the control group were 5.7 % (C282Y), 12.3 % (H63D), and 0.6 % (S65C).

Conclusions. Our results show significant differences in the frequency of C282Y mutation between the patients suspected of hereditary hemochromatosis and the control group (18.2 % vs 5.7 %). Prevalences of H63D and S65C mutations in the both groups were not statistically significant.

Key words: hemochromatosis, *HFE* gene, C282Y, H63D, S65C, PCR/RFLP.

áas. Lék. ães. 2012; 151: 428–431

ÚVOD

Hereditární (vrozená) hemochromatóza (HH) je dědičné onemocnění charakterizované zvýšenou absorpcí železa v tenkém střevě a jeho následným ukládáním do jater, myokardu, pankreatu, hypofýzy, kloubů a pokožky. Nadměrná akumulace železa v játrech má vliv na aktivaci hvězdicovitých buněk (Ito buňky, hepatic stellate cells) a jejich přeměnu v buňky podobné myofibroblastům (myofibroblast – like cells), které ve zvýšené míře produkují kolagen I., III. a IV. typu (1, 2). Hypersekrece kolagenu může vést k jaterní fibróze. Při HH jsou rovněž ve zvýšené míře Fentonovou reakcí tvořeny hydroxylové radikály, které vlivem oxidačního stresu přispívají k nekróze hepatocytů a k rozvoji hepatocelulárního karcinomu (3–5).

ADRESA PRO KORESPONDENCI:
Mgr. Monika Drastíková
Ústav klinické biochemie a diagnostiky LF a FN
Sokolská 581, 500 05 Hradec Králové e-mail:
monika.drastikova@fnhk.cz

Prevalence HH v kavkazské populaci je přibližně 1 : 200–500 (6, 7), což ji řadí mezi nejčastější geneticky podmíněná onemocnění, ale též mezi choroby výrazně „poddiagnostikované“. Hereditární hemochromatóza se dělí do pěti základních podtypů HH1–HH5. Podtyp HH1, který představuje nejběžnější formu hemochromatózy, je podmíněn mutacemi v *HFE* genu. Ostatní podtypy souvisejí s genetickými polymorfismy v genech kódujících hemojuvelin, hepcidin, transferinový receptor 2, feroportin, transferin, ceruloplazmin a H-řetězce feritinu, avšak jejich frekvence ani klinické projevy nejsou v porovnání s HH1 tak významné (8, 9).

HFE gen, poprvé popsaný v roce 1996, se nachází na krátkém raménku 6. chromozomu (6p21.3). Patří do rodiny hlavního histokompatibilního komplexu s vysokou homologií ke genům HLAI. třídy. Kódovaný HFE protein má 343 aminokyselin. Je tvořen třemi extracelulárními doménami α1–α3. Doména α3 se u zdravých osob nekovalentně váže s $ß_2$-mikroglobulinem a vzniklý heterodimer je transportován na povrch buněk, kde obsazuje receptor pro transferin (10). Transferin nesoucí železo může vytěsnit HFE protein z této vazby, čímž je zprostředkován signál o dostatečné saturaci organismu železem. Uvolněný HFE protein následně moduluje expresi hepcidinu,

který degradací feroportinu snižuje přenos železa z enterocytů, hepatocytů a makrofágů do krevního oběhu (11).

Nejčastější příčinou HH1 v kavkazské populaci je mutace C282Y ve 4. exonu *HFE* genu. Substitucí cysteinu za tyrosin v pozici 282. aminokyseliny dochází ke ztrátě jednoho ze čtyř disulfidických můstků v HFE proteinu. Tato změna konformace ovlivňuje jeho afinitu k $ß_2$-mikroglobulinu a transport na povrch buněk, a v důsledku toho i vyšší absorpci železa z gastrointestinálního traktu.

Druhou významnou genetickou změnou v *HFE* genu je mutace H63D vedoucí k substituci histidinu za aspartát. Tato mutace neovlivňuje tvorbu heterodimeru HFE s $ß_2$-mikroglobulinem, proto jsou její klinické příznaky mírné nebo se nemusí projevit vůbec. Mechanismus, jakým dochází ke zvýšenému vstřebávání železa, není u této mutace dosud přesně popsán. Třetí nejčastější mutací v *HFE* genu je S65C podmiňující substituci serinu za cystein v HFE proteinu. Ani zde není role mutace v patogenezi HH zcela objasněna.

Autozomálně recesivní přenos HH znamená, že k jejím fenotypovým projevům může docházet jen v případě přítomnosti mutace na obou alelách. Postižené osoby lze molekulárně geneticky charakterizovat buď jako homozygoty pro jeden typ mutace (nejčastěji s genotypem 282Y/282Y) nebo smíšené heterozygoty (2–6 % případů HH) (12, 13).

Hemochromatóza patří k tzv. *střádavým* onemocněním. Ke kumulaci železa dochází celoživotně a první projevy HH se manifestují mezi 40. a 50. rokem života. Klinické příznaky choroby nejsou specifické, objevuje se únava, hepatomegalie, svalové a kloubní bolesti, v pokročilejších stadiích srdeční arytmie, hypogonadismus, diabetes mellitus, jaterní cirhóza a hepatocelulární karcinom. Projevy jsou mnohdy komplikovány jiným onemocněním (steatózou jater, alkoholismem, poruchou krvetvorby, metabolickým syndromem apod.).

Pro diagnostiku HH se provádí klinické vyšetření, fyzikální vyšetření a biochemická analýza zahrnující zejména určení saturace transferinu, stanovení koncentrace feritinu, sérového železa a železa v jaterní tkáni. Nedílnou součástí diagnostického procesu je také molekulárně genetická analýza jako prostředek pro vyhledání samotné příčiny choroby a odhalující další rizikové jedince v rodině probanda. Bez laboratorní diagnostiky mohou být nespecifické projevy HH snadno přehlédnuty a choroba může zůstat dlouhodobě neléčena.

Cílem této studie bylo zjistit, jaký je výskyt mutací C282Y, H63D a S65C u souboru pacientů hepatologických poraden s příznaky akumulace železa a porovnat jej s výskytem zmíněných mutací ve zdravé populaci.

SOUBOR NEMOCN¯CH A POUÎITÉ METODY

Do studie bylo zařazeno 140 pacientů (vyšetřovaný soubor) z 12 zdravotnických center zabývajících se chorobami jater a poruchami metabolismu železa. Pro molekulárně genetickou analýzu byly použity DNAvzorky 95 mužů a 45 žen s mediánem věku 55 roků (rozsah 20–83 roků). Soubor zdravých osob (kontrolní soubor) tvořilo 167 dobrovolníků (65 mužů, 102 žen, medián 25 roků, rozsah 18–62 roků), od nichž byl získán Informovaný souhlas k DNA analýze. Studie byla provedena se svolením Etické komise Fakultní nemocnice Hradec Králové.

Izolace DNA (QIAamp Blood Mini Kit, Qiagen, Německo) byla u pacientů provedena z 200 µl nesrážlivé krve (K3EDTA) a u dobrovolníků z bukálního stěru (FlogSwabs, Copan Flock Technologies, Itálie). Pro amplifikaci byla použita polymerázová řetězová reakce (PCR). Reakční směs pro amplifikaci exonu 2 *HFE* genu (25 µl) obsahovala 100 ng DNA, 10krát koncentrovaný PCR pufr s 15mM roztokem $MgCl_2$ (TaKaRa, Japonsko), 200 µM dNTPs, 0,4 µM primerů – F: 5'-ACA TGG TTG AGG CCT GTT GC 3' a R: 5'-GCC ACA TCT GGC TTG AAA TT-3' (Generi Biotech, ČR) a 1,5 U HS *Taq* polymerázy (TaKaRa). Směs pro exon 4 se lišila pouze sekvencemi použitých primerů – F: 5'- CTG GAT AAC CTT GGC TGT ACC CCC -3' a R: 5'- CAG ATC CTC ATC TCA CTG -3'. Teplotní profil PCR reakce pro oba úseky genu se skládal z 5 minutové úvodní denaturace při 95 °C, poté následovalo 30 cyklů PCR (denaturace 30 s při 94 °C, annealing 30 s při 50 °C a elongace 30 s při 72 °C) v termocykléru Veriti™ 96-Well Thermal Cycler, Applied Biosystems, USA.

Restrikční směs se skládala z 10 µl PCR produktu, 1 µl restrikčního pufru a 1 µl příslušného restrikčního enzymu (vše New England Biolabs, USA): *RsaI* pro detekci mutace C282Y, *BclI* pro H63D a *HinfI* pro S65C. Inkubace probíhala 16 hodin při 37 °C (*RsaI* a *HinfI*) nebo při 50 °C (*BclI*). Analýza restrikčních fragmentů (RFLP) byla provedena na 3% agarózovém gelu s ethidiumbromidem. Přítomnost *wild-type* alely C282 potvrzovaly restrikční fragmenty o velikostech 171 a 18 bp, zatímco pro mutovanou alelu 282Y svědčily fragmenty 142 bp, 29 bp a 18 bp. V případě mutace 63D docházelo k zániku rozpoznávacího místa pro *BclI*, a proto byl po restrikci na gelu viditelný jeden fragment o délce odpovídající PCR produktu (208 bp). Naopak, fragmenty o délkách 138 bp a 70 bp identifikovaly *wild-type* alelu H63. Obdobně při vyšetření mutace S65C svědčil fragment dlouhý 208 bp o přítomnosti mutantní alely 65C, fragmenty 147 bp a 61 bp identifikovaly *wildtype* alelu S65.

V¯SLEDKY

Ve vyšetřovaném souboru bylo nalezeno 18 homozygotů pro mutaci C282Y (12,9 %) a deset heterozygotů (7,1 %) pro tuto mutaci. U mutace H63D bylo detekováno sedm homozygotů (5,0 %) a 32 heterozygotů (22,9 %). Heterozygotní forma mutace S65C byla prokázána u tří pacientů (2,1 %) a nebyl nalezen žádný homozygot pro S65C. Smíšená heterozygozita byla zjištěna u pěti pacientů (3,5 %), z toho u tří osob (2,1 %) se

Tab. 2. Frekvence rizikových alel *HFE* genu ve vyšetřovaném a kontrolním souboru

	Frekvence rizikové alely (%)		
	C282Y	**H63D**	**S65C**
Vyšetřovaný soubor	18,2	17,5	1,8
Kontrolní soubor	5,7	12,3	0,6

jednalo kombinaci alel 282Y/63D a u dvou osob (1,4 %) o kombinaci 282Y/65C (tab. 1).

V kontrolním souboru jsme prokázali 16 heterozygotů pro mutaci C282Y (9,6 %), 32 heterozygotů pro H63D (19,2 %), dále tři homozygoty pro H63D (1,8 %), dva heterozygoty pro S65C (1,2 %). U tří dobrovolníků (1,8 %) byla zjištěna kombinace alel 282Y/63D (smíšená heterozygozita). V souboru nebyli nalezeni žádní homozygoti pro mutace C282Y ani S65C.

Celková frekvence všech rizikových alel ve vyšetřovaném souboru byla 37,5 % (18,2 % pro C282Y, 17,5 % pro H63D a 1,8 % pro S65C), tedy dvojnásobná než v kontrolním souboru: 18,6 % (5,7 % pro C282Y, 12,3 % pro H63D a 0,6 % pro S65C) (tab. 2).

Ve vyšetřovaném souboru bylo nalezeno celkem 30 osob s jedním z genotypů podmiňujících možné klinické příznaky HH (homozygoti 282Y/282Y, 63D/63D, smíšení heterozygoti 282Y/63D a 282Y/65C); v kontrolní skupině dosáhl jejich počet šesti. Predikce rizika HH ve vyšetřovaném souboru pacientů hepatologických ambulancí byla více než sedminásobná oproti souboru kontrolnímu (odds ratio 7,32; p < 0,001; 95% konfidenční interval: 3,27–16,39 %).

DISKUZE

Od roku 1996, kdy byl poprvé popsán *HFE* gen, byla publikována celá řada prací zabývajících se mapováním výskytu mutací v tomto genu. Jejich výsledky se shodují v konstatování, že majoritní podíl (80–90 %) na rozvoji HH má mutace C282Y, zejména je-li přítomna v homozygotní formě (14, 15). Na druhou stranu je třeba poznamenat, že penetrance C282Y není kompletní a choroba se manifestuje jen u části homozygotů (u 50 % mužů a 25 % žen) (16).

Tab. 1. Frekvence genotypů *HFE* genu ve vyšetřovaném a kontrolním souboru

Genotyp	Vyšetřovaný soubor		Kontrolní soubor	
	počet osob	%	počet osob	%
homozygot 282Y/282Y	18	12,9	0	0,0
heterozygot 282Y/wt	10	7,1	16	9,6
smíšený heterozygot 282Y/63D	3	2,1	3	1,8
smíšený heterozygot 282Y/65C	2	1,4	0	0,0
homozygot 63D/63D	7	5,0	3	1,8
heterozygot 63D/wt	32	22,9	32	19,2
heterozygot 65C/wt	3	2,1	2	1,2
homozygot wt/wt	65	46,5	111	66,4
celkem	**140**	**100,0**	**167**	**100,0**

wt – wild type

Z provedených populačních studií vyplývá, že nejvyšší frekvence rizikové alely 282Y se nacházejí v severozápadní Evropě, především v Irsku (14 %) a Velké Británii (8 %). V severní části Evropy (Norsko, Švédsko, Dánsko) se frekvence alely 282Y pohybují mezi 5,7–7,5 %. Není známo, zda byla tato mutace rozšířena do ostatních oblastí Evropy starověkými Kelty nebo skandinávskými mořeplavci, Vikingy (17, 18). Ve střední Evropě je frekvence 282Y 3,4–4,0 %. Ve státech jihovýchodní Evropy (Bosna a Hercegovina, Rumunsko, Srbsko, Makedonie) její výskyt klesá na 1,0–2,2 % (19). Mimo evropský kontinent se tato mutace objevuje vzácně.

V naší studii bylo zastoupení rizikové alely 282Y v kontrolní skupině vyšší než publikovali Čimburová a kol. (5,7 % vs. 3,4 %) v roce 2005 (20). Naše výsledky mohly být zatíženy chybou vyplývající z menšího počtu vyšetřených osob (n = 167).

Výsledky analýzy alely 282Y ve vyšetřovaném souboru (n = 140) prokázaly její trojnásobně vyšší výskyt u pacientů hepatologických ambulancí (18,2 %) oproti zdravé populaci. Celkem zde bylo nalezeno 18 homozygotů pro mutaci C282Y.

Jak již bylo zmíněno, mutace C282Y je považována za nejrizikovější mutaci z hlediska HH. Některé studie udávají, že podíl homozygotů ve skupině HH může být až 96% (21, 22). U heterozygotů pro C282Y dochází ke klinické manifestaci HH jen ojediněle. Spíše se ukazuje, že mutace může u heterozygotů akcelerovat orgánové poškození jiné primární etiologie (např. chronická hepatitida C, steatóza jater, hepatitida, alkoholismus apod.).

Frekvence mutace H63D se v evropské populaci pohybuje mezi 10 a 20 %. Nejvyšší výskyt byl popsán v Baskicku (30 %), Bulharsku, Španělsku a Portugalsku (> 20 %). U nás je její výskyt okolo 15 % (16). Frekvence mutace S65C se v kavkazské populaci pohybuje od 0,5 % (jihovýchodní Itálie) do 3 % (Švédsko, populace Saami) (23, 24). V České republice je frekvence S65C okolo 1 % (16). V našem

kontrolním souboru jsme nalezli dva heterozygoty pro mutaci S65C a frekvence alely 65C byla 0,6 %.

Je známo, že u homozygotů pro H63D a smíšených heterozygotů 282Y/63D nebo 282Y/65C bývají příznaky HH mírnější. Výskyt mutací H63D (17,5 %) a S65C (1,8 %) v naší vyšetřované skupině se významně nelišil od frekvence zjištěné v kontrolním souboru i výše zmíněných populačních odhadů. Mezi heterozygoty pro S65C byla jedna žena ve věku 30 let s normálním biochemickým nálezem a 3 muži se zvýšenou sérovou koncentrací železa. Laboratorní nález však nemusí být způsoben přítomností mutace S65C.

U zbývajících 65 pacientů z vyšetřovaného souboru (46,5 %) nebyly prokázány mutace C282Y, H63D ani S65C v *HFE* genu. U těchto osob může být přetížení organismu železem způsobeno dalšími mutacemi genů, jejichž produkty se podílejí na absorpci, transportu nebo ukládání železa. K rozvoji příznaků hemochromatózy přispívají také nevhodné stravovací návyky, přítomnost toxinů v organismu, obezita, HCV infekce anebo dlouhodobě zvýšený příjem alkoholu (u mužů více než 60 g/den a u žen 40 g/den). Alkohol nejen inhibuje transkripci hepcidinu, ale v důsledku oxidačního stresu organismu také zvyšuje expresi transferinového receptoru 1 (5, 25).

Velké množství faktorů negenetického charakteru, které se objevuje v etiopatogenezi HH je jedním z důvodů, proč nelze zavést plošný populační screening mutací v *HFE* genu. Spíše je preferován tzv. *selektivní screening* osob v rizikových skupinách (16). Při diagnostice hemochromatózy je doporučováno kombinovat molekulárně genetická vyšetření s paletou biochemických testů zahrnujících určení saturace transferinu, volné vazebné kapacity séra pro železo, stanovení feritinu a železa v séru, případně v jaterní tkáni (26). Biochemické markery i přes svou nižší specifičnost a závislost na řadě faktorů (věk, dieta, stravovací návyky, menstruace a jiné ztráty krve) mohou také významně pomoci při monitorování účinnosti navržených terapeutických a dietních postupů.

ZÁVùR

Hereditární hemochromatóza je značně rozšířeným genetickým onemocněním. K určení diagnózy HH se používají biochemická a molekulárně genetická vyšetření. Vzhledem k tomu, že se v našem státě neprovádí populační screening mutací v *HFE* genu, je nezbytné cíleně vyhledávat rizikové jedince pro toto onemocnění. Jednu z rizikových skupin představují pacienti hepatologických ambulancí se známkami přetížení organismu železem. Jak ukázala naše studie, u těchto osob se vyskytuje mutace C282Y několikanásobně častěji než ve zdravé populaci. Pro potvrzení nebo vyloučení HH u těchto osob (a jejich rodinných příslušníků) by mělo být vždy provedeno molekulárně genetické vyšetření *HFE* genu.

Zkratky

BclI – *Bacillus caldolyticus*
DNA – deoxyribonucleic acid (deoxyribonukleová kyselina)
dNTPs – deoxynucleotide triphosphates (deoxynukleotid trifosfáty)
HCV – hepatitis C virus (virus hepatitidy C)
HH – hereditary hemochromatosis (vrozená (hereditární) hemochromatóza)
HinfI – *Haemophilus influenzae*
HLA – human leukocyte antigen (hlavní histokompatibilní komplex)
HS Taq – hot start Thermus aquaticus
K3EDTA – ethylene diamine tetraacetic acid trisodium salt
PCR – polymerase chain reaction (polymerázová řetězová reakce)
RFLP – restriction fragment length polymorphism (polymorfizmus délky restrikčních fragmentů)
RsaI – *Rhodopseudomonas sphaeroides*

LITERATURA

1. **Brůha R, Hůlek P, Petrtýl J.** Jaterní cirhóza. In: Ehrmann J, Hůlek P, et al. Hepatologie. Praha: Grada Publishing 2010; 399–410.
2. **Mormone E, George J, Nieto N.** Molecular pathogenesis of hepatic fibrosis and current therapeutic approaches. Chem Biol Interact. 2011; 193: 225–231.
3. **Horák J.** Genetická hemochromatóza. In: Ehrmann J, Hůlek P, et al. Hepatologie. Praha: Grada Publishing 2010; 339–445.
4. **Kovář J.** Biologický význam a fyziologické funkce železa. In: Horák J. Hemochromatóza. Praha: Grada Publishing 2010; 15–22.
5. **Fargion S, Valenti L, Fracanzani A. L.** Beyond hereditary hemochromatosis: new insights into the relationship between iron overload and chronic liver diseases. Dig Liver Dis 2011; 43: 89–95.
6. **Phatak PD, Sham RL, Raubertas RF, et al.** Prevalence of hereditary hemochromatosis in 16031 primary care patients. Ann Intern Med 1998; 129: 954–961.
7. **Lyon E, Frank EL.** Hereditary hemochromatosis since discovery of the HFE gene. Clin Chem 2001; 47: 1147–1156.
8. **Whittington CA, Kowdley KV.** Review article: haemochromatosis. Aliment Pharmacol Ther 2002; 16: 1963–1975.
9. **Novotný J.** Poruchy metabolismu železa II. Vnitř. Lék. 2005; 51: 995–1006.
10. **Feder JN, Penny DM, Irrinki A, et al.** The hemochromatosis gene product complexes with the transferrin receptor and lowers its affinity for ligand binding. Proc Natl Acad Sci USA 1998; 95: 1472–1477.
11. **Deicher R, Hörl WH.** New insights into the regulation of iron homeostasis. Eur J Clin Invest 2006; 36: 301–309.
12. **Mura C, Raguenes O, Férec C.** HFE mutations analysis in 711 hemochromatosis probands: evidence for S65C implication in mild form of hemochromatosis. Blood 1999; 93: 2502–2505.

13. **Gurrin LC, Bertalli NA, Dalton GW, et al.** HFE C282Y/H63D compound heterozygotes are at low risk of hemochromatosisrelated morbidity. Hepatology 2009; 50: 94–101.
14. **Allen KJ, Gurrin LC, Constantine CC, et al.** Iron-overloadrelated disease in HFE hereditary hemochromatosis. N Engl J Med 2008; 358: 221–230.

15. **Gómez-Llorente C, Miranda-León MT, Blanco S, et al.** Frequency and clinical expression of HFE gene mutations in a Spanish population of subjects with abnormal iron metabolism. Ann Hematol 2005; 84: 650–655.
16. **Zlocha J, Kovács L, Požgayová S, et al.** Molekulovogenetická diagnostika a skríning hereditárnej hemochromatózy. Vnitř. Lék. 2006; 52: 602–608.
17. **Pedersen P, Melsen GV, Milman N.** Frequencies of the haemochromatosis gene (HFE) variants C282Y, H63D and S65C in 6020 ethnic Danish men. Ann Hematol 2008; 87: 735–740.
18. **Olsson KS, Konar J, Dufva IH, et al.** Was the C282Y mutation an Irish Gaelic mutation that the Vikings helped disseminate– Eur J Haematol 2011; 86: 75–82.
19. **Adler G, Clark JS, Łoniewska B, et al.** Prevalence of 845G>A HFE mutation in Slavic populations: an east-west linear gradient in South Slavs. Croat Med J 2011; 52: 351–357.
20. **Čimburová M, Půtová I, Provazníková H, et al.** S65C and other mutations in the haemochromatosis gene in the Czech Population. Folia Biol 2005; 51: 172–176.
21. **Hanson EH, Imperatore G, Burke, W.** HFE gene and hereditary hemochromatosis: a HuGE review. Am J Epidemiol 2001; 154: 193–206.
22. **Cukjati M, Vaupotic T, Rupreht R, et al.** Prevalence of H63D, S65C and C282Y hereditary hemochromatosis gene mutations in Slovenian population by an improved high-throughput genotyping assay. BMC Med Genet 2007; 69: 1–9.
23. **Pietrapertosa A, Vitucci A, Campanale D, et al.** HFE gene mutations in Apulian population: allele frequencies. Eur J Epidemiol 2003; 18: 685–589.
24. **Beckman LE, Sjoberg K, Eriksson S, et al.** Haemochromatosis gene mutations in Finns, Swedes, and Swedish Saamis. Hum Hered 2001; 52: 110–112.
25. **Pietrangelo A.** Hemochromatosis: an endocrine liver disease. Hepatology 2007; 46: 1291–1301.
26. **Husová L, Dastych M, Votava M, et al.** Hereditární hemochromatóza – opomíjená diagnóza. Čes a Slov Gastroent a Hepatol 2005; 59: 188–194.

Studie byla provedena v rámci projektu Specifického vysokoškolského výzkumu č. 264902 (2012).

Dankova V, Balonova L, Straskova A, Spidlova P, **Putzova D**, Kijek T, Bozue J,Cote C, Mou S, Worsham P, Szotakova B, Cerveny L, Stulik J (2014) Characterization of tetratricopeptide repeat-likeproteins in *Francisella tularensis* and identification of a novel locus required for virulence. *Infection and Immunity* **82**: 5035–5048.

doi: 10.1128/IAI.01620-14

IAI Journals.ASM.org

Characterization of Tetratricopeptide Repeat-Like Proteins in *Francisella tularensis* and Identification of a Novel Locus Required for Virulence

Vera Dankova,[a,b] Lucie Balonova,[b] Adela Straskova,[b] Petra Spidlova,[b] Daniela Putzova,[b] Todd Kijek,[c] Joel Bozue,[c] Christopher Cote,[c] Sherry Mou,[c] Patricia Worsham,[c] Barbora Szotakova,[a] Lukas Cerveny,[d] Jiri Stulik[b]

Department of Biochemical Sciences, Faculty of Pharmacy in Hradec Kralove, Charles University in Prague, Hradec Kralove, Czech Republic[a]; Institute of Molecular Pathology, Faculty of Military Health Sciences, University of Defence, Hradec Kralove, Czech Republic[b]; Bacteriology Division, U.S. Army Medical Research Institute of Infectious Diseases, Fort Detrick, Maryland, USA[c]; Department of Pharmacology and Toxicology, Faculty of Pharmacy in Hradec Kralove, Charles University in Prague, Hradec Kralove, Czech Republic[d]

Francisella tularensis **is a highly infectious bacterium that causes the potentially lethal disease tularemia. This extremely virulent bacterium is able to replicate in the cytosolic compartments of infected macrophages. To invade macrophages and to cope with their intracellular environment, *Francisella* requires multiple virulence factors, which are still being identified. Proteins containing tetratricopeptide repeat (TPR)-like domains seem to be promising targets to investigate, since these proteins have been reported to be directly involved in virulence-associated functions of bacterial pathogens. Here, we studied the role of the *FTS_0201*, *FTS_0778*, and *FTS_1680* genes, which encode putative TPR-like proteins in *Francisella tularensis* subsp. *holarctica***
FSC200. Mutants defective in protein expression were prepared by TargeTron insertion mutagenesis. We found that the locus *FTS_1680* and its ortholog *FTT_0166c* in the highly virulent *Francisella tularensis* type A strain SchuS4 are required for proper intracellular replication, full virulence in mice, and heat stress tolerance. Additionally, the *FTS_1680*-encoded protein was identified as a membrane-associated protein required for full cytopathogenicity in macrophages. Our study thus identifies FTS_1680/
FTT_0166c as a new virulence factor in *Francisella tularensis*.

Francisella tularensis is a facultative intracellular bacterium that causes the potentially lethal disease tularemia. *F. tularensis* can infect a wide range of animal species, including humans. *F. tularensis* can be transmitted to humans through a number of routes; the most common is via the bite of an infected insect or another arthropod vector. The spectrum of human illness can range from the ulceroglandular form to the more serious pneumonic or typhoidalformoftularemia(1).Theriskofseverehumaninfection is associated mainly with two subspecies, the highly virulent *F. tularensis* subsp. *tularensis* (type A) and the less virulent *F. tularensis* subsp. *holarctica* (type B). Documented use of *F. tularensis* as a biological weapon in World War II and concerns over construction of antibiotic-resistant *F. tularensis* strains have led to an enhanced interest in unveiling mechanisms of virulence which may serve as promising targets for the development of treatments or effective prophylaxis in case of its misuse (2).

F. tularensis infects multiple cell types, including nonphagocytic and phagocytic cells (1, 2). Following entry into phagocytic host cells, *Francisella* is found in phagosomes that are characterized by the presence of early (EEA-1) and late (LAMP-1) endosomal markers (3). However, the bacterium subsequently modulates the fusion of the *Francisella*-containing phagosome with degradative lysosomes and escapes into the cytosol, where it replicates. Within 24 to 48 h after infection, *Francisella* reenters LAMP-1-positive endocytic compartments referred to as *Francisella*-containing autophagic vacuoles (3, 4).

Previous studies have identified a wide array of genes required by *F. tularensis* for adaptation to intracellular environments and/or evasion of phagocytic cell defense mechanisms. These include genes located in a 34-kb *Francisella* pathogenicity island (FPI), genes responsible for the presence of a noninflammatory lipopolysaccharide, protective capsule, and siderophores, and genes encoding proteins involved in resistance to various stress conditions (5–12).

Of the other candidates, tetratricopeptide repeat (TPR)- or SEL1-like (SLR) structural motif-containing proteins seem to be promising targets for more detailed studies. The TPR and SLR motifs share similar -helical conformations but differ in consensus sequence, length, and superhelical topology (13). Despite this distinction, both motifs represent elegant modules for the assembly of various multiprotein complexes via mediating protein-protein interactions (13, 14); thus, such proteins are often involved in numerous cellular processes in both eukaryotic and prokaryotic organisms (14, 15). Several *F. tularensis* proteins with predicted TPR/SLR motifs have already been shown to be required for the fully expressed virulent phenotype. These proteins include the hypothetical SLR-containing protein DipA, the putative TPR-containing protein FTT_1244c from *F. tularensis* subsp. *tularensis* SchuS4 (4), and the putative TPR-containing proteins PilF and FTL_0205 from *Francisella* subsp. *holarctica* LVS (16, 17).

The goal of this study was to determine whether the three putativeTPR-likeproteinsFTS_0201,FTS_0778,andFTS_1680play

Received 17 February 2014 Returned for modification 17 March 2014
Accepted 3 September 2014
Published ahead of print 22 September 2014
Editor: C. R. Roy
Address correspondence to Lukas Cerveny, cervenyl@faf.cuni.cz.
doi:10.1128/IAI.01620-14

Infection and Immunity p. 5035–5048

TABLE1 Bacterial strains and plasmids used in this study

Strain or plasmid	Relevant characteristics	Source and/or reference
E. coli strains		
-Select Gold Efficiency	F *deoR endA1 recA1 relA1 gyrA96 hsdR17* ($r_K m_K$) *supE44 thi-1 phoA* (*lacZYA argF*)U169 80*lacZ*M15	Bioline
DHM1	F= *cya-854 recA1 endA1 gyrA96* (Nal^r) *thi-1 hsdR17 spoT1 rfbD1 glnV44*(AS)	BACTH system kit; Euromedex (46)
Francisella strains		
FSC200	*F. tularensis* subsp. *holarctica*, clinical isolate	*Francisella* strain collection (18)
SchuS4	*F. tularensis* subsp. *tularensis*	USAMRIID strain collection
inFTS_0201	FSC200 *inFTS_0201*	This study
inFTS_0778	FSC200 *inFTS_0778*	This study
inFTS_1680	FSC200 *inFTS_1680*	This study
inFTS_1680 complemented	inFTS_1680 with pKK289FTS_1680	This study
inFTT_0166c	SchuS4 *inFTT_0166c*	This study
Plasmids		
pCR4-TOPO	Cloning vector, Amp^r Km^r	Invitrogen
pKEK1140	*F. tularensis*-specific TargeTron plasmid	20
pKEK1140/in0201	pKEK1140 with *FTS_0201* inserted	This study
pKEK1140/in0778	pKEK1140 with *FTS_0778* inserted	This study
pKEK1140/in1680	pKEK1140 with *FTS_1680* inserted	This study
pKEK1140/in0166c	pKEK1140 with *FTT_0166c* inserted	This study
pKK289gfp	Ft *ori*, p15a *ori*, Km^r, *groES* promoter	21
pKK289FTS_1680	pKK289 with intact *FTS_1680*	This study
pKNT25	BACTH system plasmid	46
pUT18	BACTH system plasmid	47
pUT18/1680	pUT18 with intact *FTS_1680*	This study
pKNT25/1670	pKNT25 with intact *FTS_1670*	This study
pKNT25/1167	pKNT25 with intact *FTS_1167*	This study
pKNT25/1166	pKNT25 with intact *FTS_1166*	This study
pKNT25/0277	pKNT25 with intact *FTS_0277*	This study
pKNT25/0263	pKNT25 with intact *FTS_0263*	This study

a role in *Francisella tularensis* subsp. *holarctica* FSC200 (FSC200) virulence. Using functional genomics, *in vitro* and *in vivo* characterization, and proteomic studies, we discovered that the product of the *FTS_1680* gene is a membrane-associated protein that contributestothevirulencemechanismsof*Francisella*.Wefoundthat FTS_1680 was required for intracellular replication, full virulence in mice, and heat stress tolerance. Additionally, we also tested whether inactivation of FTT_0166c, the ortholog of FTS_1680 in *F. tularensis* subsp. *tularensis* SchuS4, would result in a similar attenuated bacterial phenotype. We found that inactivation of FTT_0166c protein expression prolonged survival of mice and significantly decreased intracellular microbial replication within macrophages.

MATERIALS AND METHODS

Bacterialstrains,plasmids,andgrowthconditions. The bacterial strains and plasmids used in this study are listed in Table 1. *F. tularensis* subsp. *holarctica* FSC200 (18), acquired from the *Francisella* strain collection (FSC), was kindly provided by Åke Forsberg, Swedish Defense Research Agency, Umeå, Sweden. Wild-type FSC200 and the derived mutant strains were grown on McLeod agar supplemented with bovine hemoglobin (Becton Dickinson, Cockeysville, MD, USA) and IsoVitaleX (Becton Dickinson, Cockeysville, MD, USA) at 37°C with 5% CO_2 or in liquid Chamberlain's medium (19) at 30°C, 37°C, or 42°C. Wild-type and mutant*F.tularensis*subsp.*tularensis*SchuS4weregrownonchocolateagaror in liquid brain heart infusion broth supplemented with 1% IsoVitaleX (BectonDickinson,Cockeysville,MD,USA)at30°Cand37°C.*Escherichia coli* strains were cultivated on Luria-Bertani (LB) agar and in LB broth at either 30°C or 37°C. When necessary, penicillin (100 U/ml), ampicillin (100 g/ml), kanamycin (50 g/ml for *E. coli* and 20 g/ml for *F. tularensis*) or 0.5 mM IPTG (isopropyl--D-thiogalactopyranoside) was used.

TargeTron insertional mutagenesis. The TargeTron gene knockout system was employed to mutate the *FTS_0201*, *FTS_0784*, *FTS_1680*, and *FTT_0166c* genes as previously described (20). Target sites for insertion and retargeting PCR primers (Table 2) were generated using the TargeTron gene knockout system (Sigma-Aldrich, Steinheim, Germany), and the resulting PCR product was digested (HindIII-BsrGI) and cloned into the *Francisella* targeting vector pKEK1140 (generously provided by Karl Klose, University of Texas at San Antonio, San Antonio, TX) (20). Prepared constructs were introduced into the FSC200 or SchuS4 strain by electroporation. The presence of the TargeTron insertion was determined using an intron-specific EBS universal primer combined with a genespecific primer. Intron insertion of the targeted gene was determined using gene-specific primers that amplified across the insertion site. For the FSC200 mutants, positive clones were incubated in Chamberlain's medium at 37°C overnight and then streaked on McLeod agar (without kanamycin), with incubation at 37°C to remove the TargeTron temperature-sensitive plasmid. For the SchuS4 mutants, positive clones

were incubated in brain heart infusion broth supplemented with 1% IsoVitaleX (Becton Dickinson, Cockeysville, MD, USA) overnight at 37°C and subsequently plated onto chocolate agar and maintained at 37°C. The insertion mutants were confirmed using PCR with the gene-specific primers.

Functional complementation. To create the *FTS_1680* complemented strain, functional complementation was performed *in trans*. A DNA fragment carrying the wild-type *FTS_1680* gene was PCR ampli-

TABLE 2 Primers used in this study

Primer	Sequence (5=¡3=)
FTS_0201_IBS	AAAACTCGAGATAATTATCCTTAAAAAACAATTTAGTGCGCCCAGATAGGGTG
FTS_0201_EBS1d	CAGATTGTACAAATGTGGTGATAACAGATAAGTCAATTTAGATAACTTACCTTTCTTTGT
FTS_0201_EBS2	TGAACGCAAGTTTCTAATTTCGGTTTTTTTCCGATAGAGGAAAGTGTCT
FTS_0201_F	TAGTTTTCACGCTTGTCTCC
FTS_0201_R	GACAAAAGACCAACAGGGC
FTS_1680_IBS	AAAACTCGAGATAATTATCCTTAAACCCCAAATCAGTGCGCCCAGATAGGGTG
FTS_1680_EBS1d	CAGATTGTACAAATGTGGTGATAACAGATAAGTCAAATCATCTAACTTACCTTTCTTTGT
FTS_1680_EBS2	TGAACGCAAGTTTCTAATTTCGGTTGGGTTCCGATAGAGGAAAGTGTCT
FTS_1680_F	TATCCAAGAAACAAACTCAAG
FTS_1680_R	TCAAAGGGTAGGCATTATC
FTS_1680_pKK289_F	GCATGTCATATGAAAAACTTATCCAAGAA
FTS_1680_pKK289_R	ACATGCGAATTCCTAGTTAGTATTGTTTATAAGTTGAC
FTS_0778_IBS	AAAACTCGAGATAATTATCCTTAACAGCCAAAGACGTGCGCCCAGATAGGGTG
FTS_0778_EBS1d	CAGATTGTACAAATGTGGTGATAACAGATAAGTCAAAGACTATAACTTACCTTTCTTTGT
FTS_0778_EBS2	TGAACGCAAGTTTCTAATTTCGATTGCTGTTCGATAGAGGAAAGTGTCT
FTS_0778_F	GTTGGTGTGATTGGTAGTTGT
FTS_0778_R	AGCAGCAGCAGTTGTAAGATA
FTS_1681_IBS	AAAACTCGAGATAATTATCCTTAAAGAGCGTTGCGGTGCGCCCAGATAGGGTG
FTS_1681_EBS1d	CAGATTGTACAAATGTGGTGATAACAGATAAGTCGTTGCGCGTAACTTACCTTTCTTTGT
FTS_1681_EBS2	TGAACGCAAGTTTCTAATTTCGGTTCTCTTCCGATAGAGGAAAGTGTCT
FTS_1681_F	TTTTTGATTATGGTATTTCCG
FTS_1681_R	GTAGCAATAACTCCACCAGCA
FTS_1682_IBS	AAAACTCGAGATAATTATCCTTAGCTCCCGCAGTAGTGCGCCCAGATAGGGTG
FTS_1682_EBS1d	CAGATTGTACAAATGTGGTGATAACAGATAAGTCGCAGTAGTTAACTTACCTTTCTTTGT
FTS_1682_EBS2	TGAACGCAAGTTTCTAATTTCGATTGGAGCTCGATAGAGGAAAGTGTCT
FTS_1682_F	ACCATCAGTTTTTCTTTGCC
FTS_1682_R	TACATTCCAGGTCTTTTCTTGA
FTT_0166c_IBS-1	AAAACTCGAGATAATTATCCTTAAACCCCAAATCAGTGCGCCCAGATAGGGTG
FTT_0166c_EBS1d-1	CAGATTGTACAAATGTGGTGATAACAGATAAGTCAAATCATCTAACTTACCTTTCTTTGT
FTT_0166c-Tf	GTAATTCGCTAAGCCGCCATT
FTT_0166c-Tr	CTGAGAATGCAACTGAAACTGGG
FTS_1680_Fw	GGATCCCAAAAAC TTATCCAAGAAACA
FTS_1680_Rev	GGTACCCGGTTAGTATTGTTTATAAGTTGACT
FTS_1670_Fw	GGATCCCGCTGCAAAACAAGTT TTATTTTC
FTS_1670_Rev	GGTACCCGCATCATGCCAGGCATACCG
FTS_1167_Fw	GGAT CCCGGAAAAATAATAGGTATAGATTTAG
FTS_1167_Rev	GGTACCCGTTTTTTGTCGTCTTCAACATCC
FTS_1166_Fw	GGATCCCAGTAAGCAAGAA AAAAGTAATGTA
FTS_1166_Rev	GGTACCCGATTTTTTACTATAACAACTTTTGCA
FTS_0263_Fw	GGATCCCTCAGAAAAAAAATATACTTTTGAAAC
FTS_0263_Rev	GGTACCCGTCTGATATATTTATTCACAAGCTT
FTS_0277_Fw	GGATCCCGCAGATTATTATTCTTTACTAGG
FTS_0277_Rev	GGTACCCGAGCCCTAGGATTAAAATTCATTT

fied using FSC200 genomic DNA as a template, employing primers 1680_pKK289_F and 1680_pKK289_R (Table 2). The final PCR product was sequenced and then cloned downstream of the GroES promoter by replacing the green fluorescence protein-encoding gene in the shuttle vector pKK289gfp (21). The resulting construct, designated pKK289FTS_1680, was introduced into the mutant strain inFTS_1680 by electroporation.

Macrophage culture and infection. Bone marrow cells were isolated from femurs of 6- to 10-week-old BALB/c female mice and differentiated to bone marrow macrophages (BMMs) in Dulbecco's modified Eagle medium (DMEM) (Invitrogen) supplemented with 10% fetal bovine serum, 10% L929 cell-conditioned medium (as a source of macrophage colonystimulating factor [M-CSF]), 50 g/ml streptomycin, and 50 U/ml penicillin for 6 to 7 days (22). Briefly, the BMMs were seeded at a concentration of 5 10^5 cells per well in 24-well tissue culture plates. *F. tularensis* bacteria were diluted into cell culture medium and used for infection of BMMs at a 50:1 (bacteria/cell) multiplicity of infection (MOI). Actual infection doses were determined by plating serial dilutions of the culture inoculum. Tissue culture plates were centrifuged at 400 *g* for 5 min to start the infection and then incubated at 37°C for 30 min. Extracellular bacteria were then killed by gentamicin treatment (5 g/ml) for 30 min. At 1, 6, 12, and 24 h postinfection, the infected BMMs were washed and then lysed with 0.1% sodium deoxycholate. Lysates were

serially diluted and plated on McLeod agar to determine the number of CFU in each well.

The murine monocyte-macrophage cell line J774.2 (ECACC reference no. 85011428) was cultured in DMEM supplemented with 10% fetal bovine serum (FBS) (Gibco-BRL) at 37°C with 5% CO_2. Cells were seeded into 24-well plates at a density of approximately 3 10^5 cells/well. Cells were incubated overnight at 37°C with 5% CO_2 and subsequently infected at an MOI of 500:1 with FSC200, inFTS_0201, inFTS_0784, or inFTS_1680. Infection and proliferation were performed as described above.

For the SchuS4 macrophage proliferation assay, J774.1 cells were infected at an MOI of 100:1 with SchuS4 or inFTT_0166c. After 2 h, cells were washed once with phosphate-buffered saline (PBS), and fresh medium containing 25 g/ml gentamicin was added to kill the extracellular bacteria. Cells were harvested at 4 and 24 h postinfection, and the number of intracellular bacteria was enumerated by serial dilution and plating.

Mouse virulence studies. For survival studies, groups of five 6- to 8-week-old female BALB/c mice were infected subcutaneously with 3 10^2 CFU/mouse of the wild-type FSC200 strain, the inFTS_1680 mutant, the inFTS_1680 complemented strain, the inFTS_0201 mutant, or the inFTS_0778 mutant. An additional group of mice (n 5) was infected subcutaneously with 3 10^6 CFU/mouse of the inFTS_1680 mutant strain. Intraperitoneal challenges were carried out only with the inFTS_1680 mutant (using doses of 3 10^2 or 3 10^6 CFU/mouse), the wild-type FSC200 strain (3 10^2 CFU/mouse), and the inFTS_1680 complemented strain (3 10^2 CFU/mouse). Control groups of mice were inoculated with sterile saline only. The actual inoculation doses were confirmed by viable plate counting. Following infection, mice were observed for signs of illness or death daily for a total of 21 days.

Growth kinetic studies of the pathogen in mouse organs were performed using groups of three BALB/c mice infected intraperitoneally or subcutaneously with the wild-type strain FSC200, the inFTS_1680 complemented strain, or the inFTS_1680 mutant using a dose of 10^2 CFU/mouse of each strain. At the indicated times postinfection, livers, spleens, and lung tissues were recovered and homogenized in PBS, and the total bacterial burdens in each organ were determined by dilution plating onto McLeod agar plates.

For survival studies with the inFTT0166c mutant, groups of 6- to 8-week-old BALB/c mice (n 10) were infected subcutaneously or intranasally with increasing doses of wild-type SchuS4 or inFTT0166c mutant bacteria. Bacteria for the infection were taken from a freshly grown chocolate agar plate incubated overnight at 37°C. The bacteria were resuspended in sterile PBS to an optical density at 600 nm (OD_{600}) of 0.25 (approximately 1.5 10^9 CFU/ml) and diluted to the desired dose. Inoculum counts were verified by serial plating. Infected animals were monitored several times each day for signs of illness or death.

Colocalization of *F. tularensis* with LAMP-1 in BMMs. To examine the ability of the inFTS_1680 mutant to escape from the host cell phagosomes (23), BMMs were infected as described above. At 1 h and 6 h postinfection, the BMMs were fixed with 3.8% paraformaldehyde for 30 min, followed by neutralization with 50 mM NH_4Cl. After washing with PBS, macrophage membranes were permeabilized with 0.2% Triton X-100 for 15 min. For bacterial detection, purified rabbit polyclonal anti-*F. tularensis* serum was used at a concentration of 1:3,000 followed by detection with Alexa Fluor 488-labeled goat anti-rabbit IgG (Invitrogen, Molecular Probes, Eugene, OR, USA) at a dilution of 1:500. For the colocalization studies, BMMs were then labeled using rat monoclonal antimouse LAMP-1 antibody (1D4B; Santa Cruz Biotechnology, Santa Cruz, CA) at a concentration of 1:100, followed by detection with Alexa Fluor 594-labeled donkey anti-rat IgG (Invitrogen, Molecular Probes, Eugene, OR, USA) at a 1:500 dilution. Colocalization of bacteria with LAMP-1 was analyzed with a Nikon TE2000 confocal laser scanning microscope equipped with NIS Elements AR software.

Macrophage cytotoxicity assay. For cytotoxicity experiments, BMMs were seeded in 96-well tissue culture plates at a concentration of 2 10^4 cells/well and allowed to adhere overnight at 37°C with 5% CO_2. The next day, the BMMs were infected with bacterial cell suspensions at an MOI of 50:1. At 2 h, 24 h, and 48 h postinfection, the supernatant was collected and assayed for the presence of lactate dehydrogenase (LDH) according to manufacturer's instructions (cytotoxicity detection kit; Roche Diagnostics, Germany). Samples were measured with a Paradigm microplate reader (Beckman Coulter) at an absorbance of 490 nm. As a positive control (representing 100% cell lysis), uninfected BMMs were lysed with 0.1% natrium deoxycholate. Sample absorbance values were expressed as a percentage of the positive-control value.

Stress survival assay. *F. tularensis* strains were grown overnight at 37°C in 2.5 ml of Chamberlain's medium supplemented with the appropriate antibiotic when applicable. The cultures were diluted in fresh Chamberlain's medium to an OD_{600} of 0.1. Five aliquots of each strain (0.25 ml each) were transferred into 96-well plates and subjected to one of the following stress conditions: pH 4.0, 4% NaCl, or iron depletion. Samples were then incubated at 37°C or 42°C (in the case of heat stress) for 24 h. Bacterial growth was determined by measuring the OD_{600} every 10 min for 24 h. CFU were calculated at the end of the experiment to verify the OD_{600} measurement. For oxidative stress experiments, stationary-phase bacteria from *F. tularensis* strain FSC200 or inFTS_1680 were diluted 1:10 into fresh Chamberlain's medium and exposed to 0.03% H_2O_2. Samples were harvested at 0, 20, and 40 min postexposure and viable bacteria enumerated by serial dilution on McLeod agar plates (5, 6).

For heat stress experiments with the inFTT_0166c mutant, stationaryphase bacteria from *F. tularensis* strain SchuS4 or inFTT0166c were diluted 1:10 into fresh Chamberlain's medium and exposed to heat stress (42°C) for 50 and 100 min. Viable bacteria were enumerated by serial dilution at the start of the experiment and at the indicated time points.

BACTH assay. We performed the bacterial adenylate cyclase two-hybrid (BACTH) assay according to the manufacturer's instructions (BACTH system kit; Euromedex [reference no. EUK001]). Briefly, FTS_1680 protein was fused with the T18 adenylate cyclase subunit (Nterminal fusion to T18). Targeted proteins GroEL (FTS_1670), DnaK (FTS_1167), DnaJ2 (FTS_0277), GrpE (FTS_1166), and HtpG (FTS_0263) were fused to the T25 adenylate cyclase subunit (in-frame fusion at the N-terminal end of T25). The plasmids and primers used in this assay are listed in Tables 1 and 2, respectively. For each assay, *E. coli* DHM1 chemocompetent cells were transformed with 200 ng of each of the plasmids carrying the T25 and T18 fusions. The bacteria were then spread on LB plates containing 100 g/ml ampicillin and 50 g/ml kanamycin and incubated for 2 days at 30°C. Several clones were inoculated into 3 ml of LB containing 100 g/ml ampicillin, 50 g/ml kanamycin, and 0.5 mM IPTG and incubated overnight at 30°C. The next day, 2 l of each culture was dropped on MacConkey/maltose plates containing appropriate antibiotics and IPTG. The plates were then incubated for several days until a red coloration appeared. The empty pUT18 and pKNT25 plasmids were used as negative controls. For a positive controls, pUT18 and pKNT25 plasmids carrying the *iglA* and *iglB* genes, respectively, were used. The IglA-IglB protein/protein interaction has been previously demonstrated in *F. tularensis* (24).

Triton X-114 partitioning. Cell lysis of wild-type FSC200 and inFTS_1680 mutant bacteria was performed using a French pressure cell (16,000 lb/in^2). Fractions enriched in membrane proteins were collected by ultracentrifugation of the whole-cell lysate at 115,000 *g* for 1 h at 4°C. The supernatant was discarded; the membrane pellet was resuspended in PBS and recollected by ultracentrifugation. The final membrane protein containing pellet was resuspended in ice-cold PTX buffer (PBS containing 350 mM NaCl, 2% Triton X-114, and EDTA-free protease inhibitors) and incubated at 4°C with end-over-end rotation. After 1 h, the sample was centrifuged (12,000 rpm, 4°C, 30 min), and the supernatant was kept at 37°C for 10 min to initiate phase

partitioning. Following centrifugation (14,000 rpm, 24°C, 10 min), the upper aqueous layer was removed. An equal volume of PBS containing 350 mM NaCl was added to the organic phase. The phase separation was repeated twice. The resulting detergent phase was resuspended in PBS, and the protein content was quantified by a bicinchoninic acid assay (Sigma-Aldrich, St. Louis, MO, USA).

2D gel electrophoresis. Detergent-phase proteins were repeatedly precipitatedwithcoldacetonepriortotwo-dimensional(2D)electrophoresis. The protein precipitate was resolubilized in a rehydration buffer containing 1% (wt/vol) ASB-14 surfactant. Isoelectric focusing, reduction, alkylation, and SDS-PAGE were performed as described previously (25).

MS analysis and protein identification. The colloidal blue-stained protein spots were excised from 2D gels and subjected to an in-gel tryptic digestion according to a recently described procedure (25). The digestion wasstoppedbyacidifyingthesamplestoapHof2to3withtrifluoroacetic acid.Thein-gel-digestedproteinswereanalyzedona4800matrix-assisted laser desorption ionization–tandem time of flight (MALDI-TOF/TOF) mass spectrometer (MS) (AB Sciex, Foster City, CA). Acquisition of MS spectral data was performed in a mass range from *m/z* 800 to 4,000. Internal calibration of mass spectra was conducted utilizing tryptic autolytic peptides. Tandem mass spectra of the six most intense precursor ions having a minimum S/N ratio of 100 were acquired using a 1-kV MS/MS reflector in positive-ion mode. Data acquisition and processing were carried out using 4000 Series Explorer software v3.5 (AB Sciex). The mass spectral data obtained were analyzed using the *F. tularensis* OSU18 proteinsequencesdatabase(NC_008369.1)usingGPSExplorerSoftwarev3.6 (AB Sciex) with the Mascot search algorithm v2.2. Trypsin was selected as the proteolytic enzyme, and one missed cleavage was allowed. Carbamidomethylation of cysteine residues and methionine oxidation were set as variable and fixed modifications, respectively. The mass tolerances of the precursor and fragment ions were 100 ppm and 0.25 Da, respectively. Proteins were considered identified with confidence when the GPS protein score confidence interval (%) was equal to 100% and a minimum of two peptide sequences per protein were identified.

Ethics statement. All mouse experiments were performed in accordance with the guidelines of the Animal Care and Use Ethical Committee of the FMHS, University of Defence, Czech Republic. The research protocol was approved by this ethics committee under project no. 89–3/ 2013-3696. At USAMRIID, research was conducted under an IACUCapproved protocol in compliance with the Animal Welfare Act and other federal statutes and regulations relating to animals and experiments involving animals. The facility where this research was conducted is accredited by the Association for Assessment and Accreditation of Laboratory Animal Care International and adheres to principles stated in the Guide for the Care and Use of Laboratory Animals, National Research Council, 2011.

Statistical analysis. For each strain and time in an experiment, the assay was performed in triplicate. Each experiment was independently repeated three times. All values were expressed as mean ± standard deviation (SD) and analyzed for significance using Student's two-tailed *t* test in the statistical software GraphPad Prism 6. Differences were considered statistically significant at a *P* value of < 0.05. The 50% lethal dose (LD_{50}) determinations were calculated using probit analysis (26). The mean time-to-death (TTD) comparisons were made using two-tailed *t* tests. Survival curve comparisons were made using Kaplan-Meier survival analysis with log rank comparisons. Survival rates were compared using Fisher's exact test with step-down Bonferroni correction. All statistical analyses were done using SAS software (SAS Institute, Cary, NC).

RESULTS

SelectionofthetargetsforconstructionoftheTargeTroninsertion mutants. To investigate the involvement of TPR-like-containing proteins in FSC200 pathogenesis, several genes encoding proteins from the TPR and SLR families were chosen as targets for inactivation. Selection was performed using the web-based prediction tool TPRpred (27). TPRpred is a profile-sequence comparison method for predicting TPRs and closely related solenoid structural motifs, pentatricopeptide repeats (PPRs), and SEL1like repeats (SLRs). FTS_1680 (YP_007012402.1) contained five predicted TPRs at positions 24 to 57, 59 to 92, 94 to 127, 130 to 163, and 164 to 197 (99.83% probability); FTS_0201 (YP_007011286.1) had two predicted TPRs at positions 78 to 111 and 114 to 147 (99.95% probability); and FTS_0778 (YP_007011730) had four SLRs at positions 90 to 125, 126 to 161, 499 to 534, and 537 to 572 (100.00% probability) (Fig. 1). Disruption of *FTS_0201* (TargeTron insertion site 347/348s; strain inFTS_0201), *FTS_0778* (TargeTron insertion site 273/274s; strain inFTS_0778), and *FTS_1680* (TargeTron insertion site 177/178s; strain inFTS_1680) (Fig. 1) was performed using retargeted mobile group II introns as described previously (20).

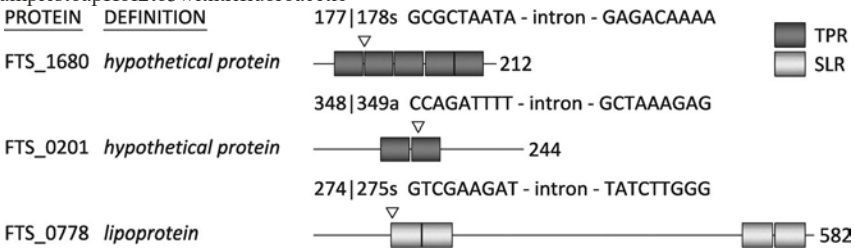

FIG1 Schematic presentation of the domain positions (predicted by the web-based tool TPRpred [27]) in proteins originating from the TPR and SLR families with the TargeTron insertion sites. The TPR domains are depicted in dark gray, while the SEL1-like domains are highlighted in light gray. Accession numbers: FTS_1680 hypothetical protein, YP_007012402.1; FTS_0201 hypothetical protein, YP_007011286.1; FTS_0778 lipoprotein, YP_007011730. DNA sequences in
which the intron is inserted are shown.

FTS_1680 is required for efficient intracellular proliferation in macrophage host cells. To explore the roles of the three TPRlike proteins FTS_0201, FTS_0778, and FTS_1680 during intracellular growth and virulence, we performed *in vitro* infection studies employing BMMs and macrophage-like cells (J774.2) as host cells. Cells were infected with the FSC200 wild-type strain or the inFTS_0201, inFTS_0778, or inFTS_1680 mutant strain, and numbers of intracellular bacteria were determined at 1, 6, 12, and 24 h after infection. The replication kinetics of the inFTS_0778 and inFTS_0201 mutant strains within BMMs (Fig. 2A) and J774.2 cells (data not shown) were indistinguishable from that of the wild-type strain. In contrast, the ability of the inFTS_1680 mutant to replicate within BMMs and J774.2 cells was significantly lower than that of the wild-type

FSC200 strain (Fig. 2A and B). The difference in the intracellular growth between the inFTS_1680 and wild-type FSC200 strains was not due to an inherent growth defect, as both strains grew similarly in Chamberlain's chemicallydefinedmedium(seeFig.8A).Astatisticallysignificant difference in intracellular replication was observed for the inFTS_1680 mutant at both 12 h and 24 h postinfection in BMMs and also at 24 h postinfection within J774.2 cells. Complementation of the inFTS_1680 strain resulted in partial restoration of the wild type phenotype, indicating that *FTS_1680* contributes to *F. tularensis* intracellular replication. Importantly, insertional mutagenesis in genes (*FTS_1681* and *FTS_1682*) from the predicted transcription unit containing *FTS_1680* did not affect intracellular proliferation (data not shown), supporting the finding that the decreased proliferation observed with the inFTS_1680 mutant is solely a consequence of *FTS_1680* disruption.

FTS_1680 is important for virulence in a murine model of tularemia. To determine whether the FTS_0201, FTS_0778, or

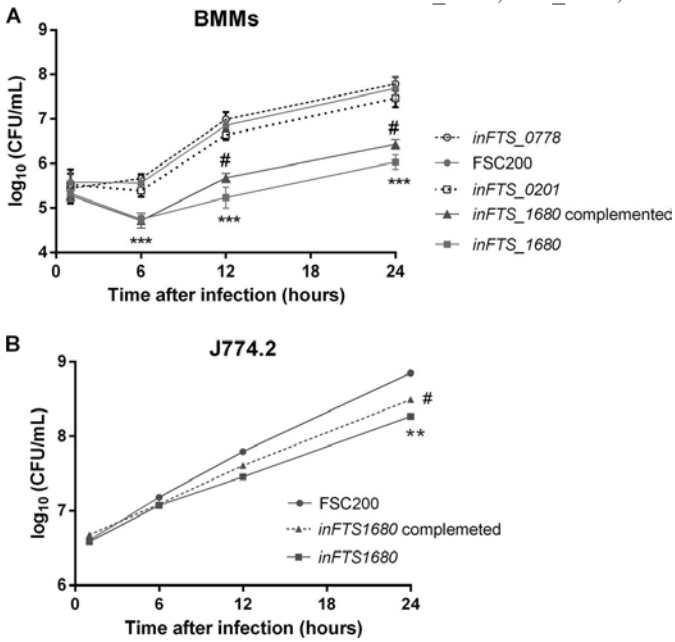

FIG2 FTS_1680 contributes to the intracellular survival in BMMs and J774.2 cells. The growth kinetics of the wild-type (filled circles), inFTS_1680 (filled squares), inFTS_1680 complemented (filled triangles), inFTS_0201 (empty squares), and inFTS_0778 (empty circles) strains inside murine bone marrowderived macrophages (BMMs) (A) or J774.2 cells (B) are shown. The number of intracellular bacteria was determined at 1, 6, 12, and 24 h postinfection. Results are shown as the average $\log_{10}$ CFU per well SD for three independent experiments performed in triplicate (n 9). Statistical significance was analyzed using an unpaired t test; *, P 0.05; **, P 0.01; ***, P 0.001 (comparing inFTS_1680 with the wild-type FSC200 strain). #, P 0.05 (comparing the complemented strain with inFTS_1680).

FTS_1680 protein contributes to the ability of *F. tularensis* to cause disease *in vivo*, groups of five BALB/c mice were infected subcutaneously with the wild-type FSC200 strain, the inFTS_0201, inFTS_0778, or inFTS_1680 mutant strain, or the inFTS_1680 complemented mutant strain. Mice were observed for signs of illness for 21 days following infection. Mice infected with either the inFTS_0201 or the inFTS_0778 mutant strain at a dose of 3 10^2 CFU/mouse succumbed to disease 5 days after infection, comparable to the case for mice infected with a similar dose of the wild-type strain. In contrast, all mice infected with the inFTS_1680 mutant strain survived the infection with both 3 10^2 CFU/mouse (data not shown) and 3 10^6 CFU/mouse (Fig. 3A), although symptoms of illness were observed at both doses. To further verify the *in vivo* attenuation of the inFTS_1680 mutant strain, we also used an intraperitoneal model of infection. Similar to the case for the subcutaneous route, all mice infected with a dose of 3 10^6 CFU/mouse of the inFTS_1680 mutant strain survived, although symptoms of illness were observed as well (Fig. 3B). Additionally, the inFTS_1680 complemented strain exhibited a 2- to 3-day delay in TTD compared to the wild-type FSC200 strain. To exclude a possible polar effect on downstream genes surrounding *FTS_1680*, we also determined the virulence phenotypes of the inFTS_1681 and inFTS_1682 mutant strains. Both mutants showed a level of virulence comparable to that of wildtype FSC200 in mice (Fig. 3A). Altogether, these findings demonstrate the importance of the product of the *FTS_1680* gene for *in vivo* virulence of *F. tularensis*.

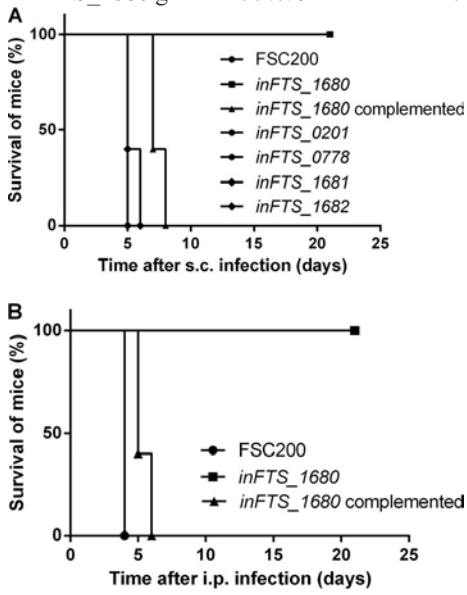

FIG 3 FTS_1680 is important for virulence in murine model of tularemia. Percent survival was determined from groups of five BALB/c mice infected subcutaneously (s.c.) with the inFTS_1680 mutant at a dose of 3 10^6 CFU/mouse, wild-type strain FSC200 (3 10^2 CFU), the inFTS_1680 complemented strain (3 10^2 CFU), the inFTS_0201 mutant (3 10^2 CFU), or the inFTS_0778mutant(3 10^2CFU)(A)orinfectedintraperitoneally(i.p.)with the inFTS_1680 mutant at a dose of 3 10^2 or 3 10^6 CFU/mouse, FSC200 (3 10^2 CFU), or the inFTS_1680 complemented strain (3 10^2 CFU) (B).

The inFTS_1680 mutant exhibits a growth defect in mouse organs. To investigate the ability of the inFTS_1680 mutant strain to persist and disseminate in host tissues, groups of three BALB/c mice were infected via the intraperitoneal route with a dose of 3 10^2CFU/mouseofthewild-typestrainortheinFTS_1680mutant. Bacterial burdens were assayed in lung, spleen, and liver tissue homogenates at 2 h and at 1, 2, 3, 5, 7, 14, 21, 28, and 35 days postinfection (Fig. 4A). Our results showed that when the wildtypestrainwasadministeredviatheintraperitonealroute,bacteria were detectable in the liver within 2 h after inoculation and in the spleen and lungs on day 1 after infection. At 3 days postinfection,

the number of bacteria rapidly increased in all organs, reaching almost 10^{10} CFU in the liver, 10^{9} CFU in the spleen, and 10^{8} CFU within the lungs. None of the mice infected with the wild-type FSC200 strain survived longer than 5 days postinoculation, due to the rapid progression of disease. Although the inFTS_1680 mutant strain initially replicated in all organs studied, the bacterial loadsbegantodeclineafter3daysandwerecompletelyeliminated from the lungs (day 14), from the liver (day 21), and from the spleen (day 35). When the subcutaneous route was used (Fig. 4B), lower levels of bacteria were present in all examined organs but intraperitoneal route of infection (Fig. 4A). These results demonstrate that the inFTS_1680 mutant is able to infect mice and to persist in infected organs, but it is unable to replicate effectively inside host tissues. We also infected mice with the inFTS_1680 complemented strain. On days 1, 2, 3, and 5 postinfection, we determined the number of bacteria in the lungs, liver, and spleen. Although the organ burdens in mice infected with the complemented strain did not reach the levels detected with the wild-type FSC200, they were significantly higher than with the inFTS_1680 mutant strain (Fig. 4A and B).

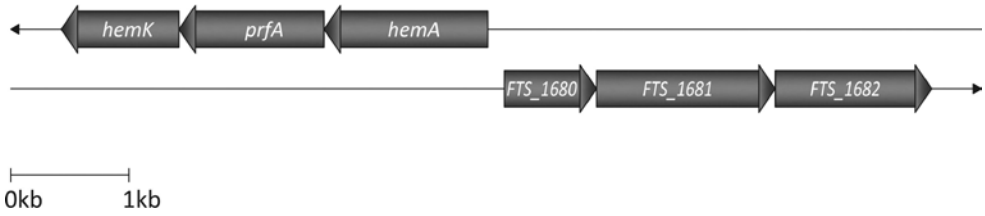

FIG 5 Schematic size-scaled diagram of the organization of the genomic region surrounding *FTS_1680* in FSC200. The genomic region surrounding *FTS_1680* is highly conserved between the various *Francisella* strains, including 3 consecutive genes in the same orientation (*FTS_1680*, *FTS_1681*, and *FTS_1682*). *FTS_1680* encodes a hypothetical protein (212 amino acids), *FTS_1681* is annotated to encode outer membrane protein assembly factor BamB (456 amino acids), and *FTS_1682* encodes the drug:H antiporter-1 (DHA1) family protein (393 amino acids) belonging to the subclass of the major facilitator superfamily (MFS).

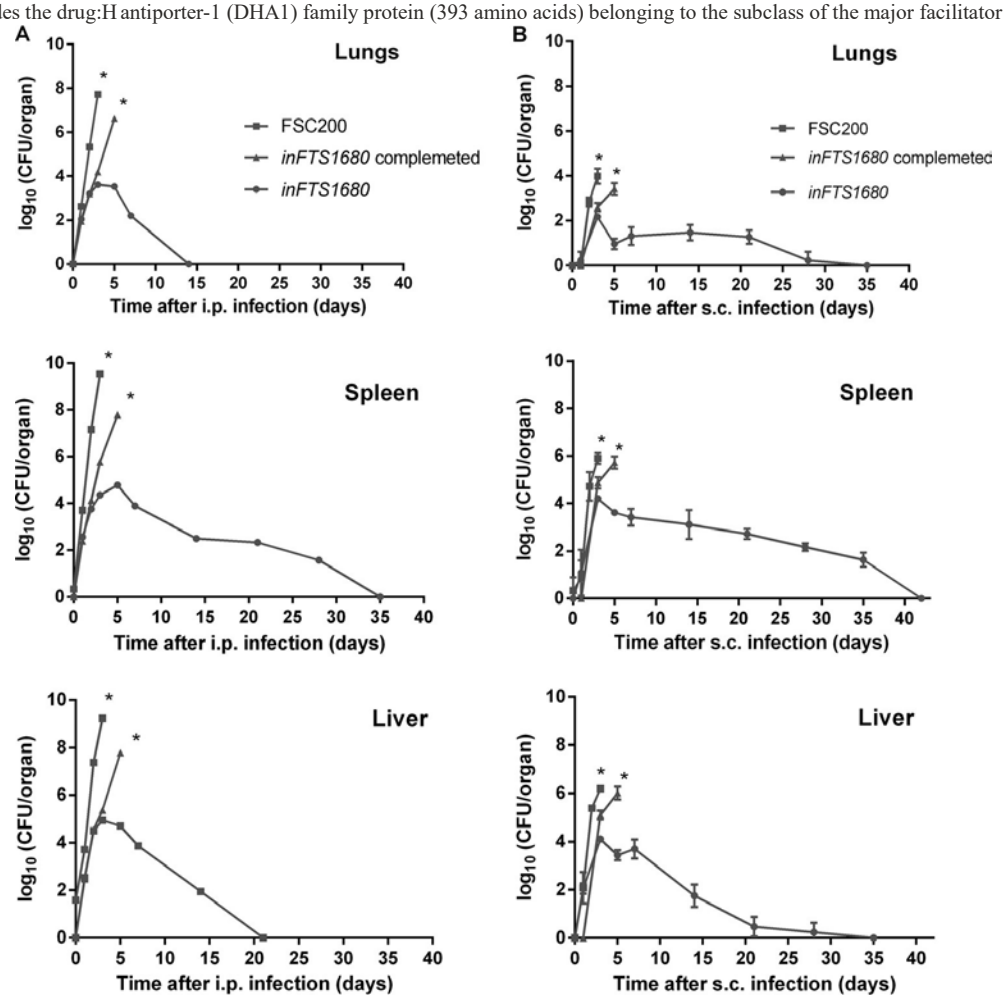

FIG4 The inFTS_1680 mutant exhibits reduced bacterial organ burdens. Bacterial burdens in the spleens, lungs, and livers of BALB/c mice infected intraperitoneally (i.p.) (A) or subcutaneously (s.c.) (B) with 3 10^{2} CFU/mouse of wild-type FSC200 (filled squares), inFTS_1680 (filled circles) or, inFTS_1680 complemented strain (filled triangles) are shown. The asterisks (*) indicate that all mice infected with the wild-type FSC200 or inFTS_1680 complemented strain died after day 5. Results are shown as the average $\log_{10}$ CFU per organ SD at the indicated time points of infection.

bacteria persisted in all organs for a longer time than with the

Description of the genomic locus surrounding *FTS_1680*. The genomic region surrounding *FTS_1680* is highly conserved between the various *Francisella* strains, including 3 consecutive genes in the same orientation (*FTS_1680*, *FTS_1681*, and *FTS_1682*)(Fig.5).*FTS_1680*encodesahypotheticalprotein(212 amino acids), the *FTS_1681* product is annotated as the outer membrane protein assembly factor BamB (456 amino acids), and *FTS_1682* encodes a drug:H antiporter-1 (DHA1) family protein (393 amino acids). Protein BLAST searches indicated that FTS_1680 and FTS_1681 share 28% identity (query cover 93%; E value 2e15) with YfgM (which contains TPR motifs) of *E. coli* K-12 and 26% identity (query cover 94%; E value 6e48) with YfgL of *E. coli* K-12. Proteins YfgM and YfgL are linked to temperature tolerance (28), and very recently YfgM has been described as a protein involved in the SecYEG system of *E. coli* (29). To exclude possible polar effects on downstream genes, we evaluated levels of

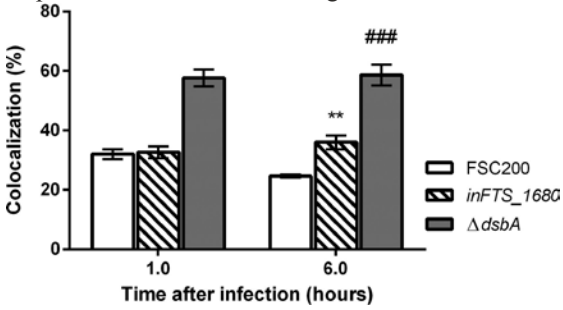

the mRNA transcripts of the genes surrounding *FTS_1680*. Quantitative reverse transcription-PCR (qRT-PCR) did not reveal any significant effect of insertional inactivation of *FTS_1680* on expression of *FTS_1681* and *FTS_1682* (data not shown).

TheinFTS_1680mutantescapesintothehostcellcytosoltoa lesserextentthanthewild-typeFSC200strain. The typical *Francisella* intramacrophage infectious cycle includes successful phagosomal escape and active multiplication in the host cell cytosol. Based on the intracellular growth defect of the inFTS_1680 mutant in BMMs, we analyzed the ability of the inFTS_1680 mutant to escape from the host cell phagosome using a colocalization study with LAMP-1 as a marker of late endosomes. As a positive control, we used the *dsbA* mutant, which has been previously shown to be unable to escape into the host cytosol (30). The inFTS_1680 mutant exhibited almost the same level of colocalization with LAMP-1 as the wild-type strain. The percentage of colocalizationofthemutantwithLAMP-1was31%at1hand35.3% at 6 h after infection. In comparison, the colocalization of the wild-type FSC200 strain with LAMP-1 was 31.3% at 1 h and significantly declined to 23.5% at 6 h after infection (Fig. 6). However, LAMP-1 colocalization of the wild-type strain or the inFTS_1680 mutant did not reach the value detected for the *dsbA* mutant strain (Fig. 6). Despite the observed statistical difference in the number of wild-type versus mutant bacteria in the phagosome at 6 h, it seems likely that the inability of inFTS_1680 to fully proliferate in the cell cytosol is responsible for attenuation rather than defects in phagosomal escape.

RoleofFTS_1680in*F.tularensis*-inducedBMMcellcytotoxicity. To investigate the role of the FTS_1680 protein in cellular cytopathogenic effects associated with *F. tularensis*, we infected BMMs with the wild-type FSC200

FIG 6 The inFTS_1680 mutant is able to escape from the phagosomes of BMMs. Quantification of colocalization of LAMP-1 with wild-type (open bars), inFTS_1680 mutant (striped bars) or *dsbA* mutant (gray bars) bacteria is shown. At each time point, 100 infected cells were examined from three different coverslips. Results are presented as the mean of triplicate samples SD, and the results shown are representative of three independent experiments. Statistical significance was analyzed using an unpaired *t* test. **, *P* 0.01 (comparing inFTS_1680 with the wild-type FSC200 strain); ###, *P* 0.001 (comparing inFTS_1680 with the *dsbA* mutant).

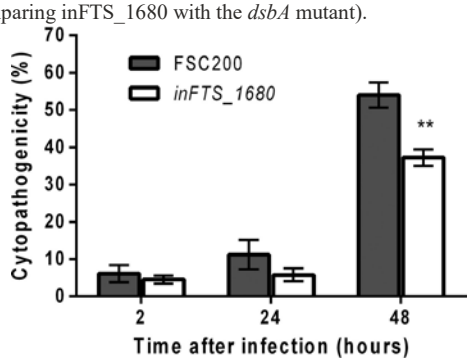

FIG 7 Induction of cytotoxicity in BMMs. BMMs were infected with the wildtype strain (gray bars) or the inFTS_1680 mutant strain (open bars). At 2 h, 24 h, and 48 h after infection, culture supernatants were collected and assayed for LDH activity using the LDH cytotoxicity detection kit (Roche). LDH activity is expressed as a percentage of the level for noninfected lysed cells (positive lysis control). Results are presented as the means of quadruplicate samples SD, and the results shown are representatives of three separate experiments. Statistical significance was analyzed using an unpaired *t* test, **, *P* 0.01.

strain or the inFTS_1680 mutant and measured the release of lactate dehydrogenase (LDH) into the cell supernatant. After 2 h of infection, the LDH level released from cells infected with the inFTS_1680 mutant (approximately 4%) was comparable to the LDH release detected in cells infected with the wild-type FSC200 strain (approximately 6%) (Fig. 7). After 24 h of infection, the LDH levels increased to 5% and 11% for the inFTS_1680 and parental FSC200 strains, respectively (Fig. 7). At 48 h postinfection, the level of LDH release was 37% for the inFTS_1680 mutant strain, which was significantly lower than the LDH release detected for the wild-type FSC200 strain (54%) (Fig. 7). The LDH assay showed that the inFTS_1680 mutant strain induces a time-dependent loss of host cell membrane integrity at levels significantly lower than those of the wildtype strain.

FTS_1680 is involved in heat stress tolerance. Growth of the inFTS_1680 mutant strain and the inFTS_1680 complemented strain in broth at 37°C was comparable to that of the wild-type FSC200 strain (Fig. 8A). To examine a possible involvement of the FTS_1680 protein in stress tolerance, we monitored the growth of the inFTS_1680, inFTS_1680 complemented, and wild-type FSC200 strains under stress-inducing culture conditions. Under heat stress conditions, the inFTS_1680 mutant strain grew substantially more slowly than the wild-type strain (Fig. 8B). Complementation of inFTS_1680 restored the growth of the mutant to a level similar to that of the parental strain (Fig. 8B). Conversely, the insertion mutants inFTS_1681 and inFTS_1682 grew similarly to FSC200 at 42°C (data not shown). This demonstrates that the observed lower resistance to heat stress of the inFTS_1680 mutant strain is solely due to the inactivation of the *FTS_1680* gene. Sensitivities of the inFTS_1680 mutant to low pH (Fig. 8C), osmotic (Fig. 8D), iron depletion (Fig. 8E), and

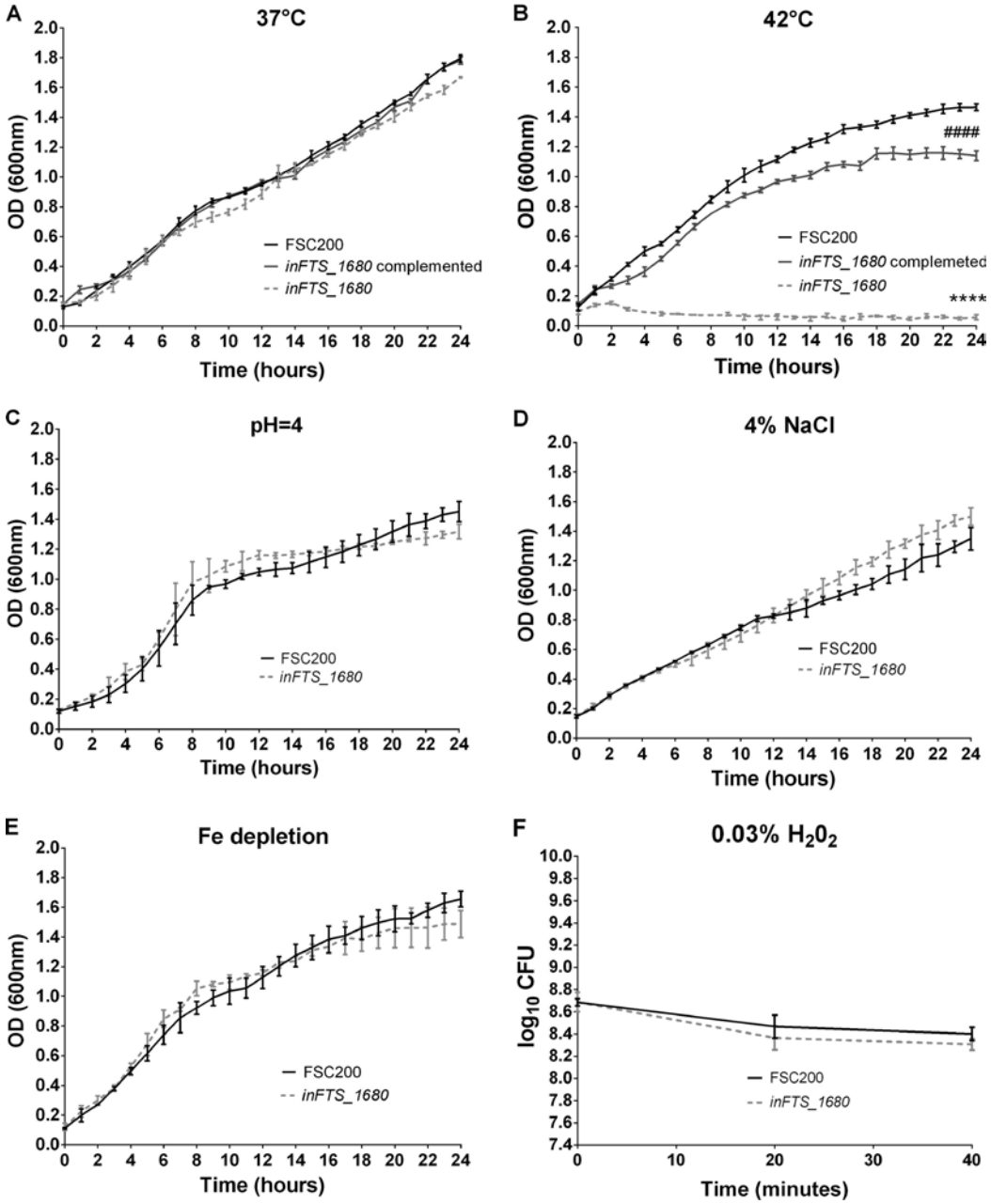

FIG8 FTS_1680 is required for heat stress tolerance. (A to E) Growth curves of *F. tularensis* strains FSC200 (black), inFTS_1680 (light gray), and complemented inFTS_1680 (dark gray) (supplemented with kanamycin at 20 g/ml) in Chamberlain's medium incubated at 37°C (A) or 42°C (B) or under the following stress conditions: pH 4.0 (C), 4% NaCl (D), or iron depletion (E). Bacterial growth was determined by measuring the OD_{600} in pentaplicate every 10 min for 24 h. CFU were analyzed at the end of the experiment to verify OD_{600} measurement. (F) Oxidative stress experiments. Stationary-phase bacteria of *F. tularensis* strains FSC200 (black) or inFTS_1680 (light gray) were diluted 1:10 in fresh Chamberlain's medium and exposed to 0.03% H_2O_2. CFU were determined at the start of the experiment and after 20 and 40 min. The results shown are representative of three independent experiments. Statistical significance was analyzed at the 24-h time point using an unpaired *t* test, ****, *P* 0.0001 (comparing inFTS_1680 with the wild-type FSC200 strain); ####, *P* 0.0001 (comparing inFTS_1680 with the complemented strain).

oxidative (Fig. 8F) stresses were comparable to those of the wild-type strain, indicating that FTS_1680 is not required for tolerance to these stress conditions.

Protein-proteininteractionanalysisofFTS_1680withrepresentatives of the heat shock proteins. Involvement of FTS_1680 in heat stress tolerance and the predicted presence of TPR motifs suggest that FTS_1680 may interact with heat shock proteins found in *F. tularensis*. Using the BACTH assay, we tested FTS_1680 interaction with GroEL (FTS_1670), DnaK (FTS_1167), DnaJ2 (FTS_0277), GrpE (FTS_1166), or HtpG (FTS_0263). Under our experimental conditions, we were unable to detect an interaction between FTS_1680 and any of the selected proteins.

FTS_1680 is detected in a lipoprotein-enriched membrane fraction. The LipPred tool for prediction of lipoprotein signal sequences (31) identified the protein FTS_1680 as a lipoprotein with a

prediction confidence of 0.99, based on the lipobox [LVI][ASTVI][GAS]Csequencevariations.Weverifiedthispredictionusing aTritonX-114phasepartitioning(32)followedbyaseparationof the detergent-phase proteins by 2D SDS-PAGE. The quality of fractionation was first verified by the immunodetection of proteins with aknownlocalization(outermembraneproteinFopA)andaffiliation to the lipoprotein class of membrane proteins (lipoprotein DsbA) in both aqueous and detergent phases (data not shown). The protein FTS_1680 was repeatedly identified among the Triton X-114 phase partitioning of the membrane protein-enriched fraction of FSC200 (Fig. 9A). The comparison of protein patterns of the detergent-enrichedfractionscollectedfromtheparentalFSC200andinFTS_1680 mutantstrainsalsoconfirmedtheabsenceoftheproteinFTS_1680in the mutant strain (Fig. 9A and B). This finding confirms membrane association of the FTS_1680 protein and also supports its predicted acylation.

Effect of inactivation of the *FTT_0166c* gene, the *FTS_1680* ortholog in the type A strain, on the phenotype of *Francisella tularensis*strainSchuS4.FTT_0166cisapredictedTPR-containing proteinwithinthefullyvirulent*F.tularensis*typeAstrainSchuS4.It shares 98% identity to FTS_1680 at the amino acid level. We hypothesized that, similar to the case for FTS_1680, inactivation of FTT_0166c may lead to an attenuated phenotype in the SchuS4 background. Using TargeTron mutagenesis, we created strain inFTT_0166c. This mutant strain carries an intron insertion at the same position in the coding sequence as in inFTS_1680, 177/178s. To investigate virulence of strain inFTT_0166c in an animal model of tularemia, we infected mice subcutaneously with increasing doses of the wild-type SchuS4 or inFTT_0166c mutant bacteria and compared LD_{50}s, survival rates, mean TTDs, and survival curves. As shown in Table 3, we found no significant difference between the wild-type and mutant strains in the calculated LD_{50} (approximately 1 CFU) or survival rate. However, we did observe that animals infected with the mutant strain survived

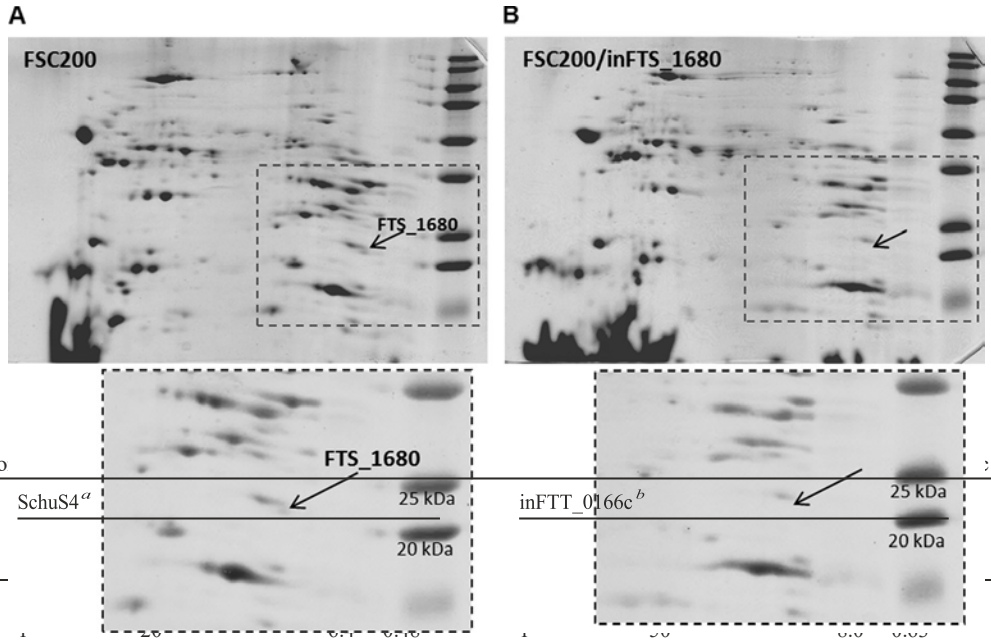

FIG 9 (A) Representative 2D SDS-PAGE separation of a lipoprotein-enriched fraction obtained by Triton X-114 phase partitioning of *F. tularensis* subsp. *holarctica* FSC200. The protein encoded by *FTS_1680* was detected in a basic region of the broad nonlinear pH range of 3 to 10 and among the masses 25 and 20 kDa (in accordance with its theoretical molecular mass and pI of 23.8 kDa and 9.39, respectively) and identified by mass spectrometry. (B) Representative 2D SDS-PAGEseparationofthelipoprotein-enrichedfractionwhichwasobtainedbyTritonX-114phasepartitioningofthemutantstrainin FTS_1680.Theprotein encoded by *FTS_1680* was not detected or identified in the neighboring spots.

TABLE 3 Compariso : mutant strain

Inoculation	SchuS4[a]				inFTT_0166c[b]				TTD comparison (*P* value)
Subcutaneous									0.0020
	8	0	5.0	0.00	10	0	6.3	0.98	0.0001
	76	0	5.0	0.00	107	0	6.4	0.66	0.0001
	756	0	4.5	0.50	1067	0	5.2	0.40	0.0092
Intranasal	0.1	90	6.0		0.1	100	NC[c]		NC
	1	70	6.0	0.00	1	90	6.0		NC
	7	0	6.0	0.00	9	30	6.6	0.50	0.0398
	74	0	5.0	0.00	89	10	6.0	0.00	0.0016
	741	0	5.0	0.00	889	0	6.0	0.00	0.0016

[a] The LD_{50} was 1 CFU for both inoculation routes.

[b] The LD_{50}s were 1 CFU and 6 CFU for the subcutaneous and intranasal inoculation routes, respectively.

[c] NC, not calculated.

longerthanwild-typeSchuS4-infectedmice.Thisobservationwas supported by a statistically significant increase in the TTD for mutant infected animals across all doses (Table 3). Additionally, comparisonofsurvivalcurvesyieldedalargersurvivalestimatefor the inFTT_0166c-infected mice than for SchuS4-infected mice (*P* 0.0001). To examine whether the observed difference was independent of route of administration, we repeated the experiment, but this time animals were challenged by the intranasal

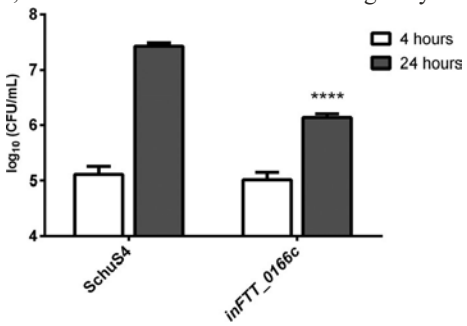

FIG10 The *FTT_0166c* gene is required for optimal intracellular replication within J774.1 cells. The number of intracellular bacteria was determined at 4 h

route. Similar to the case for the subcutaneous route, animals infected intranasally with the inFTT_0166c mutant had a statistically significantly increased TTD and survival estimate compared to the SchuS4-infected animals; however, we failed to observe a statistically significant difference in LD_{50} or survival rates (Table 3).

Furtherwe hypothesized that, similar to the case for *FTS_1680*, the inactivation of *FTT_0166c* in the fully virulent SchuS4 strain may lead to a decreased ability to proliferate in macrophages. Mouse macrophage-like J774.1 cells were infected with the wildtype SchuS4 strain or the inFTT_0166c mutant strain and assayed for intracellular replication at 4 and 24 h postinfection. No significant difference was observed between CFU counts of SchuS4 and inFTT_0166c at 4 h (Fig. 10). However, at 24 h, the inFTT_0166c mutant exhibited a significant reduction in CFU compared to SchuS4 (Fig. 10). These data demonstrated that FTT_0166c is important for intracellular replication of the fully virulent SchuS4 strain and corroborated the findings observed with the inFTS_1680 mutant of FSC200 (Fig. 2A and B).

Resistance of the inFTT_0166c mutant to heat stress (42°) was also tested, and we observed an average 1.5-log decrease in viable numbers of mutant bacteria after 50 and 100 min compared to thoseoftheparentalSchuS4strain(Fig.11).Takentogether,these data demonstrated that FTT_0166c is required for survival of SchuS4 under heat stress conditions and correlated with the findings observed with the inFTS_1680 mutant of FSC200 (Fig. 8B).

DISCUSSION

In recent years, there have been several reports indicating that TPR-containing proteins of bacterial pathogens are directly linked to virulence-associated functions. The TPRs within class II chaperones of *Yersinia*, *Pseudomonas*, *Shigella*, *Salmonella enterica*, enteropathogenic *Escherichia coli*, and *Chlamydia muridarum* (LcrH, PcrH, IpgC, SicA, CesD, and SycD, respectively)

havebeenshowntobekeyelementsforbindingthecognatetranslocators of type III secretion systems (TTSS) (33). Moreover, TPR

(open bars) and 24 h (gray bars) postinfection. Data represent the average from two independent experiments run in triplicate (*n* 6). Error bars indicate SD. Statistical significance was analyzed using an unpaired *t* test, ****, *P* 0.0001.

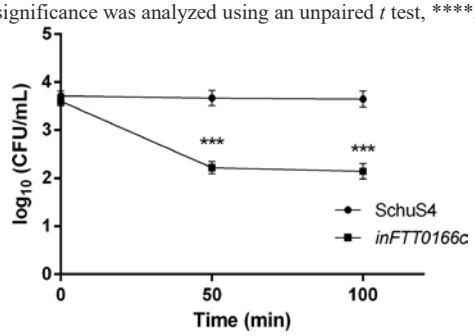

FIG 11 FTT_0166c is required for growth under heat stress conditions. Stationary-phase bacteria of *F. tularensis* strains SchuS4 (circles) or inFTT_0166c (squares) were diluted 1:10 in fresh Chamberlain's medium and then exposed to heat stress (42°C). The bacteria were spread on chocolate agar plates at 50 and 100 min, and viable bacteria were counted. Results are presented as the average CFU/ml for three independent experiments. Statistical significance was analyzed using an unpaired *t* test. ***, *P* 0.001.

domains seem to be of high importance for another TPR-containing protein, PilF, which participates in biogenesis of Tfp in *Pseudomonas* (reviewed in reference 15). SLR-containing proteins such as HcpA from *Helicobacter pylori*, EnhC and LpnE from *Legionella pneumophila*, AlgK from *Pseudomonas aeruginosa*, and ExoR from both *Sinorhizobium meliloti* and *Rhizobium leguminosarum*,MotXfrom*Vibrioparahaemolyticus*,andMerGfro m*Pseudomonas* strain K-62 have also been shown to play an important role in bacterial pathogenesis (reviewed in reference 14).

F. tularensis is able to successfully survive and cause disease in a host due to its unique strategy of intracellular survival. The mechanisms of cell entry, rapid phagosomal escape, active cytosolic multiplication, and dissemination following cell lysis are still under investigation. Since TPR-like-containing proteins are ubiquitous and fulfill many biological functions, we hypothesized that TPR-like-containing proteins might also play a role in *Francisella* virulence. Therefore, we created mutant strains with intron insertions in genes *FTS_0201*, *FTS_0778*, and *FTS_1680*, which encode TPR/SLR-containing proteins in *F. tularensis* FSC200, and also in the gene *FTT_0166c* in *F. tularensis* SchuS4 (*FTS_1680* ortholog). We subsequently investigated the effects of these mutations on *F. tularensis* virulence. First, we analyzed the abilities of the inFTS_0201, inFTS_0778, and inFTS_1680 mutants to replicate within mouse macrophages. Only the inFTS_1680 mutant exhibited a significant intracellular growth defect in primary BMMs (Fig. 2A) and slightly restricted replication in the J774.2 macrophage cell line (Fig. 2B). Although we observed differences in the levels of intracellular replication between these two cell lines, the inFTS_1680 mutant showed significantly reduced replication in both cell lines, implying its importance for optimal intracellular replication. Phenotypic differences in intracellular proliferation within differing phagocytic cell lines have been observed with other attenuated *Francisella* mutants, as previously reported (5, 6, 34).

Based on the inFTS_1680 intracellular growth defect in mouse macrophages, we also assayed intracellular growth of the inFTT_0166c mutant in the J774 macrophage cell line. Similar to

the case for the inFTS_1680 mutant, intracellular proliferation of the inFTT_0166c mutant was also significantly reduced in these cells. These results suggest that the proteins encoded by *FTS_1680* and *FTT_0166c* are required for optimal intracellular proliferation in both the type B and type A strains of *Francisella*, respectively.

TTD studies in BALB/c mice showed that the inFTS_0201 and inFTS_0778 mutant strains were as virulent as the wild-type strain, suggesting that both *FTS_0201* and *FTS_0778* are not important for virulence in the subcutaneous murine model of tularemia (Fig. 3A). In contrast to our studies with inFTS_0201, it has previously been reported that intraperitoneal infection of BALB/c mice with a disrupted *FTL_0205* gene (*FTS_0201* ortholog) in the *F. tularensis* LVS strain revealed a strong attenuation (6). A possible explanation for the discrepancy in the reported virulence between the inFTS_0201 and inFTL_0205 mutant strains could be the variable number of NKD repeats existing in these orthologs, the clear differences in the challenge model, or simply that within the FSC200 strain other virulence factors mitigate the effect of *FTS_0201* disruption, similarly to data published by Meibom et al. (35).

TTD studies with the inFTS_1680 mutant showed an attenuated phenotype. Importantly, 100% of mice infected subcutaneously with as much as 3 10^6 CFU of the inFTS_1680 mutant all survived infection. Importantly, all mice infected with either the wild-type strain or inFTS_1680 complemented strain with a dose of 3 10^2 CFU became moribund at 5 to 7 days after infection. Since virulence can vary significantly between subcutaneous and intraperitoneal models of infection (36), we also tested the inFTS_1680 and the inFTS_1680 complemented strains by the intraperitoneal route of infection. Similar to our observations with mice infected subcutaneously, all mice infected with the inFTS_1680 mutant survived infection, whereas all mice infected with the wild-type FSC200 or inFTS_1680 complemented strain succumbed to infection. These results demonstrate that the observed attenuation of the inFTS_1680 mutant occurs independent of the route of exposure. Likewise, the SchuS4-derived inFTT_0166c mutant also exhibited a route-independent attenuated phenotype. However, compared to that of its FSC200 ortholog, the attenuation observed was weaker. Nevertheless, the fact that a delay in TTD was observed across all doses for both routes supports the conclusion that this gene plays a role in virulence of the highly virulent type A strain. It is likely that the observed difference in attenuation can be attributed to the significant difference in virulence between the FSC200 and SchuS4 strains (35). Taken together, our findings support the hypothesis that *FTS_1680* and its ortholog are needed for the full virulence of both type A and type B strains.

To understand the *in vivo* attenuation of inFTS_1680, we evaluated the ability of this mutant to persist and disseminate within selectedhostorgans.TheinFTS_1680mutantwasabletoreplicate at low levels in the liver, spleen, and lungs during the first days postinfection; however, the viable number of mutant bacteria declined with time. In contrast, the wild-type and complemented inFTS_1680 mutant strains replicated to high numbers in all these organs during the first days, after which no mice survived the infection (Fig. 4). It appears in some cases that proliferation in nonmacrophage cell types is sufficient to sustain *F. tularensis* pathogenesis (34). The rapid elimination of the inFTS_1680 mutant from the organs tested suggests that this strain may be defective in replication within nonmacrophage cells as well, which may also contribute to its attenuation.

Further, we investigated the intracellular fate of the inFTS_1680 mutant inside BMMs by employing a LAMP-1 marker as an indicator of late endosomes. Our results showed that the inFTS_1680 mutant is able to escape from the phagosome, albeit at a frequency slightly lower than that of the wild-type FSC200 (Fig. 6). However, it seems likely that the predominant role of FTS_1680 might be to help *Francisella* to multiply to high numbers within the cytosol. The inFTS_1680 mutant was able to replicatewithinthecytosoliccompartment;however,itwasunableto replicate to the high number observed for wild-type bacteria. This suggests that FTS_1680 is required to maintain or support highlevel replication within the cytosol. In this respect, FTS_1680 resembles virulence factors playing a specific role during multiplication in the cytosol after phagosomal escape (reviewed in reference 37), such as the *Francisella* SEL1-like protein DipA (4). The DipA mutant does not proliferate within the cells, despite the ability to escape from the phagosome, and is completely attenuated in *in vivo* infection models (4). Additionally, we found that theFTS_1680proteinalsocontributestoFSC200cytopathogenicity (Fig. 7). As shown previously (38, 39), the inability to induce full cytotoxicity might be associated with the observed defect in cytosolic replication.

A common characteristic of TPR-like repeats is that they create multiprotein complexes and mediate protein-protein interactions, often functioning as cochaperones in particular of the heat shock proteins (15). In the present work, the inFTS_1680 mutant showed a loss of ability to resist heat stress. Therefore, we assayed protein-protein interactions of FTS_1680 with some typical representatives of the heat shock proteins by employing the BACTH system. Unfortunately, we were unable to detect any interaction between FTS_1680 and the targeted proteins. Although the BACTH system is presented as useful for detection of protein interactions outside the cytoplasm (40), the results may be false negativesincetransientinteractionsmaynotbedetected.Another possibility could be a localization of the interaction in the periplasmic space. This is a known obstacle for another bacterial two-hybrid system (41), and it is not clear if it also is a complication for analysis when employing the BACTH assay. We attempted to explore a chaperone activity, but we were unable to purify the native recombinant protein.

Interestingly, FTS_1680 also shows high similarity to YfgM from *E. coli*, that was recently shown to interact with the SecYEG translocon (29). YfgM might function in a periplasmic chaperone network while playing a role in the (E)-dependent envelope stressresponse(29).DirectinteractionwithSecAandSecEhasnot beenobservedtodate;however,itcannotberuledout.Itisworthwhile to note that both of these proteins influence replication of *Francisella* in host organs (42), which parallels our *in vivo* observations.

In order to characterize FTS_1680 in more detail, we performed proteomic characterization. FTS_1680 is predicted to be a membrane protein, and to confirm this prediction, we exploited Triton X-114 phase partitioning for isolation of *Francisella* membrane-associated proteins. Based on our results, we can conclude that FTS_1680 is a membrane protein. Taking LipPred

tool prediction into account, it can be speculated that FTS_1680 might be modified with an acyl moiety that could simply function as an anchor to the membrane, thus allowing FTS_1680 to assemble membrane-associated protein complexes. From this point of view, it is interesting that DipA was found to be on the surface of theSchuS4strain,whereitformsamembrane-associatedcomplex with the outer membrane protein FopA during intramacrophage growth (43).

We should note that for both our *in vitro* and *in vivo* experiments, we were unable to fully complement the observed phenotype by supply the native gene in *trans*. Our approach of creating insertion mutants by employing the TargeTron gene knockout system for *F. tularensis*, which utilizes retargeted mobile group II introns, raises the question of potential polar effects influencing the observed phenotype. However, we feel that for these studies this possibility is remote. In our study, we used *trans*-complementation with a plasmid where the coding sequence is cloned downstream of the GroES promoter (21). Lack of full complementation may be attributable to expression differences between the native and GroES promoters or other limitations intrinsic to *trans*-complementation (44, 45). However, the wild-type phenotype was almost fully restored in *in vivo* experiments and when assessing heat stress tolerance. Moreover, other experimental steps were performed in order to rule out potential polar effects. qRT-PCR did not show any changes in *FTL_1681*, *FTL_1682*, and *FTL_1683* expression in the inFTS_1680 mutant. Mutagenesis of *FTL_1681* and *FTL_1682* had no effect on the proliferation, virulence phenotype, and ability to resist heat stress. These observations support the conclusion that downstream genes, which are most likely to exhibit polar effects, do not influence the virulent phenotype. Thus, our observations might be the sole result of inactivation of FTS_1680.

In conclusion, the present study investigating the involvement of TPR-like proteins in the pathogenesis of *F. tularensis* identified the locus *FTS_1680/FTT_0166c* as a novel virulence factor that is required for proper intracellular replication of the microbe, heat stress tolerance, and *in vivo* virulence. Furthermore, the *FTS_1680*-encoded protein was identified as a membrane-associated protein necessary for fully expressed cytopathogenicity. Thus, FTS_1680/FTT_0166c, in addition to PilF, FTL_205, and DipA, represents another protein from the TPR-like family that is important for *Francisella* virulence. Identification of FTS_1680/FTT_0166c protein interactions and elucidation of FTS_1680/FTT_0166c functions could contribute to a deeper understanding of the unique mechanisms behind *F. tularensis* intracellular survival.

ACKNOWLEDGMENTS

We thank Karl Klose and Stephen A. Rodriguez (UTSA, San Antonio, TX) for generously providing the pKEK1140 targeting vector and Maria Safarova for technical assistance with the mouse infection studies. Additionally, we thank Steve Kerns (USAMRIID) for help with the statistical analysis for SchuS4 mouse experiments.

This work was supported by grants 160/50/15011 from the Grant Agency of Charles University, Prague, Czech Republic (SVV260065, DTRA project D-CZ-10-00001, and DTRA project CB3387 PA D-CZ-11-0001).

Theopinions,interpretations,conclusions,andrecommendationsare those of the authors and are not necessarily endorsed by the U.S. Army. The authors declare no conflicts of interest.

REFERENCES

1. **Ellis J, Oyston PC, Green M, Titball RW.** 2002. Tularemia. Clin. Microbiol. Rev. **15:**631–646. http://dx.doi.org/10.1128/CMR.15.4.631-646.2002.
2. **Oyston PC, Sjostedt A, Titball RW.** 2004. Tularaemia: bioterrorism defence renews interest in Francisella tularensis. Nat. Rev. Microbiol. **2:**967–978. http://dx.doi.org/10.1038/nrmicro1045.
3. **Santic M, Al-Khodor S, Abu Kwaik Y.** 2010. Cell biology and molecular ecology of Francisella tularensis. Cell. Microbiol. **12:**129–139. http://dx.doi.org/10.1111/j.1462-5822.2009.01400.x.
4. **Checroun C, Wehrly TD, Fischer ER, Hayes SF, Celli J.** 2006. Autophagy-mediated reentry of Francisella tularensis into the endocytic compartment after cytoplasmic replication. Proc. Natl. Acad. Sci. U. S. A. **103:**14578–14583. http://dx.doi.org/10.1073/pnas.0601838103.
5. **Meibom KL, Dubail I, Dupuis M, Barel M, Lenco J, Stulik J, Golovliov I, Sjostedt A, Charbit A.** 2008. The heat-shock protein ClpB of Francisella tularensis is involved in stress tolerance and is required for multiplication intargetorgansofinfectedmice.Mol.Microbiol.**67:**1384–1401.http://dx .doi.org/10.1111/j.1365-2958.2008.06139.x.
6. **Dieppedale J, Sobral D, Dupuis M, Dubail I, Klimentova J, Stulik J, Postic G, Frapy E, Meibom KL, Barel M, Charbit A.** 2011. Identification ofaputativechaperoneinvolvedinstressresistanceandvirulenceinFrancisella tularensis. Infect. Immun. **79:**1428–1439. http://dx.doi.org/10.1128/IAI.01012-10.
7. **Bell BL, Mohapatra NP, Gunn JS.** 2010. Regulation of virulence gene transcripts by the Francisella novicida orphan response regulator PmrA: role of phosphorylation and evidence of MglA/SspA interaction. Infect. Immun. **78:**2189–2198. http://dx.doi.org/10.1128/IAI.00021-10.
8. **Mohapatra NP, Soni S, Bell BL, Warren R, Ernst RK, Muszynski A, Carlson RW, Gunn JS.** 2007. Identification of an orphan response regulator required for the virulence of Francisella spp. and transcription of pathogenicity island genes. Infect. Immun. **75:**3305–3314. http://dx.doi.org/10.1128/IAI.00351-07.
9. **Kanistanon D, Powell DA, Hajjar AM, Pelletier MR, Cohen IE, Way SS, Skerrett SJ, Wang X, Raetz CR, Ernst RK.** 2012. Role of Francisella lipid A phosphate modification in virulence and long-term protective immune responses.Infect.Immun.**80:**943–951.http://dx.doi.org/10.1128/IAI.06109-11.
10. **Sen B, Meeker A, Ramakrishnan G.** 2010. The fslE homolog, FTL_0439 (fupA/B), mediates siderophore-dependent iron uptake in Francisella tularensis LVS. Infect. Immun. **78:**4276–4285. http://dx.doi.org/10.1128/IAI.00503-10.
11. **Llewellyn AC, Jones CL, Napier BA, Bina JE, Weiss DS.** 2011. Macrophage replication screen identifies a novel Francisella hydroperoxide resistance protein involved in virulence. PLoS One **6:**e24201. http://dx.doi .org/10.1371/journal.pone.0024201.
12. **Lenco J, Pavkova I, Hubalek M, Stulik J.** 2005. Insights into the oxidative stress response in Francisella tularensis LVS and its mutant DeltaiglC12 by proteomics analysis. FEMS Microbiol. Lett. **246:**47–54. http://dx.doi .org/10.1016/j.femsle.2005.03.040.
13. **Allan RK, Ratajczak T.** 2011. Versatile TPR domains accommodate different modes of target protein recognition and function. Cell Stress Chaperones **16:**353–367. http://dx.doi.org/10.1007/s12192-010-0248-0.
14. **Mittl PR, Schneider-Brachert W.** 2007. Sel1-like repeat proteins in signal transduction. Cell Signal. **19:**20–31. http://dx.doi.org/10.1016/j.cellsig .2006.05.034.
15. **Cerveny L, Straskova A, Dankova V, Hartlova A, Ceckova M, Staud F, Stulik J.** 2013. Tetratricopeptide repeat motifs in the world of bacterial pathogens: role in virulence mechanisms. Infect. Immun. **81:**629–635. http://dx.doi.org/10.1128/IAI.01035-12.
16. **Asare R, Abu Kwaik Y.** 2010. Molecular complexity orchestrates modulation of phagosome biogenesis and escape to the cytosol of macrophages byFrancisellatularensis.Environ.Microbiol.**12:**2559–2586.http://dx.doi .org/10.1111/j.1462-2920.2010.02229.x.

17. **Qin A, Mann BJ.** 2006. Identification of transposon insertion mutants of Francisella tularensis tularensis strain Schu S4 deficient in intracellular replication in the hepatic cell line HepG2. BMC Microbiol. **6:**69. http://dx.doi.org/10.1186/1471-2180-6-69.
18. **Johansson A, Berglund L, Eriksson U, Goransson I, Wollin R, Forsman M, Tarnvik A, Sjostedt A.** 2000. Comparative analysis of PCR versus culture for diagnosis of ulceroglandular tularemia. J. Clin. Microbiol. **38:** 22–26.
19. **Chamberlain RE.** 1965. Evaluation of live tularemia vaccine prepared in a chemically defined medium. Appl. Microbiol. **13:**232–235.
20. **Rodriguez SA, Davis G, Klose KE.** 2009. Targeted gene disruption in Francisella tularensis by group II introns. Methods **49:**270–274. http://dx.doi.org/10.1016/j.ymeth.2009.04.011.
21. **Bonquist L, Lindgren H, Golovliov I, Guina T, Sjostedt A.** 2008. MglA and Igl proteins contribute to the modulation of Francisella tularensis live vaccine strain-containing phagosomes in murine macrophages. Infect. Immun. **76:**3502–3510. http://dx.doi.org/10.1128/IAI.00226-08.
22. **Chong A, Wehrly TD, Nair V, Fischer ER, Barker JR, Klose KE, Celli J.** 2008. The early phagosomal stage of Francisella tularensis determines optimal phagosomal escape and Francisella pathogenicity island protein expression. Infect. Immun. **76:**5488–5499. http://dx.doi.org/10.1128/IAI.00682-08.
23. **Straskova A, Cerveny L, Spidlova P, Dankova V, Belcic D, Santic M, Stulik J.** 2012. Deletion of IglH in virulent Francisella tularensis subsp. holarctica FSC200 strain results in attenuation and provides protection against the challenge with the parental strain. Microbes Infect. **14:**177–187. http://dx.doi.org/10.1016/j.micinf.2011.08.017.
24. **Broms JE, Lavander M, Sjostedt A.** 2009. A conserved alpha-helix essentialforatypeVIsecretion-likesystemofFrancisellatularensis.J.Bacteriol. **191:**2431–2446. http://dx.doi.org/10.1128/JB.01759-08.
25. **Balonova L, Hernychova L, Mann BF, Link M, Bilkova Z, Novotny MV, Stulik J.** 2010. Multimethodological approach to identification of glycoproteins from the proteome of Francisella tularensis, an intracellular microorganism. J. Proteome Res. **9:**1995–2005. http://dx.doi.org/10.1021/pr9011602.
26. **Finney DJ.** 1971. Statisical logic in the monitoring of reactions to therapeutic drugs. Methods Infect. Med. **10:**237–245.
27. **Karpenahalli MR, Lupas AN, Soding J.** 2007. TPRpred: a tool for prediction of TPR-, PPR- and SEL1-like repeats from protein sequences. BMC Bioinformatics **8:**2. http://dx.doi.org/10.1186/1471-2105-8-2.
28. **Jiang M, Sullivan SM, Walker AK, Strahler JR, Andrews PC, Maddock JR.** 2007. Identification of novel Escherichia coli ribosome-associated proteins usingisobarictagsandmultidimensionalproteinidentificationtechniques.J. Bacteriol. **189:**3434–3444. http://dx.doi.org/10.1128/JB.00090-07.
29. **Gotzke H, Palombo I, Muheim C, Perrody E, Genevaux P, Kudva R, Muller M, Daley DO.** 2014. YfgM is an Ancillary Subunit of the SecYEG Translocon in Escherichia coli. J. Biol. Chem. **289:**19089–19097. http://dx.doi.org/10.1074/jbc.M113.541672.
30. **Qin A, Scott DW, Thompson JA, Mann BJ.** 2009. Identification of an essential Francisella tularensis subsp. tularensis virulence factor. Infect. Immun. **77:**152–161. http://dx.doi.org/10.1128/IAI.01113-08.
31. **Taylor PD, Toseland CP, Attwood TK, Flower DR.** 2006. LIPPRED: a web server for accurate prediction of lipoprotein signal sequences and cleavage sites. Bioinformation **1:**176–179. http://dx.doi.org/10.6026/97320630001176.
32. **Bordier C.** 1981. Phase separation of integral membrane proteins in Triton X-114 solution. J. Biol. Chem. **256:**1604–1607.
33. **Pallen MJ, Chaudhuri RR, Henderson IR.** 2003. Genomic analysis of secretionsystems.Curr.Opin.Microbiol.**6:**519–527.http://dx.doi.org/10.1016/j.mib.2003.09.005.
34. **Horzempa J, O'Dee DM, Shanks RM, Nau GJ.** 2010. Francisella tularensis DeltapyrF mutants show that replication in nonmacrophages is sufficient for pathogenesis in vivo. Infect. Immun. **78:**2607–2619. http://dx .doi.org/10.1128/IAI.00134-10.
35. **Meibom KL, Forslund AL, Kuoppa K, Alkhuder K, Dubail I, Dupuis M, Forsberg A, Charbit A.** 2009. Hfq, a novel pleiotropic regulator of virulence-associated genes in Francisella tularensis. Infect. Immun. **77:**1866– 1880. http://dx.doi.org/10.1128/IAI.01496-08.
36. **Weiss DS, Brotcke A, Henry T, Margolis JJ, Chan K, Monack DM.** 2007. In vivo negative selection screen identifies genes required for Francisella virulence. Proc. Natl. Acad. Sci. U. S. A. **104:**6037–6042. http://dx.doi.org/10.1073/pnas.0609675104.
37. **Meibom KL, Charbit A.** 2010. The unraveling panoply of Francisella tularensis virulence attributes. Curr. Opin. Microbiol. **13:**11–17. http://dx.doi.org/10.1016/j.mib.2009.11.007.
38. **Maier TM, Casey MS, Becker RH, Dorsey CW, Glass EM, Maltsev N, Zahrt TC, Frank DW.** 2007. Identification of Francisella tularensis Himar1-basedtransposonmutantsdefectiveforreplicationinmacrophages. Infect. Immun. **75:**5376–5389. http://dx.doi.org/10.1128/IAI.00238-07.
39. **Pechous R, Celli J, Penoske R, Hayes SF, Frank DW, Zahrt TC.** 2006. Construction and characterization of an attenuated purine auxotroph in a Francisella tularensis live vaccine strain. Infect. Immun. **74:**4452–4461. http://dx.doi.org/10.1128/IAI.00666-06.
40. **Battesti A, Bouveret E.** 2012. The bacterial two-hybrid system based on adenylate cyclase reconstitution in Escherichia coli. Methods **58:**325–334. http://dx.doi.org/10.1016/j.ymeth.2012.07.018.
41. **Karimova G, Ladant D, Ullmann A.** 2002. Two-hybrid systems and their usageininfectionbiology.Int.J.Med.Microbiol.**292:**17–25.http://dx.doi.org/10.1078/1438-4221-00182.
42. **Su J, Yang J, Zhao D, Kawula TH, Banas JA, Zhang JR.** 2007. GenomewideidentificationofFrancisellatularensisvirulencedeterminants.Infect. Immun. **75:**3089–3101. http://dx.doi.org/10.1128/IAI.01865-06.
43. **Chong A, Child R, Wehrly TD, Rockx-Brouwer D, Qin A, Mann BJ, Celli J.** 2013. Structure-function analysis of DipA, a virulence factor required for intracellular replication. PLoS One **8:**e67965. http://dx.doi.org /10.1371/journal.pone.0067965.
44. **Robertson GT, Child R, Ingle C, Celli J, Norgard MV.** 2013. IglE is an outer membrane-associated lipoprotein essential for intracellular survival and murine virulence of type A Francisella tularensis. Infect. Immun. **81:**4026–4040. http://dx.doi.org/10.1128/IAI.00595-13.
45. **Brotcke A, Weiss DS, Kim CC, Chain P, Malfatti S, Garcia E, Monack DM.** 2006. Identification of MglA-regulated genes reveals novel virulence factors in Francisella tularensis. Infect. Immun. **74:**6642–6655. http://dx.doi.org/10.1128/IAI.01250-06.
46. **Karimova G, Dautin N, Ladant D.** 2005. Interaction network among Escherichiacolimembraneproteinsinvolvedincelldivisionasrevealedby bacterial two-hybrid analysis. J. Bacteriol. **187:**2233–2243. http://dx.doi.org/10.1128/JB.187.7.2233-2243.2005.
47. **Karimova G, Pidoux J, Ullmann A, Ladant D.** 1998. A bacterial twohybridsystembasedonareconstitutedsignaltransductionpathway.Proc. Natl. Acad. Sci. U. S. A. **95:**5752–5756. http://dx.doi.org/10.1073/pnas.95.10.5752.

Straskova A, Spidlova P, Mou S, Worsham P, **Putzova D**, Pavkova I, Stulik J (2015) *Francisella tularensis* type B *ΔdsbA* mutant protects against type A strain and induces strong inflammatory cytokine and Th1-like antibody response *in vivo*. *Pathogens and Disease* **73**.

doi: 10.1093/femspd/ftv058

FEMS Pathogens and Disease, 73, 2015, ftv058

doi: 10.1093/femspd/ftv058

Advance Access Publication Date: 7 August 2015 Research Article

RESEARCH ARTICLE

Francisella tularensis type B *dsbA* mutant protects against type A strain and induces strong inflammatory cytokine and Th1-like antibody response *in vivo*

Adela Straskova[1],*, Petra Spidlova[1], Sherry Mou[2], Patricia Worsham[2], Daniela Putzova[1], Ivona Pavkova[1] and Jiri Stulik[1]

[1]Department of Molecular Pathology, Faculty of Military Health Sciences, University of Defence, Hradec Kralove, Trebesska 1575, Hradec Kralove 500 01, Czech Republic and [2]Bacteriology Division, U.S. Army Medical Research Institute of Infectious Diseases, Fort Detrick, MD 21702-5011, USA

*Corresponding author: Department of phototrophic microorganisms, ALGATECH Centre, Institute of Microbiology, Academy of Sciences of the Czech Republic, Trebesska 1575, Hradec Kralove 500 01, Czech Republic. Tel: 420-384-340-444; E-mail: straskova@alga.cz

One sentence summary: This work is focused on characterization of immune response during *in vivo* infection of two attenuated *Francisella tularensis* mutant (*dsbA* and *iglH*) strains; importantly, the *dsbA* mutant, but not the *iglH* mutant, induced an early innate inflammatory response leading to strong Th1-like antibody response. **Editor:** Ake Forsberg

ABSTRACT

Francisella tularensis subspecies *tularensis* is a highly virulent intracellular bacterial pathogen, causing the disease tularemia. However, a safe and effective vaccine for routine application against *F. tularensis* has not yet been developed. We have recently constructed the deletion mutants for the DsbA homolog protein (*dsbA*/FSC200) and a hypothetical protein IglH (*iglH*/FSC200) in the type B *F. tularensis* subsp. *holarctica* FSC200 strain, which exerted different protection capacity against parental virulent strain. In this study, we further investigated the immunological correlates for these different levels of protection provided by *dsbA*/FSC200 and *iglH*/FSC200 mutants. Our results show that *dsbA*/FSC200 mutant, but not *iglH*/FSC200 mutant, induces an early innate inflammatory response leading to strong Th1-like antibody response. Furthermore, vaccination with *dsbA*/FSC200 mutant, but not with *iglH*/FSC200, elicited protection against the subsequent challenge with type A SCHU S4 strain in mice. An immunoproteomic approach was used to map a spectrum of antigens targeted by Th1-like specific antibodies, and more than 80 bacterial antigens, including novel ones, were identified. Comparison of tularemic antigens recognized by the *dsbA*/FSC200 post-vaccination and the SCHU S4 post-challenge sera then revealed the existence of 22 novel SCHU S4 specific antibody clones.

Keywords: tularemia; cytokines; antibody response; protection; immunoproteomics

INTRODUCTION

Tularemia is a severe disease caused by the intracellular pathogenic bacterium *Francisella tularensis* (*F. tularensis*). Human infections are most commonly acquired through direct contact with infected material (usually animals) or through vectorborne transmission, such as bites by infected insects. By infection through skin, the ulceroglandular tularemia form develops, which represents approximately 90% of all tularemia cases (Tarnvik and Berglund 2003). A more severe form of tularemia may be caused by respiratory infections after inhalation of aerosols containing as little as 10 bacteria of subsp. *tularensis*, which may result in 30–60% mortality if untreated (Evans *et al.* 1985). The potential risk of *F. tularensis* to be misused as a biological weapon led to this bacterium being classified as a category A agent by Centers for Disease Control and Prevention, USA (Oyston, Sjostedt and Titball 2004).

In general, tularemia is treated with antibiotics where streptomycin is recommended as the drug of first choice with tetracyclines serving as potential alternatives (Russell *et al.* 1998; Dennis *et al.* 2001; Johansson *et al.* 2001). However, the successful antibiotic therapy requires prompt diagnosis which is

Received: 9 October 2014; **Accepted:** 4 August 2015

still a serious problem in some countries, and therefore, the development of a safe vaccine is urgently needed. Currently, tularemia vaccine development focuses on improvement of existing attenuated *Francisella* live vaccine strain (LVS) or on construction of new attenuated mutant strains for genes that are involved in pathogenic mechanisms of tularemic microbe (Marohn and Barry2013).Comparedtothesetwoapproaches,designingasubunit vaccine represents much more difficult task because of the current lack of knowledge of suitable immunodominant antigens. Up to now, immunoproteomics exploiting immune sera for identification of new immunoreactive antigens has been the easiest way to acquire information about candidates for protective antigens (Kilmury and Twine 2010).

Previously, we constructed two attenuated type B *F. tularensis* strains, one with deletion in gene encoding a homolog to the protein family of disulfide oxidoreductases DsbA (FTS 1067) and the second one with deletion in gene encoding the FPI protein IglH (FTS 0106/FTS _1134) (Straskova *et al.* 2009, 2012). Both mutants showed attenuated phenotype and protective potential against subsequent subcutaneous challenge with parental Europeanclinicalisolateofsubsp.*holarctica*strain,denotedasFSC200 strain. While immunization with *dsbA*/FSC200 led to complete protection of BALB/c mice against the FSC200 strain challenge, administration of the *iglH*/FSC200 mutant provided only partial dose-dependent protection with maximal protective effect when a dose of more than 3×10^7 CFUs was applied (Straskova *et al.* 2009, 2012).

In this study, we investigated the immunological parameters which might be responsible for differential protection capacity of the *dsbA*/FSC200 and the *iglH*/FSC200 mutant strains. We found that the ability of *in vivo* induction of early innate inflammatory response and the Th1-like antibody response clearly differ between both mutants. Furthermore, we demonstrated that immune response induced by the *dsbA*/FSC200 mutant is also sufficient for protection against challenge with *Francisella* type A strain SCHU S4. Finally, using an immunoproteomic approach, we defined the profile of *Francisella* membrane proteins recognized by post-vaccination and post-challenge sera and their comparison enabled the determination of novel immunoreactive SCHU S4 antigens.

MATERIALS AND METHODS

Animals

Female BALB/c mice were purchased from Velaz, s.r.o. (Unetice, Czech Republic) and entered experiments at 6–8 weeks of age. All procedures using mice were performed in accordance with guidelines of Animal Care and Use Ethical Committee of the Faculty of Military Health Sciences, University of Defence, Czech Republic. At USAMRIID, research was conducted under an IACUC approved protocol in compliance with the Animal Welfare Act and other federal statutes and regulations relating to animals and experiments involving animals. The facility where this research was conducted is accredited by the Association for Assessment and Accreditation of Laboratory Animal Care International and adheres to principles stated in the Guide for the Care and Use of Laboratory Animals, National Research Council, 2011.

Bacteria and culture conditions

Wild-type*F.tularensis*subsp.*tularensis*SCHUS4strain(Collection of Animal Pathogenic Microorganisms, No. 5600, Veterinary ResearchInstitute,Brno,CzechRepublicorUSAMRIIDstraincollection) and *F. tularensis* subsp. *holarctica* FSC200 strain were used. Generation of mutant strains with the *in frame* deletion of the *iglH* gene in the FSC200 strain (*iglH*/FSC200) and with the deletion of the *dsbA* gene in FSC200 (*dsbA*/FSC200) strain has been described previously (Straskova *et al.* 2009, 2012). Bacterial stocks of each strain were grown on McLeod agar supplemented with bovine hemoglobin (Becton Dickinson San Jose, CA) and IsoVitalex (Becton Dickinson) for 24 h at 37◦C and 5% CO_2. Before each experiment, bacteria were grown for 24 h at 37◦C and 5% CO_2 on McLeod agar plates and thereafter suspended in PBS (phosphate-buffered saline, pH 7.4) to an $OD_{600} = 1$, which is approximately 3×10^9 bacteria mL^{-1}. Studies involving *F. tularensis* SCHU S4 strain were conducted at the BSL-3 facility at the Faculty of Military Health Sciences following appropriate biosafety requirements.

Animal infection, cytokine and antibody assays

For immunological assays, groups of BALB/c mice (n = 3) were subcutaneously (s.c.) infected with 10^2 CFU/mouse of *F. tularensis* strain FSC200 and with 10^7 CFU/mouse of the *iglH*/FSC200 or the *dsbA*/FSC200 mutant strain. After 1, 3, 5, 7, 14, 21 and 28 days post-infection, mice were killed and sera together with livers and spleens were collected. Blood was obtained from *vena cava* and pooled for each strain from three mice per treatment. Sera were then separated from blood, filtered through a 0.22μm filter and stored at −80◦C until needed. Individual livers and spleens were aseptically removed from each mouse, homogenized in PBS and stored frozen at −20◦C until needed. Organ homogenates and sera samples were used undiluted and analyzed for levels of cytokines and antibodies using Custom Quantibody Array technology (RayBiotech, Inc., Norcross GA, USA) following the manufacturer´s protocol. The cytokine/antibody concentrations were calculated against the standards using software H20 OV Q-Analyzer v8.10.4 (Raybiotech, Inc., Norcross, GA).

To determine bacterial burden in targeted organs, BALB/c mice (n = 3 for each treatment) were infected with 10^2 CFU/ mouse of the *F. tularensis* FSC200 parental strain or with 10^7 CFU/mouse of the *dsbA*/FSC200 mutant. Control group of mice was inoculated with sterile saline solution only. After 1, 3, 5, 7, 14, 21 and 28 days of infection, livers, spleens and lungs were aseptically removed, homogenized in 2 mL of PBS, serially diluted and plated on McLeod agar plates enriched with 100 U mL^{-1} of penicillin to minimize unwanted contamination. After 3 days of incubation at 37◦C in 5% CO_2, the bacterial colonies were enumerated and CFUs per organ were calculated.

For *in vivo* subcutaneous protection studies, groups of BALB/c mice (n = 5) were s.c. inoculated with 10, 10^2, 10^3, 10^4, 10^5 and 10^7 CFU/mouse of the *dsbA*/FSC200 mutant or with 10^7 CFU/mouse of the *iglH*/FSC200 mutant strain. After 3 weeks of immunization, mice were challenged s.c. with 10^2 CFU/mouse of virulent SCHU S4 strain. For intranasal protection studies, groups of BALB/c mice (n = 10) were vaccinated intranasally (i.n.) with 10,

10^2, 10^3, 10^4, 10^5 or 10^6 CFU/mouse of the *dsbA*/FSC200 mutant. After 4 weeks, mice were challenged i.n. using 10^2 CFU/mouse of the *F. tularensis* SCHU S4 strain. In both studies, mice were monitored daily for morbidity and mortality. The study endpoint was euthanasia when moribund or survival to 21 days following exposure.

For immunoproteomic studies, BALB/c mice (n = 10) were s.c. vaccinated with 10^7 CFU/mouse of the *dsbA*/FSC200 mutant strain. After 21 days, five *dsbA*/FSC200-vaccinated mice were killed to obtain sera. The remaining *dsbA*/FSC200-immunized mice were further s.c. challenged with 10^2 CFU/mouse of highly virulent SCHU S4 strain. After 21 days of infection, sera were collected and stored at −80◦C until needed.

Detergent-enriched fraction preparation

The detergent-enriched fraction was prepared using the Triton X-114 phase separation similar to those described by Shimizu, Kida and Kuwano (2005). Briefly, *F. tularensis* SCHU S4 was grown in chemically defined Chamberlain medium until up to an OD_{600nm} of 0.8. Culture was then pelleted by centrifugation and washed twice with cold PBS. The cell pellet was resuspended in ice-cold PBS supplemented with proteases inhibitors cocktail Complete EDTA-free (Roche, A.G., Switzerland) and disintegrated by French Pressure Cell Press. Then, the whole cell lysate was ultracentrifuged at 100 000 × g for 1 h at 4◦C to pellet membrane-associated proteins. Pellets were resuspended in icecold PTX buffer (PBS supplemented with 350 mm NaCl, 2% Triton X-114, protease inhibitor mixture) and incubated at 4◦C for 1 h under end-over-end rotation. Samples were centrifuged at 12 000 rpm 4◦C for 30 min, and the supernatants were kept at 37◦C for 10 min to induce detergent phase separation. Following centrifugation at 14 000 rpm for 10 min at room temperature, the upper aqueous phase was discarded and replaced with the same volume of PBS supplemented with 350 mm NaCl. This phase separation was repeated three times, and the final detergent phase was resuspended in PBS to the original volume. Protein concentration in the suspension was measured with a BCA protein assay kit (Sigma-Aldrich, St. Louis, MO, USA).

Pilin protein-enriched fraction preparation

Francisella tularensis SCHU S4 was grown on McLeod plates for 48 h and then the bacteria were harvested from the plates and suspended in PBS. The supernatant enriched for the pili was acquired by vortexing the suspension at the maximum speed for 2 min. The bacteria were pelleted by centrifugation at 13 000 rpm for 10 min and the supernatant was collected, which was then heated at 65◦C for 2 h to eliminate any remaining bacteria. The pili were left to aggregate on an orbital shaker at 4◦C for 18 h. The suspension was then ultracentrifuged at 150 000 × g 4◦C for 1 h, the pellets were resuspended in PBS and the protein concentration was quantified using a BCA protein assay kit (SigmaAldrich).

Two-dimensional polyacrylamide gel electrophoresis (2D PAGE), Western Blotting and MALDI TOF/TOF protein identification

Protein samples were precipitated with cold acetone, solubilized in ASB-D buffer (7 M urea, 2 M thiourea, 40 mM Tris, 1% Triton X-100, 1% ASB-14, 0.5% bromphenol blue and 1.2% DeStreak) and separated using immobilized pH gradient strips (IPG), nonlinear pH 3–10, 18 cm or linear pH 6–11, 18 cm (GE Healthcare, Uppsala, Sweden) using 150 or 200 µg of protein/gel for western blots and 1 mg of protein/gel for Coomassie blue staining (Colloidal Blue Stain Kit, Invitrogen). Following IEF, the IPG strips were equilibrated for 15 min in equilibration buffer (2% SDS, 50 mM Tris-HCl (pH 8.8), 6 M urea, 30% glycerol and 1% DTT) followed by a second 15 min equilibration step (2% SDS, 50 mM Tris-HCl (pH 8.8), 6 M urea, 30% glycerol and 14% iodoacetamide). Approximately 9–16% gels were used for second dimension separations. Proteins from the gels were transferred onto BioTrace PVDF membrane (Pall Corporation, Pensacola, FL) and subjected to immunoblotting using the pooled sera either from the *dsbA*/FSC200 vaccinated or SCHU S4-challenged immunized BALB/c mice. As a secondary antibody, the polyclonal goat anti-mouse immunoglobulins/HRP(Dako, Denmark), which recognizes IgG, IgA and IgM isotypes, was used. Chemiluminiscence detection was performed using a BM chemiluminiscence blotting substrate POD according to the manufacturer's instructions (Roche Applied Science). For these experiments, three biological replicates of detergent and pilin protein-enriched fractions were prepared.

Alignments of immunoreactive spots on 2D blots with Coomassie blue-stained gels were done manually.

Protein spots corresponding to immunoreactive spots on western blots were excised from Coomassie blue-stained 2Dgels and in-gel tryptically digested as described elsewhere (Balonova *et al.* 2010). The mass spectra were recorded in positive MS and MS/MS modes on a 4800 MALDI-TOF/TOF mass analyzer (AB Sciex, Forster City, CA). Internal calibration of mass spectra was performed using tryptic autolytic peptides. Acquired data were processed using GPS Explorer software version 3.6 (AB Sciex) cooperating with the Mascot search algorithm version 2.2 and the search was done against a *Francisella tularensis* SCHU S4 database (NC 006570.2). Trypsin was selected as the proteolytic enzyme and one missed cleavage was allowed. Carbamidomethylation of cysteine residues and methionine oxidation was set as a variable and fixed modification, respectively. Proteins were considered identified with the confidence when GPS protein score confidence interval was 100% and at least two peptides per protein were identified.

STATISTICS

Differences in cytokine levels were compared by two-way ANOVA followed by Tukey´s multiple-comparison post-test as appropriate, using GraphPad Prizm 5 software. In all cases, differences were considered significant at $P < 0.05$, where the group of wt FSC200 infected mice and the *dsbA*/FSC200 vaccinated mice were compared and the group of wt FSC200 strain and the *iglH*/FSC200 mutant were compared. Each experiment was independently repeated two times.

RESULTS

In vivo cytokine immune responses elicited in BALB/c mice after *dsbA*/FSC200 and *iglH*/FSC200 s.c. vaccination

To determine whether the *dsbA*/FSC200 mutant or the *iglH*/FSC200 mutant elicited different immune responses in BALB/c mice, the levels of IFN-γ, IL-10, IL-12, IL-17, IL-1β, IL-2, IL-23, IL-4, IL-6 and TNF-α were measured in spleens, livers and sera on days 1, 3, 5, 7, 14, 21 and 28 post-vaccination.

Immunization of BALB/c mice with the *dsbA*/FSC200 mutant led to significantly upregulated levels of IFN-γ and IL-12 in

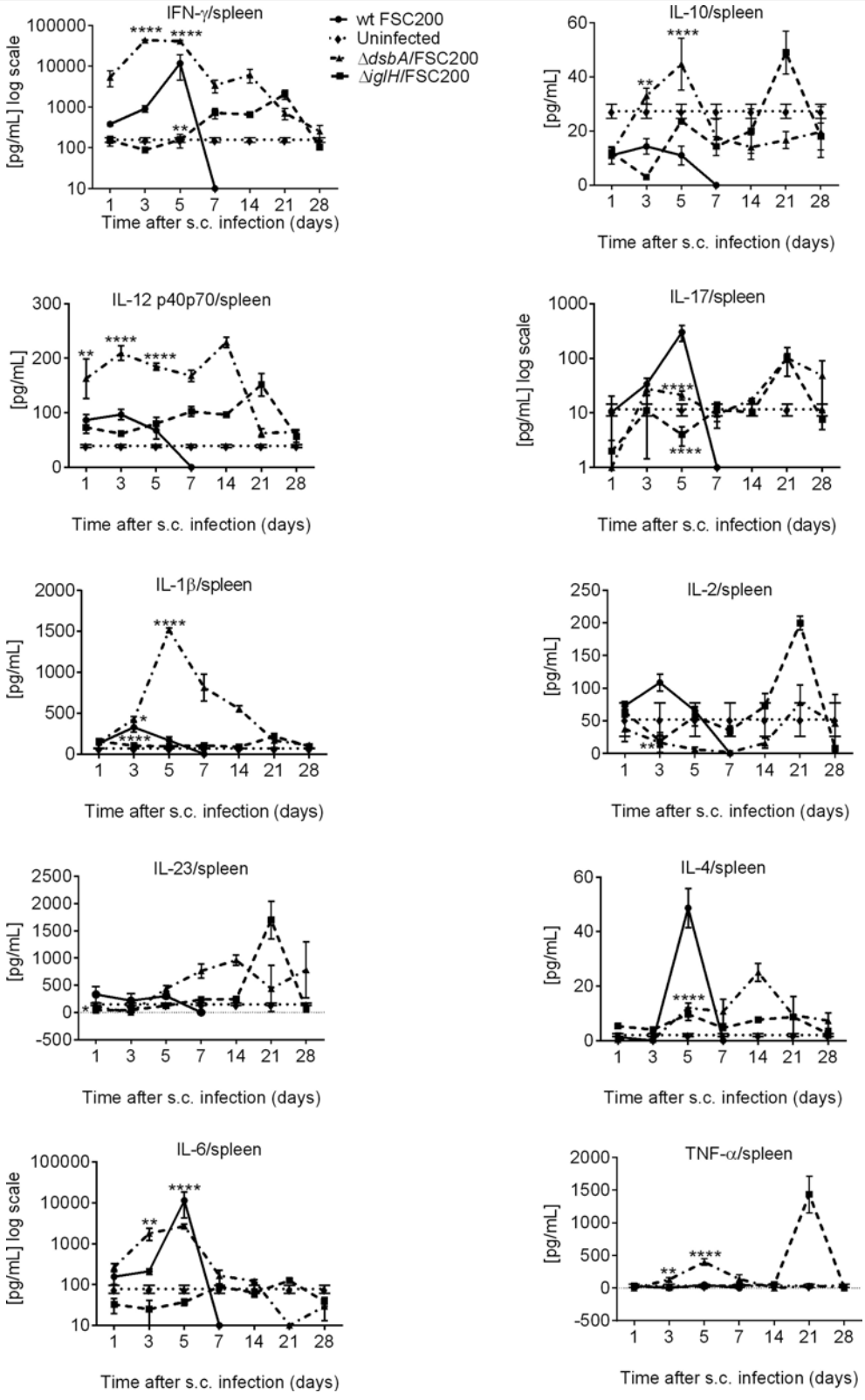

Figure 1. *In vivo* cytokine immune responses elicited in BALB/c mice spleens after *dsbA*/FSC200 and *iglH*/FSC200 vaccination. Groups of BALB/c mice (n = 3) were s.c. inoculated either with 10^2 CFU/mouse of wt FSC200 strain (circles) or with 10^7 CFU/mouse of *dsbA*/FSC200 (triangles) or 10^7 CFU/mouse of *iglH*/FSC200 (squares) mutant strains. Individual spleen was removed at given time interval and analyzed for cytokine levels using cytokine arrays. Statistical comparison was done between groups vaccinated with *dsbA*/FSC200 mutant and wt FSC200 strain and between groups vaccinated with *iglH*/FSC200 mutant and wt FSC200 strain. Results represent means ± standard errors, where $P < 0.05$ was considered to be significant. The results shown are representatives of two separate experiments.

spleen compared to the group infected with wt strain (Fig. 1; Fig. S1, Supporting Information). The increased levels of these cytokines started very early on day 3 after vaccination and persisted till day 14 (Fig. 1). Similarly, IL-6 production increased significantly on day 3, which was maintained until day 5 but then declined by day 7. Day 5 after *dsbA*/FSC200 immunization was also characterized by steep production of IL-1β and TNF-α. In contrast to TNF-α,

the increased level of IL-1β in spleen declined more slowly and persisted till day 21 (Fig. 1; Fig. S1, Supporting Information). Cytokine profile after 2 weeks of *dsbA*/FSC200 infection is associated with the peaks of IL-4 and IL-23 production (Fig. 1). The immunization with the *iglH*/FSC200 mutant influenced expression of IFN-γ, IL-2, IL-17, IL-10, IL-23 and IL-12 cytokines in spleen; nevertheless, their levels appeared with a delay of more than 3 weeks in comparison to the *dsbA*/FSC200 mutant (Fig. 1; Fig. S1, Supporting Information).

Likewise in spleen, the *dsbA*/FSC200 mutant was also able to induce strong upregulation of IFN-γ, IL-1β and IL-12 levels in liver (Fig. 2; Fig. S2, Supporting Information). The increased production of IL-6 was shifted to day 7 after infection in liver, and on day 7 also the upregulation of IL-17 production occurred. Both *dsbA*/FSC200 and *iglH*/FSC200 mutants then stimulated secretion of IL-2 and IL-4 on day 7 in liver and TNF-α on day 14 after immunization (Fig. 2; Fig. S2, Supporting Information).

Investigation of cytokine patterns in sera of vaccinated BALB/c mice confirmed that the *dsbA*/FSC200 mutant can upregulate the early IFN-γ, IL-12 and IL-6 responses (Fig. 3; Fig. S3, Supporting Information). Furthermore, there was strong increase of IL-1β, IL-4, TNF-α and IL-10, but in these cases the response was divided in two phases, one on day 5 and the second 3 weeks after infection (Fig. 3; Fig. S3, Supporting Information). The complicated kinetics exhibited production of IL-2 with three maxima on days 1, 5 and 14. Late time responses are associated with increased levels of IL-17 and IL-23. Like in spleen and liver, the *iglH*/FSC200 mutant induced only a weak inflammatory cytokine response in serum (Fig. 3; Fig. S3, Supporting Information). The only exception was TNF-α production, but even in this case the *dsbA*/FSC200 mutant was more efficient than the *iglH*/FSC200 mutant (Fig. 3; Fig. S3, Supporting Information).

As for infection with parental FSC200 strain, there was a distinct early induction of IL-2, IL-23 and IL-4 in liver and of IFN-γ, Il-6 and IL-17 in serum (Figs 2 and 3). Although these mice succumbing to the infection within 5 days after inoculation.

Humoral immune response in BALB/c mice after vaccination with the *dsbA*/FSC200 and the *iglH*/FSC200 mutant strains

As an additional correlate of *in vivo* protection, we measured the development of humoral adaptive immune response. Groups of BALB/c mice (n = 3) were s.c. inoculated with 10^7 CFU/mouse of *dsbA*/FSC200 or 10^7 CFU/mouse of *iglH*/FSC200 mutant strains. The levels of IgM, IgG1, IgG2a, IgG2b and IgA antibodies were analyzed on days 1, 3, 5, 7, 14, 21 and 28 post-vaccination and compared to antibody levels generated in uninfected mice and mice infected with the parental FSC200 strain.

Mice vaccinated with the *dsbA*/FSC200 mutant showed an early increase of all examined antibody classes except for IgG1 (Fig. 4; Fig. S4, Supporting Information). The most pronounced differencewasfoundintheproductionofIgAandIgG2aantibodies soon after *dsbA*/FSC200 vaccination (Fig. 4; Fig. S4, Supporting Information). It was striking that production of both antibody classes exerted the same kinetics with two peaks on days 5 and 21 post-vaccination (Fig. 4; Fig. S4, Supporting Information).

Surprisingly, the antibody levels detected after the *iglH*/FSC200 mutant vaccination did not rise over the cut off levels of uninfected mice except for IgG1, where the concentration increased early at day 3 and later at day 21 post-infection (Fig. 4; Fig. S4, Supporting Information).

Bacterial burdens in mice organs after the *dsbA*/FSC200 mutant vaccination

The presence of mutant bacteria in mice organs without causing animal disease is an efficient stimulus for the immune system. The groups of BALB/c mice (n = 3) were infected s.c. with the *dsbA*/FSC200 mutant using a dose of 10^7 CFU/mouse. Mice tissues were then collected on days 1, 3, 5, 7, 14, 21 and 28 following infection, and bacterial numbers were determined in homogenates of spleen, lungs and liver.

As shown in Fig. 5, the *dsbA*/FSC200 mutant strain was able to spread to the spleen, liver and lungs of BALB/c mice after s.c. infection. The highest level of recoverable bacteria was found in spleen and liver, where the CFUs reached more than 10^5 within 5 days of infection (Fig. 5). Thereafter, the mutant bacteria recovered from spleen and liver declined throughout the remaining study period (Fig. 5). The mutant bacteria were completely eliminated from liver samples within 21 days of infection and from spleen within 28 days (Fig. 5). It is necessary to mention that bacterial burdens in spleen and liver roughly followed level of cytokines and antibodies detected in these organs. In contrast to the liver and spleen, significantly lower CFUs were detected in lung tissue early after infection and bacteria were completely eliminated within 1 week of infection (Fig. 5).

Protection of the *dsbA*/FSC200 and the *iglH*/FSC200 mutant strains against *F. tularensis* SCHU S4 challenge

Based on previous data documenting protective potential of both mutants, we decided to examine their ability to protect against the challenge with highly virulent *F. tularensis* SCHU S4 strain. The *dsbA*/FSC200 or the *iglH*/FSC200 immunized mice were s.c. challenged with 100 CFU ofSCHU S4 strain. Miceimmunized with the *iglH*/FSC200 mutant showed rapid signs of illness and four mice died within 6–14 days post-challenge. The remaining mice returned to health by day 21 (Table 1A). The group of mice inoculated with the *dsbA*/FSC200 mutant survived the challenge with SCHU S4 strain without any post-infection clinical signs of tularemia (Table 1A). The control group of nonimmunized animals died on days 4–5 post-challenge (Table 1A).

Next, we titrated the immunization doses of the *dsbA*/FSC200 mutant to find the lowest possible dose with protection capability. Therefore, mice were s.c. inoculated with different doses of the *dsbA*/FSC200 mutant and after 3 weeks s.c. challenged with 100 CFU/mouse of SCHU S4 strain. We observed that the complete protection of animals against the SCHU S4 infection can be reached with doses of as low as 10^4 CFU/mouse (Table 1A). In addition, we tested the intranasal protection ability of the *dsbA*/FSC200 mutant against the i.n. SCHU S4 challenge. Mice were vaccinated with different doses of the *dsbA*/FSC200 mutant strain, where none of mice showed sickness during 28 days of observation after immunization. Immunized mice were further infected i.n. with 10^2 CFU/mouse of SCHU S4 strain. All mice in the groups vaccinated with 10, 10^2 and 10^3 CFU/mouse died on day 4 post-challenge. Protection was observed in the groups of animals vaccinated with 10^4, 10^5

and 10^6 CFU/mouse, where two of ten, three of ten and five of ten mice survived, respectively (Table 1B).

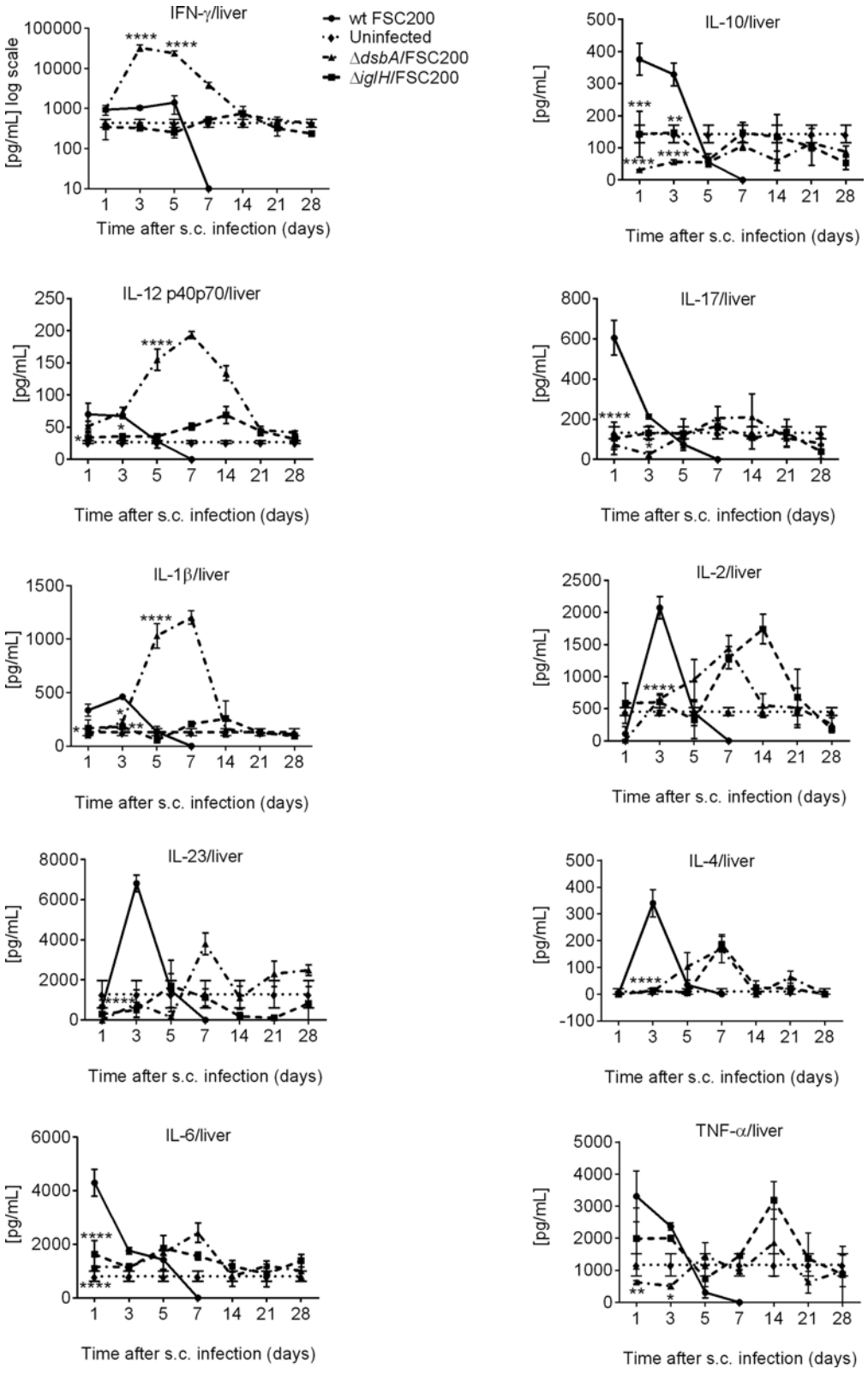

Figure 2. *In vivo* cytokine immune responses elicited in BALB/c mice livers after *dsbA*/FSC200 and *iglH*/FSC200 vaccination. Groups of BALB/c mice (n = 3) were s.c. inoculated either with 10^2 CFU/mouse of FSC200 strain (circles) or with 10^7 CFU/mouse of *dsbA*/FSC200 (triangles) or 10^7 CFU/mouse of *iglH*/FSC200 (squares) mutant strains. At selected time intervals after infection, individual livers were removed and further analyzed for cytokine levels using cytokine arrays. Statistical comparison was done between groups vaccinated with *dsbA*/FSC200 mutant and wt FSC200 strain and between groups vaccinated with *iglH*/FSC200 mutant and wt FSC200 strain. Results represent means ± standard errors, where $P < 0.05$ was considered to be significant. The results shown are representatives of two independent experiments.

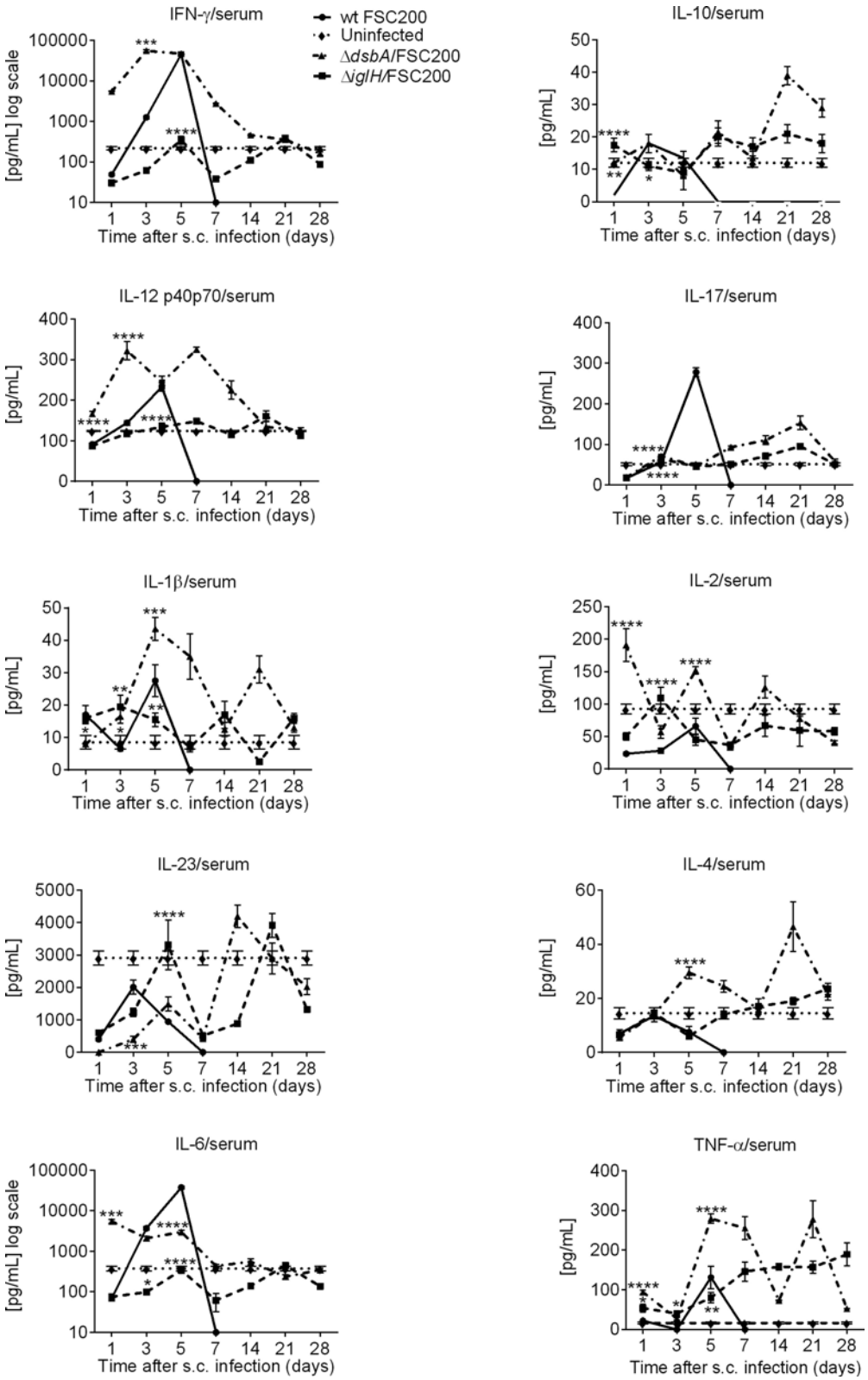

Figure 3. *In vivo* cytokine immune responses elicited in BALB/c mice sera after *dsbA*/FSC200 and *iglH*/FSC200 vaccination. Groups of BALB/c mice ($n = 3$) were s.c. inoculated either with 10^2 CFU/mouse of FSC200 strain (circles) or with 10^7 CFU/mouse of *dsbA*/FSC200 (triangles) or 10^7 CFU/mouse of *iglH*/FSC200 (squares) mutant strains. Mice were killed at given time interval after vaccination and cytokine levels were determined in the serum using cytokine arrays. The results shown are representatives of two independent experiments.

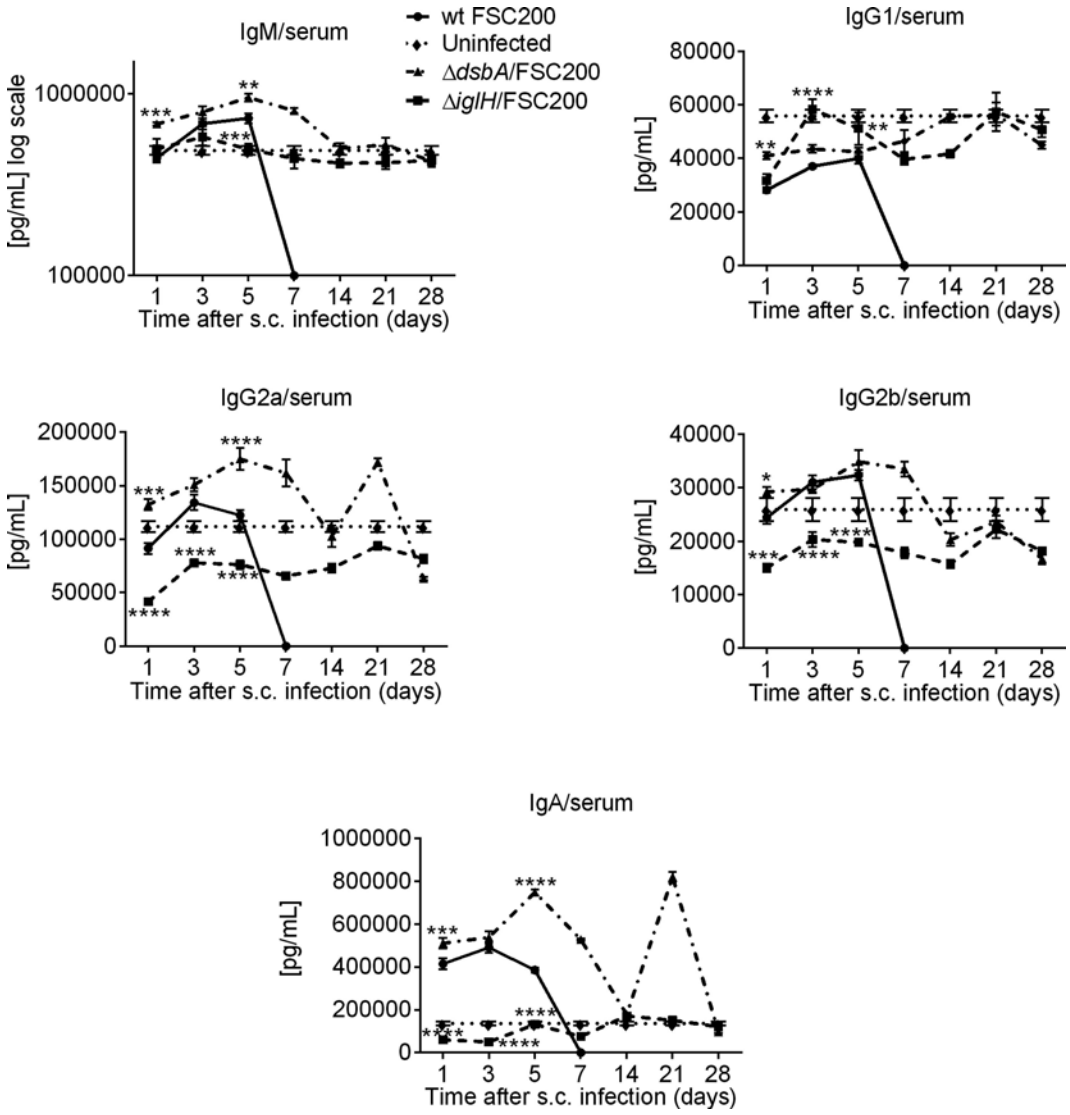

Figure 4. Humoral immune responses in BALB/c mice after *dsbA*/FSC200 and *iglH*/FSC200 vaccination. Groups of BALB/c mice (n = 3) were s.c. inoculated either with 10^2 CFU/mouse of FSC200 strain (circles) or with 10^7 CFU/mouse of *dsbA*/FSC200 (triangles) or 10^7 CFU/mouse of *iglH*/FSC200 (squares) mutant strains. Mice were killed at given time interval after vaccination and antibody levels were determined in the serum using cytokine arrays. The results shown are representatives of two separate experiments.

Our results show that the *dsbA*/FSC200 mutant is attenuated for s.c. and i.n. infection of BALB/c mice. Moreover, the *dsbA*/FSC200 mutant has protective ability against lethal dose of SCHU S4 strain in s.c. infection and is able to partially protect against respiratory SCHU S4 challenge.

Mapping of *dsbA*/FSC200 post-vaccination and SCHU S4 post-challenge immunoproteome

As we have shown, the protective response of the *dsbA*/FSC200 mutant strain is accompanied by increased levels of IgA and IgG2a antibody production. Thus, we decided to examine the profile of the antibody-recognized antigens after s.c. vaccination with the *dsbA*/FSC200 mutant strain. Assuming that the surface-exposed and membrane-associated proteins are crucial antibody targets, detergent-enriched and pilin protein-enriched subproteomes were analyzed using a classical immunoproteomic approach with sera pooled from *dsbA*/FSC200 vaccinated BALB/c mice. Overall, we identified 63 antigens, 22 of which had not been previously described (Table 2; Table S1, SupportingInformation)(Pelletier,RaoultandLaScola2009;Kilmury and Twine 2010; Fulton *et al.* 2011; Golovliov *et al.* 2013). It is interesting that most of them, 19 antigens in total, were found in pilin protein-enriched subproteome which seems to be a valuable source for antibody-inducing antigens. The group of novel immunoreactive antigens covered the spectrum of enzymes, as well as ribosomal and stress proteins. It is worth to mention acid phosphatase (FTT 0221), DipA (FTT 0369c), D-alanyl-Dalanine carboxypeptidase (FTT 1029), IglE (FTT 1701/FTT 1346), PdpE (FTT 1710/FTT _1355), PilA orthologs (FTT 0889c, FTT 0890c) and hypothetical proteins (FTT 0704, FTT 0903, FTT 1407c and FTT 1653). Because *dsbA*/FSC200 vaccination helps mice to survive SCHU S4 infection, we also collected sera from SCHU S4 challenged mice to measure possible seroconversion to SCHU S4 specific antigens. In this case, we identified 71 antigens recognized by SCHU S4 post-challenge sera (Table S1, Supporting Information). Of them eight new antibody-binding antigens not found in *dsbA*/FSC200 post-vaccination sera were

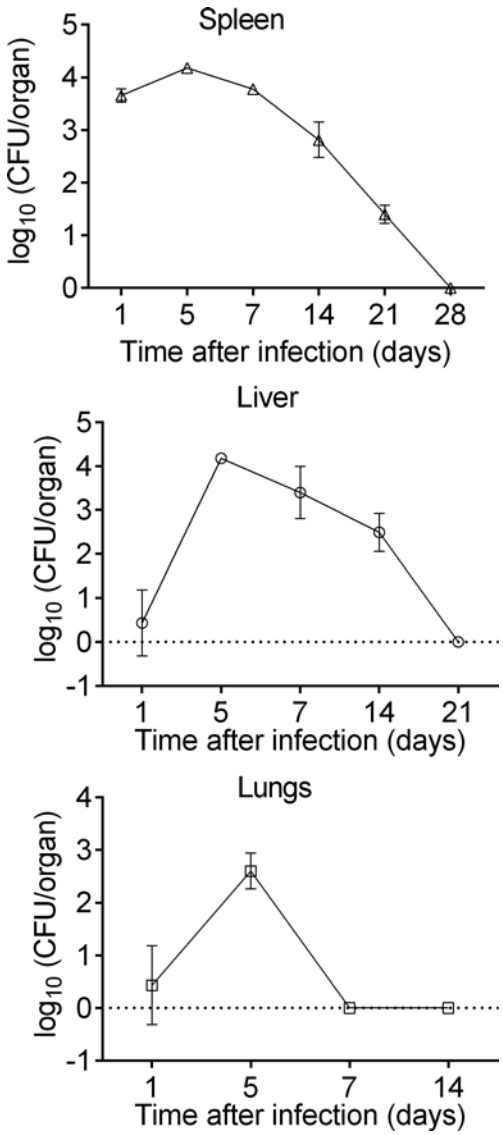

Figure 5. Bacterial burdens in mice organs after *dsbA*/FSC200 mutant vaccination. BALB/c mice (n = 3 per group) were inoculated s.c. with 10^7 CFU/mouse of the *dsbA*/FSC200 mutant and CFUs were determined for the lung, liver and spleen tissues at each time point indicated. Results represent means ± standard errors of CFU counts. The data are representative of three independent experiments.

discovered (Table 2). These antigens recognized uniquely by SCHU S4 post-challenge sera also formed a functionally heterogeneous group involving proteins with the known role in *Francisella* pathogenesis such as superoxide dismutase Fe (FTT 0068), superoxide dismutase Cu-Zn (FTT 0879) and hypothetical protein (FTT 0910).

DISCUSSION

So far, the development of safe and effective vaccine against tularemia is still far from realization (Pechous, McCarthy and Zahrt 2009). Recently, a hypothetical lipoprotein with high homology to the protein family of disulphide oxidoreductases DsbA was identified as a new essential virulence factor of *F. tularensis*. The *dsbA* deletion mutants in both type A and type B *F. tularensis* strains were constructed and exerted pronounced attenuation in mouse infection models (Qin *et al.* 2009; Straskova *et al.* 2009). Furthermore, an intranasal immunization with the *dsbA* mutant in type A strain or subcutaneous immunization with the *dsbA* mutant in type B strain reliably protected against the challenge with parental virulent strains (Qin *et al.* 2009; Straskova *et al.* 2009). Besides *dsbA*/FSC200 mutant strain, our laboratory has also constructed the deletion mutant for the FPI protein encoded by *iglH* gene in FSC200 strain. However, compared to the *dsbA*/FSC200 mutant, its preventive effect was dose dependent and complete protection against the wild-type parental strain was only found after administration of the highest immunization dose of 3×10^7 CFU/mouse used (Straskova *et al.* 2009).

In this study, we explored the features of innate and adaptive immunity induced by these two attenuated mutants with differential protective capacity. In agreement with these findings, we were able to measure an early increase of IFN-γ and IL-6 in spleen and serum in the *dsbA*/FSC200 immunized BALB/c mice. Higher levels of IFN-γ but not IL-6 were also observed in liver samples. The strong early inflammatory response to *dsbA*/FSC200 vaccination was further corroborated by the increased levels of IL-12 and IL-1β in spleen, liver and serum and TNF-α in spleen and serum. Furthermore, liver and serum samples exhibited an increased response of IL-2 production after *dsbA*/FSC200 immunization. Furthermore, spleen tissue was also found to be a source of IL-23 overproduction with a maximum on day 14 post-infection. The same time interval of IL23 upregulation was observed for serum samples. Mice deficient in IL-12p40 but not in IL-12p35 are susceptible to *F. tularensis* LVS infections indicating that IL-12p70 is not necessary for bacteria elimination (Elkins *et al.* 2002). As the IL-23 is a complex of p40 subunit with a 19-kDa protein, it is possible that only IL-23 can participate in the development of T-cell-mediated bacterial clearance. Furthermore, IL-23 is an inducer of IL-17 production. As for IL-17, we detected increased levels of this cytokine in liver tissue; however, an even more pronounced expression was found in serum with maximum at late time point (21 days post-infection). There is controversy about the role of IL-17 in protection against respiratory challenge with SCHU S4. While Skyberg *et al.* (2013) showed that IL-17 is inefficient for intratracheal infection of mice with SCHU S4 strain, Golovliov *et al.* (2013) demonstrated that increased efficacy of FSC200 *clpB* mutant strain in induction protective response against SCHU S4 respiratory infection is associated with the increased IL-17 pulmonaryproductionafterSCHUS4challenge.Asignificantupregulation of IL-4 expression was also observed in liver and spleen samples on days 7 and 14 post-infection, respectively. Mast cells were found to be major source of IL-4 capable to restrict intramacrophage growth of *F. tularensis* LVS (Thathiah *et al.* 2011), and the production of this cytokine was dependent on mast cell TLR2 signaling (Rodriguez *et al.* 2012). In agreement with less efficient *in vivo* protection of mice against parental virulent strain, the *iglH*/FSC200 mutant strain exerted, besides TNF-α level in serum, weak and delayed production of inflammatory cytokines compared to the *dsbA*/FSC200. Recently, a similar study was published in which four defined gene deletion mutants of SCHU S4 were examined for their abilities to induce protective responses against dermal and respiratory challenge with SCHU S4 strain. Two of them, deletion mutants for *clpB* and γglutamyl transpeptidase exhibited the most efficient protection in both dermal and resiratory models. Likewise in our study, the protective capacity of these two mutants correlated, among others, with the increased levels of IFN γ, TNF α in serum and IFN γ,

Table 1A. Survival of BALB/c mice following subcutaneous immunization with the *dsbA*/FSC200 mutant or the *iglH*/FSC200 mutant against SCHU S4 s.c. challenge.

Bacterial strain	s.c. dose CFU/mouse on day 0 (vaccination dose)	s.c. dose of SCHU S4 CFU/mouse on day 21 after vaccination (challenge dose)	Nr. of deaths/total
	0 (mock solution only)	10^2	5/5
dsbA/FSC200		10^2	4/5
	10	10^2	4/5
	10^2		
	10^3		
	4	10^2	1/5
	10	10^2	0/5
	10^5	10^2	0/5
	10^7	10^2	0/5
iglH/FSC200	10^7	10^2	4/5

BALB/c mice (n = 5) were immunized subcutaneously with the *dsbA*/FSC200 mutant or the *iglH*/FSC200 mutant. Animals were challenged subcutaneously 3 weeks later with virulent SCHU S4 strain. The mice were monitored daily for morbidity and mortality. The study endpoint was euthanasia when moribund or survival to 21 days following exposure.

Table 1B. Survival of BALB/c mice following intranasal immunization with the *dsbA*/FSC200 mutant against SCHU S4 i.n. challenge.

Bacterial strain	i.n. dose CFU/mouse on day 0 (vaccination dose)	i.n. dose of SCHU S4 CFU/mouse on day 28 after vaccination (challenge dose)	Nr. of deaths/total
	0 (mock solution only)	10^2	10/10
dsbA/FSC200	10	10^2	10/10
	10^2	10^2	10/10
	10^3	10^2	10/10
	10^4	10^2	8/10
	10^5	10^2	7/10
	10^6	10^2	5/10

BALB/c mice (n = 10) were immunized i.n. with the *dsbA*/FSC200 mutant, animals were challenged i.n. 28 days later with virulent SCHU S4 strain. The mice were monitored daily for morbidity and mortality. The study endpoint was euthanasia when moribund or survival to 21 days following exposure.

TNF α, IL-1β, IL-6, IL-17 in spleen (Ryden *et al.* 2013). Generally, the cytokine pattern induced by the *dsbA*/FSC200 mutant indicates the development of a strong Th1 protective response. This finding was further supported by the array analysis of antibody induction in serum of mice immunized with the *dsbA*/FSC200 and the *iglH*/FSC200 mutants. We found that *dsbA*/FSC200 vaccination induced all antibody classes; nevertheless, the most robust response concerned the IgA and IgG2a production, which had two maxima, of which the early one paralleled the traditional quick IgM antibody secretion. Very recent publication demonstrated that IgA-deficient mice exhibited enhanced susceptibility to pulmonary *F. tularensis* LVS infection. Additionally, these mice had significantly reduced pulmonary levels of IFN-γ and IL-12. The decline in IFN-γ amount reflects the diminished numbers of $CD4_+$ and $CD8_+$ T cells in the lungs (Furuya *et al.* 2013). In contrast to *dsbA*/FSC200, the *iglH*/FSC200 infected mice only upregulated IgG1 levels typical for a Th2 response. Previously, we had observed that subcutaneous vaccination of mice with *dsbA*/FSC200 can reliably protect mice against 4 × 10^5 CFU of the wild-type B isolate FSC200 (Straskova *et al.* 2009). In this study, we looked at distribution and persistence of the *dsbA*/FSC200 microbes in selected organs of vaccinated mice. We have shown that the bacterial burdens following s.c. infection with the mutant strain were highest in spleen followed by liver and lungs (Fig. 5). Importantly, the mutant bacteria were eliminated from all analyzed organs during the time period of 4 weeks (Fig. 5). This finding shows the ability of the host to mount the effective immune response after the *dsbA*/FSC200 administration that even protects BALB/c mice against subcutaneous and respiratory SCHU S4 challenge (Tables 1A and 1B).

Table 2. Novel immunoreactive SCHU S4 antigens.

SCHU S4 gene locus	Protein name	Detected by *dsbA*/200 serum	Detected by *dsbA*/200 + SCHU S4 serum	Antigen
FTT 0034*	NADH dehydrogenase I, D subunit		x	LP fraction
FTT 0068	Superoxide dismutase [Fe]		x	Pilin fraction
FTT 0080	Triosephosphate isomerase		x	Pilin fraction
FTT 0139	Transcription antitermination protein nusG	x	x	Pilin fraction
FTT 0142	50S ribosomal protein L10	x	x	Pilin fraction
FTT 0339	30S ribosomal protein S8	x	x	Pilin fraction
FTT 0369c	Hypothetical protein	x	x	Pilin fraction
FTT 0372c	AcetylCoA carboxylase beta subunit	x	x	Pilin fraction
FTT 0624	ATP-dependent Clp protease subunit P		x	Pilin fraction
FTT 0704	Hypothetical protein	x	x	Pilin fraction
FTT 0879	Superoxide dismutase (Cu-Zn) precursor		x	LP fraction
FTT 0889c	Type IV pili fiber building block protein PilE	x	x	LP fraction
FTT 0890c	Type IV pili fiber building block protein PilA	x	x	LP fraction
FTT 0903	Hypothetical protein	x	x	Pilin fraction LP fraction
FTT 0910	Hypothetical protein		x	LP fraction
FTT 1241	Serine hydroxymethyltransferase	x	x	Pilin fraction
FTT 1260	Hypothetical lipoprotein		x	LP fraction
FTT 1375	3-Oxoacyl-(acyl-carrier-protein) reductase	x	x	Pilin fraction
FTT 1407c	Hypothetical membrane protein	x	x	Pilin fraction
FTT 1459c	NAD-dependent epimerase		x	Pilin fraction
FTT 1701, FTT 1346	Hypothetical protein	x	x	Pilin fraction
FTT 1710, FTT 1355	Conserved hypothetical protein	x	x	Pilin fraction

*Criteria for identification not fulfilled (C.I. 92% and only one peptide per protein was identified), but the protein was identified repeatedly.

Using comparative proteome analyses, we had already showed that there are differences in protein expression between type B and type A strains (Hubalek *et al.* 2004; Pavkova *et al.* 2006). Nevertheless, the protective ability of the *dsbA*/FSC200 mutant against type A strain indicates that some immunoreactive antigens can be shared. Data from our present immunoproteomic study confirmed that 14 antigens were recognized by both types of immune sera (Table 2). On the other hand, seroconversion to SCHU S4 unique response was reflected by production of antibodies against another eight bacterial proteins (Table 2). Among identified proteins, DipA, FTT 1407c, PilA, PdpE, FTT 0903, IglE, acid phosphatase, superoxide dismutase Fe and superoxide dismutase Cu-Zn represent potential or well-known virulence factors (Weiss *et al.* 2007; Melillo *et al.* 2009; Akimana, Al-Khodor and Abu Kwaik 2010; Forslund *et al.* 2010; Chong *et al.* 2013; Mohapatra *et al.* 2013; Robertson *et al.* 2013). It was already described that IglE, PdpE superoxide dismutase Fe and acid phosphatase can be secreted during *Francisella* growth (Konecna *et al.* 2010; Broms *et al.* 2012). Additionally, we observed that DipA and IglE can accumulate in a membrane of the *dsbA*/LVS mutant (Straskova *et al.* 2009) and unpublished observation. It might be that these proteins are misfolded due to the loss of the DsbA protein, which has both thiol/disulfide oxidoreductase and chaperone function (Straskova *et al.* 2009; Schmidt *et al.* 2013) and are, therefore, not delivered to proper location. This situation can lead to the increased immunogenicity of these misfolded proteins.

Our results show that the *dsbA*/FSC200 mutant is able to mount strong Th1 type immune response *in vivo* that is even efficient against a subcutaneous and intranasal challenge with type A *Francisella* SCHU S4 strain. Moreover, identification of novel immunoreactive antigens which are common or unique for the *dsbA*/FSC200 vaccination or the SCHU S4 challenge then contributes to the listof proteins useful for a subunit vaccine design.

SUPPLEMENTARY DATA

Supplementary data are available at FEMSPD online.

ACKNOWLEDGEMENTS

We are grateful to Evelyn Lawrenz for critical reading of the manuscript, to Maria Safarova for her technical assistance with mouse experiments and Jitka Zakova for help with 2D electrophoresis.

FUNDING

TheworkwassupportedbySpecificResearchgrantofMinistryof Education, Youth and Sports of Czech Republic (SV/FVZ201202), DTRA project CB3387 PA D-CZ-11-0001 and by a long-term organization development plan 1011.

Conflict of interest. None declared.

REFERENCES

Akimana C, Al-Khodor S, Abu Kwaik Y. Host factors required for modulation of phagosome biogenesis and proliferation of *Francisella tularensis* within the cytosol. *PLoS One* 2010;**5**:e11025.

Balonova L, Hernychova L, Mann BF, *et al.* Multimethodological approach to identification of glycoproteins from the proteome of *Francisella tularensis*, an intracellular microorganism. *J Proteome Res* 2010;**9**:1995–2005.

Broms JE, Meyer L, Sun K, *et al.* Unique substrates secreted by the type VI secretion system of *Francisella tularensis* during intramacrophage infection. *PLoS One* 2012;**7**:e50473. Chong A, Child R, Wehrly TD, *et al.* Structure-function analysis of DipA, a virulence factor required for intracellular replication. *PLoS One* 2013;**8**:e67965.

Dennis DT, Inglesby TV, Henderson DA, *et al.* Tularemia as a biological weapon: medical and public health management. *JAMA* 2001;**285**:2763–73.

Elkins KL, Cooper A, Colombini SM, *et al. In vivo* clearance of an intracellular bacterium, *Francisella tularensis* LVS, is dependent on the p40 subunit of interleukin-12 (IL-12) but not on IL-12 p70. *Infect Immun* 2002;**70**:1936–48.

Evans ME, Gregory DW, Schaffner W, *et al.* Tularemia: a 30-year experience with 88 cases. *Medicine* 1985;**64**:251–69.

Forslund AL, Salomonsson EN, Golovliov I, *et al.* The type IV pilin, PilA, is required for full virulence of *Francisella tularensis* subspecies tularensis. *BMC Microbiol* 2010;**10**:227.

Fulton KM, Zhao X, Petit MD, *et al.* Immunoproteomic analysis of the human antibody response to natural tularemia infection with Type A or Type B strains or LVS vaccination. *Int J Med Microbiol* 2011;**301**:591–601.

Furuya Y, Kirimanjeswara GS, Roberts S, *et al.* Increased susceptibility of IgA-deficient mice to pulmonary *Francisella tularensis* live vaccine strain infection. *Infect Immun* 2013;**81**: 3434–41.

Golovliov I, Twine SM, Shen H, *et al.* A deltaclpB mutant of *Francisella tularensis* subspecies holarctica strain, FSC200, is a more effective live vaccine than *F. tularensis* LVS in a mouse respiratory challenge model of tularemia. *PLoS One* 2013;**8**:e78671.

Hubalek M, Hernychova L, Brychta M, *et al.* Comparative proteome analysis of cellular proteins extracted from highly virulent *Francisella tularensis* ssp. tularensis and less virulent *F. tularensis* ssp. holarctica and *F. tularensis* ssp. mediaasiatica. *Proteomics* 2004;**4**:3048–60.

Johansson A, Berglund L, Sjostedt A, *et al.* Ciprofloxacin for treatment of tularemia. *Clin Infect Dis* 2001;**33**:267–8.

Kilmury SL, Twine SM. The *Francisella tularensis* proteome and its recognition by antibodies. *Front Microbiol* 2010;**1**:143.

Konecna K, Hernychova L, Reichelova M, *et al.* Comparative proteomic profiling of culture filtrate proteins of less and highly virulent *Francisella tularensis* strains. *Proteomics* 2010;**10**: 4501–11.

Marohn ME, Barry EM. Live attenuated tularemia vaccines: recent developments and future goals. *Vaccine* 2013;**31**: 3485–91.

Melillo AA, Mahawar M, Sellati TJ, *et al.* Identification of *Francisella tularensis* live vaccine strain CuZn superoxide dismutase as critical for resistance to extracellularly generated reactive oxygen species. *J Bacteriol* 2009;**191**: 6447–56.

Mohapatra NP, Soni S, Rajaram MV, *et al.* Type A *Francisella tularensis* acid phosphatases contribute to pathogenesis. *PLoS One* 2013;**8**:e56834.

Oyston PC, Sjostedt A, Titball RW. Tularaemia: bioterrorism defencerenewsinterestin*Francisellatularensis*.*NatRevMicrobiol* 2004;**2**:967–78.

Pavkova I, Reichelova M, Larsson P, *et al.* Comparative proteome analysis of fractions enriched for membrane-associated proteins from *Francisella tularensis* subsp. tularensis and *F. tularensis* subsp. holarctica strains. *J Proteome Res* 2006;**5**: 3125–34.

Pechous RD, McCarthy TR, Zahrt TC. Working toward the future: insights into *Francisella tularensis* pathogenesis and vaccine development. *Microbiol Mol Biol R* 2009;**73**:684–711.

Pelletier N, Raoult D, La Scola B. Specific recognition of the major capsid protein of Acanthamoeba polyphaga mimivirus by sera of patients infected by *Francisella tularensis*. *FEMS Microbiol Lett* 2009;**297**:117–23.

QinA,ScottDW,ThompsonJA,*etal.*Identificationofanessential *Francisella tularensis* subsp. tularensis virulence factor. *Infect Immun* 2009;**77**:152–61.

Robertson GT, Child R, Ingle C, *et al.* IglE Is an outer membraneassociated lipoprotein essential for intracellular survival and murine virulence of type A *Francisella tularensis*. *Infect Immun* 2013;**81**:4026–40.

Rodriguez AR, Yu JJ, Guentzel MN, *et al.* Mast cell TLR2 signaling is crucial for effective killing of *Francisella tularensis*. *J Immunol* 2012;**188**:5604–11.

Russell P, Eley SM, Fulop MJ, *et al.* The efficacy of ciprofloxacin and doxycycline against experimental tularaemia. *J Antimicrob Chemoth* 1998;**41**:461–5.

Ryden P, Twine S, Shen H, *et al.* Correlates of protection following vaccination of mice with gene deletion mutants of *Francisella tularensis* subspecies tularensis strain, SCHU S4 that elicit varying degrees of immunity to systemic and respiratory challenge with wild-type bacteria. *Mol Immunol* 2013;**54**: 58–67.

Schmidt M, Klimentova J, Rehulka P, *et al. Francisella tularensis* subsp. holarctica DsbA homologue: a thioredoxin-like protein with chaperone function. *Microbiology* 2013;**159**:2364–74.

Shimizu T, Kida Y, Kuwano K. A dipalmitoylated lipoprotein from *Mycoplasma pneumoniae* activates NF-kappa B through TLR1, TLR2, and TLR6. *J Immunol* 2005;**175**:4641–6.

Skyberg JA, Rollins MF, Samuel JW, *et al.* Interleukin-17 protects against the *Francisella tularensis* live vaccine strain but not against a virulent *F. tularensis* type A strain. *Infect Immun* 2013;**81**:3099–105.

Straskova A, Cerveny L, Spidlova P, *et al.* Deletion of IglH in virulent *Francisella tularensis* subsp. holarctica FSC200 strain resultsinattenuationandprovidesprotectionagainstthechallenge with the parental strain. *Microbes Infect* 2012;**14**:177–87.

Straskova A, Pavkova I, Link M, *et al.* Proteome analysis of an attenuated *Francisella tularensis* dsbA mutant: identification of potential DsbA substrate proteins. *J Proteome Res* 2009;**8**: 5336–46.

Tarnvik A, Berglund L. Tularaemia. *Eur Respir J* 2003;**21**:361–73.

Thathiah P, Sanapala S, Rodriguez AR, *et al.* Non-FcepsilonR bearing mast cells secrete sufficient interleukin-4 to control *Francisellatularensis*replicationwithinmacrophages.*Cytokine* 2011;**55**:211–20.

Weiss DS, Brotcke A, Henry T, *et al. In vivo* negative selection screen identifies genes required for Francisella virulence. *P Natl Acad Sci USA* 2007;**104**:6037–42.

Fabrik I, Link M, **Putzova D**, Plzakova L, Lubovska Z, Philimonenko V, Pavkova I, Rehulka P, Krocova Z, Hozak P, et al. (2018) The Early Dendritic Cell Signaling Induced by Virulent *Francisella tularensis* Strain Occurs in Phases and Involves the Activation of Extracellular Signal-Regulated Kinases (ERKs) and p38 In the Later Stage. *Molecular & Cellular Proteomics* **17**: 81–94.

doi: 10.1074/mcp.RA117.000160

The Early Dendritic Cell Signaling Induced by Virulent *Francisella tularensis* Strain Occurs in Phases and Involves the Activation of Extracellular Signal-Regulated Kinases (ERKs) and p38 In the Later Stage*[□S]

Ivo Fabrik‡, Marek Link‡, Daniela Putzova‡, Lenka Plzakova‡, Zuzana Lubovska§, Vlada Philimonenko§¶, Ivona Pavkova‡, Pavel Rehulka‡, Zuzana Krocova‡, Pavel Hozak§¶, Marina Santic, and Jiri Stulik‡**

Dendritic cells (DCs) infected by *Francisella tularensis* are poorly activated and do not undergo classical maturation process. Although reasons of such unresponsiveness are not fully understood, their impact on the priming of immunity is well appreciated. Previous attempts to explain the behavior of *Francisella*-infected DCs were hypothesisdriven and focused on events at later stages of infection. Here, we took an alternative unbiased approach by applying methods of global phosphoproteomics to analyze the dynamics of cell signaling in primary DCs during the first hour of infection by *Francisella tularensis*. Presented results show that the early response of DCs to *Francisella* occurs in phases and that ERK and p38 signaling modules induced at the later stage are differentially regulated by virulent and attenuated *dsbA* strain. These findings imply that the temporal orchestration of host proinflammatory pathways represents the integral part of *Francisella* life-cycle inside hijacked DCs. ***Molecular & Cellular Proteomics 17: 10.1074/mcp.RA117.000160, 81–94, 2018.***

From the ‡Department of Molecular Pathology and Biology, Faculty of Military Health Sciences, University of Defence, 500 01 Hradec Kralove, Czech Republic; §Institute of Molecular Genetics ASCR v.v.i., Microscopy Centre, Electron Microscopy Core Facility, 142 20 Prague 4, Czech Republic; ¶Institute of Molecular Genetics ASCR v.v.i., Department of Biology of the Cell Nucleus, 142 20 Prague 4, Czech Republic; Department of Microbiology, Faculty of Medicine, University of Rijeka, 51000 Rijeka, Croatia

Received June 27, 2017, and in revised form, September 22, 2017
Published, MCP Papers in Press, October 18, 2017, DOI 10.1074/mcp.RA117.000160

Author contributions: I.F. and J.S. designed research; I.F., M.L., D.P., L.P., Z.L., V.P., I.P., P.R., and Z.K. performed research; I.F., M.L., D.P., L.P., Z.L., V.P., Z.K., and M.S. analyzed data; I.F. and J.S. wrote the paper; P.H. contributed new reagents/analytic tools.

Francisella tularensis is a Gram-negative bacterium and intracellular pathogen that is responsible for tularemia disease (1). Although humans are not the primary hosts, *Francisella* capacity to cause respiratory infections with the relatively high mortality rates prompted the classification of the bacterium as a potential biological weapon (2). The disease itself is characterized by the delayed onset of the adaptive immunity which is then followed by the hypercytokinemia (3). The suboptimal host response comes as a consequence of *Francisella* ability to avoid the activation of phagocytes in which the bacterium replicates (4). *Francisella* initiates its intracellular life cycle by the entry into the host cell where it transiently resides within the phagosome. Following 30–60 min post infection (p.i.)[1], *Francisella* escapes from the vacuole into

[1] The abbreviations used are: p.i., post infection; AMPK, AMPactivated protein kinase; AP-1, activator protein 1; BMDC, bone marrow-derived dendritic cell; CREB, cAMP-responsive elementbinding protein; DC, dendritic cell; ERK, extracellular signal–regulated kinase; GAP, GTPase-activating protein; GEF, guanine nucleotide exchange factor; GM-CSF, granulocyte-macrophage colony-stimulating factor; GSK, glycogen synthase kinase; HILIC, hydrophilic interaction chromatography; IFN-, interferon-; IKK, inhibitor of NF-B kinase; JNK, c-Jun N-terminal kinase; LPS, lipopolysaccharide; MAPK, mitogen-activated protein kinase; MAPKAPK, MAPK-activated protein kinase; MOI, multiplicity of infection; mTOR, mammalian target of rapamycin;

the host cell cytosol and it replicates there (5). Dendritic cells (DCs), as professional phagocytes, are also susceptible to *Francisella* infection. Like the situation in other host cells, *Francisella*infected DCs are not sufficiently stimulated, do not produce proinflammatory cytokines and do not undergo the classical process of maturation (6). Consequently, these DCs have only a limited capacity to prime the adaptive response and they serve rather as migrating bacterial reservoirs. The weak immunostimulatory phenotype of infected DCs correlates with *Francisella* tendency to evade the host proinflammatory signaling. *Francisella*-mediated activation of nuclear factor -light-chain-enhancer of activated B cells (NF-B) is dependent on toll-like receptor 2 (TLR2)/myeloid differentiation primary response protein 88 (MyD88) stimulation (7). However, the bacterium can reduce the NF-B-driven gene expression either through the modulation of phosphoinositide 3-kinase (PI3K)/Akt pathway or by the rapid escape from the phagosome (7, 8). In cytosol, the sensing of *Francisella* DNA triggers stimulator of interferon genes (STING)-dependent type I interferon (IFN) response which helps to orchestrate the inflammasome assembly and caspase 1 activation (9, 10). Nevertheless, although virulent *Francisella* stimulates in DCs the expression of IFN-, the pyroptosis is suppressed (11). *Francisella* manipulation of DC response therefore evolves in time and follows the bacterial needs. From this perspective, the early *Francisella*-DC interactions represent the crucial phase which directs the future events of DC activation and potentially shapes the adaptive immune response.

To better understand these early processes, we analyzed the cell signaling dynamics of primary DC during the first hour of *Francisella* infection by SILAC (stable isotope labeling by amino acids in cell culture) based phosphoproteomic approach. Our results reveal the existence of distinct phases of protein phosphorylation in infected DCs. Although the initial stage seems to relate to the general process of the bacterial entry, the induction of extracellular signal-regulated kinase (ERK) and p38 signaling during the later phase is regulated differently by the used virulent and attenuated *Francisella* strains.

EXPERIMENTAL PROCEDURES

Cultivation of Bacteria—All *Francisella tularensis* strains were cultured on McLeod agar enriched for bovine hemoglobin and IsoVitalex (both Becton Dickinson, Franklin Lakes, NJ) at 37 °C.

Generation/SILAC Labeling of Bone Marrow-Derived DCs (BMDCs) and J774.2 Cultivation—BMDCs were generated from bone marrow progenitors isolated from femurs and tibias of 6- to 8-week-old female C57BL/6 mice. Approximately 1 10^7 bone marrow cells were seeded on 10 cm tissue plastic Petri dish into 10 ml of RPMI 1640 media containing 10% (v/v) fetal bovine serum (FBS; Sigma Aldrich, St. Louis, MO) and penicillin/streptomycin and these were left at 37 °C in a humidified atmosphere of 5% CO_2. After overnight depletion of adherent cells, suspension cells were seeded on a new dish in RPMI 1640, 10% FBS, and 5% (v/v) supernatant from Ag8653 cells transfected by cDNA of murine granulocyte-macrophage colonystimulating factor (GM-CSF). Cells were passaged every 2–3 days. Suspension cells were harvested on the day 9 of cultivation. SILAC labeling of BMDCs was performed as previously described (12). All experiments using mice were performed in accordance with guidelines of the Animal Care and Use Ethical Committee of the Faculty of Military Heath Sciences, University of Defense, Czech Republic (project no. 50–6/2016–684800). The murine macrophage-like cell line J774.2 was obtained from the European Collection of Cell Culture (EACC, ref No. 85011428). J774.2 were cultured in high glucose DMEM containing 10% (v/v) FBS (Sigma Aldrich) and kept at 37 °C in a humidified atmosphere of 5% CO_2. Cells were passaged every 2–3 days.

Infections and Treatments—Unless otherwise noted, all infection experiments were performed as described: harvested BMDCs were seeded into fresh RPMI 1640 medium containing 10% FBS (or SILAC medium with 10% dialyzed FBS in the case of proteomics experiments) at 2.5 10^6 cells/ml. Infection was initiated by the addition of bacteria suspended in the medium of the same composition followed by thorough mixing. Multiplicity of infection (MOI) was 50. Infected cells were kept at 37 °C/5% CO_2 and the infection was stopped by the addition of excess of ice-cold PBS followed by centrifugation of suspension at 4 °C. For 24 h infection intervals, BMDCs were seeded at 2 10^6 cells/ml and MOI was 10. Cells treated by *E. coli* 055:B5 lipopolysaccharide (LPS; 500 ng/ml) were used as a positive control. In experiments with killed *Francisella*, bacteria were first fixed by 3.7% (w/v) paraformaldehyde (PFA) at 4 °C overnight and then used as an infection agent at apparent MOI 100. For synchronization of BMDC infection, bacterial suspension was mixed with the suspension of 7.5 10^6 cells (MOI 50) in flat-bottom falcon tube and immediately copelleted in centrifuge (400 *g*, 5 min, RT). Following the centrifugation (*t* 0), cells were kept at 37 °C/5% CO_2 for the indicated time p.i. Mock-infected BMDCs were centrifuged without bacteria. When indicated, seeded BMDCs were pretreated either by DMSO or by bafilomycin A1 or SB203580 (both Sigma Aldrich) for 1 h at final concentrations of 100 nM or 10 M, respectively, followed by the addition of bacteria. DMSO/inhibitors were present in the medium throughout the infection. Adherent J774.2 cells were infected in 6-well plates (1 10^6 cells/well) by cocentrifugation (400 *g*, 5 min, RT) with bacteria (MOI 50) and left for 60 min at 37 °C/5% CO_2.

Cell Lysis and Protein Digestion—BMDC pellets were lysed by sodium deoxycholate (SDC)-containing buffer as previously described (13). Protein concentrations were measured using the Micro BCA kit (Thermo Pierce, Waltham, MA) and the corresponding light and heavy isotope-labeled lysates were mixed in a 1:1 ratio based on protein content. Proteins were reduced by the addition of DTT (final concentration 10 mM) for 1 h at 37 °C, followed by the alkylation with iodoacetamide (IAA; final concentration 20 mM) for 30 min at room temperature in the dark. The excess of IAA was quenched by the addition of DTT to a final concentration of 20 mM and the reaction was left to proceed for 15 min at room temperature. Proteins were digested by trypsin (Promega, Madison, WI) at a ratio 50:1 (w/w) at 37 °C

NF-B, nuclear factor -light-chain-enhancer of activated B cells; p70S6K, p70 ribosomal S6 kinase; PAK, p21activated kinase; PI3K, phosphoinositide 3-kinase; RSK, p90 ribosomal protein S6 kinase; SILAC, stable isotope labeling by amino acids in cell culture; TLR, toll-like receptor.

overnight. Digestion was stopped by the addition of TFA to a final concentration of 1% (v/v) to precipitate SDC. Suspension was then mixed with an equal volume of ethyl acetate, vortexed and centrifuged. Upper organic phase was removed and the extraction process was repeated four times to completely extract SDC (14). Water phase containing peptides was then desalted on Discovery DSC-18 SPE cartridges (500 mg/3 ml; Sigma Aldrich) and the eluate in 80% ACN/0.1% TFA was vacuum-dried.

HPLC Fractionation—Fractionation of peptides was performed using Alliance 2695 liquid chromatograph (Waters, Milford, MA). For phosphoproteome analysis, BMDC digests were fractionated by hydrophilic interaction chromatography (HILIC) (15). Peptide material of 3 to 5 mg was injected onto TSKgel Amide-80 HR column (5 m, 4.6 250 mm) with guard column (5 m, 4.6 10 mm; both Tosoh Bioscience, Tokyo, Japan) under conditions of 20% mobile phase A (2% ACN/0.1% TFA) and 80% mobile phase B (98% ACN/0.1% TFA) at flow rate of 0.5 ml/min. Peptide separation was performed by a linear gradient formed by mobile phase A and mobile phase B, from 80 to 60% of mobile phase B in 40 min and from 60 to 0% of mobile phase B in 5 min. Through the gradient elution window, 20 fractions were manually collected into microcentrifuge tubes. For analysis of BMDC proteome at 60 min p.i., 200–300 g of peptides were fractionated by high-pH reversed phase liquid chromatography as previously described (16) and 10 fractions were manually collected through the gradient elution window. Prior LC-MS analysis, fractions 1 and 2 were pooled with fractions 9 and 10, respectively.

Phosphopeptide Enrichment—Collected HILIC fractions were first acidified by 2% (v/v) TFA solution containing 100 mM glutamic acid as an excluder, followed by the addition of 1.5–2.5 mg of TiO_2 particles (10 m, GL Sciences, Tokyo, Japan). Suspensions were then vor-

texed for 20 min at room temperature and centrifuged. Pellets of TiO_2 were sequentially washed in buffers A (65% ACN/2% TFA/100 mM glutamic acid), B (65% ACN/0.5% TFA), and C (65% ACN/0.1% TFA). TiO_2-bonded phosphopeptides were eluted by vortexing particles for 10 min at room temperature in ammonia solution (pH 11) followed by the acidification of supernatants by TFA to reach pH 2. Each HILIC fraction was subjected to two identical cycles of the enrichment and TiO_2-eluates from the same fraction were pooled, desalted on 3M Empore SPE cartridges (Sigma Aldrich) and the eluates in 65% MeOH/0.1% TFA were vacuum-dried.

Liquid Chromatography-Mass Spectrometry—The Ultimate 3000 RSLCnano system connected through Nanospray Flex ion source with Q Exactive mass spectrometer (Thermo Scientific, Waltham, MA) were used for instrumental analysis (17). For phosphoproteome analysis, approximately one third of sample material from each phosphopeptide fraction was introduced onto trap column (PepMap100 C18, 3 m, 0.075 20 mm) and then separated by running a linear gradient (0.1% FA in water as phase A; 80% ACN, 20% water and 0.1% FA as phase B) from 4 to 34% B in 48 min and from 34 to 55% B in 10 min, at a flow rate of 300 nl/min, on analytical column (PepMap C18, 2 m, 0.075 150 mm). The full MS/Top10 setup was used for mass spectra acquisition. The positive ion MS spectra from 350–1750 *m*/*z* range were obtained in the Orbitrap at a resolution of 70,000 (at *m*/*z* 200). Multiply charged precursors ions with minimal threshold intensity of 5 10^4 counts and not fragmented during previous 30 s were admitted for higher energy collisional dissociation (HCD). Tandem mass spectra were acquired with following settings; resolution at 17,500, AGC target value at 1 10^5, maximum ion injection time at 100 ms, and normalized collision energy set to 27. Data acquisition was under control of Xcalibur software v3.0. Proteome samples fractions were analyzed by the same instrumentation using a linear gradient from 4 to 30% B in 88 min and from 30 to 55% B in 25 min for separation. Mass spectrometer operated in Top12 setup and collected MS spectra were in range of 350–1650 m/z. Intensity threshold for triggering MS/MS was 6 10^4 counts. The rest of instrumental parameters were identical to those of phosphoproteome analysis.

Phosphosite and Protein Identification and Quantification—Phosphoproteome and proteome data sets were processed by MaxQuant ver. 1.5.2.8 coupled with Andromeda search engine (18). Data were searched against FASTA database consisting of reference proteome for *Mus musculus* (UP000000589; June 16, 2015; 53,245 sequences) and Swiss-Prot TrEMBL database entry for *Francisella tularensis* subsp. *holartica* FSC200 strain (January 27, 2015; 1424 sequences), both downloaded from Uniprot site. MaxQuant-implemented database was used for the identification of contaminants. False discovery rate (FDR) estimation of peptide identification was based on targetdecoy approach using reverted search database as a decoy. Phosphosite identification and quantification was performed using these MaxQuant parameters: mass tolerance for the first search 20 ppm, for the second search from recalibrated spectra 4.5 ppm (with individual mass error filtering enabled); maximum of 2 missed cleavages; maximal charge per peptide z 7; minimal length of peptide 7 amino acids, maximal mass of peptide 4600 Da; carbamidomethylation (C) as fixed and phosphorylation (STY), oxidation (M) and acetylation (protein N-term) as variable modifications with the maximum number of variable modifications per peptide set to 5. Trypsin with no cleavage restriction was set as a protease. Mass tolerance for fragments in MS/MS was 20 ppm, taking the 12 most intensive peaks per 100 Da for search (with enabled possibility of cofragmented peptide identification). Minimal Andromeda score for modified peptides was 40 and minimal delta score for modified peptides was 6. FDR filtering on peptide spectrum match was 0.01 with separate FDR filtering for each modification set to 0.01. For peptide quantitation, Arg6 [$^{13}C_6$] and Lys6 [$^{13}C_6$] were set as labels in heavy channel (or in light channel for label-swap experiments to obtain inverted H/L ratios) with requantify function enabled. Ratios for individual phosphosites were derived from normalized ratios of the least modified phosphopeptides in a given replicate. MaxQuant parameters for processing of proteome data were identical except for only oxidation (M) and acetylation (protein N-term) were allowed as variable modifications. For protein quantitation, only protein groups with at least one unique or razor peptide having SILAC ratio and only those protein groups passing protein FDR filtering set to 0.01 were considered (18). All hits identified in searches as contaminants were filtered out.

Experimental Design and Statistical Rationale—SILAC experiments were performed in biological triplicate for each time point and bacterial strain used and the respective mock-treated BMDCs served as a control. In two replicates, light BMDCs were infected and heavy cells were mock-treated. In one replicate, SILAC groups were swapped (supplemental Fig. S1). In total, 18 digests (three time points/two bacterial strains/triplicate) were fractionated by HILIC. Aliquots of 6 digests (60 min p.i./two bacterial strains/triplicate) were also subjected to proteome analysis. Significantly regulated phosphosites for each triplicate (time point/bacterial strain) were found by global mean rank test (GMRT) (19) using R package MeanRankTest (https://www.evotec.com/MeanRankTest) with parametric FDR level set to 0.05. Only those phosphosites quantified in all three replicates of the given experimental condition were allowed for testing. With respect to the obtained phosphoproteomic data, GMRT was chosen for two reasons: (1) rank tests in general are advantageous for global methods when fold changes are relatively low (20) and (2) GMRT was shown to reliably control FDR even for small number of replicates (19).

Phosphosite Fuzzy c-means Clustering—Fuzzy *c*-means clustering (21) of phosphosites with localization probability 0.75 (22, 23), which were quantified in all three time points for WT-infected BMDC samples with the relative standard deviation (RSD) 30%, was performed by *Mfuzz* R package (24). For a given phosphosite, normalized log_2ratios from replicates were first averaged and multiplied by 1 for each time point and then normalized by Z-score. Fuzzifier was set to 3.65 (25) and the number of clusters was 4. Human protein reference database (HPRD) (26) kinase motifs enriched in phosphosite clusters were found by Fisher exact test (Benjamini-Hochberg (BH) FDR level set to 0.05) using Perseus software ver. 1.5.4.1 (27).

InnateDB Terms Enrichment and the Construction of Protein-Protein Interaction Network—For the comparison of BMDC response induced by WT and *dsbA Francisella* strains, normalized log_2-ratios of phosphosites quantified in all three replicates of WT-infected BMDCs samples were tested by unpaired two sample Student's *t* test against those quantified in all three replicates of *dsbA*-infected BMDCs samples of the same time interval. Phosphosites (and corresponding phosphoproteins) having p 0.05 were further considered as differentially regulated between BMDCs infected by WT and *dsbA*. For InnateDB term analysis, phosphoproteins were first annotated by Pathway analysis web-based tool from InnateDB database (http://www.innatedb.com/) (28) and Fisher exact test was then used to find enriched InnateDB Pathway name terms in the group of differentially regulated phosphosites (BH FDR level set to 0.05). Only terms containing at least 3 regulated phosphosites are reported. In case in which the same group of phosphosites was annotated by several similar enriched InnateDB terms, one representative term was selected. Using the described approach, none InnateDB terms were found enriched for 10 and 30 min p.i. For the construction of proteinprotein interaction network, only proteins bearing phosphosites differentially regulated between WT- and *dsbA*-infected

BMDCs at 60 min p.i. were considered. Sequences were mapped to murine protein sequences on STRING (v10) (29) using BLAST to obtain database identifiers and best matches with at least 80% identity were used. STRING interaction network containing interactions with 700 score was then loaded into Cytoscape ver 3.2.1 and only differentially regulated phosphoproteins or proteins having at least two differentially regulated neighbors ("connecting" nodes) were kept. The emerging network was then reduced to contain smallest possible number of "connecting" nodes while keeping all regulated phosphoproteins in one network (*i.e.* removing "connecting" nodes with relatively low number of neighbors). In cases where it could not be decided, all equivalent nodes were kept.

Immunofluorescence Microscopy—Bacteria were incubated for 1 h with 5 μM 5-(and 6)-carboxyfluorescein diacetate succinimidyl ester (CFDA-SE) prior the infection. BMDCs were then infected as described under Experimental Procedures, transferred to glass slide using cytospin and fixed by 3.7% PFA. The excess of PFA was quenched by 50 mM NH_4Cl and cells were permeabilized by 50 g/ml digitonin for 1 min. BMDCs were then stained for 20 min by Alexa Fluor 594 Phalloidin (6.6 μM) and for 5 min by 4 ,6-diamidino-2phenylindole (DAPI, 300 nM) and mounted by Mowiol. Microscope slides were viewed by fluorescence microscopy on Nikon Eclipse Ti (Nikon, Tokyo, Japan). Percentage of infected cells was calculated as an average of 500 cross-sectional images per time point.

Transmission Electron Microscopy—Infected or uninfected cells were quickly washed with Sörensen buffer (0.1 M sodium/potassium phosphate buffer, pH 7.3; SB) at 37 °C, fixed with 2.5% glutaraldehyde in SB for 2 h, washed with SB, embedded in blocks of 1% low-melting point agarose (type VII, Sigma Aldrich), and postfixed with 1% OsO_4 solution in SB for 2 h. The cells were dehydrated in series of ethanol with increasing concentration, subsequently in propyleneoxide, and embedded in Epon-Durcupan resin. Polymerized blocks were cut into 80 nm ultrathin sections, collected on 200 mesh size copper grids, and stained with saturated aqueous solution of uranyl acetate for 4 min. The sections were examined in FEI Morgagni 268 transmission electron microscope operated at 80 kV. The images were captured using Mega View III CCD camera (Olympus Soft Imaging Solutions, Münster, Germany).

Flow Cytometry—Following 24 h of infection, suspension BMDCs were harvested and stained by following antibodies: anti-CD11cphycoerythrin (PE)-Cy7 (BD Pharmingen, San Jose, CA), antiCD80-PE (Beckman Coulter, Brea, CA), anti-CD86-PE (Beckman Coulter), and anti-I-A/I-E major histocompatibility complex II (MHC II) conjugated with biotin (Novus Biologicals, Littleton, CO), respectively. Anti-MHC II antibodies were then stained by streptavidin-FITC (Invitrogen, Carlsbad, CA). Cells were fixed and before analysis on CyAn ADP flow cytometer (Beckman Coulter) stained by propidium iodide. Data acquisition and interpretation were performed using Summit 4.3 software (Beckman Coulter).

ELISA—Quantification of cytokines in cell culture supernatants was performed using DuoSet ELISA kits (R&D Systems, Minneapolis, MN) according to manufacturer instructions.

Quantitative Real-time PCR—RNA was isolated from cells using RNeasy kit from Qiagen. 1 g of total RNA was reverse transcribed using oligo (dT) primers (New England Biolabs, Ipswich, MA). Quantitative real-time PCR analysis was performed and analyzed using ABI Prism 7500 Fast RT-PCR System (Applied Biosystems, Foster City, CA). Data were normalized to the housekeeping gene 18S rRNA (*Rn18S1*) and expressed as fold change relative to RNA samples from mock-treated cells using the comparative Ct method (Ct). The following TaqMan Gene Expression Assays were used (Applied Biosystems): *Il10* (Mm01288386_m1), *Il12b* (Mm01288989_m1), *Ifnb1* (Mm00439552_s1), and *Rn18S1* (Mm03928990_g1).

Western Blot—Cell pellets were lysed in RIPA buffer containing protease (Roche, Basel, Switzerland) and phosphatase (cocktail set II, Merck, Darmstadt, Germany) inhibitors. Denatured and reduced proteins were separated by SDS-PAGE and transferred to PVDF membranes. Blots were blocked by milk and incubated with primary antibody overnight followed by secondary antibody conjugated with horseradish peroxidase (Dako, Glostrup, Denmark). Bands were visualized by ECL (Amersham Biosciences, Little Chalfont, United Kingdom). Anti-actin and anti-tubulin antibodies were purchased from Sigma Aldrich and Abcam (Cambridge, United Kingdom), respectively. The rest of primary antibodies were obtained from Cell Signaling (Danvers, MA).

RESULTS

Francisella Induces Two Waves of Protein Phosphorylation in BMDCs During the First Hour of Infection—SILAC-labeled primary murine bone marrow-derived DCs (BMDCs) (12) were infected by fully virulent *Francisella tularensis* subsp. *holarctica* FSC200 strain (WT) in suspension without the synchronization by centrifugation to avoid TLR2-MyD88-dependent NF-B activation caused by a mechanical force (30). BMDCs were lysed at 10, 30, and 60 min p.i. and the lysates were processed and analyzed as described under Experimental Procedures (supplemental Fig. S1). In total, 17,535 phosphosites from *Francisella*-infected BMDC proteome were identified. From these, more than 5000 were quantified in all replicates of each experimental condition (time/bacterial strain; supplemental Fig. S2 and supplemental Table S1). In general, *Francisella*-induced phosphorylation events in BMDCs were most apparent at 10 min p.i. (Fig. 1*A*). Consistently, the highest number of phosphosites was classified as significantly regulated at 10 min p.i. (Fig. 1*B* and supplemental Fig. S3). Surprisingly, following the drop at 30 min p.i., there was a new increase in BMDC protein phosphorylation at 60 min p.i. This observation was not caused artificially by the variability of data. Phosphoproteome samples were grouped together according to the time p.i. in PCA (supplemental Fig. S4*A*). Although the relatively small phosphorylation changes and suboptimal SILAC labeling efficiency of primary BMDCs (12) led to the low correlation of label swap replicates, there was no difference between 30 and 60 min p.i. data sets in terms of the distribution of RSDs for phosphosites SILAC ratios (supplemental Fig. S4*B*). The increase in BMDC signaling at 60 min p.i. was also not affected by the changes in protein expression or degradation (supplemental Fig. S5). To further analyze phosphorylation dynamics in infected BMDCs, fuzzy *c*-means clustering was used to group reproducibly quantified phosphosites according to their time profiles (Fig. 1*C* and 1*D*). In line with results shown in Fig. 1*B*, cluster peaking at 10 min p.i. (cluster A) contained the highest number of phosphosites (Fig. 1*C*). To identify potentially involved kinases, clustered phosphosites were searched for Human Protein Reference

Database (HPRD) kinase motifs (Table I). Activities of several kinases seemed to follow the profile of the largest phosphosite cluster A; *e.g.* p70 ribosomal S6 kinase (p70S6K), Akt or p21-activated kinase 2 (PAK2) (Table I). Importantly, activities of these kinases were confirmed by Western blot (Fig. 1*E*). The large part of phosphoproteins regulated at 10 min p.i. was functionally linked to regulation of cytoskeleton and vesicular transport (supplemental Table S1). Among them, GTPaseactivating proteins (GAPs) and guanine nucleotide exchange

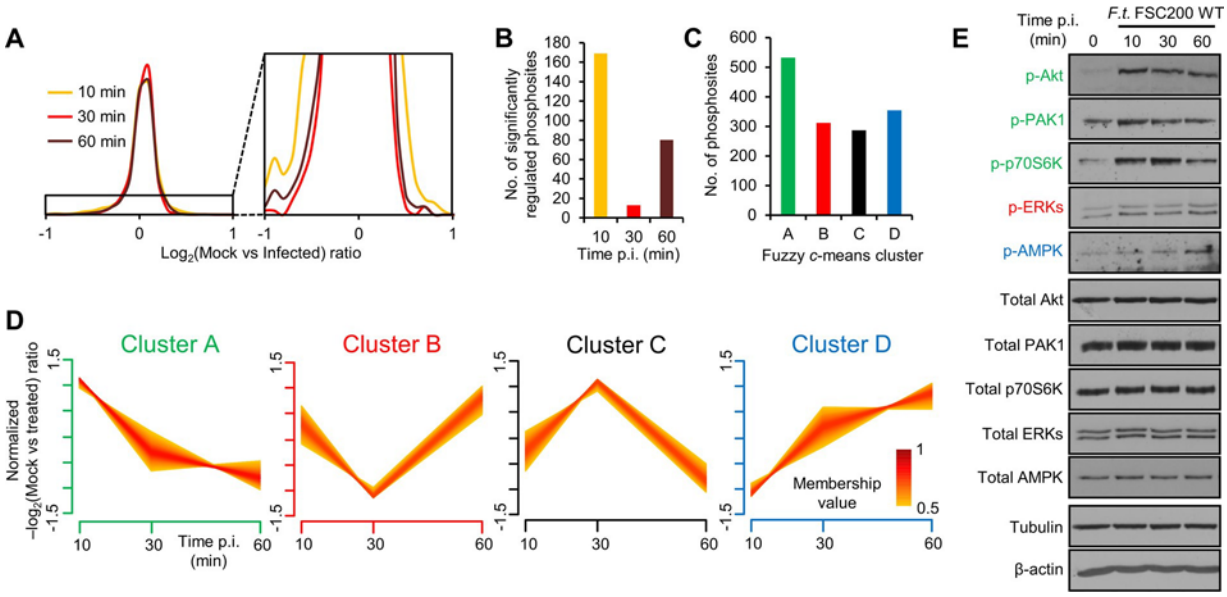

FIG. 1. **Protein phosphorylation induced in BMDCs during the first hour of infection by *Francisella tularensis* subsp. *holarctica* FSC200 (WT) strain.** SILAC-labeled BMDCs were infected with WT (MOI 50) for 10, 30, or 60 min (supplemental Fig. S1) and processed as described under Experimental Procedures. *A*, Histograms of normalized SILAC log_2-ratios (Mock/WT) of phosphosites from infected BMDCs. Data collected from means of three biological replicates with RSD 30%. *B*, Count of significantly regulated phosphosites per given time p.i. (Global Mean Rank Test, FDR 0.05). *C*, Count of phosphosites which were assigned to fuzzy *c*-means clusters. *D*, Fuzzy *c*-means clustered phosphosites from infected BMDCs. *E*, Western blot analysis of selected kinases. Data are representative from biological duplicate.

TABLE I

HPRD motifs enriched in phosphosite clusters from Fig. 1D. Motifs were found by Fisher exact test (BH FDR 0.05). Only those with enrichment factor 1.2 are presented. None motif was found for cluster C

Cluster	HPRD motif	Enrichment factor	FDR
A	p70 Ribosomal S6 kinase	2.33	$3.02 10^{7}$
	Aurora-A kinase	1.97	$6.82 10^{4}$
	Phosphorylase kinase	1.64	$1.50 10^{5}$
	Akt kinase	1.57	$3.82 10^{4}$
	MAPKAPK1 kinase	1.55	$2.39 10^{4}$
	PAK2 kinase	1.53	$2.65 10^{3}$
	PKC epsilon kinase	1.46	$6.21 10^{3}$
	MAPKAPK2 kinase	1.30	$7.85 10^{3}$
	14–3-3 domain binding motif	1.27	$2.05 10^{4}$
	Calmodulin-dependent protein kinase II	1.21	$1.30 10^{3}$
B	Growth associated histone HI kinase	1.48	$2.38 10^{3}$
	ERK1,2 kinase	1.26	$7.96 10^{5}$
	WW domain binding motif	1.21	$3.31 10^{4}$
	GSK-3, ERK1, ERK2, CDK5	1.21	$3.68 10^{4}$
D	Calmodulin-dependent protein kinase I	2.10	$1.14 10^{2}$
	AMP-activated protein kinase	1.70	$1.49 10^{2}$

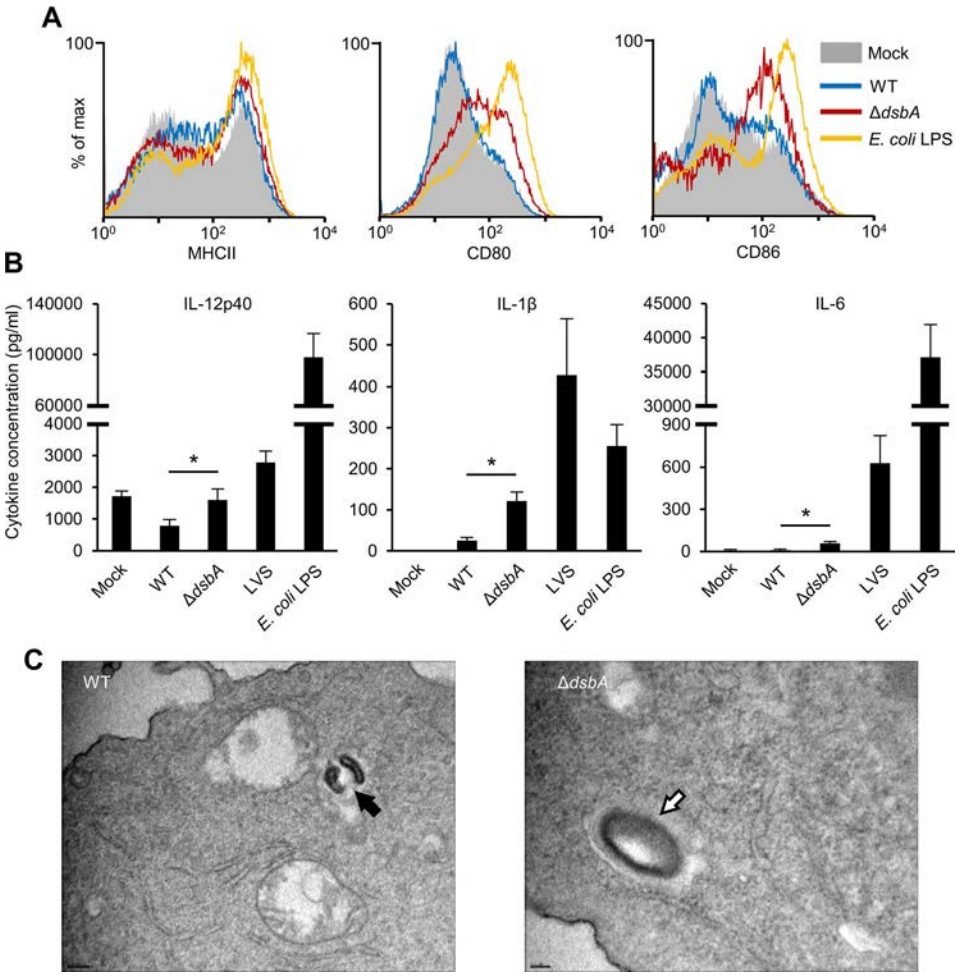

FIG. 2. ***Francisella dsbA* mutant stimulates *in vitro* BMDC activation and maturation.** BMDCs were infected by FSC200 WT, FSC200 *dsbA* or LVS at MOI 10 or treated by *E. coli* LPS (500 ng/ml) and left for 24 h. *A*, Flow cytometric analysis of cell surface expression of MHC II, CD80 and CD86. Histograms are representative from biological triplicate. *B*, Concentrations of IL-12p40, IL-1 and IL-6 in culture supernatants were determined by ELISA. Data are presented as means S.E. of independent replicates; *n* 3; **p* 0.05 (Student's *t* test). *C*, Electron micrographs of BMDCs infected by WT and *dsbA* at 60 min p.i. (MOI 50). Black arrow shows free bacteria in the cytosol. White arrow indicates the damaged phagosomal membrane. Lengths of scale bars are 0.2 m and 0.1 m for micrographs showing WT and *dsbA*, respectively. Data are representative from biological triplicate.

factors (GEFs) of Rac and Cdc42 GTPases (*e.g.* Arhgaps, Arhgefs or Docks) represented the most notable examples. GEFs activate Rac/Cdc42 and promote their binding to PAKs, which in turn stimulates PAK autophosphorylation and activation. Such autophosphorylation of PAK1 (S204) and PAK2 (S55 and S197) was indeed detected at 10 min p.i., therefore indirectly confirming previous kinase motif analysis (Fig. 1*D*, 1*E* and Table I) and supporting the active role of Rho GTPasePAK signaling in *Francisella* internalization. In contrast to 10 min p.i., only few potential kinases could be associated with the second signaling maximum occurring 60 min p.i. (clusters B and D in Fig. 1*D* and Table I, respectively). Although the activity of AMP-activated protein kinase (AMPK) gradually increased and peaked at 60 min p.i. (cluster D in Fig. 1*D* and Fig. 1*E*), ERKs displayed more complex behavior as their kinase motif was enriched in phosphosite cluster displaying maxima at 10 and 60 min p.i. (cluster B in Fig. 1*D*).

Francisella Mutant Lacking dsbA Gene May Serve As An Avirulent Control to WT Strain in BMDCs—The identification of DC signaling pathways regulated in response to *Francisella* virulent behavior could be facilitated by the confrontation of results with experiments in which attenuated strain was used as a control. *Francisella* strains lacking *dsbA* gene (*dsbA*) are attenuated *in vivo* and provide the protection against subsequent challenge by parental strain (31–33). The engagement of adaptive immunity suggests that *dsbA* would represent suitable alternative to WT in terms of DC response. To assess *in vitro* ability of *dsbA* to induce

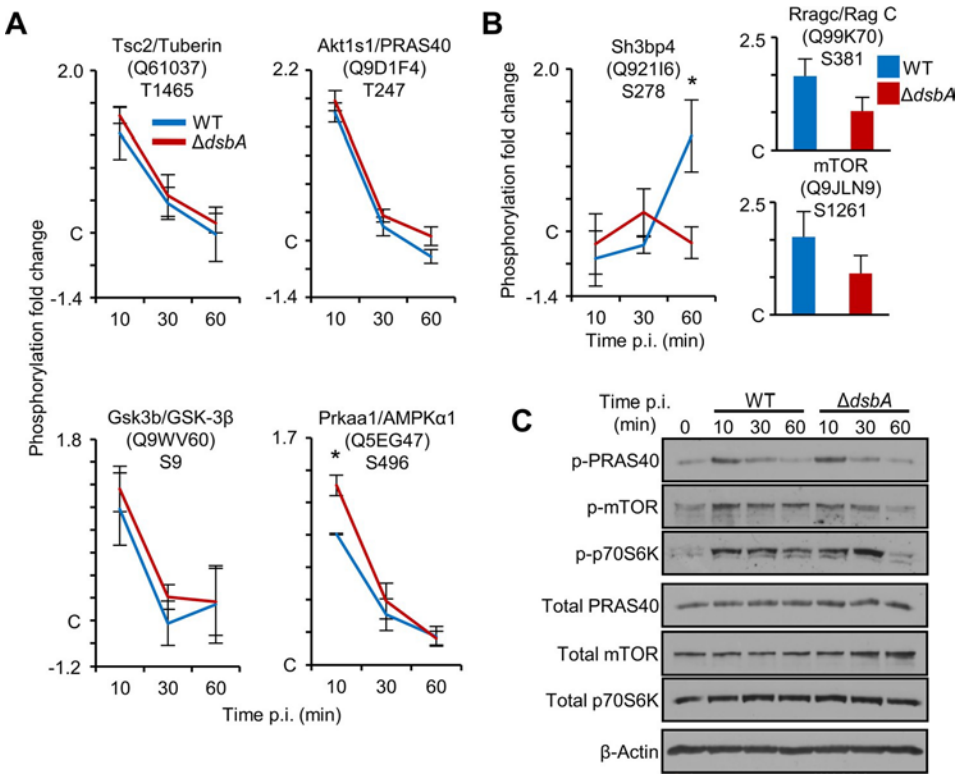

FIG. 3. **BMDCs infected by WT maintain mTOR/p70S6K signaling at 60 min p.i.** *A*, Time-dependent changes in phosphorylation of known Akt targets in WT- and *dsbA*-infected BMDCs. *B*, Time-dependent site phosphorylation in proteins connected to mTOR localization to lysosome - all sites were significantly upregulated at 60 min p.i. only in WT-infected BMDCs (Global Mean Rank Test, FDR 0.05). Bar graphs show the situation at 60 min p.i. for sites quantified only at this time point. Headings of graphs in (*A*) and (*B*) contain gene name/protein name, Uniprot accession number and phosphosite position. SILAC-based phosphorylation changes are expressed as a mean S.E. (n 3) of normalized fold change (FC, infected/mock) at respective time p.i.; $^*p$ 0.05 (Student's t test applied on normalized SILAC $\log_2$-ratios). In graphs, "C" designates no change (FC 1) and up- and downregulated phosphosites are represented by positive and negative FC values, respectively. *C*, Western blot analysis of phosphosites connected to mTOR activity in infected BMDCs. Data are representative from biological duplicate.

BMDC maturation, cells were infected by FSC200 WT and *dsbA* mutant of the same background and surface expression of MHC II, CD80 and CD86 was measured 24 h p.i. by flow cytometry (Fig. 2*A*). For all presented maturation markers, *dsbA*-infected BMDCs showed higher expressions than cells infected by WT. Similarly, *in vitro* secretion of proinflammatory cytokines IL-12p40, IL-1, and IL-6 was higher in BMDCs infected by *dsbA* at 24 h p.i. (Fig. 2*B*). The observed differences between strains were not skewed by BMDC cell death (supplemental Fig. S6*A*). Note however, that both WT and *dsbA* strains were relatively poor inducers of BMDC cytokine secretion compared with *Francisella* Live Vaccine Strain (LVS; Fig. 2*B*). Moreover, the viability of cells in general (supplemental Fig. S6*A*) might further affect the cytokine production because the levels of IL-12p40 secreted by *dsbA*-infected BMDCs did not exceed those of uninfected cells and the production in WT-infected BMDCs was even lower (Fig. 2*B*). Consistently, the levels of IL-12p70 and IL-23 secreted by BMDCs infected with either WT or *dsbA* were below the level of detection. To explore the intracellular fate of bacterial strains, WT- and *dsbA*-infected BMDCs were subjected to transmission electron microscopy at 60 min p.i. Similarly to what was previously reported (34), WT bacteria were located primarily in the cytosol at this time p.i. (Fig. 2*C*). In contrast, the majority of *dsbA* bacteria (60%) were surrounded by the damaged vacuolar membrane (Fig. 2*C*) which suggested the intracellular trafficking of *dsbA* in BMDCs differed from that of virulent strain. Importantly, although the unsynchronized infection reduced BMDC infectivity, the dynamics of WT and *dsbA* host entry did not differ significantly (supplemental Fig. S6*B*). Taken together, the results confirmed the attenuated nature of *dsbA* in BMDCs *in vitro* and encouraged its use as an avirulent control for phosphoproteomics experiments where WT was an infection agent (supplemental Fig. S1).

Signaling of mTOR/p70S6K is Sustained 60 min p.i. in WTinfected BMDCs—BMDCs infected by *dsbA* mutant were processed and analyzed for phosphoproteome changes exactly as for WT-treated cells. Dominant feature of WT-infected BMDCs was an early Akt activation (see above) (8). To examine whether WT and *dsbA* mutant differed in their ability to trigger Akt signaling, time profiles of several identified Akt targets phosphorylated in both WT- and *dsbA*-infected BMDCs at 10 min p.i. were compared (Fig. 3*A*,

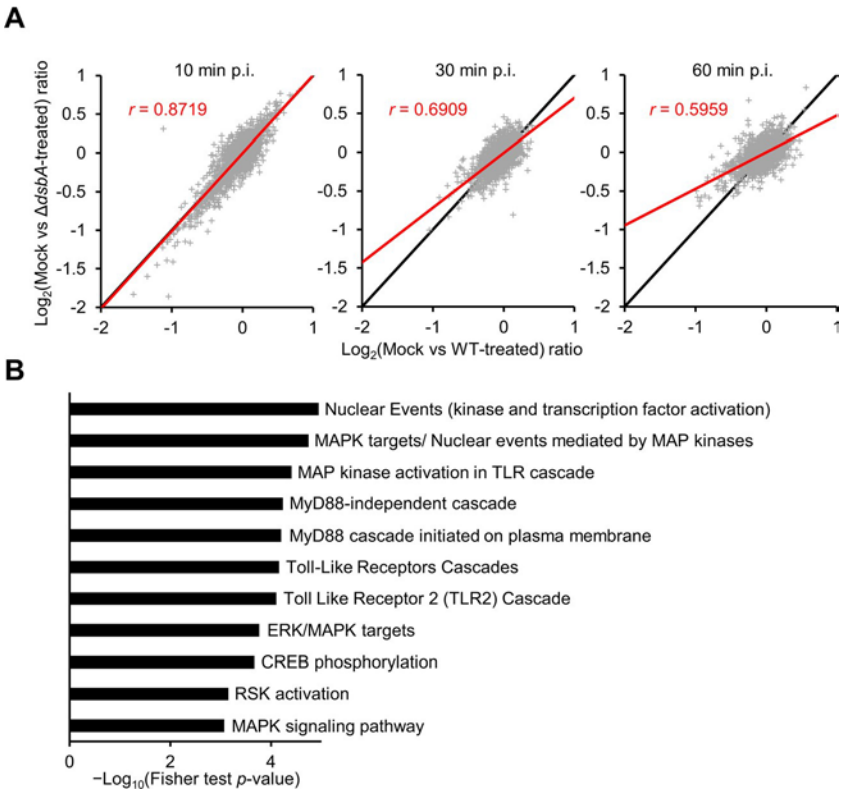

FIG. 4. **Signaling in BMDCs infected by WT and *dsbA* starts to diverge at 60 min p.i.** *A*, Means of normalized $\log_2$-ratios of phosphosites quantified in all three biological replicates of SILAC experiment with RSD 30% per given time p.i. in WT-infected BMDCs were correlated with the corresponding values of the same site in *dsbA*-infected cells. Black line represents *x y* function, red line shows the actual correlation with Pearson coefficient (*r*) for the given time p.i. *B*, Innate DB terms enriched in the group of proteins differentially phosphorylated in WT- and *dsbA*-infected BMDCs at 60 min p.i. (Fisher exact test; BH FDR 0.05). Only those terms containing at least 3 differentially regulated phosphosites are presented.

supplemental Table S1). Phosphorylation trends of Tuberin (Tsc2; T1465), proline-rich AKT1 substrate 1 (PRAS40; T247), glycogen synthase kinase-3 (GSK-3; S9) or AMPK 1 (S496) followed the predicted Akt activity (cluster A in Fig. 1*D*) similarly in both WT- and *dsbA*-infected BMDCs. Importantly, these proteins are responsible for the suppression of mammalian target of rapamycin complex 1 (mTORC1) activity and Akt-mediated phosphorylation release mTORC1 from their inhibition (35– 38). This suggested that mTOR activity should follow that of Akt in both WT- and *dsbA*-infected BMDCs (Fig. 1*D*). However, several phosphosites associated with mTOR signaling were found to be upregulated at 60 min p.i. in BMDCs infected by WT (Fig. 3*B*, supplemental Table S1). Although phosphorylation of mTOR on S1261 was shown to be crucial for the induction of mTORC1 activity (39), functional roles of phosphosites S278 on SH3 domain-binding protein 4 (SH3BP4) and S381 on RagC are unknown. Interestingly, SH3BP4 negatively regulates mTORC1 activity on lysosome lumen through binding of Rag complex via SH3BP4 region containing S278 (40). Differential regulation of mTOR between WT- and *dsbA*-infected BMDCs at 60 min p.i. was confirmed by Western blot (Fig. 3*C*). Independently of the bacterial strain used, PRAS40 (T247) phosphorylation (compare with Fig. 3*A*) and mTOR/p70S6K signaling were induced 10 min p.i. However, mTOR/p70S6K crosstalk at 60 min p.i. was preserved only in WT-infected BMDCs. These results suggest that in contrast to BMDCs infected by *dsbA*, mTOR/p70S6K signaling is maintained in WT-infected BMDCs at 60 min p.i. and that this activity is Akt-independent.

Cell Signaling of BMDCs Infected by WT and dsbA Starts to Diverge at 60 min p.i.—Observed differences in mTOR activity prompted further inspection of phosphoproteomic data to search for system-wide variations in WT- and *dsbA*induced BMDC signaling. To determine correlations in phosphoproteomes, phosphosites quantified in the given time point p.i. in both WT- and *dsbA*-infected BMDCs were plotted against each other in scatter plots (Fig. 4*A*). Phosphorylation changes induced by WT and *dsbA* invasion at 10 min p.i. correlated well. However, WT-infected BMDCs showed more prominent protein phosphorylation with increasing time p.i. (Fig. 4*A*). This behavior affected also counts of regulated phosphosites (supplemental Fig. S3 and supplemental Table S1). Although at 10 min p.i. the numbers of significantly regulated phosphosites in BMDCs infected by WT and *dsbA* were comparable, almost three times more

phosphosites from WT-infected cells passed the significance test when compared with *dsbA* at 60 min p.i. (supplemental Fig. S3). Similarly, the numbers of phosphosites, which were considered as differentially regulated between WT- and *dsbA*infected BMDCs (see Experimental Procedures), were almost two times higher at 60 min p.i. (125 sites) than those at 10 or 30 min p.i. (70 and 56, respectively; supplemental Fig. S7). Interestingly, the weak correlation of strain-specific signaling temporally corresponded to the second wave of protein phosphorylation at 60 min p.i. in WT-infected BMDCs (Fig. 1*B*). BMDC signaling pathways engaged differentially by WT and *dsbA* at 60 min p.i. were found by InnateDB terms enrichment analysis (Fig. 4*B*). Taken together, WT and *dsbA* induce similar patterns of protein phosphorylation in BMDCs during the entry. BMDC cell signaling starts to diverge in later time points p.i. and this is largely because of activation of TLR- and mitogen-activated protein kinase (MAPK)-related pathways in WT-infected cells.

ERKs and p38 Modules are Major Components of WTinduced BMDC Signaling at 60 min p.i.—To explore phosphoproteins differentially regulated at 60 min p.i. to a greater depth, protein-protein interaction network was constructed (supplemental Fig. S8). The assembly of the network was subjected to two requirements: (1) the network should contain as many phosphoproteins differentially regulated in WT- and *dsbA*-infected BMDCs at 60 min p.i. as possible and (2) unidentified proteins should also be included to keep the network together (see Experimental Procedures). Notably, the center of the network was formed by a cluster of closely interacting nodes corresponding to MAPKs and MAPK-activated protein kinases (MAPKAPKs) (Fig. 5*A*). The kinetics of phosphorylation for sites with available quantitative data is shown in Fig. 5*B*. The phosphorylation profiles of ERK2 and p38 in their activation loops (Y185 and T180, respectively) suggested that these MAPKs are activated at 60 min p.i. only in WT-infected BMDCs. Interestingly, although the activation of p38 in WT-infected BMDCs peaked at 60 min p.i., the phosphorylation of ERK2 was upregulated also at 10 min p.i. in both WT- and *dsbA*-infected BMDCs. Of note, the time profile of ERK2-activation phosphosite in WT-infected BMDCs resembled the V-like shaped phosphosite cluster B (Fig. 1*D*) for which ERKs kinase motif was enriched (Table I). Although not passing the significance level for differential regulation in WT- and *dsbA*-infected BMDCs at 60 min p.i., phosphosite from the activation loop of ERK1 (Y205) followed the trend of ERK2 (Fig. 5*B*). These findings confirmed ERKs as participants in both waves of WT-induced signaling in BMDCs during the first hour of the infection. Differential regulation of ERKs and p38 in WT- and *dsbA*-infected BMDCs affected also the phosphorylation state of MAPKAPKs acting downstream (Fig. 5*B* and 5*C*). ERK-dependent phosphorylation of p90 ribosomal protein S6 kinases (RSKs) RSK1 and RSK2 (S352 and T365, respectively) plays a crucial role in their activation (41, 42). Similarly, p38-induced phosphorylation of MAP kinase-activated protein kinase 2 (MAPKAPK2 or MK2) site T320 is a

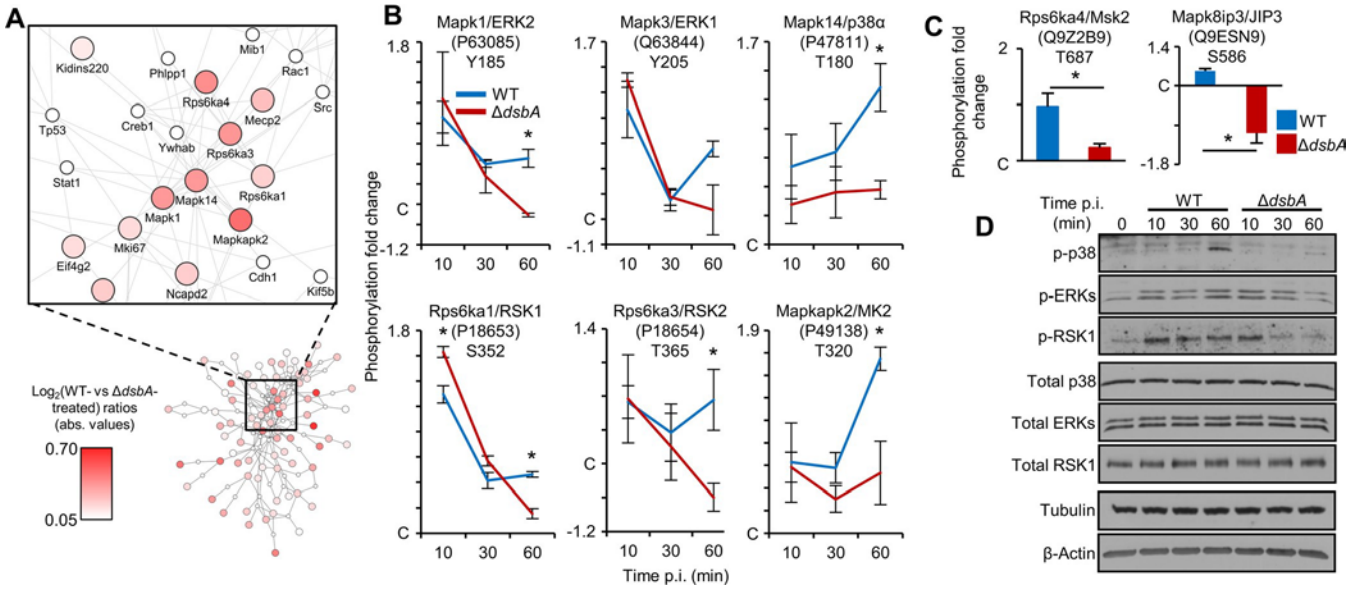

FIG. 5. **ERK and p38 modules are induced in WT-infected BMDCs at 60 min p.i.** *A*, Protein-protein interaction network constructed on STRING background containing 80 proteins differentially phosphorylated in WT- and *dsbA*-infected BMDCs at 60 min p.i. (large circles). Magnified part shows MAPK interaction cluster. The color of large circles corresponds to the absolute value of the difference between means of phosphosite normalized SILAC log_2-ratios in WT- and *dsbA*-infected BMDCs at 60 min p.i. The whole network is in supplemental Fig. S8. For details see Experimental procedures. *B*, Time-dependent and (*C*) 60 min p.i. changes in phosphorylation of MAPK-connected phosphosites in WT- and *dsbA*-infected BMDCs. See Fig. 3 legend for the description of the graphs. *D*, Western blot analysis of phosphosites connected to MAPKs activity in infected BMDCs. Data are representative from biological duplicate.

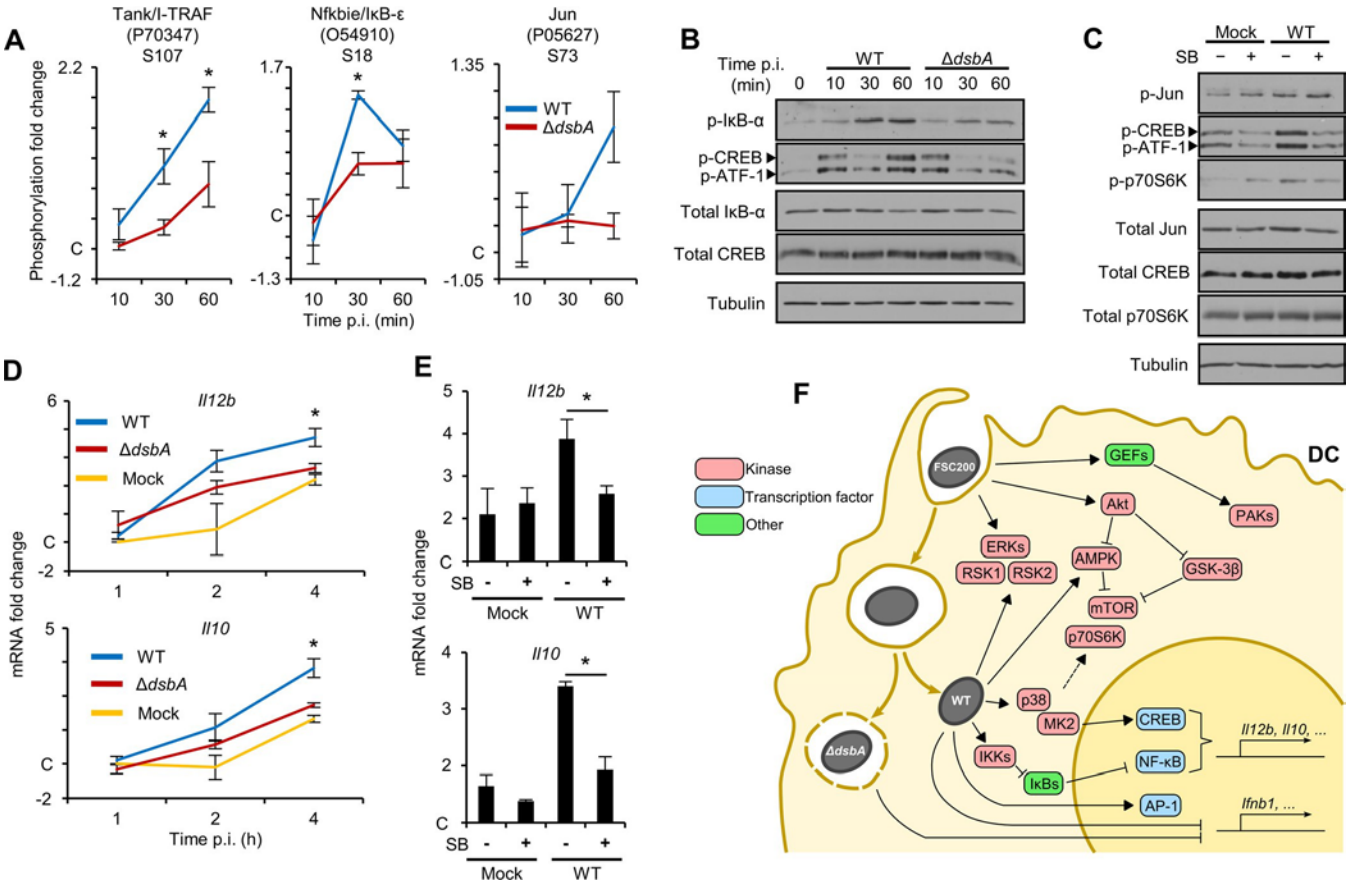

FIG. 6. **p38-regulates the gene expression in WT-infected BMDCs.** *A*, Time-dependent changes in phosphorylation of selected phosphosites in WT- and *dsbA*-infected BMDCs. *B*, Phosphorylation of IB- and CREB in WT- and *dsbA*-infected BMDCs (MOI 50) during the first hour of infection. *C*, Phosphorylation of Jun, CREB and p70S6K in WT-infected BMDCs at 60 min p.i. Cells were pretreated either by DMSO or p38-inhibitor SB203580 for 60 min before infection. *D*, Stable expression of *Il12b* and *Il10* mRNA in WT- and *dsbA*-infected BMDCs (MOI 50) and in mock-treated cells during 4 h p.i. *E*, Stable expression of *Il12b* and *Il10* mRNA at 2 h p.i. in WT-infected BMDCs. Cells were pretreated either by DMSO or p38-inhibitor SB203580 for 60 min before infection. F, A model of phosphorylation-mediated early DC signaling in response to infection by *Francisella tularensis* subsp. *holarctica* FSC200. For the description of graphs in (*A*), see Fig. 3 legend. The changes in mRNA transcription in (*D*) and (*E*) are expressed as a mean S.E. (*n* 3) FC (infected over mock left for 1 h); **p* 0.05 (Student's *t* test applied on Ct values from WT- and *dsbA*-infected BMDCs). In graphs, "C" designates no change (FC 1). Western blots are representative from biological duplicates.

part of MK2-activating cascade (43). Downstream of ERKs and p38 lies also mitogen- and stress-activated kinase 2 (Msk2) whose activity is positively regulated by phosphorylation of T687 (44). As expected, all these sites were significantly more phosphorylated in WT-infected BMDCs at 60 min p.i. (Fig. 5*B* and 5*C*). Importantly, phosphorylation kinetics paralleled the time profiles of phosphosites in activation loops of the respective upstream MAPK (Fig. 5*B*). Although there was no direct proof of c-Jun N-terminal kinases (JNKs) involvement in WT-induced BMDC signaling at 60 min p.i., the phosphorylation of JNK-interacting protein 3 (JIP3) (45) was differentially regulated in WT- and *dsbA*infected BMDCs at this time p.i. (Fig. 5*C*). To confirm SILACbased results, the activation states of ERKs, p38 and RSK1 were assessed by Western blot (Fig. 5*D*). In line with phosphoproteomics data, ERKs and RSK1 were activated in both WT- and *dsbA*-infected BMDCs at 10 min p.i. However, in contrast to WT-infected BMDCs, both kinases returned to their near-basal states in *dsbA*-infected cells at 60 min p.i. As expected, the induction of p38 at 60 min p.i. was observed only in BMDCs infected by WT strain (Fig. 5*D*). The described MAPK activation profiles were not biased by the efficiency or by the synchronization of the infection (supplemental Fig. S9). WT-specific induction of ERKs and p38 at 60 min p.i. raised a question whether the altered host signaling could be related to the increased presence of WT in the cytosol (Fig. 2*C*). Bafilomycin A1 treatment is employed to block *Francisella* phagosomal escape in host cells (46, 47). However, bafilomycin A1 alone was a potent inducer of p38 in BMDCs (supplemental Fig. S10*A*) which ruled out its use in this case. Nevertheless, BMDCs treated by escape-negative (47) paraformaldehyde (PFA)-killed bacteria showed a similar level of ERK activation as in WT-infected cells and only p38 activity was dependent on the viability of bacteria (supplemental Fig.

S10*B*). Altogether, the results indicate that ERKs and p38 and their downstream effectors RSK1, RSK2, Msk2 and MK2 represent major signaling modules specifically induced in WT-infected cells at 60 min p.i. and that the induction of p38 branch requires viable bacteria.

WT-induced p38 Signaling Regulates the Early Expression of Pro- and Anti-inflammatory Cytokines in Infected BMDCs—The induction of MAPK/MAPKAPK cascades in WT-infected BMDCs suggested that these cells might also mobilize their transcriptional machinery. Indeed, the observation of WTdriven phosphorylation of proteins associated with inhibitor of NF-B kinase (IKK) signaling indicated the upregulation of gene expression. Tab2 protein, needed for IKK/ activation, was phosphorylated (S450) in WT-infected BMDCs at 60 min p.i. (supplemental Table S1). Similarly, a known substrate of both canonical IKKs and IKK-related kinases (48) - Tank - was phosphorylated on two residues (S107 and S258; Fig. 6*A* and supplemental Table S1, respectively). Finally, IKK targets NF-B inhibitor- (IB-; S18) (Fig. 6*A*), IB- (Fig. 6*B*) and Abin2 (S147) (supplemental Table S1) were found to be phosphorylated in WT-infected BMDCs at 30 min or 60 min p.i., respectively, and these events are known to have a positive impact on NF-B-dependent gene expression (49, 50). In addition, the transcriptional activity of activator protein 1 (AP-1) was also upregulated in BMDCs infected by WT as inferred from the phosphorylation of Jun (S73) (Fig. 6*A*). The described situation favored the expression of *Il12b* in WTinfected BMDCs (Fig. 6*D*) as the gene transcription is NF-Band AP-1-dependent (51, 52). Notably, although the phosphorylation of Jun was p38-independent (Fig. 6*C*), the expression of *Il12b* relied on p38 activity (Fig. 6*E*) which suggests that WT-induced p38 might support NF-B-dependent transcription (53). The early *Il12b* expression, followed by IL-12p40 secretion (1–6 h p.i.; Fig. 6*D* and supplemental Fig. S11), contrasted with the situation at 24 h p.i., in which the levels of IL-12p40 produced by WT-infected BMDCs were below those produced by *dsbA*-infected cells (Fig. 2*B* and supplemental Fig. S11). The nature of the attenuation of IL-12p40 production in WT-infected BMDCs could not be explained based on the presented phosphoproteomic data as these describe the very early moments of the infection. Nevertheless, several lines of evidence suggested that triggering of MAPK/MAPKAPK signaling in WT-infected BMDCs at 60 min p.i. leads to the activation of cAMP-responsive element-binding protein (CREB) which is responsible for the transcription of genes with immunosuppressive functions (54). First, InnateDB terms connected to events in the nucleus (including "CREB phosphorylation") were found enriched in the group of proteins differentially phosphorylated in WT- and *dsbA*-infected BMDCs at 60 min p.i. (Fig. 4*B*). Second, although none of CREB phosphosites were identified as regulated in phosphoproteomic screen, CREB represented an interaction hub in MAPK signaling cluster in the constructed protein-protein interaction network (Fig. 5*A*). CREB-regulated transcription coactivator 2 (TORC2) was phosphorylated in WT-infected BMDCs at 60 min p.i. (supplemental Table S1) at 2 position (S612) to calcineurin binding motif (55). Finally, WT-induced MK2 and Msks MAPKAPKs (see above) can phosphorylate the regulatory S133 CREB site (56, 57). In line with the latter, CREB was phosphorylated in WT-infected BMDCs at 60 min p.i. (Fig. 6*B*) in p38-dependent manner (Fig. 6*C*). Notably, CREB was also phosphorylated at 10 min p.i. in both WT- and *dsbA*-infected BMDCs and the biphasic activation profile in WT-infected cells implied the participation of either ERKs (Fig. 1*D* and 5*B*) and/or Akt (see Discussion) in the process. The activation of CREB in infected macrophages and DCs leads to the expression of anti-inflammatory genes such as *Il10* (54). Consistently with WT-induced CREB phosphorylation, the increase in *Il10* mRNA was more prominent in WT-infected BMDCs (Fig. 6*D*) and the stable expression relied on p38 activity (Fig. 6*E*). The dominant position of MAPK-regulated transcription factors in BMDC transcriptional response to WT might seem surprising considering the cytosolic localization of bacteria at 60 min p.i. (Fig. 2*C*). Indeed, cytosolic *Francisella* is known to induce expression of type I IFN-related genes through the activation of interferon-regulatory factor 3 (IRF3) by TANK-binding kinase 1 (TBK1) in STING-dependent manner (9, 10, 58, 59). The interaction network in supplemental Fig. S8 contained group of proteins potentially involved in cytosolic sensing of bacteria (supplemental Fig. S12*A*). However, the cluster was relatively small and both participants identified in phosphoproteomic screen, Tank (Fig. 6*A*) and Trafd1 (supplemental Fig. S12*B*), were also shown to participate in the regulation of NF-B activity (Fig. 6*B*) (48, 60, 61). In line with the inconclusive findings, the expression of *Ifnb1* was low in both WT- and *dsbA*-infected BMDCs when compared with cells infected by LVS (supplemental Fig. S12*C*). Taken together, these results show that signaling cascades responsible for the activation of NF-B and CREB in BMDCs are stimulated during the first hour of WT infection and the induced early expression of both *Il12b* and *Il10* genes depends on WT-activated p38 signaling.

DISCUSSION

In this work, we explored phosphorylation signaling of DCs during their early (1 h) interactions with either virulent *Francisella tularensis* subsp. *holarctica* FSC200 (WT) or its avirulent *dsbA* mutant. Such events are known to be differentially regulated in host cells infected by virulent and attenuated strains (7, 62–64) and they represent the initial point of divergence in the activation and the immunogenic development of DCs (6). We demonstrate here that virulent *Francisella* triggers two distinct waves of DC protein phosphorylation within the first hour of infection (Fig. 6*F*). The initial phagocytosis-induced DC response (10 min p.i.) involves Akt-mediated stimulation of mTOR, the activation of ERK-RSK module, and the regulation of Rac/Cdc42 GAPs and GEFs and PAK autophosphorylation. The active role of ERKs and mTOR in *Francisella* internalization was reported before (65, 66), but this is the first study to show the involvement of PAKs in the process. Their function however remains unclear because PAK activation is associated with macropinocytic uptake (67) which is not the primary mechanism of *Francisella* entry into phagocytes (68). The initial DC response induced by the bacterial engulfment rapidly declines at 30 min p.i. The notable exception represents the upregulation of IKK signaling (*e.g.* phosphorylation of IBs and Tank) which occurs more prominently in DCs infected by WT bacterium. The difference between strains becomes even more evident at 60 min p.i. when WT induces the new wave of host proteome phosphorylation. The most active components of this second signaling peak are ERK1/ 2-RSK1/2 and p38-MK2 kinase modules. The lower potency of *dsbA* to stimulate such response represents an interesting feature of the invasion. DsbA protein is TLR2 ligand (69) but it is unlikely that its loss affected TLR-dependent MAPK activation because there is no quantitative difference in the initial signaling response of DCs to WT and *dsbA*. Rather, the existence of two temporally separated host phosphorylation waves suggests that infected DCs react to two distinct events. Considering the bacterial uptake as the origin of the initial DC response, we speculate that the second signaling wave detected at 60 min p.i. might be functionally linked to the rapid escape of WT bacteria into the cytosol. Two findings support this notion: (1) only viable WT bacteria are able to trigger p38 activation and (2) although the majority of *dsbA*containing phagosomes lose their integrity at 60 min p.i., bacteria are still surrounded by vacuolar membranes and therefore not fully released. It is however impossible to conclude whether the activation of p38/ERKs at 60 min p.i. results from the enhanced cytosolic sensing of bacterial products, WT-specific rapid disruption of phagosome, or the activity of unidentified bacterial effector. In this light, it is interesting that components of cytosolic DNA-sensing pathways are not among phosphoproteins differentially regulated between WTand *dsbA*-infected DCs. It was previously shown that *dsbA* of LVS background stimulates the higher production of IFN- than its WT counterpart (70). In contrast, the expression of *Ifnb1* in DCs infected by FSC200 WT and *dsbA* is lower than in LVS-infected DCs and virtually indistinguishable from uninfected cells. This suggests that the observed upregulation of MAPK signaling in WT-infected BMDCs is unrelated to STING-dependent cytosolic sensing of *Francisella* DNA (9, 10, 58, 59). The activation of MAPKs is a part of the host proinflammatory response and it is usually associated rather with attenuated *Francisella* strains (62, 63). For example, previous analysis of host phosphoproteome showed that p38-target tristetraproline (TPP) was phosphorylated in response to *F. novicida lpcC* mutant and that this positively affected the stability of proinflammatory transcripts (63). In contrast, we observe p38-mediated TPP phosphorylation (S52; supplemental Table S1) and p38-dependent *Il12b* expression rather in DCs infected by virulent strain. These contradictory findings might be explained if we consider that the extent of MAPK activity induced by virulent *Francisella* is assessed only relatively by the comparison with attenuated bacteria. For illustration, mutants defective in phagosomal escape are known to prolong the stimulation of TLRs from within the phagosome (7) and the comparison of these strains with WTs may lead to the conclusion that virulent *Francisella* avoids MAPK activation. Here, we employ *dsbA* as a reference. The mutant is attenuated and provides protection *in vivo* (33). However, the production of IL-1 in infected DCs suggests that *dsbA* probably reaches the host cytosol. Such behavior would explain the relatively low ability of *dsbA* to induce TLR-dependent early MAPKs signaling when compared with phagosome-residing mutants (7). On the other hand, different kinetics of *dsbA*-driven phagosomal disruption and of the cellular stress connected with the process might be responsible for the apparently high MAPKs activity in WT-infected DCs at 60 min p.i. Collectively, the presented comparative study reveals that the early MAPKs signaling in *Francisella*infected DCs is selectively engaged rather than suppressed. The preservation of mTOR activity observed at 60 min p.i. in WT-activated DCs probably helps to stimulate gene transcription and to re-configure the cell metabolism (71). Interestingly, although Akt mediated the suppression of mTOR inhibitors during the bacterial entry, mTOR activity at 60 min p.i. was partially supported by p38 (Fig. 6*C*) and possibly also by ERKs (66). The initial proinflammatory directing of WT-infected DCs is however lost during *Francisella*-DC interaction and, in contrast to *dsbA*-infected cells, DCs infected by virulent bacteria are not activated or matured 24 h p.i. Although the transient early activation of p38 and IB-phosphorylation was in *Francisella*-infected cells observed before (64), implications for bacterial virulence remain unclear. It is known that the activation of p38 helps *Francisella* to suppress the early cell death of the host (72, 73) and to

downregulate MHC II (74). We propose that the positive regulation of CREB transcription factor is another side effect of p38 activation which favors *Francisella*-mediated host survival and immunity bypass (54). It was previously shown that GSK-3 inhibition led to CREB activation and IL-10 production in LVS-infected macrophages (75). Akt-mediated inhibition of GSK-3 could be indeed responsible for CREB induction at 10 min p.i. observed in both WT- and *dsbA*-infected DCs. However, phosphorylation of CREB at 60 min p.i. and the early expression of *Il10* in DCs infected by WT was p38-dependent. Although the levels of secreted IL-10 were below the limit of detection, we speculate that p38-dependently produced IL-10 may through autocrine/ paracrine stimulation instruct DCs to suppress the initial inflammation and to alter the maturation (76). Taken together, our phosphoproteomic data show that the very early DC response to *Francisella* is divided into temporally separate phases which correspond to different stages of bacterial infection. We report that cytosolic virulent *Francisella* induces MAPKs and early gene expression and that these processes are the earliest events regulated differentially in DCs infected by WT and attenuated *dsbA* strains of fully virulent FSC200 bacterial background. The temporal orchestration of host proinflammatory pathways therefore represents the integral part of *Francisella* life-cycle inside hijacked DCs. In this regard, the detailed analysis of earlyintermediate gene expression in cells exposed to the bacterium may provide new insights into how DCs acquire their unproductive phenotype.

Acknowledgments—We thank Prof. Yousef Abu Kwaik for critical reading of the manuscript and Jitka Zakova and Lenka Luksikova (University of Defense) for excellent technical assistance.

DATA AVAILABILITY

Proteomics data were deposited to the ProteomeXchange Consortium (http://proteomecentral.proteomexchange.orgx) via the PRIDE partner repository with the data set identifiers PXD005747 (phosphoproteome) and PXD006759 (proteome) and MS/MS spectra can be viewed on MS-Viewer (http://msviewer.ucsf.edu/prospector/cgi-bin/msform.cgi?formmsviewer) using the search keys uomohcoiy9 (phosphoproteome) and oqiga3hn5r (proteome).

* This work was supported by the Czech Science Foundation (15–02584S). Marina Santic was supported by the Croatian Science Foundation (HRZZZ-9003). The Microscopy Centre - Electron Microscopy CF, IMG AS CR is supported by the Czech-BioImaging large RI project (LM2015062 funded by MEYS CR) and by OP RDE (CZ.02.1.01/0.0/0.0/16_013/0001775).

□S This article contains supplemental material.

** To whom correspondence should be addressed: Department of Molecular Pathology and Biology, Faculty of Military Health Sciences, University of Defence, 500 01 Hradec Kralove, Czech Republic. Tel.: 00420-973-253-220; Fax: 00420-495-513-018; E-mail: jiri.stulik@unob.cz.

REFERENCES

1. Kubelkova, K., and Macela, A. (2015) Putting the Jigsaw Together - A BriefInsight Into the Tularemia. *Open Life Sci.* **10,**
2. Oyston, P. C. F., Sjostedt, A., and Titball, R. W. (2004) Tularaemia: bioterrorism defence renews interest in *Francisella tularensis. Nat. Rev. Microbiol.* **2,** 967–978
3. Sharma, J., Mares, C. A., Li, Q., Morris, E. G., and Teale, J. M. (2011) Features of sepsis caused by pulmonary infection with *Francisella tularensis* Type A strain. *Microb. Pathog.* **51,** 39–47
4. Asare, R., and Kwaik, Y. A. (2010) Exploitation of host cell biology andevasion of immunity by *Francisella tularensis. Front. Microbiol.* **1,** 145
5. Santic, M., Al-Khodor, S., and Abu Kwaik, Y. (2010) Cell biology andmolecular ecology of *Francisella tularensis. Cell. Microbiol.* **12,** 129–139
6. Fabrik, I., Ha¨ rtlova, A., Rehulka, P., and Stulik, J. (2013) Serving the newmasters - dendritic cells as hosts for stealth intracellular bacteria. *Cell. Microbiol.* **15,** 1473–1483
7. Cole, L. E., Santiago, A., Barry, E., Kang, T. J., Shirey, K. A., Roberts, Z. J.,Elkins, K. L., Cross, A. S., and Vogel, S. N. (2008) Macrophage proinflammatory response to *Francisella tularensis* live vaccine strain requires coordination of multiple signaling pathways. *J. Immunol.* **180,** 6885–6891
8. Cremer, T. J., Butchar, J. P., and Tridandapani, S. (2011) *Francisella* subverts innate immune signaling: focus on PI3K/Akt. *Front. Microbiol.* **5,** 13
9. Storek, K. M., Gertsvolf, N. A., Ohlson, M. B., and Monack, D. M. (2015) cGAS and Ifi204 cooperate to produce type I IFNs in response to *Francisella* infection. *J. Immunol.* **194,** 3236–3245
10. Jones, J. W., Kayagaki, N., Broz, P., Henry, T., Newton, K., O'Rourke, K.,Chan, S., Dong, J., Qu, Y., Roose-Girma, M., Dixit, V. M., and Monack, D. M. (2010) Absent in melanoma 2 is required for innate immune recognition of *Francisella tularensis. Proc. Natl. Acad. Sci. U.S.A.* **107,** 9771–9776
11. Bauler, T. J., Chase, J. C., and Bosio, C. M. (2011) IFN- mediates suppression of IL-12p40 in human dendritic cells following infection with virulent *Francisella tularensis. J. Immunol.* **187,** 1845–1855
12. Fabrik, I., Link, M., Ha¨ rtlova, A., Dankova, V., Rehulka, P., and Stulik, J.(2014) Application of SILAC labeling to primary bone marrow-derived dendritic cells reveals extensive GM-CSF-dependent arginine metabolism. *J. Proteome Res.* **13,** 752–762
13. Rogers, L. D., Fang, Y., and Foster, L. J. (2010) An integrated globalstrategy for cell lysis, fractionation, enrichment and mass spectrometric analysis of phosphorylated peptides. *Mol. Biosyst.* **6,** 822–829
14. Yeung, Y.-G., and Stanley, E. R. (2010) Rapid detergent removal frompeptide samples with ethyl acetate for mass spectrometry analysis. *Curr. Protoc. Protein Sci.* Chapter **16,** Unit 16.12
15. McNulty, D. E., and Annan, R. S. (2008) Hydrophilic interaction chromatography reduces the complexity of the phosphoproteome and improves global phosphopeptide isolation and detection. *Mol. Cell. Proteomics MCP* **7,** 971–980
16. Ha¨rtlova, A., Link, M., Balounova, J., Benesova, M., Resch, U., Straskova, A.,Sobol, M., Philimonenko, A., Hozak, P., Krocova, Z., Gekara, N., Filipp, D., and Stulik, J. (2014) Quantitative proteomics analysis of macrophagederived lipid rafts reveals induction of autophagy pathway at the early time of *Francisella tularensis* LVS infection. *J. Proteome Res.* **13,** 796–804
17. Michalski, A., Damoc, E., Hauschild, J.-P., Lange, O., Wieghaus, A., Makarov, A., Nagaraj, N., Cox, J., Mann, M., and Horning, S. (2011) Mass spectrometry-based proteomics using Q Exactive, a high-performance benchtop quadrupole Orbitrap mass spectrometer. *Mol. Cell. Proteomics MCP* **10,** M111.011015
18. Cox, J., and Mann, M. (2008) MaxQuant enables high peptide identificationrates, individualized p.p.b.-range mass accuracies and proteome-wide protein quantification. *Nat. Biotechnol.* **26,** 1367–1372
19. Klammer, M., Dybowski, J. N., Hoffmann, D., and Schaab, C. (2014) Identification of significant features by the Global Mean Rank test. *PloS One* 9:e104504,

20. Zhou, Y., Cras-Me´ neur, C., Ohsugi, M., Stormo, G. D., and Permutt, M. A.(2007) A global approach to identify differentially expressed genes in cDNA (two-color) microarray experiments. *Bioinformation* **23,** 2073–2079
21. Futschik, M. E., and Carlisle, B. (2005) Noise-robust soft clustering of geneexpression time-course data. *J. Bioinform. Comput. Biol.* **3,** 965–988
22. Olsen, J. V., Blagoev, B., Gnad, F., Macek, B., Kumar, C., Mortensen, P.,and Mann, M. (2006) Global, in vivo, and site-specific phosphorylation dynamics in signaling networks. *Cell* **127,** 635–648
23. Sharma, K., D'Souza, R. C. J., Tyanova, S., Schaab, C., Wis´niewski, J. R.,Cox, J., and Mann, M. (2014) Ultradeep human phosphoproteome reveals a distinct regulatory nature of Tyr and Ser/Thr-based signaling. *Cell Rep.* **8,** 1583–1594
24. Kumar, L., and E Futschik, M. (2007) Mfuzz: a software package for softclustering of microarray data. *Bioinformation* **2,** 5–7
25. Schwa¨ mmle, V., and Jensen, O. N. (2010) A simple and fast method todetermine the parameters for fuzzy *c*-means cluster analysis. *Bioinformation* **26,** 2841–2848
26. Keshava Prasad, T. S., Goel, R., Kandasamy, K., Keerthikumar, S., Kumar,S., Mathivanan, S., Telikicherla, D., Raju, R., Shafreen, B., Venugopal, A., Balakrishnan, L., Marimuthu, A., Banerjee, S., Somanathan, D. S., Sebastian, A., Rani, S., Ray, S., Harrys Kishore, C. J., Kanth, S., Ahmed, M., Kashyap, M. K., Mohmood, R., Ramachandra, Y. L., Krishna, V., Rahiman, B. A., Mohan, S., Ranganathan, P., Ramabadran, S., Chaerkady, R., and Pandey, A. (2009) Human Protein Reference Database–2009 update. *Nucleic Acids Res.* **37,** D767–D772
27. Tyanova, S., Temu, T., Sinitcyn, P., Carlson, A., Hein, M. Y., Geiger, T.,Mann, M., and Cox, J. (2016) The Perseus computational platform for comprehensive analysis of (prote)omics data. *Nat. Methods* **13,** 731–740
28. Breuer, K., Foroushani, A. K., Laird, M. R., Chen, C., Sribnaia, A., Lo, R.,Winsor, G. L., Hancock, R. E. W., Brinkman, F. S. L., and Lynn, D. J. (2013) InnateDB: systems biology of innate immunity and beyond–recent updates and continuing curation. *Nucleic Acids Res.* **41,** D1228–D1233
29. Szklarczyk, D., Franceschini, A., Wyder, S., Forslund, K., Heller, D., HuertaCepas, J., Simonovic, M., Roth, A., Santos, A., Tsafou, K. P., Kuhn, M., Bork, P., Jensen, L. J., and von Mering, C. (2015) STRING v10: proteinprotein interaction networks, integrated over the tree of life. *Nucleic Acids Res.* **43,** D447–D452
30. Kim, H. G., Kim, J. Y., Gim, M. G., Lee, J. M., and Chung, D. K. (2008) Mechanical stress induces tumor necrosis factor- production through Ca^2 release-dependent TLR2 signaling. *Am. J. Physiol. Cell Physiol.* **295,** C432–C439
31. Qin, A., Scott, D. W., Thompson, J. A., and Mann, B. J. (2009) Identificationof an essential *Francisella tularensis subsp. tularensis* virulence factor. *Infect. Immun.* **77,** 152–161
32. Straskova, A., Pavkova, I., Link, M., Forslund, A.-L., Kuoppa, K., Noppa, L.,Kroca, M., Fucikova, A., Klimentova, J., Krocova, Z., Forsberg, A., and Stulik, J. (2009) Proteome analysis of an attenuated *Francisella tularensis dsbA* mutant: identification of potential DsbA substrate proteins. *J. Proteome Res.* **8,** 5336–5346
33. Straskova, A., Spidlova, P., Mou, S., Worsham, P., Putzova, D., Pavkova, I.,and Stulik, J. (2015) *Francisella tularensis* type B *dsbA* mutant protects against type A strain and induces strong inflammatory cytokine and Th1-like antibody response *in vivo. Pathog. Dis.* **73,** ftv058
34. Straskova, A., Cerveny, L., Spidlova, P., Dankova, V., Belcic, D., Santic, M.,and Stulik, J. (2012) Deletion of IglH in virulent *Francisella tularensis subsp. holarctica* FSC200 strain results in attenuation and provides protection against the challenge with the parental strain. *Microbes Infect.* **14,** 177–187
35. Hashimoto, M., Sagara, Y., Langford, D., Everall, I. P., Mallory, M., Everson,A., Digicaylioglu, M., and Masliah, E. (2002) Fibroblast growth factor 1 regulates signaling via the glycogen synthase kinase-3 pathway. Implications for neuroprotection. *J. Biol. Chem.* **277,** 32985–32991
36. Manning, B. D., Tee, A. R., Logsdon, M. N., Blenis, J., and Cantley, L. C.(2002) Identification of the tuberous sclerosis complex-2 tumor suppressor gene product tuberin as a target of the phosphoinositide 3-kinase/akt pathway. *Mol. Cell* **10,** 151–162
37. Ning, J., Xi, G., and Clemmons, D. R. (2011) Suppression of AMPK activation via S485 phosphorylation by IGF-I during hyperglycemia is mediated by AKT activation in vascular smooth muscle cells. *Endocrinology* **152,** 3143–3154
38. Vander Haar, E., Lee, S.-I., Bandhakavi, S., Griffin, T. J., and Kim, D.-H.(2007) Insulin signalling to mTOR mediated by the Akt/PKB substrate PRAS40. *Nat. Cell Biol.* **9,** 316–323
39. Acosta-Jaquez, H. A., Keller, J. A., Foster, K. G., Ekim, B., Soliman, G. A.,Feener, E. P., Ballif, B. A., and Fingar, D. C. (2009) Site-specific mTOR phosphorylation promotes mTORC1-mediated signaling and cell growth. *Mol. Cell. Biol.* **29,** 4308–4324
40. Kim, Y.-M., Stone, M., Hwang, T. H., Kim, Y.-G., Dunlevy, J. R., Griffin, T. J.,and Kim, D.-H. (2012) SH3BP4 is a negative regulator of amino acid-Rag GTPase-mTORC1 signaling. *Mol. Cell* **46,** 833–846
41. Dalby, K. N., Morrice, N., Caudwell, F. B., Avruch, J., and Cohen, P. (1998) Identification of regulatory phosphorylation sites in mitogen-activated protein kinase (MAPK)-activated protein kinase-1a/p90rsk that are inducible by MAPK. *J. Biol. Chem.* **273,** 1496–1505
42. Kang, S., Dong, S., Gu, T.-L., Guo, A., Cohen, M. S., Lonial, S., Khoury,H. J., Fabbro, D., Gilliland, D. G., Bergsagel, P. L., Taunton, J., Polakiewicz, R. D., and Chen, J. (2007) FGFR3 activates RSK2 to mediate hematopoietic transformation through tyrosine phosphorylation of RSK2 and activation of the MEK/ERK pathway. *Cancer Cell* **12,** 201–214
43. Engel, K., Schultz, H., Martin, F., Kotlyarov, A., Plath, K., Hahn, M., Heinemann, U., and Gaestel, M. (1995) Constitutive activation of mitogenactivated protein kinase-activated protein kinase 2 by mutation of phosphorylation sites and an A-helix motif. *J. Biol. Chem.* **270,** 27213–27221
44. Toma´ s-Zuber, M., Mary, J. L., Lamour, F., Bur, D., and Lesslauer, W. (2001) C-terminal elements control location, activation threshold, and p38 docking of ribosomal S6 kinase B (RSKB). *J. Biol. Chem.* **276,** 5892–5899
45. Matsuura, H., Nishitoh, H., Takeda, K., Matsuzawa, A., Amagasa, T., Ito,M., Yoshioka, K., and Ichijo, H. (2002) Phosphorylation-dependent scaffolding role of JSAP1/JIP3 in the ASK1-JNK signaling pathway. A new mode of regulation of the MAP kinase cascade. *J. Biol. Chem.* **277,** 40703–40709
46. Santic, M., Asare, R., Skrobonja, I., Jones, S., and Abu Kwaik, Y. (2008) Acquisition of the vacuolar ATPase proton pump and phagosome acidification are essential for escape of *Francisella tularensis* into the macrophage cytosol. *Infect. Immun.* **76,** 2671–2677
47. Chong, A., Wehrly, T. D., Nair, V., Fischer, E. R., Barker, J. R., Klose, K. E.,and Celli, J. (2008) The early phagosomal stage of *Francisella tularensis* determines optimal phagosomal escape and *Francisella* pathogenicity island protein expression. *Infect. Immun.* **76,** 5488–5499
48. Clark, K., Peggie, M., Plater, L., Sorcek, R. J., Young, E. R. R., Madwed,J. B., Hough, J., McIver, E. G., and Cohen, P. (2011) Novel cross-talk within the IKK family controls innate immunity. *Biochem. J.* **434,** 93–104 49. Shirane, M., Hatakeyama, S., Hattori, K., Nakayama, K., and Nakayama, K. (1999) Common pathway for the ubiquitination of IB, IB, and IB mediated by the F-box protein FWD1. *J. Biol. Chem.* **274,** 28169–28174
50. Leotoing, L., Chereau, F., Baron, S., Hube, F., Valencia, H. J., Bordereaux,D., Demmers, J. A., Strouboulis, J., and Baud, V. (2011) A20-binding inhibitor of nuclear factor-B (NF-B)-2 (ABIN-2) is an activator of inhibitor of NF-B (IB) kinase (IKK)-mediated NF-B transcriptional activity. *J. Biol. Chem.* **286,** 32277–32288
51. Sanjabi, S., Hoffmann, A., Liou, H. C., Baltimore, D., and Smale, S. T. (2000) Selective requirement for c-Rel during IL-12 P40 gene induction in macrophages. *Proc. Natl. Acad. Sci. U.S.A.* **97,** 12705–12710
52. Zhu, C., Gagnidze, K., Gemberling, J. H., and Plevy, S. E. (2001) Characterization of an activation protein-1-binding site in the murine interleukin-12 p40 promoter. Demonstration of novel functional elements by a reductionist approach. *J. Biol. Chem.* **276,** 18519–18528
53. Olson, C. M., Hedrick, M. N., Izadi, H., Bates, T. C., Olivera, E. R., andAnguita, J. (2007) p38 mitogen-activated protein kinase controls NF-B transcriptional activation and tumor necrosis factor alpha production through RelA phosphorylation mediated by mitogen- and stress-activated protein kinase 1 in response to *Borrelia burgdorferi* antigens. *Infect. Immun.* **75,** 270–277

54. Wen, A. Y., Sakamoto, K. M., and Miller, L. S. (2010) The role of thetranscription factor CREB in immune function. *J. Immunol.* **185,** 6413–6419
55. Screaton, R. A., Conkright, M. D., Katoh, Y., Best, J. L., Canettieri, G., Jeffries,S., Guzman, E., Niessen, S., Yates, J. R., Takemori, H., Okamoto, M., and Montminy, M. (2004) The CREB coactivator TORC2 functions as a calciumand cAMP-sensitive coincidence detector. *Cell* **119,** 61–74
56. Tan, Y., Rouse, J., Zhang, A., Cariati, S., Cohen, P., and Comb, M. J. (1996) FGF and stress regulate CREB and ATF-1 via a pathway involving p38 MAP kinase and MAPKAP kinase-2. *EMBO J.* **15,** 4629–4642
57. Deak, M., Clifton, A. D., Lucocq, L. M., and Alessi, D. R. (1998) Mitogenand stress-activated protein kinase-1 (MSK1) is directly activated by MAPK and SAPK2/p38, and may mediate activation of CREB. *EMBO J.* **17,** 4426–4441
58. Tanaka, Y., and Chen, Z. J. (2012) STING specifies IRF3 phosphorylation byTBK1 in the cytosolic DNA signaling pathway. *Sci. Signal.* **5,** ra20 59. Henry, T., Brotcke, A., Weiss, D. S., Thompson, L. J., and Monack, D. M. (2007) Type I interferon signaling is required for activation of the inflammasome during *Francisella* infection. *J. Exp. Med.* **204,** 987–994
60. Mashima, R., Saeki, K., Aki, D., Minoda, Y., Takaki, H., Sanada, T.,Kobayashi, T., Aburatani, H., Yamanashi, Y., and Yoshimura, A. (2005) FLN29, a novel interferon- and LPS-inducible gene acting as a negative regulator of toll-like receptor signaling. *J. Biol. Chem.* **280,** 41289–41297
61. Sanada, T., Takaesu, G., Mashima, R., Yoshida, R., Kobayashi, T., andYoshimura, A. (2008) FLN29 deficiency reveals its negative regulatory role in the Toll-like receptor (TLR) and retinoic acid-inducible gene I (RIG-I)-like helicase signaling pathway. *J. Biol. Chem.* **283,** 33858–33864
62. Huang, M. T.-H., Mortensen, B. L., Taxman, D. J., Craven, R. R., Taft-Benz, S., Kijek, T. M., Fuller, J. R., Davis, B. K., Allen, I. C., Brickey, W. J., Gris, D., Wen, H., Kawula, T. H., and Ting, J. P.-Y. (2010) Deletion of *ripA* alleviates suppression of the inflammasome and MAPK by *Francisella tularensis*. *J. Immunol.* **185,** 5476–5485
63. Nakayasu, E. S., Tempel, R., Cambronne, X. A., Petyuk, V. A., Jones, M. B.,Gritsenko, M. A., Monroe, M. E., Yang, F., Smith, R. D., Adkins, J. N., and Heffron, F. (2013) Comparative phosphoproteomics reveals components of host cell invasion and post-transcriptional regulation during *Francisella* infection. *Mol. Cell. Proteomics MCP* **12,** 3297–3309
64. Telepnev, M., Golovliov, I., and Sjo¨ stedt, A. (2005) Francisella tularensisLVS initially activates but subsequently down-regulates intracellular signaling and cytokine secretion in mouse monocytic and human peripheral blood mononuclear cells. *Microb. Pathog.* **38,** 239–247
65. Parsa, K. V. L., Butchar, J. P., Rajaram, M. V. S., Cremer, T. J., andTridandapani, S. (2008) The tyrosine kinase Syk promotes phagocytosis of *Francisella* through the activation of Erk. *Mol. Immunol.* **45,** 3012–3021
66. Edwards, M. W., Aultman, J. A., Harber, G., Bhatt, J. M., Sztul, E., Xu, Q.,Zhang, P., Michalek, S. M., and Katz, J. (2013) Role of mTOR downstream effector signaling molecules in *Francisella tularensis* internalization by murine macrophages. *PloS One* **8,** e83226
67. Van den Broeke, C., Radu, M., Chernoff, J., and Favoreel, H. W. (2010) Anemerging role for p21-activated kinases (Paks) in viral infections. *Trends Cell Biol.* **20,** 160–169
68. Moreau, G. B., and Mann, B. J. (2013) Adherence and uptake of *Francisella* into host cells. *Virulence* **4,** 826–832
69. Thakran, S., Li, H., Lavine, C. L., Miller, M. A., Bina, J. E., Bina, X. R., andRe, F. (2008) Identification of *Francisella tularensis* lipoproteins that stimulate the toll-like receptor (TLR) 2/TLR1 heterodimer. *J. Biol. Chem.* **283,** 3751–3760
70. Putzova, D., Panda, S., Ha¨ rtlova, A., Stulík, J., and Gekara, N. O. (2017) Subversion of innate immune responses by *Francisella* involves the disruption of TRAF3 and TRAF6 signalling complexes. *Cell. Microbiol.* doi: 10.1111/cmi.12769
71. Sukhbaatar, N., Hengstschla¨ ger, M., and Weichhart, T. (2016) mTOR-Mediated Regulation of Dendritic Cell Differentiation and Function. *Trends Immunol.* **37,** 778–789
72. Hrstka, R., Stulík, J., and Vojtesek, B. (2005) The role of MAPK signalpathways during *Francisella tularensis* LVS infection-induced apoptosis in murine macrophages. *Microbes Infect.* **7,** 619–625
73. Santic, M., Pavokovic, G., Jones, S., Asare, R., and Kwaik, Y. A. (2010) Regulation of apoptosis and anti-apoptosis signalling by *Francisella tularensis*. *Microbes Infect.* **12,** 126–134
74. Brummett, A. M., Navratil, A. R., Bryan, J. D., and Woolard, M. D. (2014) Januskinase 3 activity is necessary for phosphorylation of cytosolic phospholipase A2 and prostaglandin E2 synthesis by macrophages infected with *Francisella tularensis* live vaccine strain. *Infect. Immun.* **82,** 970–982
75. Zhang, P., Katz, J., and Michalek, S. M. (2009) Glycogen synthase kinase-3 (GSK3) inhibition suppresses the inflammatory response to *Francisella* infection and protects against tularemia in mice. *Mol. Immunol.* **46,** 677–687
76. Corinti, S., Albanesi, C., la Sala, A., Pastore, S., and Girolomoni, G. (2001) Regulatory activity of autocrine IL-10 on dendritic cell functions. *J. Immunol. Baltim. Md 1950* **166,** 4312–4318